

กรดอะมิโนรีเซปเตอร์และเซนเซอร์ที่มีอะครีตินและสเตอรอยด์



นางสาว อัญชลี สิริกุลขจร

ศูนย์วิทยทรัพยากร

วิทยานิพนธ์นี้เป็นส่วนหนึ่งของการศึกษาตามหลักสูตรปริญญาวิทยาศาสตรดุษฎีบัณฑิต


สาขาวิชาเคมี ภาควิชาเคมี

คณะวิทยาศาสตร์ จุฬาลงกรณ์มหาวิทยาลัย

ปีการศึกษา 2550

ลิขสิทธิ์ของจุฬาลงกรณ์มหาวิทยาลัย

ACRIDINE- AND STEROID-BASED AMINO ACID RECEPTORS AND SENSORS



Miss Anchalee Sirikulajorn

ศูนย์วิจัยทรัพยากร
A Dissertation Submitted in Partial Fulfillment of the Requirements

for the Degree of Doctor of Philosophy Program in Chemistry

Department of Chemistry
จุฬาลงกรณ์มหาวิทยาลัย

Faculty of Science

Chulalongkorn University


Academic year 2007

Copyright of Chulalongkorn University


501970

Thesis Title	ACRIDINE- AND STEROID-BASED AMINO ACID RECEPTORS AND SENSORS
By	Miss Anchalee Sirikulakajorn
Field of Study	Chemistry
Thesis Advisor	Associate Professor Thawatchai Tuntulani, Ph.D.
Thesis Co-advisor	Assistant Professor Boosayarat Tomapatanaget, Ph.D.


Accepted by the Faculty of Science, Chulalongkorn University in Partial Fulfillment of the Requirements for the Doctoral Degree

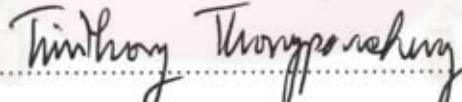

 Dean of the Faculty of Science
 (Professor Supot Hannongbua, Dr. rer. nat.)


THESIS COMMITTEE



 Chairman
 (Associate Professor Sirirat Kokpol, Ph.D.)



 Thesis Advisor
 (Associate Professor Thawatchai Tuntulani, Ph.D.)


 Thesis Co-advisor
 (Assistant Professor Boosayarat Tomapatanaget, Ph.D.)


 External Member
 (Assistant Professor Tienthong Thorngpanchang, Ph.D.)


 Member
 (Associate Professor Supason Wanichweacharunguang, Ph.D.)


 Member
 (Assistant Professor Worawan Bhanthumnavin, Ph.D.)


 Member
 (Assistant Professor Soamwadee Chaianansutcharit, Ph.D.)

อัญชลี สิริกุลขจร: กรดอะมิโนรีเซปเตอร์และเซนเซอร์ที่มีอะครีดีนและสเตอรอยด์ (ACRIDINE- AND STEROID-BASED AMINO ACID RECEPTORS AND SENSORS) อ. ที่ปรึกษา : รศ.ดร. ธวัชชัย ต้นทุลानी, อ. ที่ปรึกษาร่วม : ผศ.ดร. บุญยรัตน์ ธรรมพัฒน์กิจ, 161 หน้า.

ได้ทำการสังเคราะห์อนุพันธ์ของอะครีดีนและอะครีดีเนียม 4 ชนิดที่มีหมู่ไทโอยูเรียสำหรับจับกับกรดอะมิโนโมเลกุล L1 L2 L1H และ L2H ศึกษาความสามารถในการจับกับกรดอะมิโน 5 ชนิด คือ ทริปโตฟาน ฟีนิลอะลานีน ลิวซีน อะลานีนและ โกลซีน โดยใช้เทคนิค $^1\text{H-NMR}$ ยูวี-วิสิเบิลและฟลูออเรสเซนส์ พันธะไฮโดรเจนระหว่างหมู่ไทโอยูเรียของลิแกนด์และหมู่คาร์บอกซิลเลตของกรดสวิตเทอร์ไอออนิกอะมิโน คือ อันตรกิริยาหลักที่พบในสารประกอบเชิงซ้อน จากการทดลองพบว่า L1 และ L2 ที่เป็นกลางจับกับกรดอะมิโน ได้ไม่ดีดังผลของค่า K จำนวนเมื่อจับกับทริปโตฟานเท่ากับ 266 และ 307 M^{-1} ตามลำดับ เนื่องจากผลของแรงผลักระหว่างความหนาแน่นของอิเล็กตรอนที่ไนโตรเจนอะตอมของหมู่อะครีดีนกับประจุลบที่หมู่คาร์บอกซิลเลตของกรดอะมิโน อัตราส่วนของลิแกนด์ต่อกรดอะมิโนในสารประกอบเชิงซ้อนพบว่าเป็น 1:1 อย่างไรก็ตาม L2 ซึ่งมีโครงสร้างเป็นวงจับกับกรดอะมิโนที่มีหมู่อะโรมาติกได้ดีกว่า ในขณะที่ L1 ซึ่งมีโครงสร้างไม่เป็นวงไม่แสดงความจำเพาะเจาะจงในการจับกับกรดอะมิโน ลิแกนด์ L1H และ L2H ซึ่งมีหมู่อะครีดีเนียมไอออนเมื่อจับกับกรดอะมิโนพบว่านอกจากการเกิดพันธะไฮโดรเจนแล้วยังพบว่าเกิดการเคลื่อนที่ของโปรตรอนจากหมู่อะครีดีเนียมไปที่หมู่คาร์บอกซิลเลตของกรดอะมิโน นอกจากนี้ยังพบว่า L1H และ L2H จับกับกรดอะมิโนได้ดีกว่า L1 และ L2 โดยจะจับกับทริปโตฟานได้ดีที่สุด ยืนยันจากผลของค่า K จำนวนเมื่อจับกับทริปโตฟานได้ค่าดังนี้ K เท่ากับ 2873 และ 3157 M^{-1} สำหรับ L1H และ L2H ตามลำดับ ผลที่ได้แสดงว่าหมู่อะครีดีเนียมไอออนทำให้ความสามารถในการจับกับกรดอะมิโนดีขึ้น เนื่องจากมีแรงดึงดูดระหว่างประจุในสารประกอบเชิงซ้อนที่เกิดขึ้น

ได้ทำการสังเคราะห์อนุพันธ์สเตอรอยด์ซึ่งมีหมู่ยูเรียที่ตำแหน่งคาร์บอน C3 C7 และ C12 โมเลกุล L3 สำหรับศึกษาความสามารถในการเกิดสารประกอบเชิงซ้อนกับกรดอะมิโนชนิด L และ D ของทริปโตฟาน ฟีนิลอะลานีน ลิวซีน อะลานีนและ โกลซีน โดยใช้เทคนิค $^1\text{H-NMR}$ ยูวี-วิสิเบิล และการศึกษาทางเคมีคำนวณ จากผลการทดลองด้วยเทคนิค NMR พบว่าสารประกอบเชิงซ้อนระหว่าง L3 กับกรดอะมิโนเกิดผ่านพันธะไฮโดรเจนระหว่างหมู่ยูเรียที่ตำแหน่ง C7 และ C12 กับหมู่คาร์บอกซิลเลตของกรดอะมิโน รวมทั้งพันธะ $\pi-\pi$ ระหว่างหมู่อะโรมาติกของโมเลกุล L3 กับกรดอะมิโน นอกจากนี้ยังพบอีกว่า L3 มีความสามารถในการจับกับทริปโตฟานโดยเฉพาะอย่างยิ่งกับทริปโตฟานชนิด L ได้ดีกว่าชนิด D โดยให้ค่า $\log K$ เท่ากับ 4.54 และ 2.08 ตามลำดับเนื่องจากโครงสร้างของสารประกอบเชิงซ้อนที่ต่างกัน กรดอะมิโนตัวอื่นซึ่งมีหมู่แทนที่ขนาดเล็กพบว่าทั้งชนิด L และ D ไม่พบความแตกต่างเมื่อเกิดสารประกอบเชิงซ้อนกับ L3

ภาควิชา.....เคมี.....ลายมือชื่อนิสิต.....อัญชลี สิริกุลขจร.....
 สาขาวิชา.....เคมี.....ลายมือชื่ออาจารย์ที่ปรึกษา.....ธวัชชัย ต้นทุลानी.....
 ปีการศึกษา.....2550.....ลายมือชื่ออาจารย์ที่ปรึกษาร่วม.....บุญยรัตน์ ธรรมพัฒน์.....

4673840523 : MAJOR CHEMISTRY

KEY WORD: ACRIDINE/ ACRIDINIUM/ THIOUREA/ AMINO ACIDS/ STEROIDAL RECEPTOR/ UREA/ FLUORESCENCE/ HYDROGEN BONDING INTERACTION

ANCHALEE SIRIKULKAJORN: ACRIDINE- AND STEROID-BASED AMINO ACID RECEPTORS AND SENSORS. THESIS ADVISOR: ASSOC. PROF. THAWATCHAI TUNTULANI, Ph.D., THESIS COADVISOR: ASST. PROF. BOOSAYARAT TOMAPATAGET, Ph.D., 161 pp.

Four derivitized acridine and acridinium compounds (L1, L2, L1H and L2H) comprised of thiourea binding site were synthesized. Binding abilities of receptors L1, L2, L1H and L2H toward amino acids (Trp, Phe, Leu, Ala and Gly) were studied by $^1\text{H-NMR}$, UV-vis and fluorescence spectrophotometry. Hydrogen bonding interactions between thiourea binding site of the ligand and carboxylate groups in zwitterionic amino acids were found to be main interactions driving complexation to take place. Neutral ligands L1 and L2 showed weak binding (K for Trp = 266 M^{-1} and 307 M^{-1} for L1 and L2, respectively) due to repulsion between the host and the guest. The cyclic ligand L2 showed selective binding with aromatic amino acids while the acyclic ligand L1 did not. The stoichiometry of 1:1 complex was observed. In case of L1H and L2H (the protonated ligands), all results revealed the movement of the NH^+ -proton toward the carboxylate group of the amino acids. A large enhancement of emission band upon amino acid addition, especially in Trp suggested that the protonation of N-acridine could improve the binding ability (K for Trp = 2873 M^{-1} and 3157 M^{-1} for L1H and L2H, respectively) of the ligand toward amino acid due to a complementary from electrostatic forces.

A steroidal compound L3 comprised of urea binding site at C3, C7 and C12 positions processing an intrinsic chiral structure was synthesized to investigate binding abilities for amino acids (Trp, Phe, Leu, Ala and Gly). Binding studies of L3 toward both L- and D-forms of amino acids were carried out using $^1\text{H-NMR}$ spectroscopy, UV-vis spectrophotometry and modeling studies. Changes in $^1\text{H-NMR}$ spectra of L3 revealed that the complexes of L3 and amino acids occurred via hydrogen bond interactions (between urea groups and carboxylate unit) and π - π stacking interactions (between phenyl rings of a receptor and amino acid side chains). Results from all techniques exhibited the preference of L3 toward L-Trp ($\log K = 4.54$) over D-Trp ($\log K = 2.08$) and other amino acids. The preference over L-form amino acids, therefore, diminished in cases of the less bulky-side-chain amino acids (Phe, Leu and Ala).

Department: Chemistry

Student's signature: Anchalee Sivikulkaajorn

Field of study: Chemistry

Advisor's signature: S. Tuntulani

Academic year: 2007

Co-advisor's signature: Boosayarat Tomapataget

ACKNOWLEDGEMENTS

I wish to express deepest appreciation to my thesis advisor and co-advisor, Assoc. Prof. Thawatchai Tuntulani and Assist. Prof. Boosayarat Tomapatanaget, for their regularly close supervision, invaluable guidance, willing assistance, generous encouragement, sincere forgiveness and personal friendship throughout my postgraduate career. In addition, I would like to thank and pay my respect to Assoc. Prof. Sirirat Kokpol, Assist. Prof. Tientong Thongpanchang, Assoc. Prof. Supason Wanichweacha rungruang, Assist. Prof. Worawan Bhanthumnavin and Assist. Prof. Soamwadee Chaianansutcharit for their valuable suggestions and comments as committee members and thesis examiners. Furthermore, I would like to thank and express my gratitude to all staffs in Supramolecular Chemistry Research Unit especially Assoc. Prof. Vithaya Ruangponvisuti, Assoc. Prof. Nuanphun Chantarasiri and Assoc. Prof. Buncha Pulpoka for their generous helps and useful suggestions.

Definitely, this thesis cannot be completed without kindness and helpful of many people. Firstly, I would like to thank the Scientific and Technological Research Equipment Center of Chulalongkorn University, particularly, Miss Amporn Aengpakornkaew for elemental analysis results. Absolutely, I am grateful to the University of Bristol to furnish many facilities for my research; and all staffs in the Department of Chemistry for their generous helps. I would like to thank Prof. Anthony P. Davis; my supervisor and Dr. Germinal Margo; my co-supervisor during research working in Bristol UK for his invaluable guidance and willing assistance for the synthesis of steroidal receptor. Finally, the Development and Promotion of Science and Technology Talents Project (DPST) and the Thailand Research Fund are gratefully acknowledged for the grant during my Ph.D. degree study and research.

I would like to express my highest gratitude to my family for their love, kindness, encouragement and financial support throughout my life. Additionally, I would like to thank Mrs. Thongsuk Chalermkuanmongkon for her residence during my study in last year. Finally, my appreciation would be expressed to all members in Tuntulani's, Tomapatanaget's and Davis's group as well as all my friends in Bristol in the past and present for their very nice friendship, sincere helps and encouragement throughout my doctoral course, especially when I was away from home.

CONTENTS

	Page
ABSTRACT (THAI)	iv
ABSTRACT (ENGLISH)	v
ACKNOWLEDGEMENTS	vi
CONTENTS	vii
LIST OF TABLES	xiii
LIST OF FIGURES	xv
LIST OF ABBREVIATIONS	xviii
CHAPTER I SUPRAMOLECULAR CHEMISTRY AND FLUOROGENIC CHEMOSENSORS	1
1.1 Molecular Recognition.....	1
1.2 Complementary in Biology: How Things Fit Together.....	2
1.3 Fluorogenic Chemosensors.....	3
1.3.1 Fluorogenic Principles of Sensing.....	3
1.3.1.1 Photoinduced Electron Transfer (PET).....	3
1.3.1.2 Intramolecular Charged Transfer (ICT).....	5
1.3.1.3 Monomer-Excimer Formation.....	6
CHAPTER II AMINO ACID RECEPTORS CONTAINING ACRIDINE MOIETY	7
2.1 Introduction.....	7
2.1.1 Amino Acids: How Important in Biology.....	7
2.1.2 Amino Acids Recognition.....	8
2.1.3 Anion Recognition.....	9
2.1.4 Determination of Binding Constant.....	11
2.1.4.1 Determination of Binding Constant by NMR spectroscopy.....	11
2.1.4.2 Determination of Binding Constant by UV-vis and Fluorescence Spectroscopy.....	12
2.1.5 Literature Review of Amino Acid Receptors.....	13

	Page
2.1.6 Objectives and Scope of This Research.....	21
2.2 Experimental Section.....	22
2.2.1 General Procedure for Synthesis of Receptors Containing Acridine Moiety.....	22
2.2.1.1 Analytical Instruments.....	22
2.2.1.2 Materials for Synthesis.....	23
2.2.1.3 Synthesis of Acridine Derivatives.....	23
2.2.1.3.1 Preparation of <i>o</i> -Methoxyphenol (1).....	23
2.2.1.3.2 Preparation of 2-Methoxy-4-nitrophenol (2).....	24
2.2.1.3.3 Preparation of 2-Methoxy-1-(2-(2-(2-(2-(2-methoxy-4-nitrophenoxy) ethoxy)ethoxy)ethoxy)ethoxy)-4-nitrobenzene (3).....	25
2.2.1.3.4 Preparation of 3,6-[3-Methoxy-4-(2-(2-(2-(2-(3-methoxy-1-thiourea benzene)ethoxy)ethoxy) ethoxy)ethoxy)-1-thiourea benzene]acridine (L2)....	26
2.2.1.3.5 Preparation of 3,6-Dithiocyanate acridine.....	27
2.2.1.3.6 Preparation of 3,6-Bis(thiourea phenyl)acridine (L1).....	28
2.2.1.3.7 Preparation of 3,6-Bis(thiourea phenyl)acridinium ion (L1H).....	29
2.2.1.3.8 Preparation of 3,6-[3-Methoxy-4-(2-(2-(2-(2-(3-methoxy-1-thiourea benzene)ethoxy)ethoxy) ethoxy)ethoxy)-1-thiourea benzene]acridinium ion (L2H).....	30
2.2.2 Experimental Procedures in Complexation Studies.....	31
2.2.2.1 ¹ H-NMR Titration Studies for Complexes of Ligands L1 and L2 with Amino Acids.....	31
2.2.2.2 ¹ H-NMR Titration Studies for Complexes of Ligand L1H with Amino Acids.....	33
2.2.2.3 ¹ H-NMR Titration Studies for Complexes of Ligand L2H with Amino Acids.....	33
2.2.2.4 UV-vis Titration Studies for Complexes of Ligand L1 and L2 with Amino Acid.....	35
2.2.2.5 UV-vis Titration Studies for Complexes of Ligand L1H and L2H with Amino Acids.....	36

	Page
2.2.2.6 Fluorescence Titration Studies for Complexes of Ligand L1 and L2 with Amino Acids.....	37
2.2.2.7 Fluorescence Titration Studies for Complexes of Ligand L1H and L2H with Amino Acids.....	38
2.3 Results and Discussion.....	39
2.3.1 Synthesis and Characterization of Acridine Derivative Receptors.....	39
2.3.1.1 Synthesis and Characterization of 3,6-Bis(thiourea phenyl)acridine (L1)	39
2.3.1.2 Synthesis and Characterization of 3,6-[3-Methoxy-4-(2-(2-(2-(3-methoxy-1-thiourea benzene)ethoxy)ethoxy) ethoxy)ethoxy)-1-thiourea benzene] acridine (L2).....	40
2.3.1.3 Synthesis and Characterization of 3, 6-Bis(thiourea phenyl)acridinium ion (L1H) and 3,6-[3-methoxy-4-(2-(2-(2-(3-methoxy-1-thiourea benzene)ethoxy)ethoxy)ethoxy)ethoxy)-1-thiourea benzene]acridinium ion (L2H).....	43
2.3.2 The Complexation Studies of Ligand L1 and L2 with Amino Acids by ¹ H-NMR technique.....	44
2.3.3 The Complexation Studies by UV-vis Technique.....	51
2.3.3.1 The Complexation Studies of Ligands L1 and L2 with Amino Acids by UV-vis Technique.....	51
2.3.3.2 The Complexation Studies of Ligands L1H and L2H with Amino Acids by UV-vis Technique.....	54
2.3.4 The Complexation Studies of Ligands L1H and L2H with Amino Acids by ¹ H-NMR Titration Technique.....	58
2.3.5 The Complexation Studies of Ligands L1 , L2 , L1H and L2H with Amino Acids by Fluorescence Technique.....	63
CHAPTER III STEROIDAL RECEPTORS FOR AMINO ACIDS.....	71
3.1 Introduction.....	71
3.1.1 Steroids in Supramolecular Chemistry.....	71
3.1.2 Steroid-Based Anion and Amino Acid Receptors.....	72
3.1.3 Literature Review for Steroidal receptors for amino acids.....	74

	Page
3.1.4 Objectives and Scope of this research.....	77
3.2 Experimental Section.....	78
3.2.1 Synthesis of Steroidal Receptor.....	78
3.2.1.1 Preparation of Methyl 3 α -acetoxy-7 α , 12 α -dihydroxy-5 β -cholan-24-oate (1.2).....	78
3.2.1.2 Preparation of Methyl 3 α -acetoxy-7 α , 12 α -dioxo-5 β -cholan-24-oate (1.3).....	79
3.2.1.3 Preparation of Methyl 3 α -acetoxy-7 α , 12 α -dioximino-5 β -cholan-24-oate (1.4).....	79
3.2.1.4 Preparation of Methyl 3 α -acetoxy-7 α , 12 α -di[N-(t-butyloxycarbonyl)amino]-5 β -cholan-24-oate (1.5).....	80
3.2.1.5 Preparation of Methyl 3 α -hydroxy-7 α , 12 α -di[N-(t-butyloxycarbonyl)amino]-5 β -cholan-24-oate (1.6).....	81
3.2.1.6 Preparation of Methyl 3 α -azido-7 α , 12 α -di[N-(t-butyloxycarbonyl)amino]-5 β -cholan-24-oate (1.7).....	82
3.2.1.7 Preparation of Methyl 3 α -azido-7 α , 12 α -bis-amino-5 β -cholan-24-oate (1.8).....	83
3.2.1.8 Preparation of Methyl 3 α -azido-7 α , 12 α -bis-[(phenylaminocarbonyl)amino]-5 β -cholan-24-oate (1.9).....	84
3.2.1.9 Preparation of Methyl 3 α -amino-7 α , 12 α -bis-[(phenylaminocarbonyl)amino]-5 β -cholan-24-oate (1.10).....	85
3.2.1.10 Preparation of 4-Isocyanato-4'-nitroazobenzene (1.11).....	86
3.2.1.11 Preparation of Methyl 3 α -[(4-nitroazobenzene-4'-aminocarbonyl)amino]-7 α ,12 α -bis-[(phenylamino carbonyl)amino]-5 β -cholan-24-oate (L3)...	86
3.2.2 Experimental procedures in complexation studies.....	88
3.2.2.1 ¹ H-NMR Titration Studies for Complexes of Ligand L3 with Amino Acids.....	88
3.2.2.2 UV-vis Titration Studies for Complexes of Ligand L3 with Amino Acids.....	89
3.3 Results and Discussion.....	90

	Page
3.3.1 Design Concept.....	90
3.3.2 Synthesis and Characterization of Steroidal Receptor L3	91
3.3.2.1 Synthesis and Characterization of Methyl 3 α -acetoxy-7 α , 12 α -dihydroxy-5 β -cholan-24-oate (1.2).....	91
3.3.2.2 Synthesis and Characterization of Methyl 3 α -acetoxy-7 α , 12 α -dioxo-5 β -cholan-24-oate (1.3).....	91
3.3.2.3 Synthesis and Characterization of Methyl 3 α -acetoxy-7 α , 12 α -dioximino-5 β -cholan-24-oate (1.4).....	92
3.3.2.4 Synthesis and Characterization of Methyl 3 α -acetoxy-7 α , 12 α -di[N-(t-butylloxycarbonyl) amino]-5 β -cholan-24-oate (1.5).....	92
3.3.2.5 Synthesis and Characterization of Methyl 3 α -hydroxy-7 α , 12 α -di[N-(t-butylloxycarbonyl) amino]-5 β -cholan-24-oate (1.6).....	93
3.3.2.6 Synthesis and Characterization of Methyl 3 α -azido-7 α , 12 α -di[N-(t-butylloxycarbonyl) amino]-5 β -cholan-24-oate (1.7).....	93
3.3.2.7 Synthesis and Characterization of Methyl 3 α -azido-7 α , 12 α -bis-amino-5 β -cholan-24-oate (1.8).....	94
3.3.2.8 Synthesis and Characterization of Methyl 3 α -azido-7 α , 12 α -bis-[(phenyl aminocarbonyl) amino]-5 β -cholan-24-oate (1.9).....	94
3.3.2.9 Synthesis and Characterization of Methyl 3 α -amino-7 α , 12 α -bis-[(phenyl aminocarbonyl) amino]-5 β -cholan-24-oate (1.10).....	95
3.3.2.10 Synthesis and Characterization of 4-Isocyanato-4'-nitroazobenzene (1.11).....	95
3.3.2.11 Synthesis and Characterization of Methyl 3 α -[(4-nitroazobenzene-4'-aminocarbonyl) amino]-7 α , 12 α -bis-[(phenylamino carbonyl) amino]-5 β -cholan-24-oate (L3).....	96
3.3.3 The Complexation Studies with Amino Acids.....	98
3.3.3.1 The Complexation Studies of Ligand L3 with Amino Acids by Using ¹ H-NMR Technique.....	98
3.3.3.2 The Complexation Studies of L3 with Amino Acids by UV-vis Technique.....	110

	Page
CHAPTER IV CONCLUSION.....	114
4.1 Conclusion.....	114
4.2 Suggestion for Future Work.....	117
REFERENCES.....	118
APPENDICES.....	127
VITA.....	161



ศูนย์วิทยทรัพยากร
จุฬาลงกรณ์มหาวิทยาลัย

LIST OF TABLES

Table	Page
2.1 Amounts of amino acids that used in complexation studies with ligand L1 and L2 for NMR titration studies.....	31
2.2 Amounts of solutions of amino acids used to prepare various amino acids: L1 ratios for NMR titration studies.....	32
2.3 Amounts of amino acids that used in complexation studies with ligand L1H for NMR titration studies.....	33
2.4 Amounts of amino acids that used in complexation studies with ligand L2H for NMR titration studies.....	34
2.5 Amounts of solutions of amino acids used to prepare various amino acids: L2H ratios for NMR titration studies.....	34
2.6 Amounts of amino acids that used in complexation studies with ligand L1 and L2 for UV-vis titration studies.....	35
2.7 Amounts of amino acids that used in complexation studies with ligand L1H and L2H for UV-vis titration studies.....	36
2.8 Amounts of amino acids that used in complexation studies with ligand L1 and L2 for fluorescence titration studies.....	37
2.9 Amounts of amino acids that used in complexation studies with ligand L1H and L2H for fluorescence titrations studies.....	38
2.10 The basicity of various amino acids.....	58
2.11 The binding constants of interaction between L1 , L1H , L2 and L2H with amino acids calculated from fluorescence titration using Benesi-Hildebrand equation.....	69
2.12 Fluorescence enhancement factors (FE) of receptors L1 , L1H , L2 and L2H with various guests.....	69
3.1 Amounts of amino acids that used in complexation studies with ligand L3 for NMR titration studies.....	88
3.2 Amounts of amino acids that used in complexation studies with ligand L3 for UV-vis titration studies.....	90

Table	Page
3.3 Chemical shifts (ppm) of ligand L3 and their changes at complexation with various amino acids.....	99
3.4 Binding constants (K) of ligand L3 complexes with varioud amino acids using the EQNMR program.....	110
3.5 Summary of the binding constants (log K) of ligand L3 for various amino acids using the SPECFIT32 program.....	112



ศูนย์วิทยทรัพยากร
จุฬาลงกรณ์มหาวิทยาลัย

LIST OF FIGURES

Figure	Page
1.1	The molecular recognition of guest inside active pore..... 1
1.2	The lock and key principle: receptor sites in the host (lock) are complementary to the guest (key)..... 2
1.3	PET process with the participation of the HOMO and LUMO of the fluorophore and an external molecular orbital..... 4
1.4	PET process with the participation of the HOMO and LUMO of the fluorophore and an empty external molecular orbital..... 5
1.5	Schematic diagram of spectral displacement of ADD resulting from interaction of anion with an electron donating group in receptor..... 6
2.1	Structures of acridine derivatives containing thiourea (L1 , L2 , L1H and 2H) 22
2.2	The synthetic pathway of final product L1 39
2.3	The synthetic pathway of final product L2 42
2.4	The synthetic pathway of final products L1H and L2H 44
2.5	The structures of all zwitterionic amino acids in this experiment..... 45
2.6	¹ H-NMR (400 MHz) of L1 in DMSO- <i>d</i> ₆ upon addition of excess amount of (1) Trp, (2) Phe, (3) Leu, (4) Ala, and (5) Gly..... 46
2.7	¹ H-NMR (400 MHz) of L2 in DMSO- <i>d</i> ₆ upon addition of excess amount of (1) Trp, (2) Phe, (3) Leu, (4) Ala, and (5) Gly..... 46
2.8	¹ H-H ROESY of L1 ·Trp complex..... 47
2.9	¹ H-H NOESY of L2 ·Trp complex..... 48
2.10	The proposed structure of (a) L1 ·Trp and (b) L2 ·Trp complexes, consistent with the cross relationship from ROESY and NOESY and the signal of both receptors and Trp..... 49
2.11	Job's plots of the complexation of (a) L2 ·Phe, (b) L2 ·Trp, (c) L1 ·Phe and (d) L1 ·Trp on the chemical shift of NH thiourea..... 50
2.12	The mass spectrum of L2 ·Trp complex..... 51
2.13	The UV-vis absorption spectra of (a) ligand L1 (3×10 ⁻⁵ M) and (b) ligand L2 (2.5×10 ⁻⁵ M)..... 52
2.14	Absorption spectra of ligand L1 upon addition of Phe 50 equiv..... 53

Figure	Page
2.15	Absorption spectra of ligand L2 upon addition of Phe 40 equiv..... 53
2.16	The UV-vis absorption spectra of (a) ligand L1H (2.5×10^{-5} M) and (b) ligand L2H (2.0×10^{-5} M)..... 55
2.17	Absorption spectra of ligand L1H upon addition of Phe 30 equiv..... 56
2.18	Absorption spectra of ligand L2H upon addition of Phe 30 equiv..... 56
2.19	Plot of absorbance of (a) L1H (2.5×10^{-5} M) and (b) L2H (2.0×10^{-5} M) at 460 nm in DMSO as a function of equivalent of amino acids addition..... 57
2.20	$^1\text{H-NMR}$ titration spectra of L1H (3.0×10^{-3} M) in $\text{DMSO-}d_6$ upon addition of Trp 1.0, 2.0 and 4.0 equivalent, in comparison with $^1\text{H-NMR}$ spectra of L1 (3.0×10^{-3} M)..... 59
2.21	$^1\text{H-NMR}$ titration spectra of L2H (3.0×10^{-3} M) in $\text{DMSO-}d_6$ upon addition of Trp 0.5, 1.0, 2.0 and 4.0 equivalent, in comparison with $^1\text{H-NMR}$ spectra of L2 (3.0×10^{-3} M)..... 59
2.22	$^1\text{H-NMR}$ titration spectra of L1H (3.0×10^{-3} M) in $\text{DMSO-}d_6$ upon addition of Phe 0.4, 1.0, 1.4, 1.8, 2.0, 3.0 and 4.0 equivalent..... 61
2.23	$^1\text{H-NMR}$ titration spectra of L2H (3.0×10^{-3} M) in $\text{DMSO-}d_6$ upon addition of Phe 0.6, 1.0, 2.0, 2.5, 3.0, 4.0 and 5.0 equivalent..... 62
2.24	The emission spectra of L1 (2.0×10^{-4} M) upon adding Trp 30 equivalent..... 64
2.25	The emission spectra of L1 (2.0×10^{-4} M) upon adding Phe 30 equivalent..... 64
2.26	The emission spectra of L2 (2.0×10^{-4} M) upon adding Trp 30 equivalent..... 65
2.27	The emission spectra of L2 (2.0×10^{-4} M) upon adding Phe 30 equivalent..... 65
2.28	The emission spectra of L1H (2.0×10^{-4} M) upon adding Trp 25 equivalent... 66
2.29	The emission spectra of L1H (2.0×10^{-4} M) upon adding Phe 25 equivalent... 67
2.30	The emission spectra of L2H (2.0×10^{-4} M) upon adding Trp 30 equivalent... 67
2.31	The emission spectra of L2H (2.0×10^{-4} M) upon adding Phe 30 equivalent... 68
3.1	Structure of Cholapod with Multiple NH Units..... 73
3.2	Structure of the Steroidal Receptor L3 77

Figure	Page	
3.3	Reagents and conditions: (a) p-TsOH, MeOAc, reflux; (b) Ca(ClO) ₂ , HOAc; (c) NH ₂ OH .HCl, NaOAc, reflux; (d) H ₂ (1 atm), PtO ₂ , HOAc; Zn, HOAc; (Boc) ₂ O, NaHCO ₃ aq., THF; (e) NaOMe, MeOH; (f) Ph ₃ P, DEAD, MeSO ₃ H, DMAP, THF; NaN ₃ , DMF, 47°C; (g) TFA, DCM; (h) PhNCO, Et ₃ N, DMAP, THF, 50°C; (i) activated zinc, HOAc; (j) 4-Isocyanato-4'-nitroazobenzene 1.11, DMAP, THF.....	97
3.4	Partial ¹ H-NMR spectra of L3 and L3 complexes with various amino acid...	100
3.5	Partial ¹ H-NMR titration spectra of L3 (4.0x10 ⁻³ M) upon adding L-Trp 4.0 equivalent in DMSO-d ₆	101
3.6	Partial ¹ H-NMR titration spectra of L3 (4.0x10 ⁻³ M) upon adding D-Trp 4.0 equivalent in DMSO-d ₆	102
3.7	Job's plots of NH _b in (a) L3'L-Trp, (b) L3'L-Phe, (c) L3'L-Leu, (d) L3'L-Ala and (e) L3'Gly complexes.....	104
3.8	¹ H-H NOESY NMR of L3'D-Trp complex.....	105
3.9	¹ H-H COSY NMR of L3'D-Trp complex.....	106
3.10	¹ H-H COSY NMR of L3'L-Trp complex.....	107
3.11	Structures of (a) L3'D-Trp and (b) L3'L-Trp complexes derived from computer-based molecular modeling. Intramolecular and intermolecular hydrogen bonds are shown as broken lines.....	109
3.12	The UV-vis absorption spectra of ligand L3 (2.0x10 ⁻⁵ M).....	111
3.12	UV-vis titration spectra of L3 (2x10 ⁻⁵ M) upon adding L-Trp 40 eq.....	113
3.13	UV-vis titration spectra of L3 (2x10 ⁻⁵ M) upon adding D-Trp 300 eq.....	113

LIST OF ABBREVIATIONS

A	Absorbance of the solution at a given wavelength
Å	Angstrom
A ₀	Absorbance of free ligand
Ac	Acetyl
ADD	Acridinedione Fluorophore
Ala	Alanine
Arg	Arginine
bs	Broad Singlet
^t Bu	Tert-butyl
°C	Degree Celcius
Cad.2HCl	Cadaverine Dihydrochloride
CDCl ₃	Deuterated Chloroform
(CD ₃) ₂ CO	Deuterated Acetone
CEAA	Luminescent Crown Ether Amino Acid
cm ⁻¹	Wave Number
cm	centimeter
¹³ C-NMR	Carbon-13 Nuclear Magnetic Resonance
COSY	Correlation Spectroscopy
Cyc	Diaminocyclohexane
d	Doublet
DCM	Dichloromethane
DEAD	Diethyl Azodicarboxylate Solution
dd	Doublet of doublet
DMAP	4-(Dimethylamino)pyridine
DMF	Dimethylformamide
DMSO	Dimethylsulfoxide
DMSO- <i>d</i> ₆	Deuterated Dimethylsulfoxide
equiv	Equivalent
ESI	Electro Spray Ionization
EtOAc	Ethyl acetate

FE	Fluorescence Enhancement Factor
g	Gram
[G]	Guest Concentration
GABA.HCl	γ -Aminobutyric Acid
Gly	Glycine
[HG]	Complex Concentration
His	Histidine
$^1\text{H-NMR}$	Proton-1 Nuclear Magnetic Resonance
HOMO	Highest Occupied Molecular Orbital
ICT	Intermolecular Charged Transfer
J	Coupling Constant
K_a	Association Constant
K_{assoc}	Association Constant
Kg	Kilogram
K_s	Stability Constant
[L]	Ligand Concentration
Leu	Leucine
LUMO	Lowest Unoccupied Molecular Orbital
Lys	Lysine
Lys-OMe.2HCl	L-Lysine Methyl Ester Dihydrochloride
m	Multiplet
[M]	Metal Concentration
MeCN	Acetonitrile
MeOH	Methanol
MHz	Megahertz
min	Minute
mL	Milliliter
[ML]	Complex Concentration
mm	Millimeter
MS	Mass Spectroscopy
m/z	Mass per Charge Ratio

nm	Nanometer
NMR	Nuclear Magnetic Resonance
NOESY	Nuclear Overhauser Enhancement Spectroscopy
OAc	Acetate
Orn	Ornithine
PET	Photoinduced Electron Transfer
Ph	Phenyl
Phe	Phenylalanine
ppm	Part per Million
Pro	Proline
ROESY	Rotational Nuclear Overhauser Effect Spectroscopy
r.t.	Room Temperature
s	Singlet
sec	Second
Spd.3HCl	Spermidine Trihydrochloride
t	Triplet
THF	Tetrahydrofuran
TLC	Thin Layer Chromatography
Trp	Tryptophan
UV-vis	Ultraviolet-visible
Val	Valine
β_i	Association Constant
$\Delta\delta$	Changes in Chemical Shift
ϵ -Ahx	6-Aminohexanoic Acid
δ	Chemical Shift

CHAPTER I

SUPRAMOLECULAR CHEMISTRY AND FLUOROGENIC CHEMOSENSORS

The field of *supramolecular chemistry* has been defined as “chemistry beyond the molecule” and involves investigating new molecular systems in which the most important feature is that the components are held together reversibly by *intermolecular forces of non-covalent bonds*. There are a number of such interactions that can be utilized.[1] They include:

- (a) electrostatics (ion-ion, ion-dipole and dipole-dipole);
- (b) hydrogen bonding;
- (c) π - π stacking interactions;
- (d) van der Waals forces;
- (e) hydrophobic or hydrophilic effects.

1.1 Molecular Recognition

Supramolecular chemistry[2] based on molecular recognition has added a new dimension to chemistry. Given any substrates (neutral molecules, cations or anions), an appropriate receptor, possessing structural features suitable for substrate recognition, can be designed. This concept is illustrated in Figure 1.1.

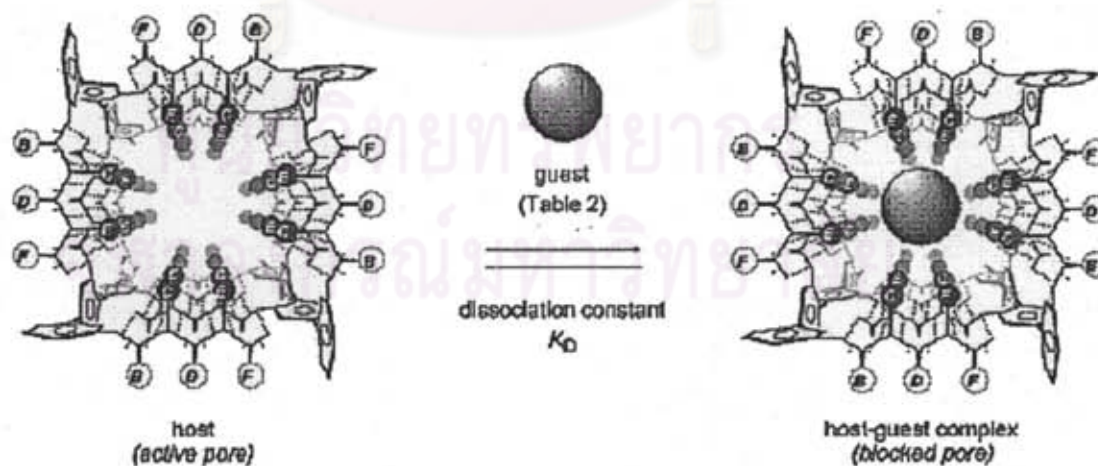


Figure 1.1 The molecular recognition of guest inside active pore.

Synthetic receptors have been the challenge of designing and building molecules having shapes and dimensions suitable for hosting any kind of substrates and ability of establishing with substrate interactions of a sufficient energy. Binding interactions gave several applications in chemical and biochemical processes.[3]

1.2 Complementarity in Biology: How Things Fit Together

One of the most important concepts is *complementarity*. The enzyme may catalyze a single reaction with high or total specificity; the active site of the enzyme being complementary to the substrate. In other words, the size, shape and position of the binding sites within the active site are ideal for specific substrate recognition. Emil Fischer described this idea in 1894 as the '*Lock and Key*' principle. Figure 1.2 shows a stylized representation of the lock and key. The arrangement of binding sites in the host (lock) is complementary to the guest (key) with both sterically and electronically.[1]

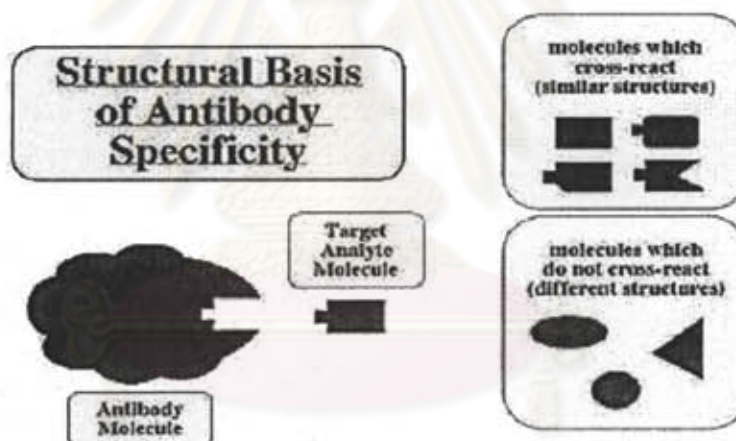


Figure 1.2 The lock and key principle: receptor sites in the host (lock) are complementary to the guest (key).

An example of the lock and key principle in Nature is provided by carboxypeptidase-A, an enzyme that selectively catalyzes the hydrolysis of the C-terminal amino acid residues of proteins. It is the zinc ion at the enzyme active site that catalyzes the removal of an amino acid residue from the carbon end of the polypeptide chain.

1.3 Fluorogenic Chemosensors

1.3.1 Fluorogenic Principles of Sensing[4]

Luminescence can be defined as a spontaneous emission of radiation from an excited state. Depending on the mode of excitation, the terms chemoluminescence, electroluminescence, radioluminescence, etc. are used. The luminescence phenomenon can be classified as fluorescence when the excited molecule results in a new molecule with the same multiplicity and as phosphorescence when it involves luminescence with a change in spin multiplicity. An observing in a fluorescence molecule is that absorption of light at a given wavelength results in an almost instantaneous emission of light at a longer wavelength.

In relation to the use of fluorescence for sensing or detecting, the principal advantage over other light-based methods such as absorbance is its high sensibility. This is so because the emission fluorescence signal is proportional to the substance concentration. In absorbance measurements, the substance concentration is proportional to the absorbance which is related to the ratio between intensities measured before and after the beam passes through the sample. Therefore, in fluorescence, an increase of the intensity of the incident beam results in a larger fluorescence signal whereas this is not so for absorbance. Fluorescence techniques can measure concentration even one million times smaller than absorbance techniques. It is interesting to understand the basis of the nature of the photoinduced processes that are responsible for the photophysical changes upon anion coordination. These effects are specifically related with the use of the binding site-signaling subunit approach.

1.3.1.1 Photoinduced Electron Transfer (PET)[4]

This photoinduced process has been extensively studied and widely used for sensing purposes of cation and anions. As described above, fluorescence in a molecule is observed when an excited electron, for instance in the lowest unoccupied molecular orbital (LUMO), goes to the highest occupied molecular orbital (HOMO), releasing the

excess of energy as light. Over this scheme, it might happen that an orbital from another part of the molecule or from another molecular entity could have energy between that of the HOMO and that of the LUMO of the fluorophore. When this “alien” orbital is full (having a donor group), a PET from this full orbital to the HOMO of the fluorophore can take place. A further electron transfer from the LUMO of the fluorophore to the external orbital retrieves the stable ground state. Following this sequence, fluorescence quenching occurs because the transition from the excited to the ground state takes place following a nonradiative path (see Figure 1.3). What is macroscopically observed is a decrease of the emission intensity or no fluorescence at all. A similar process can take place when there is an empty orbital from another part of the molecule or from another molecular entity between both the HOMO and the LUMO of the fluorophore. In this case, a PET from the excited LUMO to the empty orbital can occur, followed by a further electron transfer from this orbital to the HOMO of the fluorophore. Again, relaxation occurs without radiation and fluorescence quenching is observed (see Figure 1.4).

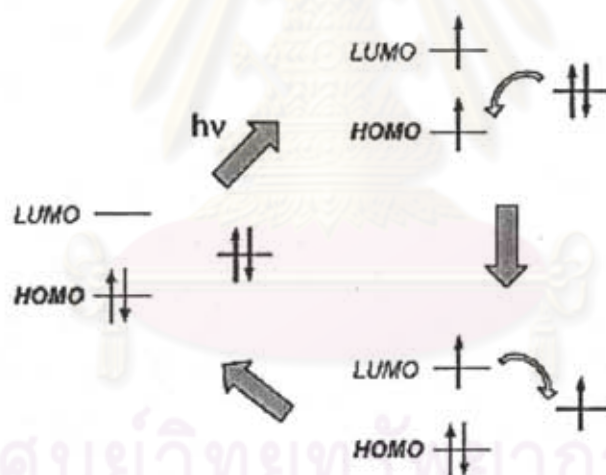


Figure 1.3 PET process with the participation of the HOMO and LUMO of the fluorophore and an external molecular orbital.[4]

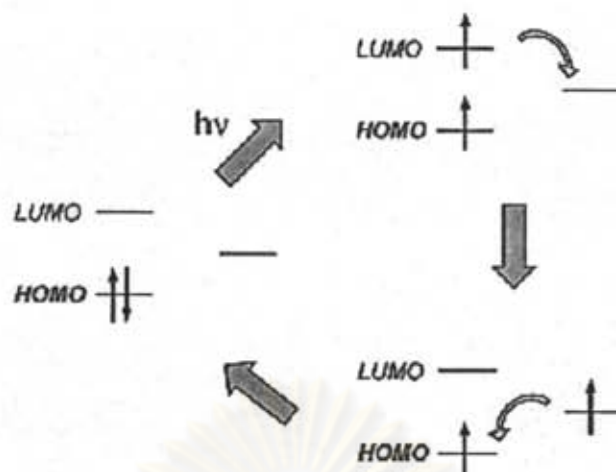


Figure 1.4 PET process with the participation of the HOMO and LUMO of the fluorophore and an empty external molecular orbital.[4]

1.3.1.2 Intramolecular Charged Transfer (ICT)[4]

This phenomenon can be occurred when a fluorophore contains and electron-donating group conjugated to an electron-withdrawing group. It undergoes intramolecular charge transfer from the donor to the acceptor upon excitation by light. The consequent change in dipole moment results in a Stokes shift that depends on the microenvironment of the fluorophore. Notably, the polarity probes have been designed on this basis. It was found from the literature that very few ICT-based fluorescent sensors for anions have been reported due to the weaker binding forces of these guests, which could entail only weak spectroscopic effects upon complexation.[5, 6] ICT fluorescent anion receptor relies on the choice of a spacer that links the ICT fluorophore and the anion-binding or anion-recognition site to allow for a highly efficient communication of the anion-recognizing messages to the fluorophore. As with the ICT fluorophore, the photophysics and emission of the charge transfer state are subjected to the electron donor/acceptor strength, and the anion-binding site is assumed to be better incorporated in either the electron donor or acceptor moiety. This will change the photophysical properties of fluorophore because the complexed anion affects the efficiency of ICT. An example of this phenomenon showed that anion hydrogen bonding with the donor moiety caused

increasing the electron-donating character of the donor group as shown in Figure 1.5. This increase in charge density results in the red shift of absorption and emission together with an increase in the fluorescence intensity.[7]

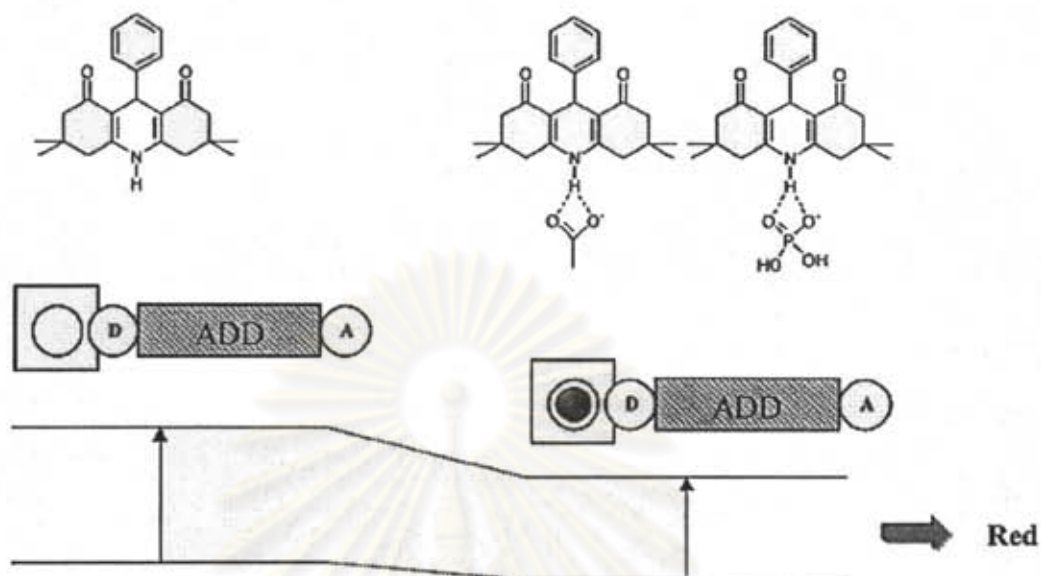


Figure 1.5 Schematic diagram of spectral displacement of ADD resulting from interaction of anion with an electron donating group in receptor.[7]

1.3.1.3 Monomer-Excimer Formation[4]

A phenomenon that can be observed when using fluorophores is the formation of excimers. An excimer can be defined as a complex formed by interaction of a fluorophore in the excited state with a fluorophore of the same structure in the ground state.[8] An important aspect is that the emission spectrum of the excimer is red-shifted with respect to that of the monomer, and in many cases, the dual emission of the monomer and the excimer is observed. Therefore, excimer formation or excimer rupture upon anion addition results in anion sensing by simple monitoring of the emission excimer band. In general, it is assumed that flat highly π -delocalized systems such as pyrene and anthracene show greater tendency to form excimers. An additional requirement for excimer formation is that two monomers need to be in close proximity in order to give stacking interactions and the molecular excimer state.

CHAPTER II

AMINO ACID RECEPTORS CONTAINING ACRIDINE MOIETY

2.1 Introduction

2.1.1 Amino Acids: How Important in Biology[9]

The primary function of amino acids is to provide the precursors for protein synthesis. In addition, amino acids serve as precursors of other important nitrogenous compounds such as biologically active amines (e.g., epinephrine, dopamine, etc.), purine and pyrimidine nucleotides, small peptide hormones, glutathione, carnitine, and many others. Finally, amino acids can be oxidized to provide metabolic energy.

The amount of free amino acids in the human body, both extracellular and intracellular, is relatively small (about 40 g in a 70-kg man). This pool of free amino acids is not a mixable whole-body pool, since amino acids do not pass freely through cell membranes. The major flux of amino acids into and out of this pool occurs by **protein turnover**. Intracellular enzymes are constantly being synthesized and degraded. As a rule, inducible enzymes, such as δ -amino levulinate synthetase, have short half-lives on the order of hours or minutes. In contrast, structural proteins, such as muscle proteins, have much longer half-lives on the order of months.

The healthy human adult usually exhibits **nitrogen balance**, which is defined as a steady state in which nitrogen ingestion is balanced by nitrogen loss. The minimum daily protein requirement for a 70-kg man has been determined to be about 20 g, equaling the obligatory amino acid losses. This value is obtained under special experimental conditions and is probably not compatible with health under normal life conditions. No mechanism exists for storing excess amino acids. The amino acids derived from excess dietary proteins are metabolized, and the nitrogen is excreted in the form of urea.

Several amino acid **transport systems** are known in humans. Each system is responsible for a class of structurally similar amino acids. For example, there is a system for **acidic** amino acids (aspartate, asparagine, glutamate and glutamine), a system for **basic** amino acids (arginine, lysine and histidine), a **proline-glycine** system, and several systems for **neutral amino acids** (glycine, alanine, valine, leucine, isoleucine, proline, phenylalanine, tyrosine, tryptophan, serine, threonine, cysteine and methionine). A limited extent amino acids can also be absorbed in the form of short peptides. Many of the amino acid transport systems are coupled with sodium transport. The amino acid crosses the cell membrane accompanied by a sodium ion, which is subsequently pumped back out of the cell by the Na^+/K^+ pump.

2.1.2 Amino Acids Recognition

Amino acids and their derivatives are among the most important molecules in natural living systems. They are chiral molecules and have both the active groups of an amine and carboxylic acid acting as acid and base (though their natural pH is usually influenced by the side chain group). In aqueous media, the amine group gains a positive charge and the acid group a negative charge known as a zwitterion. Molecular recognition of amino acids and their derivatives has been one of most attractive objects of host-guest chemistry. It is partly due to their potential characteristics which make amino acids suitable for guest molecules in artificial recognition systems. One of these characteristics of amino acids is their versatile ability to form complexes with other molecules via various types of interaction modes which cover almost all kinds of intermolecular interactions ever found in the chemistry of molecular recognition.[10-19]

Amino and carboxyl groups in amino acids are expected to act as binding sites for hydrogen bonding and electrostatic interactions such as Coulombic and dipole-dipole interactions. Residual groups on the α -carbon can also form additional recognition sites, where not only electrostatic interactions but also other types of interactions such as van der Waals or hydrophobic interactions and/or even steric repulsion may operate according to the chemical and physical properties of the residual groups. Supramolecular chemistry has allowed the development of probes for amino acids. In order to recognize

the zwitterionic form of an amino acid effectively, binding of the ammonium and the carboxylate groups is required. Amino acids exist largely as strongly solvated zwitterionic structures in neutral aqueous solutions. The electronic densities at the carboxylate and ammonium functions are greatly affected by their mutual vicinity, causing the binding forces of complementary groups of the receptor to be less effective for the complexation.[20]

Thus, the design of a model receptor for amino acids in zwitterionic form is still a challenging problem, and most works have been performed with single-charged substrates, under acidic (amino acid or amino ester salts) or basic (carboxylate salts) conditions. Most receptors reported in the literature have been achieved for binding with amino acids undergone various interactions; hydrogen bonding, metal-ligand interaction, electrostatic interaction.[21-23]

2.1.3 Anion Recognition

Anion recognition via artificial receptors is of current interest in supramolecular chemistry because of their importance in biological and environmental assays. Anions play a central role in physiology and in healthcare. They are prevalent in both heavy industry and in farming, and as such in the environment. They are often harmful pollutants, for example, phosphates from fertilizers. Many anions are also used as the products of the degradation (hydrolysis) of chemical warfare agents such as fluoride which is the breakage product of the sarin gas and organophosphates found in many nerve agents[24] or cyanide which is extremely toxic to mammals, leading to vomiting, convulsions, loss of consciousness, and eventual death.[25]

Anion recognition chemistry actually grew from its beginnings in the same period as cation and neutral molecule recognition. Non-covalent interactions used in anion-host binding can be actually categorized into 4 types; hydrogen-bonding, electrostatic interactions, metal or Lewis acid center or hydrophobic effects.[26] In the case of receptors containing one or more urea subunits, the selectivity is related to the energy of the receptor-anion interaction; in this sense, strong hydrogen bond interactions are established with anions containing the most electronegative atom: F (fluoride) and O

(carboxylates, inorganic oxoanions). According to this view, all hydrogen bonds can be considered as incipient proton-transfer reactions, and for strong hydrogen bonds, this reaction can be in a very advanced state.[27] Thus, for a given-NH-containing receptor (the acid), the selectivity should be mainly related to the basicity of the anion; the higher anion basicity, the stronger the hydrogen-bonding interaction.

In comparison to cation and neutral molecule coordination chemistry, design and synthesis of anion receptors are recent development due to a number of reasons. Firstly, the ordinary interaction is electrostatic forces. Most anion sizes are greater than isoelectronic cations, thus their charge to radius ratios are lower. This means that electrostatic binding interaction is less effective in the case of larger anions. Secondly, some anions such as carboxylates, phosphates and sulphates exist in narrow pH window. Thus, the stability and the basicity of anions should be considered for a well-match between hosts and anions. Finally, there are wide varieties of geometry and coordination number. Therefore, a higher degree of design may be required to construct receptors complementary to their anionic guests. A well-designed host molecule would gain both high selective and great sensitive binding.

The chemistry of anion coordination has some special features that need to be considered. Thus, when making the choice of a receptor for a certain anion, the shape, geometry of the anion and its charge, which can be varied as a function of the pH; and its hydrophobicity should be taken into account.[2] In general, it can be said that abiotic receptors for anions use similar type of interactions as biological receptors. Those can be classified basically in electrostatic interactions, formation of hydrogen bonds, and interactions with metal centers.

Electrostatic interactions with anions are found when using positively charged receptors having for instance guanidinium[28-31] groups or quaternary ammoniums.[32, 33] These two groups have a positive charge that basically does not depend on the pH of the medium. Amines can also give electrostatic interactions with anions as they are usually protonated and exist in the charged form at neutral and acidic aqueous solutions.[34-36]

Hydrogen bonding groups have been widely used in binding sites for anion recognition. Poly amines and guanidinium groups can form hydrogen bonds with anions.

Other hydrogen bonding sites typically used in chromogenic or fluorogenic chemosensors are ureas[37], thioureas[38, 39], calix[4]pyrroles[40-42], porphyrins[43, 44] and amides.[45, 46]

Metal complexes have also been used as anion binding sites. Metal complexes can bind anions forming stronger bonds than those generally observed using electrostatic or hydrogen-bonding interactions.[47, 48]

2.1.4 Determination of Binding Constants

In the viewpoint of molecular recognition systems, the weak chemical interaction is amplified, integrated and converted to physical signal that can readily read out and record. These data are related to complexation process. There are several methodologies to determine the binding constant such as NMR spectroscopy, UV-vis spectroscopy, fluorescence and electrochemical techniques depending on the molecular design.

2.1.4.1 Determination of Binding Constants by NMR spectroscopy[49, 50]

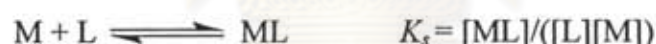
¹H-NMR titration is one of the most useful techniques which is available to chemists for the investigation of dynamic molecular processes. Appeared NMR spectra are basically treated to display a qualitative description of reversible dynamic processes. This topic is often introduced with a discussion of simple two-site exchange systems; slow and fast exchange. It is stated that the spectrum consists of two signals under “*slow-exchange*” conditions. The binding constant can be evaluated by ratio of integration of the NMR signals for free and bound hosts. The bound and free molecules give rise to discrete NMR signals that can be integrated to determine [G] and [HG] directly and association constant (β_i) finally. There is just one signal at the population-averages chemical shift under “*fast-exchange*” conditions. Most of the host-guest equilibria are fast on the NMR time scale. Basically, the association constant of either slow or fast exchange process is represented by the following equation.

$$\beta_i = [HG]/[H][G]^i$$

In a typical fast exchange NMR titration experiment, a small aliquot of a guest may be added to a known concentration solution of a host in a deuterated solvent and the NMR spectrum is monitored as a function of the guest concentration or a host to guest ratio. Commonly, changes in chemical shift ($\Delta\delta$) are noted for various atomic nuclei attributed to the influence of guest binding on their magnetic environments. As a result, two kinds of information are gained. Firstly, the location of nuclei most affected may give qualitative information about the selectivity of guest binding. More importantly, the shape of the titration curve plot of chemical induced shift against added guest concentration gives quantitative information about the binding constant. Such titration curves are often analyzed by modern curve fitting procedure; for instance, EQNMR.

2.1.4.2 Determination of the Stability Constants by UV-vis and Fluorescence Spectroscopy[51]

The stability constant K_s which controls the equilibrium between the free ligand L and the complex ML with the metal may be obtained from the variation of either absorbance or fluorescence intensity at proper observation wavelengths.



It is easy to derive the following relation involving the absorbance A_0 of the free ligand and the absorbance A of the solution at a given wavelength

$$\frac{A_0}{A_0 - A} = \frac{\epsilon_L}{\epsilon_L - \epsilon_{ML}} \left(\frac{1}{K_s[M]} + 1 \right)$$

where ϵ_L and ϵ_{ML} are the molar extinction coefficients of the ligand and the complex, respectively. The quantity $A_0/(A_0 - A)$ is plotted versus $[M]^{-1}$, and the stability constant is then given by the ratio of intercept/slope.

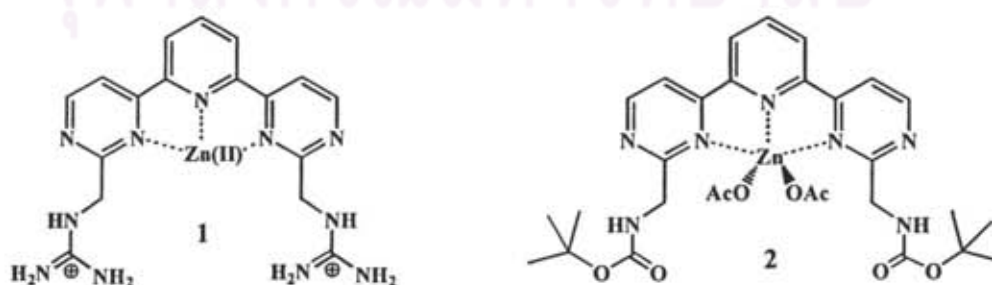
The various methods for determining the stability constants from fluorimetric data were previously discussed.[52] The best of them uses the relation

$$\frac{I_F^0}{I_F^0 - I_F} = \frac{\epsilon_L \Phi_L}{\epsilon_L \Phi_L - \epsilon_{ML} \Phi_{ML}} \left(\frac{1}{K_s[M]} + 1 \right)$$

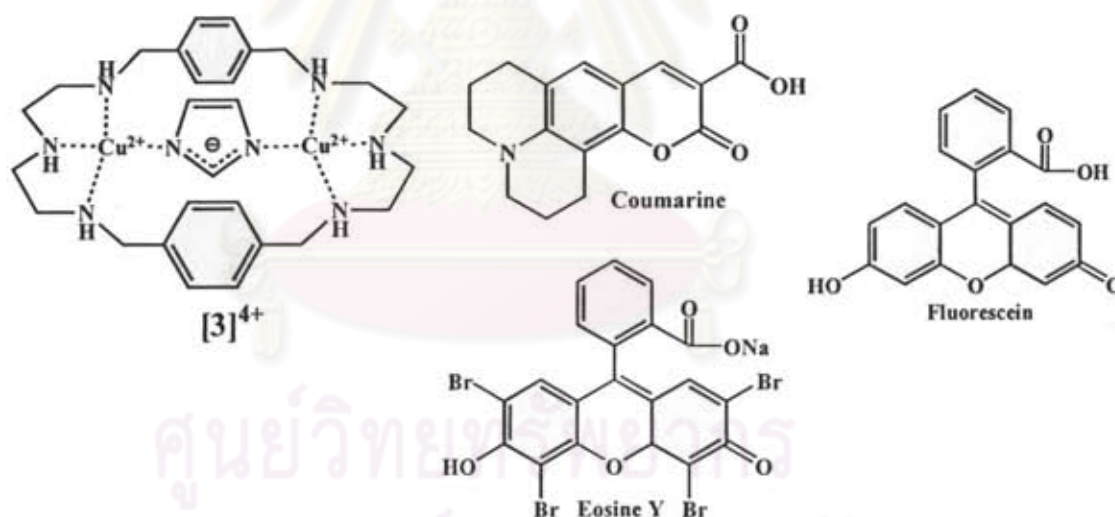
where Φ_L and Φ_{ML} are the quantum yields of the ligand and the complex, respectively. The quantity $I_F^0/(I_F^0 - I_F)$ is plotted versus $[M]^{-1}$, and the stability constant is then given by the ratio of intercept/slope.

2.1.5 Literatures Review of amino acid receptors

The cooperativity between coordination chemistry and organic molecular recognition has been studied by achieving large color changes in indicator displacement. Pyrocatechol and Zn (II) complexes **1** and **2** were used as indicator and receptors for aspartate and glutamate, respectively. Both receptors were firstly investigated the binding affinity with the indicator. The color changed from yellow ($\lambda_{\max} = 445$ nm) to a deep blue ($\lambda_{\max} = 647$ nm) upon addition of $1(\text{OAc})_2$ to a solution of the indicator. The binding constants for 1:1 complex showed 3.75×10^5 and $6.0 \times 10^4 \text{ M}^{-1}$ for 1:3 and 2:3, respectively. The addition of various amino acids to an ensemble of 1:3 or 2:3 resulted in a color change from deep blue to yellow, indicating the displacement of the indicator. The binding constants of **1** with hydrophobic amino acids such as glycine, valine and phenylalanine are in the range of $1 \times 10^4 \text{ M}^{-1}$. A slightly enhanced affinity was found for asparagines ($2.3 \times 10^4 \text{ M}^{-1}$). The carboxylate (benzoic acid) and dicarboxylate (succinate, aspartate and glutamate) guests were also studied the binding with **1** and **2**. A comparison between **1** and **2** is instructive. The binding constants for **2** with aspartate, glutamate and phenylalanine are almost identical. The difference is found in the case of aspartate and other amino acids.[41]

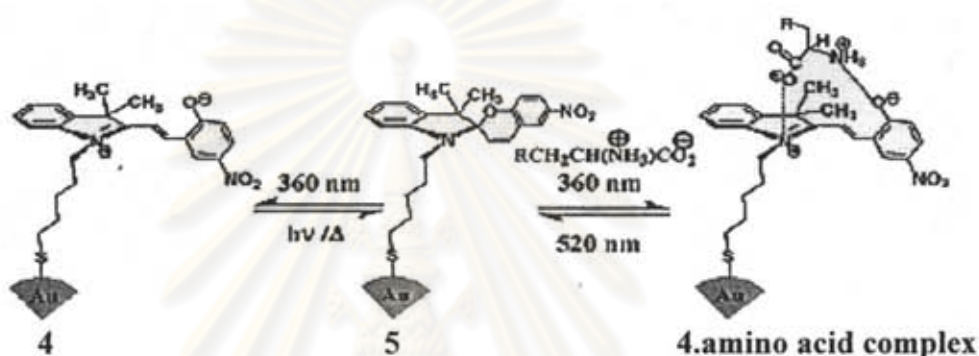


A novel type of off/on fluorescent chemosensor for selective detection of histidine has been described. A heteroditopic system containing crown fragment and quanidinium subunit is used as receptor for linear analytes. Selective binding with histidine from dicopper (II) complex (3) was proceeded from non covalent interaction between imidazole side chain of histidine and Cu^{II} ions. The fluorescent indicators; coumarine, fluorescein and eosine Y are bound through non covalent interactions (carboxylate group of each dye bridge the two Cu^{II} ions), which quenches their emission. The addition of histidine displaces the indicator which displays its full fluorescence when it is released to the solution. Titration of each indicator indicated formation of 1:1 adducts. Each receptor/indicator pair was studied the binding with L-amino acids: His, Ala, Phe, Leu, Pro and Gly. There are only two amino acids (His and Gly) displace the indicator. The highest sensing selectivity is observed with the $[\text{3}]^{4+}$ /eosin Y which sufficiently discriminates histidine from glycine and other investigated amino acids. The observed trend of stability constant ($\text{His} > \text{Gly} > \text{Ala} > \text{Phe} > \text{Val} > \text{Leu} > \text{Pro}$) seems to be related to the increasing steric repulsive effects by the amino acids side chain.[53]

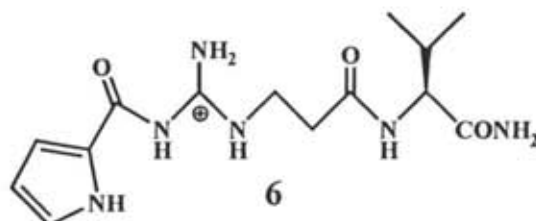


Photoswitchable double-shell structure on a Au nanoparticle core, consisting of photochromic spiropyran (5) was prepared for amino acid binding and releasing study. Under dark conditions, the majority of spiropyran molecules exist in their “closed” spiro form (colorless, nonpolar and no strong emission), which when excited with UV light (360nm) undergo photoisomerization to the “open” merocyanine form 4 (highly polar

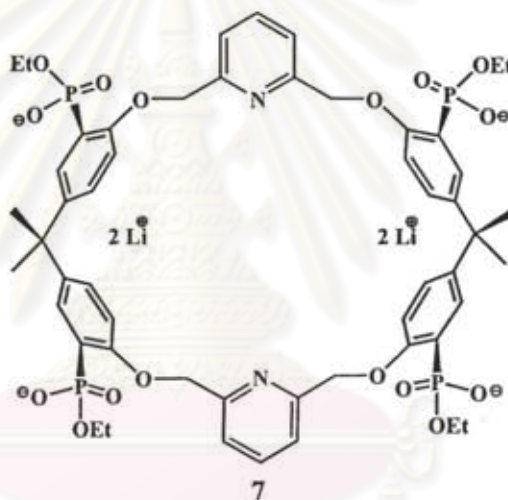
and zwitterionic) absorbing in the visible region and emission around 650 nm. The binding studies of zwitterionic merocyanine towards amino acids: L-Trp, L-Tyr, L-DOPA and α -methyl-L-DOPA, were investigated. Compound **4** can undergo the quick thermal ring closure in the absence of amino acids. The two-point electrostatic interaction between **4** and amino acids resulted in the formation of a stable complex which prevents the thermal ring closure. In case of **4**, the emission intensity decreased gradually with time and the solution became nonfluorescent after 120 min. In the presence of various amino acids, an initial decrease in emission intensity was observed and persisted for a long time. The long-lived species is assigned to the binding with Trp.[54]



N-substituted guanidiniocarbonyl pyrrole **6** is efficient receptor for the complexation of amino acid carboxylates in water. This receptor strongly binds carboxylate through a combination of ion pairing and multiple hydrogen bonds. Additional binding interactions by a side chain attached to the N' of the guanidiniocarbonyl pyrrole could help to stabilize the complex and increase the selectivity of the recognition. The complexation properties were firstly studied with valine using UV-vis titration. The result showed that the pyrrole **6** strongly bound amino acid carboxylates even in aqueous buffer solution with association constants of $K_{\text{assoc}} > 10^3 \text{ M}^{-1}$. The stability of the complex seemed to depend on the nature of the amino acid side chain. Valine bound nearly two times better than alanine ($K_{\text{assoc}} = 1750$ and 1000 M^{-1} , respectively).[55]

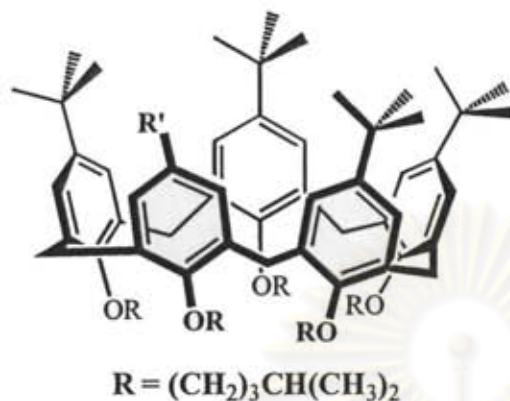


A macrocycle (7) having two chelating bisphosphonate moieties was successfully used as the selective receptor for lysine methyl ester dication. This compound was very soluble in polar solvents such as methanol and water but insoluble in DMSO and MeCN. Complex stoichiometries with lysine, arginine, ornithine and histidine were obtained from Job plots. The smaller amino acid esters including histidine, ornithine and arginine produced a clear 2:1 stoichiometry but lysine was bound by 7 in a clean 1:1 complex. In methanol, association constants for the complexes of amino acids with receptor 7 showed that the four-point interactions in case of the lysine is more powerful than the two-point interactions in the related assemblies with ornithine and arginine. However, histidine is even superior to lysine because it is able to form two strong hydrogen bonds between the imidazolium moiety and the bisphosphonate ions. Lysine formed complex 5-7 times more strongly than ornithine and arginine and even twice as strongly as histidine.[56]



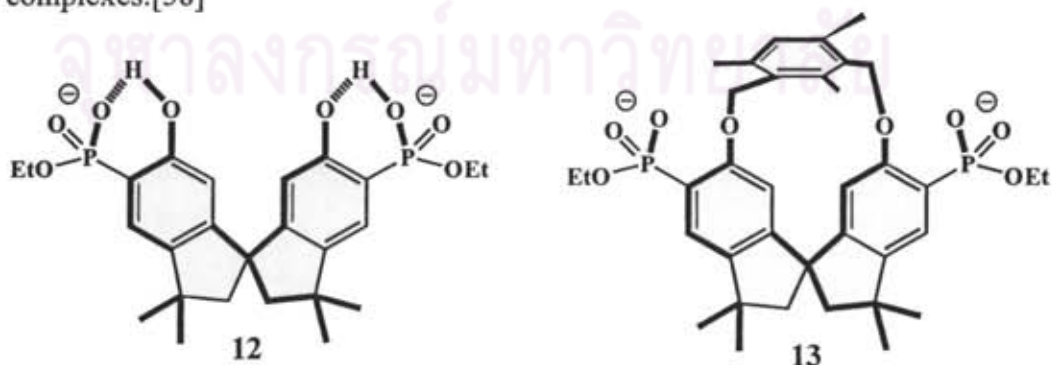
Calix[5]arene **8**, **9**, **10**, **11a** and **11b** have been reported for an affinity with biogenic amines (Cad.2HCl and Spd.3HCl), ω -amino acids (ϵ -Ahx, Lys-OMe.2HCl and GABA.HCl). A preliminary NMR screening of binding affinities of all receptors toward N ^{α} -Ac-L-Lys-OMe.HCl found that **11a** in the presence of a *p*-ureido showed the highest association constants. The receptor **11** was further investigated the binding with Cad.2HCl, ϵ -Ahx and Lys-OMe.2HCl. The 1:1 stoichiometry was determined. Complex formation is proposed to be 1:1 endocavity complexes which were supported by shifts in ¹H-NMR spectrum of both receptors and guest protons. The binding of the pentylenammonium chain inside the calix[5]arene cavity takes advantage of a

combination of cation- π , CH- π and hydrogen bond interactions with the phenolic oxygens. In case of Spd.3HCl guest, the inclusion inside the calixarene cavity was also observed. On the other hand, zwitterionic GABA showed a likely single-point interaction without the inclusion.[57]

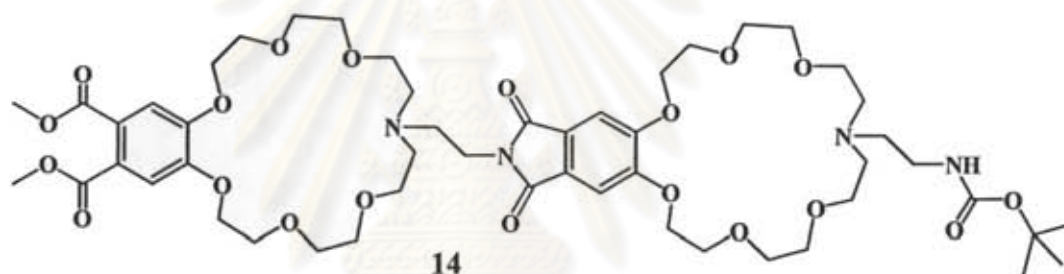


- 8 ; R = *t*Bu
- 9 ; R = NO₂
- 10 ; R = NH₂
- 11a ; R = (R)-PhMe CHNHC(O)NH
- 11b ; R = (S)-PhMe CHNHC(O)NH

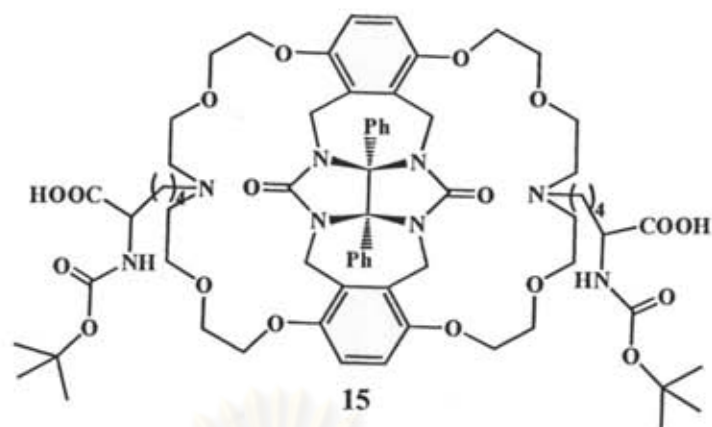
A new class of cleftlike receptor molecules based on bisphosphonates was presented as a chiral sensor for arginine and lysine. The spirobisindane skeleton in **12** and **13** guarantees a high degree of rigidity. The mesitylene spacer in **13** was chosen to prevent rotation of the bridge. Job plots from the NMR technique of **12**, **13** with α,ω -diammonium compounds (Cyc, L-His, L-Orn, L-Lys and L-Arg) supported that **12** forms 1:1 complexes with lysine or arginine. From the association constants, it was found that the open chain host **12** is selective for short rigid α,ω -amines (K_a up to $8 \times 10^3 \text{ M}^{-1}$) and macrocycle **13** prefers longer dications (K_a up to $1.2 \times 10^4 \text{ M}^{-1}$). No enantiodiscrimination is found for the open chain host **12**, and even **13** can only distinguish among enantiometric guests in the attribution of N⁺...N⁺ distance of more than five bonds. Hydrogen bonds between phosphonates and ammonium cation are main interactions of the complexes.[58]



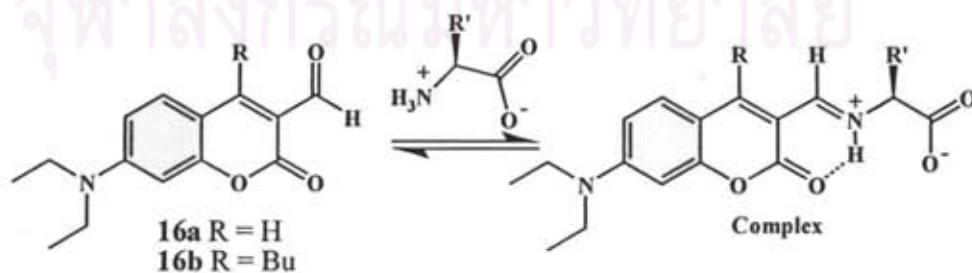
Luminescent crown ether amino acid (CEAA) has been synthesized. It has affinity to ammonium ions and signal the binding process by an increase in emission. 18-crown-6 can be easy to oligomerize with other recognition moieties with use of standard peptide synthesis methods to obtain CEAA dipeptide **14**. Furthermore, a fluorescent phthalic ester or phthalimide moiety was incorporated as a luminescent probe for binding events. In receptor **14**, both crown ether parts bind independently to monoammonium guests with affinity similar to that of monomeric CEAs. A bisammonium guest, such as lysine methyl ester, is cooperatively bound with a much higher affinity. Isomeric tripeptides containing one Lys show different emission response with **14** depending on the distance between ammonium ions with the peptides. Moving the Lys into the peptide chain and thus increasing the distance of N-terminal and the side chain ammonium group leads to a significant decrease of the affinity and emission. The highest affinity was obtained in the case of N-terminal lysine.[59]



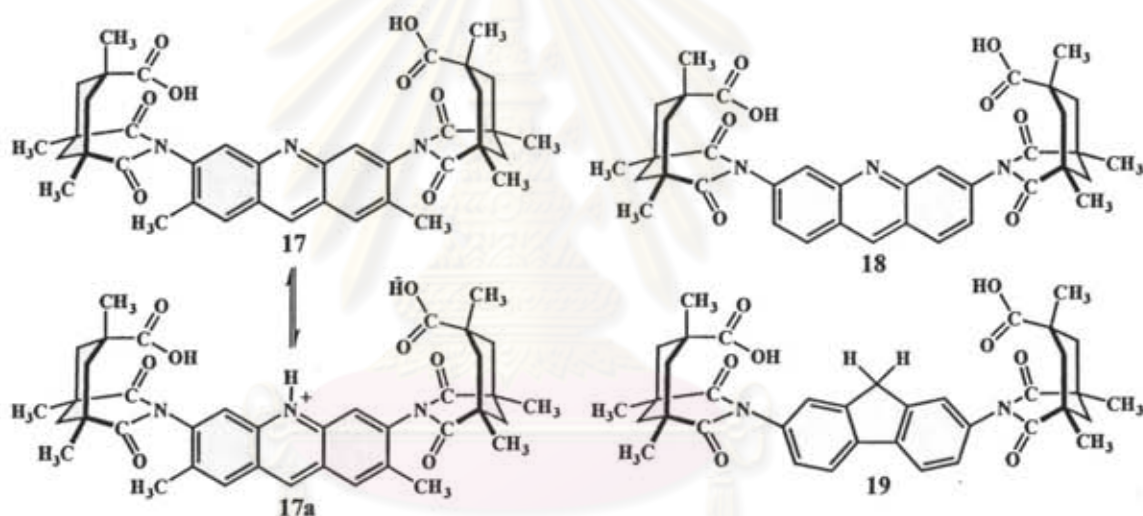
Diphenylglycoluril based clip molecules (**15**) having cavity for amino acids binding inside was studied. This host allows the binding of different phenolic guests via a combination of several non covalent interactions (H-bonding, π - π stacking and the cavity effect). The binding properties were investigated by using a competing dye (Magneson) for a competition experiment. The binding of Magneson with **15** caused an increasing in the absorbance at 452 nm. This complex bound in a 1:1 host-guest ratio. The binding of the complex with different guests showed a decreasing of Magneson absorption band at 450 nm and the presence of an isobestic point at ca. 290 nm. The complexation with guests fitted a 1:1 complex stoichiometry. The binding constants calculated for **15** with guests were moderate to high and a remarkable enantioselectivity for D-tyrosine, L-phenylalanine and D-tryptophan.[60]



Novel receptors which explore aldehyde containing chromophores (coumarin aldehyde **16a** and its 4-butyl derivative **16b**) were chosen to detect amines and amino acids via the reversible formation of imines. Results from UV/vis spectroscopy showed that the two aldehydes displayed a red shift in absorption toward the addition of glycine. The formation of the iminium ion was more favorable for **16b** than **16a**. The red shift is consistent with the proposed mechanism of hydrogen bonding of the iminium ion to the chromophore carbonyl. The dramatic difference in spectroscopic properties of **16a** and **16b** is supposed to steric effects. Fluorescence studies of compound **16b** exhibited a strong increase in fluorescence upon addition of an amine. Results from a number of amines and amino acids indicated that all primary amines give strong fluorescence responded with compound **16b**. The acidic amino acids (aspartate and glutamate) had smaller equilibrium constants and larger fluorescence increases than the neutral amino acids (glycine, lysine, serine and alanine). Finally, in agreement with the absorption data, compound **16a** did not give the significant fluorescence changes upon addition of amines or amino acids.[61]

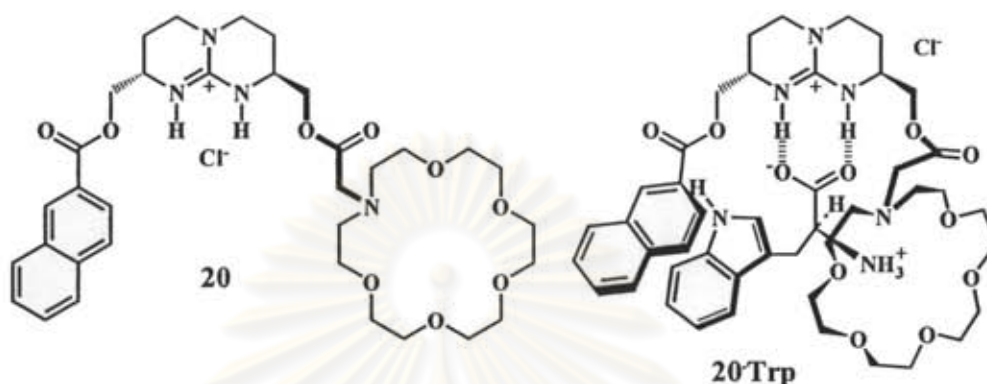


Acridine derivatives (**17-19**) were described their binding with amino acids. NMR spectra of **17** indicated the presence of its zwitterionic form, namely **17a**. It was found that phenylalanine, tryptophan and tyrosine O-methyl ether were extracted from their aqueous solutions with high efficiency by **17**. NMR spectroscopy indicated that these amino acids occupied nearly 50% of the available receptor **17**. In contrast, leucine, isoleucine and valine were not extracted. The NMR spectrum of the phenylalanine complex showing a dramatic upfield shift of the phenyl protons were most easily rationalized by the stacking interactions. Similar spectra were observed with tryptophan and tyrosine derivatives. Extraction studies of **18** complexed with these aromatic amino acids were much reduced but still of the same stacking nature. The fluorene **19**, lacking both zwitterionic character and a well-placed aromatic ring, showed no evidence of binding to these amino acids at all.[62]



A receptor **20** was investigated the affinity toward amino acids by liquid-liquid extraction experiments. Properties of **20** feature as follow: (i) non-self-complementary binding sites for carboxylate (a guanidinium function) and ammonium (a crown ether); (ii) an aromatic planar surface for an additional selective stacking interaction with the side chain of aromatic amino acids; (iii) a chiral structure (S,S-isomer) for enantioselective recognition. Results from the extraction of L-Trp, L-Phe or L-Val which determined by NMR showed 40% extraction for L-Trp and L-Phe but L-Val, without any aromatic side chain, was not detected. A competition experiment with a mixture of all

three amino acids resulted in 100:97:6 Phe/Trp/Val ratios. In case of the extraction of a mixture of 13 amino acids, selectivity of Phe was enhanced. Reciprocally, use of (R,R)-**20** allowed the extraction of D-Phe or D-Trp, but not of the L-enantiomers. $^1\text{H-NMR}$ data (upfield shifts for the naphthoyl protons) supported the binding for a 1:1 complex of (S,S)-**20** with Trp.[63]



2.1.6 Objectives and Scope of This Research

The main goals of this research are to synthesize fluorescent receptors based on acridine derivatives **L1**, **L2**, **L1H** and **L2H** for determination of amino acids binding. All acridine derivatives employed NH-based thiourea to serve as binding sites for the carboxylate group of amino acid guests and acridine is used as fluorophore. Amino acids studied in this work are classified into two types including aliphatic amino acids; alanine (Ala), glycine (Gly) and leucine (Leu) and aromatic amino acids; phenylalanine (Phe) and tryptophan (Trp). The complexation studies are also investigated by several techniques: $^1\text{H-NMR}$ spectroscopy, UV-vis spectrophotometry, fluorescence spectrophotometry and mass spectroscopy.

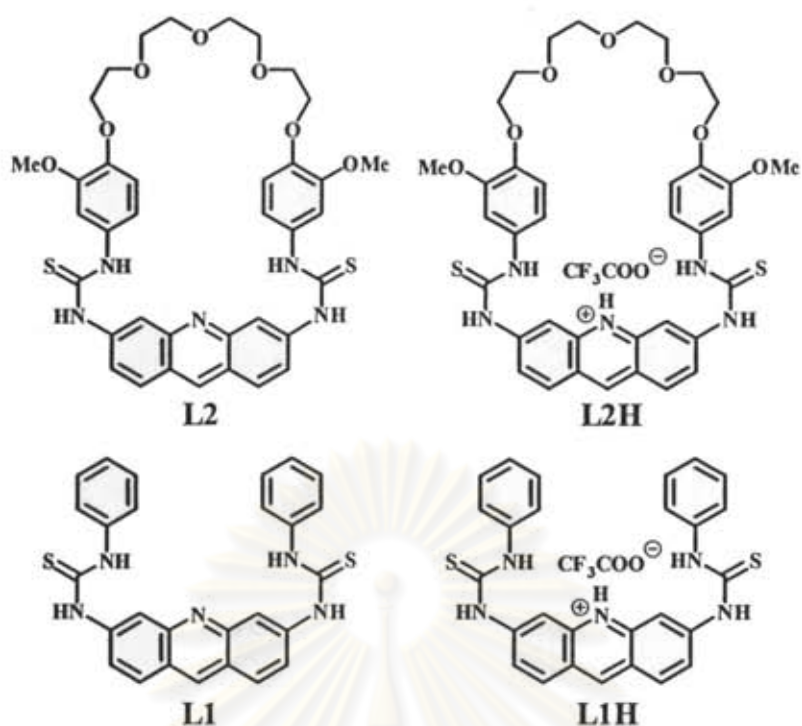


Figure 2.1 Structures of acridine derivatives containing thiourea (L1, L2, L1H and L2H).

2.2 Experimental Section

2.2.1 General procedures for syntheses of receptors containing acridine moiety

2.2.1.1 Analytical instruments

The ¹H-NMR, ¹³C-NMR and two dimensional NMR spectra were recorded on a Varian 400 MHz nuclear magnetic resonance spectrometer. In all cases, samples were dissolved in deuterated chloroform or dimethylsulfoxide, and chemical shifts were recorded using a residual proton signal as internal reference. Coupling constants were given in Hertz. Elemental analyses were analyzed on a Perkin Elmer CHNO/S analyzer (PE2400 series II) by ignition combustion gas chromatography separated by frontal analyses and quantitatively detected by thermal conductivity detector. UV-vis absorption

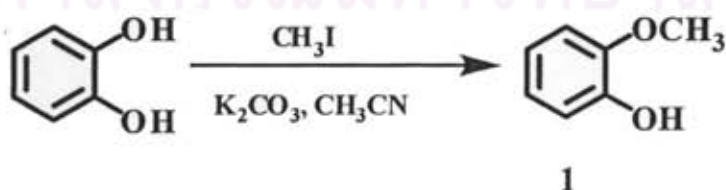
spectra were acquired on a Varian Cary 50 Probe UV-vis spectrophotometer. Samples were contained in 10 mm path length quartz cuvettes (3.5 mL volume). Fluorescence emission spectra were obtained on Varian Cary Eclipse Fluorescence spectrophotometer by personal computer data processing unit. The light source is a pulse xenon lamp and a detector is a photomultiplier tube. Unless otherwise noted, the spectroscopic grade solvent was employed as purchased without further purification. Electrospray mass spectra were determined on a Micromass Platform quadrupole mass analyzer with an electrospray ion source using acetonitrile as solvent. All melting points were obtained on Electrothermal 9100 apparatus. Infrared spectra were carried out on a Nicolet Impact 410 FTIR spectrometer at room temperature with the potassium bromide (KBr) disk method.

2.2.1.2 Materials for synthesis

All materials were standard analytical grade, purchased from Fluka, Aldrich or Merck and used without further purification. Commercial grade solvents such as acetone, dichloromethane, hexane, methanol and ethyl acetate were purified by distillation before used. Acetonitrile and dichloromethane for set up the reaction were dried over calcium hydride and freshly distilled under nitrogen atmosphere prior to use. Chromatographic separations were performed on silica gel columns (kieselgel 60, 0.063-0.200 mm, Merck). Thin layer chromatography (TLC) was carried out using silica gel plates (kieselgel 60 F₂₅₄, 1mm, Merck). All guests as salts and ligands were dried *in vacuo* prior to use.

2.2.1.3 Synthesis of acridine derivatives

2.2.1.3.1 Preparation of *o*-methoxy phenol (1)

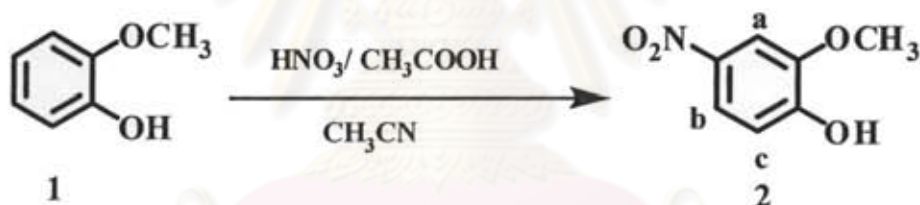


To a stirred solution of pyrocatechol (2.8390g, 0.025 mol) and potassium carbonate (3.5225g, 0.025 mol) in 80 mL acetonitrile was slowly added with a solution of iodomethane (1.57 mL, 0.025 mol) in acetonitrile. The solution was heated to reflux under nitrogen for 8 hours and then allowed to cool to room temperature. The solvent was removed under vacuum and the solid residue was taken up in dichloromethane. The solvent was further treated with 3M hydrochloric acid (50 mL) and extracted with dichloromethane (3x50 mL). The organic layer was dried over anhydrous sodium sulfate and the organic solvent was removed under reduced pressure. The residue was purified by silica gel column and eluted with dichloromethane. The desired product (**1**) was obtained as yellowish oil (54% yield).

Characterization data for 1:

¹H-NMR spectrum (CDCl₃): δ = 6.935 (4H, m, Ar-H), 5.755 (1H, d, *J* = 4.0 Hz, -OH), 3.924 (3H, d, *J* = 3.6 Hz, -OCH₃).

2.2.1.3.2 Preparation of 2-methoxy-4-nitrophenol (2)



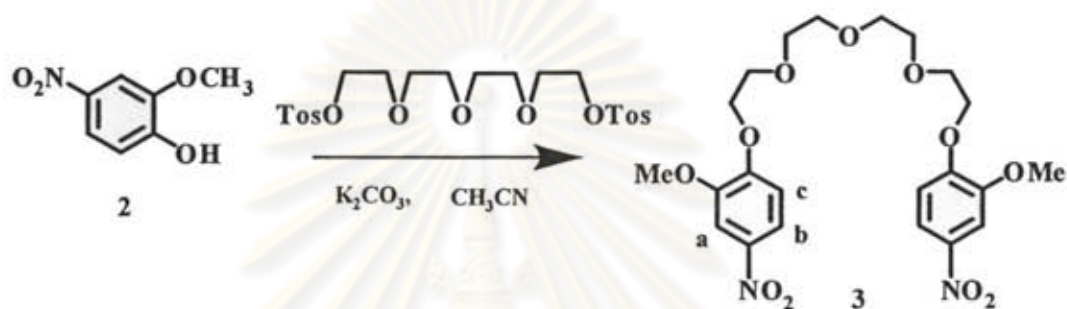
Glacial acetic acid (20 mL) and **1** (3.0586g, 0.025 mol) was mixed and stirred in 80 mL acetonitrile. A solution of concentrated nitric acid (1.8602 mL, 0.025 mol) was slowly added. The mixture was refluxed gently under nitrogen for 4 hours. After cooling to room temperature, the reaction was poured into ice/water and added with sodium hydrogencarbonate until pH reached 9. The mixture was extracted with dichloromethane (3x50 mL). The organic solvent was removed and then the residue was purified on a silica gel column using dichloromethane as eluent. The purified product (**2**) was obtained as yellow crystalline solid after dryness in 10% yield.

Characterization data for 2:

¹H-NMR spectrum (CDCl₃): δ = 7.825 (1H, dd, J = 7.8, 2.4 Hz, Ar- H_b), 7.704 (1H, d, J = 2.4 Hz, Ar- H_a), 6.921 (1H, d, J = 8.8 Hz, Ar- H_c), 6.131 (1H, s, -OH), 3.936 (3H, s, -OCH₃).

IR spectrum (KBr, cm⁻¹) 3369, 3100, 3015, 1590, 1513, 1341, 1267, 1088

2.2.1.3.3 Preparation of 2-Methoxy-1-(2-(2-(2-(2-(2-methoxy-4-nitrophenoxy) ethoxy)ethoxy)ethoxy) ethoxy)-4-nitrobenzene (3)



A mixture of 2 (0.2011g, 0.0012 mol), the catalytic amount of tetrabutylammonium bromide and potassium carbonate (1.6530g, 0.012 mol) in 80 mL acetonitrile was stirred at room temperature for 30 minutes. Then, a solution of tetraethylene glycol ditosylate (0.3010g, 0.006 mol) in acetonitrile was added and the reaction mixture was heated under nitrogen atmosphere for 5 days. After the mixture cooled down to room temperature, the solvent was removed to dryness *in vacuo*. The residue was dissolved in dichloromethane and then washed with 3M hydrochloric acid (50 mL) and extracted with dichloromethane (3x50 mL). The organic phase was dried over anhydrous sodium sulfate and the solvent was removed. The desired product (3) was obtained as a bright yellow crystalline solid (40% yield) after recrystallization in dichloromethane/methanol.

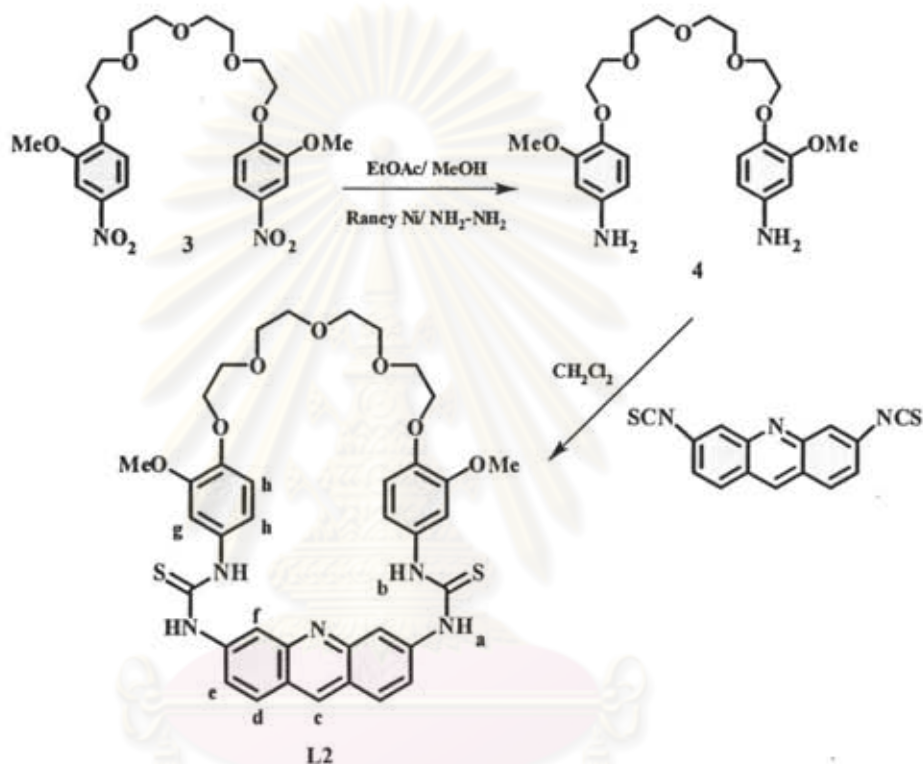
Characterization data for 3:

¹H-NMR spectrum (CDCl₃): δ = 7.916 (2H, d, J = 8.8 Hz, Ar- H_b), 7.765 (2H, s, Ar- H_a), 6.985 (2H, d, J = 8.4 Hz, Ar- H_c), 4.308 (4H, t, J = 4.8 Hz, Ar-O-CH₂-CH₂-O-), 3.966

(10H, br s, Ar-O-CH₂-CH₂-O- + -OCH₃), 3.766 (4H, m, *J* = 2.8 Hz, Ar-O-CH₂-CH₂-O-CH₂-CH₂-O-), 3.710 (4H, m, *J* = 2.8 Hz, Ar-O-CH₂-CH₂-O-CH₂-CH₂-O-).

IR spectrum (KBr, cm⁻¹) 3443, 3093, 2898, 1590, 1520, 1334, 1275, 1139, 1092

2.2.1.3.4 Preparation of 3,6-[3-methoxy-4-(2-(2-(2-(2-(3-methoxy-1-thiourea benzene)ethoxy)ethoxy) ethoxy)ethoxy)-1-thiourea benzene]acridine (L2)



Hydrazine (0.4876 g, 0.021 mol) and Raney nickel (0.3073g) was added to a vigorously stirred solution of **3** (0.2095 g, 0.004 mol) in 60 mL of 1:1 ethyl acetate:methanol. After 2 hours, the mixture was filtered to remove Raney nickel and the filtrate was freed of solvent. The residue was dissolved in dichloromethane and dried over sodium sulfate anhydrous. Evaporation of the solvent gave the product **4**, as yellow liquid which was immediately used in the next step by dissolving it in 150 mL dichloromethane and cooling to 0°C. A solution of proflavinedithiocyanate (1.1677g, 0.004 mol) in dichloromethane was slowly added into the solution of **4** with the controlled temperature at 0°C and the reaction was stirred at room temperature overnight.

The reaction mixture was filtered to remove dimer product (dark red powder) and then the organic solvent was evaporated under reduced pressure. The residue was dissolved in DMF and then methanol was added to precipitate the desired product **L2** as an orange powder (16% yield).

Characterization data for L2:

$^1\text{H-NMR}$ spectrum (DMSO- d_6): $\delta = 10.092$ (2H, s, $-\text{NH}_a$), 9.975 (2H, s, $-\text{NH}_b$), 8.855 (1H, d, $J = 12.0$ Hz, $\text{Ar}_{\text{acridine-}H_c}$), 8.234 (2H, s, $\text{Ar}_{\text{acridine-}H_f}$), 8.001 (2H, d, $J = 8.0$ Hz, $\text{Ar}_{\text{acridine-}H_e}$), 7.680 (2H, d, $J = 9.6$ Hz, $\text{Ar}_{\text{acridine-}H_d}$), 7.181 (2H, s, $\text{Ar-}H_g$), 6.954 (4H, s, $\text{Ar-}H_h$), 4.041 (4H, s, $\text{Ar-O-CH}_2\text{-CH}_2\text{-O-}$), 3.727 (10H, s, $\text{Ar-O-CH}_2\text{-CH}_2\text{-O-} + \text{-OCH}_3$), 3.571 (8H, d, $J = 7.6$ Hz, $\text{Ar-O-CH}_2\text{-CH}_2\text{-O-CH}_2\text{-CH}_2\text{-O-}$).

$^{13}\text{C}\{^1\text{H}\}$ -NMR spectrum (DMSO- d_6): $\delta = 179.4, 149.2, 148.6, 145.4, 141.6, 135.1, 132.5, 128.3, 123.3, 123.0, 117.6, 116.3, 113.2, 109.3, 69.9, 69.8, 68.9, 68.1, 55.6$.

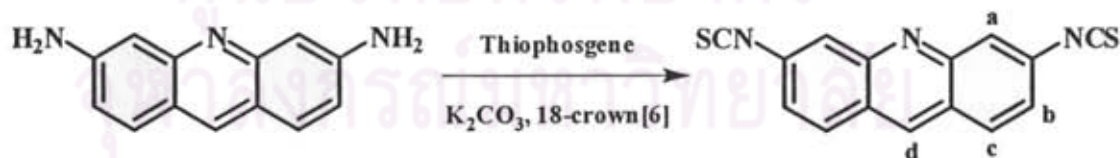
IR spectrum (KBr, cm^{-1}) 3338, 2921, 2867, 1602, 1513, 1458, 1225, 1131

MS(ESI): m/z for $\text{C}_{37}\text{H}_{39}\text{N}_5\text{O}_7\text{S}_2 = 729.23$ [M^+].

Elemental analysis:

Anal. Calcd for $\text{C}_{37}\text{H}_{39}\text{N}_5\text{O}_7\text{S}_2 \cdot 0.6 \text{CH}_2\text{Cl}_2 \cdot 0.4 \text{DMF}$	C, 57.47; H, 5.31; N, 9.33
Found	C, 57.14; H, 5.32; N, 9.60

2.2.1.3.5 Preparation of 3,6-dithiocyanateacridine



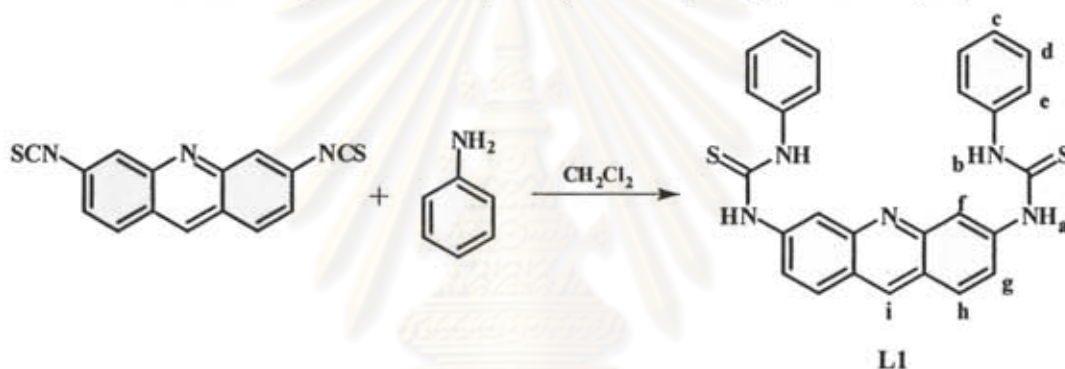
To a solution of proflavine hemisulfatedihydrate (0.2763 g, 0.001 mol) in dichloromethane 100 mL, potassium carbonate (1.1000 g, 0.008 mol) and a catalytic amount of 18-crown[6] were added and the mixture was stirred at room temperature for

30 min. Thiophosgene (0.30 mL, 0.004 mol) was added and the reaction was stirred at room temperature overnight until the clear orange solution was observed. This solution was poured into water (100 mL) and extracted with dichloromethane (3x50 mL). Purification of this solid by silica gel column chromatography using dichloromethane as eluent and the recrystallization with dichloromethane/hexane were carried out to give yellow crystals as products (70 % yield).

Characterization data:

¹H-NMR spectrum (CDCl₃): δ = 8.773 (1H, s, H_d), 8.035 (4H, m, H_a and H_b), 7.435 (2H, dd, J = 8, 2.4 Hz, H_c)

2.2.1.3.6 Preparation of 3,6-bis(thioureaphenyl)acridine (L1)



To a solution of aniline (0.1026 mL, 0.0011 mol) in 30 mL dichloromethane was cooled to 0°C and slowly added with a solution of proflavinedithiocyanate (0.1500g, 0.0005 mol) in dichloromethane. After the reaction mixture was stirred at room temperature overnight, a yellow solid was precipitated and the solid was filtered under vacuum and washed with dichloromethane to yield a pale orange powder as the final product (L1) (52% yield).

Characterization data for L1:

¹H-NMR spectrum (DMSO-*d*₆): δ = 10.284 (2H, s, -NH_a), 10.144 (2H, s, -NH_b), 8.894 (1H, s, Ar_{acridine}-H_i), 8.251 (2H, s, Ar_{acridine}-H_f), 8.037 (2H, d, J = 8.8 Hz, Ar_{acridine}-H_g), 7.697 (2H, dd, J = 8.8, 3.0 Hz, Ar_{acridine}-H_h), 7.526 (4H, d, J = 7.2 Hz, Ar-H_e), 7.350 (4H, m, J = 7.6 Hz, Ar-H_d), 7.142 (2H, m, Ar-H_c).

$^{13}\text{C}\{^1\text{H}\}$ -NMR spectrum (DMSO- d_6): $\delta = 179.6, 149.3, 142.1, 139.8, 135.4, 129.2, 124.8, 124.0, 123.8, 123.5, 118.0$.

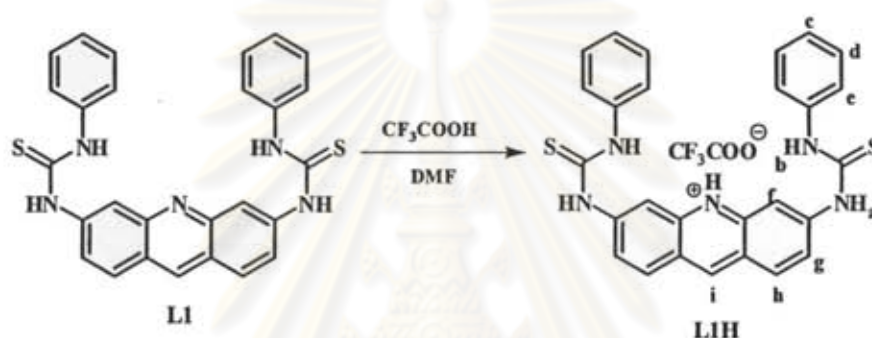
IR spectrum (KBr, cm^{-1}) 3217, 3027, 1618, 1544, 1446, 1252, 1147

Elemental analysis:

Anal. Calcd for $\text{C}_{27}\text{H}_{21}\text{N}_5\text{S}_2$ C, 67.61; H, 4.41; N, 14.60.

Found C, 67.59; H, 4.42; N, 14.61.

2.2.1.3.7 Preparation of 3,6-bis(thioureaphenyl)acridinium ion (L1H)



To a solution of L1 (0.0031g, 0.0405 mmol) in DMF, an excess amount of trifluoroacetic acid (0.1000 mL) was added and then stirred at room temperature for 2 days. The desired product (L1H) was obtained as an orange solid in 65 % yield after an addition of methanol into the reaction mixture.

Characterization data for L1H:

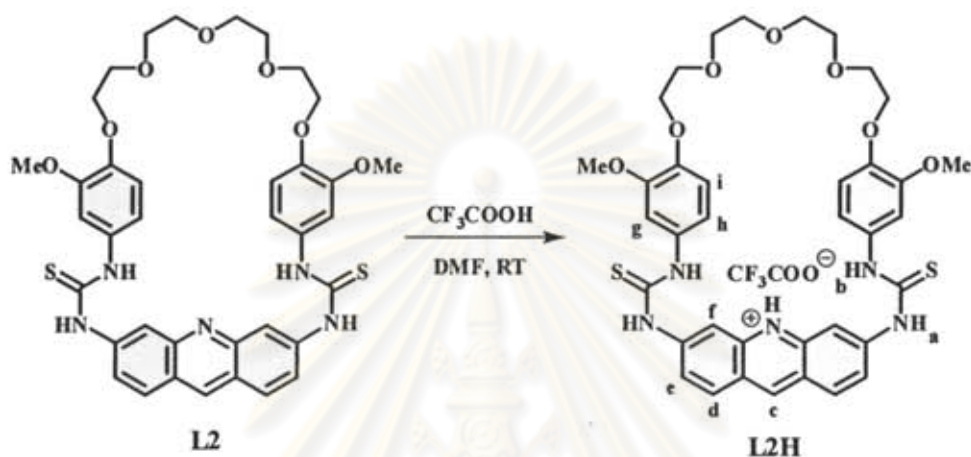
^1H -NMR spectrum (DMSO- d_6): $\delta = 11.085$ (2H, s, $-\text{NH}_a$), 10.804 (2H, s, $-\text{NH}_b$), 9.453 (1H, s, $\text{Ar}_{\text{acridine}}-\text{H}_i$), 8.885 (2H, s, $\text{Ar}_{\text{acridine}}-\text{H}_f$), 8.274 (2H, m, $\text{Ar}_{\text{acridine}}-\text{H}_g$), 7.784 (2H, d, $J = 9.2$ Hz, $\text{Ar}_{\text{acridine}}-\text{H}_h$), 7.545 (4H, d, $J = 7.6$ Hz, $\text{Ar}-\text{H}_e$), 7.364 (4H, t, $J = 8.0$ Hz, $\text{Ar}-\text{H}_d$), 7.171 (4H, t, $J = 7.2$ Hz, $\text{Ar}-\text{H}_c$).

$^{13}\text{C}\{^1\text{H}\}$ -NMR spectrum (DMSO- d_6): $\delta = 179.3, 159.7, 159.4, 159.0, 139.3, 130.8, 129.0, 125.6, 124.4, 123.3, 122.1, 118.9$

IR spectrum (KBr, cm^{-1}) 3478, 3050, 2781, 1696, 1536, 1458, 1193

MS(ESI): m/z for $\text{C}_{32}\text{H}_{29}\text{F}_3\text{N}_6\text{O}_3\text{S}_2 = 665.752$ [M^+ +DMF].

2.2.1.3.8 Preparation of 3,6-[3-methoxy-4-(2-(2-(2-(2-(3-methoxy-1-thiourea benzene)ethoxy)ethoxy) ethoxy)ethoxy)-1-thiourea benzene]acridinium ion (L2H)



The protonation of **L2** was prepared similarly to that of **L1**. The final product (**L2H**) was as a dark red solid in 60% yield.

Characterization data for L2H:

$^1\text{H-NMR}$ spectrum ($\text{DMSO-}d_6$): $\delta = 10.843$ (2H, bs, $-\text{NH}_a$), 10.555 (2H, bs, $-\text{NH}_b$), 9.425 (1H, bs, $\text{Ar}_{\text{acridine}}-\text{H}_c$), 8.866 (2H, bs, $\text{Ar}_{\text{acridine}}-\text{H}_f$), 8.255 (2H, bs, $\text{Ar}_{\text{acridine}}-\text{H}_e$), 7.756 (2H, bs, $\text{Ar}_{\text{acridine}}-\text{H}_d$), 7.201 (2H, s, $\text{Ar}-\text{H}_g$), 7.005 (2H, m, $\text{Ar}-\text{H}_h$), 6.968 (2H, s, $\text{Ar}-\text{H}_i$), 4.057 (4H, s, $\text{Ar}-\text{O}-\text{CH}_2-\text{CH}_2-\text{O}-$), 3.732 (10H, s, $\text{Ar}-\text{O}-\text{CH}_2-\text{CH}_2-\text{O}- + -\text{OCH}_3$), 3.563 (8H, d, $J = 8.4$ Hz, $\text{Ar}-\text{O}-\text{CH}_2-\text{CH}_2-\text{O}-\text{CH}_2-\text{CH}_2-\text{O}-$).

IR spectrum (KBr, cm^{-1}) 3529, 2918, 2867, 1676, 1509, 1458, 1201, 1123

MS(ESI): m/z for $\text{C}_{39}\text{H}_{40}\text{F}_3\text{N}_5\text{O}_9\text{S}_2 = 844.864$ [$\text{M}+\text{H}^+$].

2.2.2 Experimental procedures in complexation studies

2.2.2.1. $^1\text{H-NMR}$ titration studies for complexes of ligands L1 and L2 with amino acids

Typically, a 0.002 M solution of a ligand (1.18×10^{-6} mol) in $\text{DMSO-}d_6$ (0.6 mL) was prepared in a 5-mm NMR tube. An initial $^1\text{H-NMR}$ spectrum of the solution of the ligand was recorded. A 0.012 M stock solution of guest molecules (6.00×10^{-6} mol) in $\text{DMSO-}d_6$ (0.5 mL) was prepared in a vial (shown in Tables 2.1). The solution of a guest molecule (0.4 mL) was added *via* microsyringe (10 and 50 μL portions) to the NMR tube to have guest:host ratios shown in Table 2.2. $^1\text{H-NMR}$ spectra were recorded after each addition.

Table 2.1 Amounts of amino acids that used in complexation studies with ligand L1 and L2 for NMR titration studies.

Ligands	Amino acids	Weight (gram)
L1 or L2	Glycine	0.00045
	Alanine	0.00053
	Leucine	0.00079
	Phenylalanine	0.00099
	Tryptophan	0.00122

ศูนย์วิทยทรัพยากร
จุฬาลงกรณ์มหาวิทยาลัย

Table 2.2 Amounts of solutions of amino acids used to prepare various amino acids:L1 ratios for NMR titration studies.

ratio of guest:ligand	volume guest added (μL)
0.0:1.0	0
0.1:1.0	10
0.2:1.0	10
0.3:1.0	10
0.4:1.0	10
0.5:1.0	10
0.6:1.0	10
0.7:1.0	10
0.8:1.0	10
0.9:1.0	10
1.0:1.0	10
1.2:1.0	20
1.4:1.0	20
1.6:1.0	20
1.8:1.0	20
2.0:1.0	20
2.5:1.0	50
3.0:1.0	50
3.5:1.0	50
4.0:1.0	50

2.2.2.2 ¹H-NMR titration studies for complexes of ligand L1H with amino acids

Typically, a 0.003 M solution of a ligand L1H (1.8×10^{-6} mol) in DMSO-*d*₆ (0.6 mL) was prepared in a 5-mm NMR tube. An initial ¹H-NMR spectrum of the solution of the ligand was recorded. A 0.014 M stock solution of guest molecules (9.00×10^{-6} mol) in DMSO-*d*₆ (0.5 mL) was prepared in a vial (shown in Tables 2.3). The solution of a guest molecule (0.4 mL) was added *via* microsyringe (10 and 50 μL portions) to the NMR tube to have guest:host ratios shown in Table 2.2. ¹H-NMR spectra were recorded after each addition.

Table 2.3 Amounts of amino acids that used in complexation studies with ligand L1H for NMR titration studies.

Ligand	Amino acids	Weight (gram)
L1H	Glycine	0.00068
	Alanine	0.00080
	Leucine	0.00118
	Phenylalanine	0.00148
	Tryptophan	0.00184

2.2.2.3 ¹H-NMR titration studies for complexes of ligand L2H with amino acids

Typically, a 0.005 M solution of a ligand L2H (1.75×10^{-6} mol) in DMSO-*d*₆ (0.35 mL) was prepared in a 5-mm NMR tube. An initial ¹H-NMR spectrum of the solution of the ligand was recorded. A 0.029 M stock solution of guest molecules (1.16×10^{-5} mol) in DMSO-*d*₆ (0.4 mL) was prepared in a vial (shown in Tables 2.4). The solution of a guest molecule (0.3 mL) was added *via* microsyringe (10 and 50 μL portions) to the NMR tube have guest:host ratios shown in Table 2.5. ¹H-NMR spectra were recorded after each addition.

Table 2.4 Amounts of amino acids that used in complexation studies with ligand **L2H** for NMR titration studies.

Ligand	Amino acids	Weight (gram)
L2H	Glycine	0.00088
	Alanine	0.00104
	Leucine	0.00153
	Phenylalanine	0.00193
	Tryptophan	0.00239

Table 2.5 Amounts of solutions of amino acids used to prepare various amino acids:**L2H** ratios for NMR titration studies.

ratio of guest:ligand	volume guest added (μL)	ratio of guest:ligand	volume guest added (μL)
0.0:1.0	0	1.0:1.0	7.5
0.1:1.0	7.5	1.2:1.0	15
0.2:1.0	7.5	1.4:1.0	15
0.3:1.0	7.5	1.6:1.0	15
0.4:1.0	7.5	1.8:1.0	15
0.5:1.0	7.5	2.0:1.0	15
0.6:1.0	7.5	2.5:1.0	37.5
0.7:1.0	7.5	3.0:1.0	37.5
0.8:1.0	7.5	3.5:1.0	37.5
0.9:1.0	7.5	4.0:1.0	37.5

2.2.2.4 UV-vis titration studies for complexes of ligand L1 and L2 with amino acids

Typically, 0.01 M solution of $[\text{Bu}_4\text{N}][\text{PF}_6]$ (0.3874 g) in 100 mL of DMSO (spectroscopic grade) was prepared and used as a solvent in all UV-vis experiment. Solution of 0.00003 M of a ligand L1 (3.00×10^{-7} mol) or 0.000025 M solution of ligand L2 (2.50×10^{-7} mol) in 10 mL of DMSO were prepared in a volumetric flask. The ligand solution (2 mL) was pipetted into a 1 cm pathlength quartz cuvette and absorption spectrum of each ligand was recorded from 330 to 550 nm at room temperature. A solution of a guest in DMSO was prepared in a 10 mL volumetric flask (shown in Tables 2.6 for L1 and L2). The solution of a guest (total volume 1.5 mL) was added directly to the cuvette by microburette and stirred for 30 sec prior to measurement. The absorption spectra of solution were recorded after each addition until absorbance of a new peak at 460 nm was constant.

Table 2.6 Amounts of amino acids that used in complexation studies with ligand L1 and L2 for UV-vis titration studies.

Ligands	Amino acids	Weight (gram)	Ligand:Guest (equiv)
L1	Glycine	0.00150	1:50
	Alanine	0.00178	1:50
	Leucine	0.00262	1:50
	Phenylalanine	0.00330	1:50
	Tryptophan	0.00408	1:50
L2	Glycine	0.00100	1:40
	Alanine	0.00119	1:40
	Leucine	0.00175	1:40
	Phenylalanine	0.00220	1:40
	Tryptophan	0.00273	1:40

2.2.2.5 UV-vis titration studies for complexes of ligand L1H and L2H with amino acids

Typically, 0.01 M solution of $[\text{Bu}_4\text{N}][\text{PF}_6]$ (0.3874 g) in 100 mL of DMSO (spectroscopic grade) was prepared and used as a solvent in all UV-vis experiment. Solution of 0.000025 M of a ligand L1H (2.50×10^{-7} mol) or 0.00002 M solution of ligand L2H (2.00×10^{-7} mol) in 10 mL of DMSO (spectro grade) were prepared in a volumetric flask. The ligand solution (2 mL) was pipetted into a 1 cm pathlength quartz cuvette and absorption spectrum of each ligand was recorded from 330 to 550 nm at room temperature. A solution of a guest in DMSO was prepared in a 10 mL volumetric flask (shown in Tables 2.7 for L1H and L2H). The solution of a guest (total volume 1.5 mL) was added directly to the cuvette by microburette and stirred for 30 sec prior to measurement. The absorption spectra of solution were recorded after each addition until absorbance of a new peak at 400 nm was constant.

Table 2.7 Amounts of amino acids that used in complexation studies with ligand L1H and L2H for UV-vis titration studies.

Ligand	Amino acids	Weight (gram)	Ligand:Guest (equiv)
L1H	Glycine	0.00075	1:30
	Alanine	0.00089	1:30
	Leucine	0.00131	1:30
	Phenylalanine	0.00165	1:30
	Tryptophan	0.00204	1:30
L2H	Glycine	0.00060	1:30
	Alanine	0.00071	1:30
	Leucine	0.00105	1:30
	Phenylalanine	0.00132	1:30
	Tryptophan	0.00163	1:30

2.2.2.6 Fluorescence titration studies for complexes of ligand L1 and L2 with amino acids

Typically, 0.01 M solution of $[\text{Bu}_4\text{N}][\text{PF}_6]$ (0.3874 g) in 100 mL of DMSO (spectroscopic grade) was prepared and used as a solvent in all fluorescence experiment. Solution of 0.0002 M of a ligand L1 (2.00×10^{-6} mol) or 0.0002 M solution of ligand L2 (2.00×10^{-6} mol) in 10 mL of DMSO (spectro grade) was prepared in a volumetric flask. The ligand solution (2 mL) was pipetted into a 1 cm pathlength quartz cuvette and emission spectrum of each ligand recorded from 430 to 650 nm (excitation at 400 nm) at room temperature. A solution of a guest in DMSO was prepared in a 10 mL volumetric flask (shown in Tables 2.8 for L1 and L2). The solution of a guest (total volume 1.5 mL) was introduced in portions to the cuvette by microburette and stirred for 30 sec prior to measurement. The emission spectra of solution were recorded toward all titrations.

Table 2.8 Amounts of amino acids that used in complexation studies with ligand L1 and L2 for fluorescence titration studies.

Ligand	Amino acids	Weight (gram)	Ligand:Guest (equiv)
L1	Glycine	0.00400	1:30
	Alanine	0.00475	1:30
	Leucine	0.00699	1:30
	Phenylalanine	0.00880	1:30
	Tryptophan	0.01088	1:30
L2	Glycine	0.00600	1:30
	Alanine	0.00713	1:30
	Leucine	0.01050	1:30
	Phenylalanine	0.01321	1:30
	Tryptophan	0.01634	1:30

2.2.2.7 Fluorescence titration studies for complexes of ligand L1H and L2H with amino acids

Typically, 0.01 M solution of $[\text{Bu}_4\text{N}][\text{PF}_6]$ (0.3874 g) in 100 mL of DMSO (spectroscopic grade) was prepared and used as a solvent in all fluorescence experiment. Solution of 0.0002 M of a ligand L1H (2.00×10^{-6} mol) or 0.0002 M solution of ligand L2H (2.00×10^{-6} mol) in 10 mL of DMSO (spectro grade) was prepared in a volumetric flask. The ligand solution (2 mL) was pipetted into a 1 cm pathlength quartz cuvette and emission spectrum of each ligand recorded from 470 to 650 nm (excitation at 460 nm) at room temperature. A solution of a guest in DMSO was prepared in a 10 mL volumetric flask (shown in Tables 2.9 for L1H and L2H). The solution of a guest (total volume 1.5 mL) was introduced in portions to the cuvette by microburette and stirred for 30 sec prior to measurement. The emission spectra of solution were recorded toward all titrations.

Table 2.9 Amounts of amino acids that used in complexation studies with ligand L1H and L2H for fluorescence titration studies.

Ligand	Amino acids	Weight (gram)	Ligand:Guest (equiv)
L1H	Glycine	0.00500	1:25
	Alanine	0.00594	1:25
	Leucine	0.00875	1:25
	Phenylalanine	0.01102	1:25
	Tryptophan	0.01362	1:25
L2H	Glycine	0.00600	1:30
	Alanine	0.00713	1:30
	Leucine	0.01050	1:30
	Phenylalanine	0.01321	1:30
	Tryptophan	0.01634	1:30

2.3 Results and discussion

2.3.1 Synthesis and characterization of acridine derivative receptors

2.3.1.1 Synthesis and characterization of 3,6-bis(thioureaphenyl)acridine (L1)

Synthesis of compound **L1** is outlined in Figure 2.2. Proflavinedithiocyanate was synthesized from a reaction between proflavine hemisulfatedihydrate and thiophosgene in the presence of anhydrous potassium carbonate as a base and 18-crown[6] as a catalyst. The desired compound was separated on a silica gel column with dichloromethane as eluent to give proflavinedithiocyanate as a yellow solid. **L1** was prepared by a coupling reaction of proflavinedithiocyanate with aniline in dry dichloromethane. During an addition of a proflavinedithiocyanate solution, temperature was kept at 0°C to protect a forming of dimer by-product. After that, this reaction was stirred at room temperature for 2 days. The ¹H-NMR spectrum of **L1** showed the presence of three phenyl proton signal at range 7.1-7.6 ppm with a consistent of one doublet and two multiplets. The acridine protons appeared two singlets at 8.89 and 8.25 ppm, one doublet at 8.04 ppm and one doublet of doublet at 7.69 ppm. The ¹H-NMR spectra showed NH thiourea resonance in downfield position at 10.28 and 10.14 ppm adjacent to acridine and phenyl ring, respectively. IR spectra showed a N-H stretching band at 3217 cm⁻¹, C-H aromatic stretching band at 3027 cm⁻¹, C=C stretching band at 1618 cm⁻¹ and C=S stretching band at 1544 cm⁻¹. The result from elemental analysis also supported the structure of this compound.

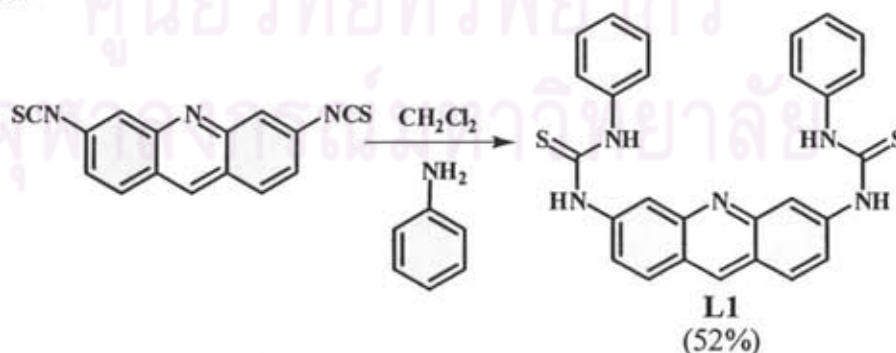


Figure 2.2 The synthetic pathway of final product **L1**.

2.3.1.2 Synthesis and characterization of 3,6-[3-methoxy-4-(2-(2-(2-(2-(3-methoxy-1-thiourea benzene) ethoxy) ethoxy) ethoxy) ethoxy) ethoxy)-1-thiourea benzene] acridine (L2)

Synthesis of compound **L2** is outlined in Figure 2.3. The synthesis pathway of **L2** was started from a conversion of pyrocatechole to *o*-methoxy phenol (**1**) using a simple nucleophilic substitution reaction. Pyrocatechole was reacted with iodomethane in the presence of anhydrous potassium carbonate as based in dry acetonitrile yielding *o*-methoxy phenol as yellowish oil in 54% yield after purification by silica gel column chromatography using dichloromethane as eluent. The $^1\text{H-NMR}$ spectrum of **1** showed a doublet for methoxy proton at 3.92 ppm and a doublet for phenolic hydroxyl proton at 5.76 ppm, with an integral ratio of 3:1. It is thus in good agreement with the proposed structure.

2-Methoxy-4-nitrophenol (**2**) was prepared by electrophilic substitution reaction of *o*-methoxy phenol under mild condition for generating nitronium ion in order to prevent oxidation of the phenol group. The reaction of **1** with nitric acid and glacial acetic acid in acetonitrile gave 2-methoxy-4-nitrophenol. A by-product; 2-methoxy-6-nitrophenol, was found from the reaction. Consequently, the hydroxyl group is a stronger activating group on the stability of intermediate than the methoxy group, which influence on the stability of arenium ion intermediate at the para position more than the ortho and the meta positions.[64] However, a difficulty in separation both compounds from column chromatography causes the obtaining of **2** in low %yield. The $^1\text{H-NMR}$ spectrum of **2** showed aromatic protons at 7.82, 7.70 and 6.92 ppm as well as phenolic hydroxyl proton at 6.13 ppm which existed at a lower field compared to **1**. IR spectrum of **2** showed O-H stretching band at 3369 cm^{-1} and N=O stretching band at 1590 cm^{-1} .

Synthesis of compound **3** was achieved by the coupling a unit of tetraethyleneglycol ditosylate with 2-methoxy-4-nitrophenol (**2**) which has a stable protonation form of aryloxide ion acting as a good nucleophile because of the para-directing of nitro group. From this reaction, product **3** was obtained as a yellowish crystalline solid in 40% yield. The $^1\text{H-NMR}$ spectrum of **3** showed an absence of the characteristic peaks of the tosyl groups in tetraethyleneglycol ditosylate. In addition, the

methoxy protons and the bridging glycolic protons appeared at 3.96 and 4.31-3.71 ppm, respectively. IR spectrum of **3** showed O-H stretching band at 3443 cm^{-1} , C-H (aromatic) stretching at 3093 cm^{-1} , C-H (aliphatic) stretching at 2898 cm^{-1} , N=O stretching band at 1590 cm^{-1} and C-O stretching at 1139 cm^{-1} .

Compound **4** was synthesized by a reduction of nitro groups in **3** using hydrazine and a hydrogenation catalyst, namely Raney nickel, in a mixed solvent of methanol/ethyl acetate. This amine product was immediately used in the next step because it is air sensitive and easily to decompose.

The final product (**L2**) was accomplished by a coupling reaction of compound **4** with proflavinedithiocyanate in dry dichloromethane under nitrogen atmosphere with high dilute condition. During an addition of a proflavinedithiocyanate solution, temperature was kept at 0°C and then stirred at room temperature overnight. Dark red solid which is a dimer product was firstly precipitated and filtered out. **L2** was found in the filtrate. The desired product (**L2**) as orange solid (17% yield) was obtained from a crystallization in DMF/methanol. The dimer product was proved by mass spectrometry showing signal at $m/z\ 1459\ [M^+]$. The $^1\text{H-NMR}$ spectrum of **L2** showed a downfield shift of NH thiourea signals at 10.09 and 9.98 ppm due to the intramolecular hydrogen bonding with N-acridine, acridine protons were assigned at 8.85, 8.23, 8.00 and 7.68 ppm. IR spectrum of **L2** showed N-H stretching band at 3447 cm^{-1} , C-H (aliphatic) stretching at 2921 cm^{-1} , C=C stretching band at 1600 cm^{-1} , C=S stretching band at 1513 cm^{-1} and C-O stretching at 1131 cm^{-1} . ESI mass spectra also supported the structure of this compound showing an intense line at $729.23\ m/z$, corresponding to **L2**. Moreover, the result of elemental analysis is good agreement with compound **L2**.

ศูนย์วิทยทรัพยากร
จุฬาลงกรณ์มหาวิทยาลัย

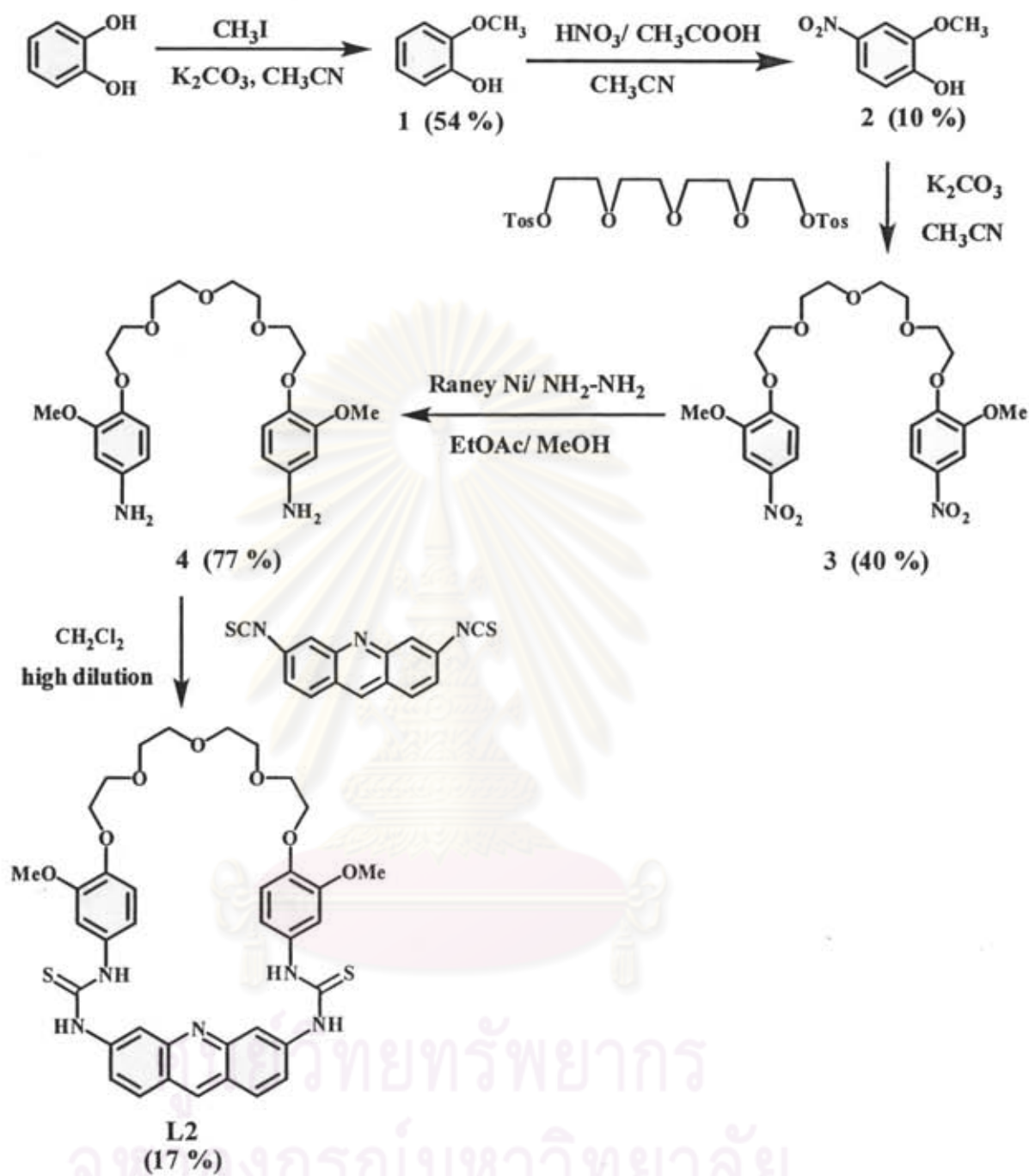


Figure 2.3 The synthetic pathway of final product L2.

2.3.1.3 Synthesis and characterization of 3, 6-bis(thioureaphenyl)acridinium ion (L1H) and 3,6-[3-methoxy-4-(2-(2-(2-(2-(3-methoxy-1-thiourea benzene)ethoxy)ethoxy)ethoxy)ethoxy)-1-thiourea benzene]acridinium ion (L2H)

Synthesis of compound **L1H** and **L2H** is outlined in Figure 2.4. Compounds **L1H** and **L2H** are in protonated form of **L1** and **L2**, respectively. A protonation at N-acridine group of **L1** and **L2** using trifluoroacetic acid in dimethylformamide provided **L1H** and **L2H** as a red solid in 65% yield and a dark red solid in 60% yield, respectively. Both final products are in salt-form which has trifluoroacetate as counteranion. The $^1\text{H-NMR}$ spectra of **L1H** and **L2H** showed a farther downfield shift of NH thiourea protons at 11.08 and 10.80 ppm for **L1H** and 10.84 and 10.55 ppm for **L2H**. The acridine protons were also observed at a downfield shift due to a transformation from N-acridine to NH^+ -acridinium. IR spectra of **L1H** showed shifts of IR bands to longer wavenumber; N-H stretching band at 3478 cm^{-1} , C-H aromatic stretching band at 3050 cm^{-1} , C=C stretching band at 1696 cm^{-1} . In case of **L2H**, the same result in IR band shifts was observed; N-H stretching band at 3529 cm^{-1} and C=C stretching band at 1676 cm^{-1} . ESI mass spectra also supported the structure of **L1H** and **L2H** showing an intense line at $m/z = 665.752$ [$\text{M}^+ + \text{DMF}$] and 844.864 [$\text{M} + \text{H}^+$] for **L1H** and **L2H**, respectively.

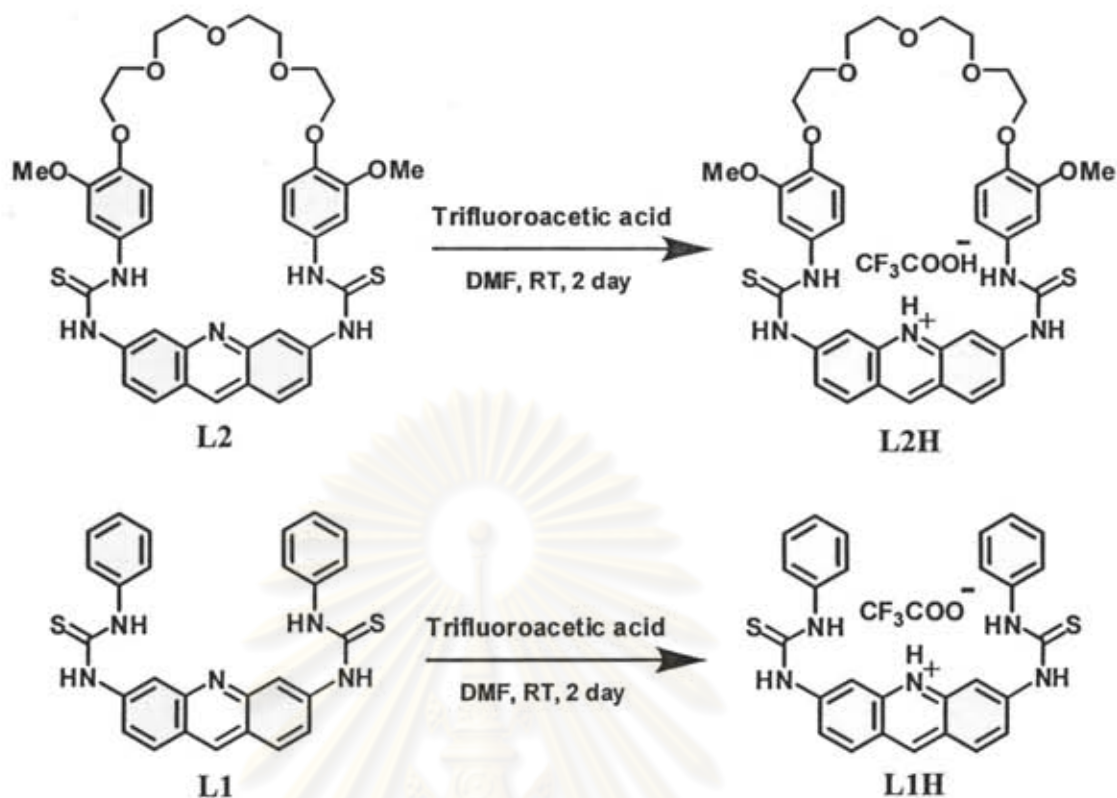


Figure 2.4 The synthetic pathway of final products L1H and L2H.

2.3.2 The complexation studies of ligand L1 and L2 with amino acids by ¹H-NMR technique

Ligand L1 (acyclic form) has thiourea binding site for binding with carboxylate terminal of zwitterions amino acids guest while ligand L2 (cyclic form) has two binding sites which are thiourea and crown-ether like to bind with carboxylate terminal and ammonium terminal of zwitterions amino acids guest, respectively. Moreover, L2 has more rigid structure than the open ligand L1. The chiral recognition is not expected due to the lacking of stereochemically dependent. The amino acids are expected to be zwitterionic form in polar organic solvent (using DMSO as solvent). Thus, complexation studies of both ligands with amino acids such as tryptophan (Trp), phenylalanine (Phe), leucine (Leu), alanine (Ala) and glycine (Gly) as shown in Figure 2.5 were investigated for searching the effect of receptor structure in the binding with amino acids. All amino

acids are used as the optically pure L-enantiomer due to the important species for life and cheaper cost.

The binding properties of **L1** and **L2** toward various amino acids with $^1\text{H-NMR}$ technique were firstly investigated by an addition of excess amount of amino acids (2.5 equiv.) into a solution of **L1** and **L2** in $\text{DMSO-}d_6$. It resulted in remarkable downfield shifts of the NH thiourea resonances particularly, Trp and Phe as shown in Figures 2.6 and 2.7. The complexes of both receptors and guests took through the hydrogen bonding between thiourea based on receptor and carboxylate of zwitterionic amino acids.[65, 66] Beside the downfield shifts of the NH thiourea protons, the changes of acridine protons in case of **L1** (downfield shift of H_d and H_f protons and upfield shift of H_e and H_g protons) upon adding Trp indicated a possibility of the complementary π - π stacking interaction between aromatic amino acid and acridine of host. However, slightly shifts of the acridine protons were observed in case of Phe addition. This result probably caused by the limited solubility of Phe in $\text{DMSO-}d_6$. In addition, a ROESY spectrum of a [**L1**.Trp] clarified the complexation structure observed by the correlation at the aryl protons (H_s and H_y) of Trp and acridine assignments (H_d , H_e and H_f) (shown in Figure 2.8). This strong evidence signified that aromatic moiety based Trp positioned at the acridine group underwent the π - π stacking interaction. An observation of slightly shifts to downfield of NH thiourea protons in the complexation of **L1** with aliphatic amino acids (Leu, Ala and Gly) indicated a weaker interaction due to a lacking of π - π stacking interaction.

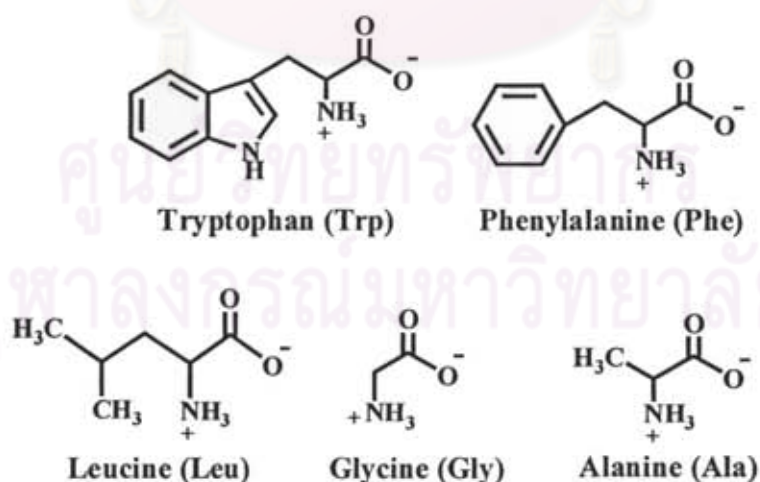


Figure 2.5 The structures of all zwitterionic amino acids in this experiment.

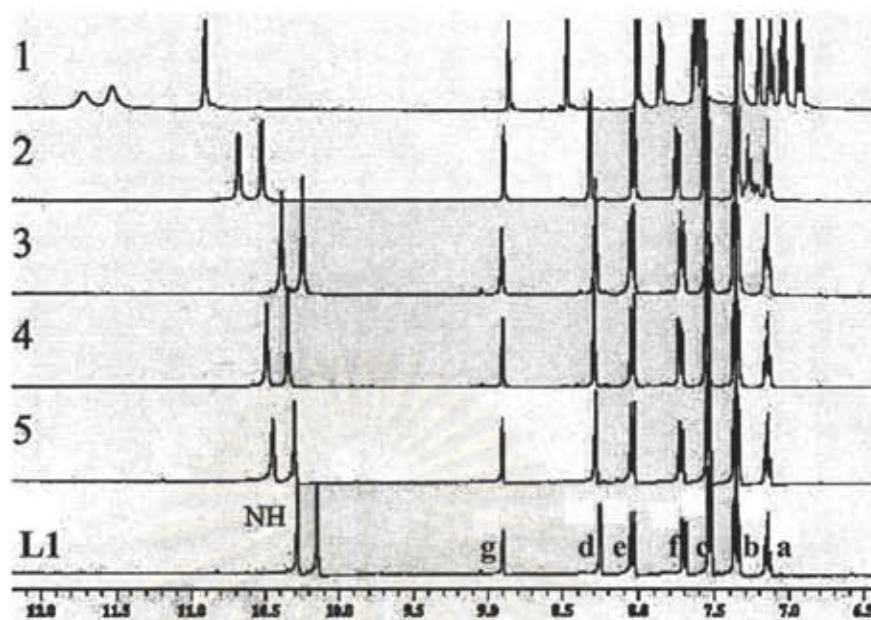


Figure 2.6 $^1\text{H-NMR}$ (400 MHz) of L1 in $\text{DMSO-}d_6$ upon addition of excess amount of (1) Trp, (2) Phe, (3) Leu, (4) Ala, and (5) Gly.

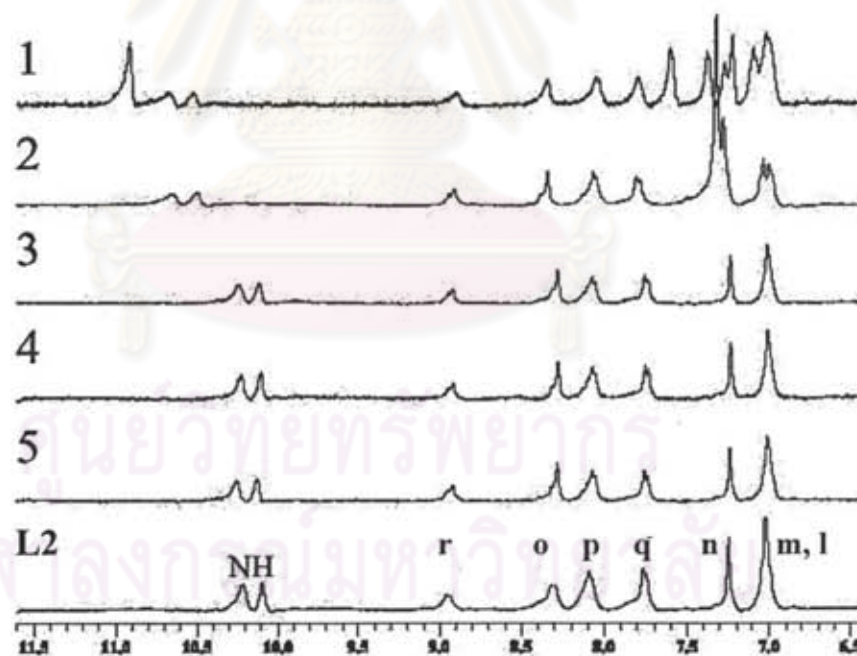


Figure 2.7 $^1\text{H-NMR}$ (400 MHz) of L2 in $\text{DMSO-}d_6$ upon addition of excess amount of (1) Trp, (2) Phe, (3) Leu, (4) Ala, and (5) Gly.

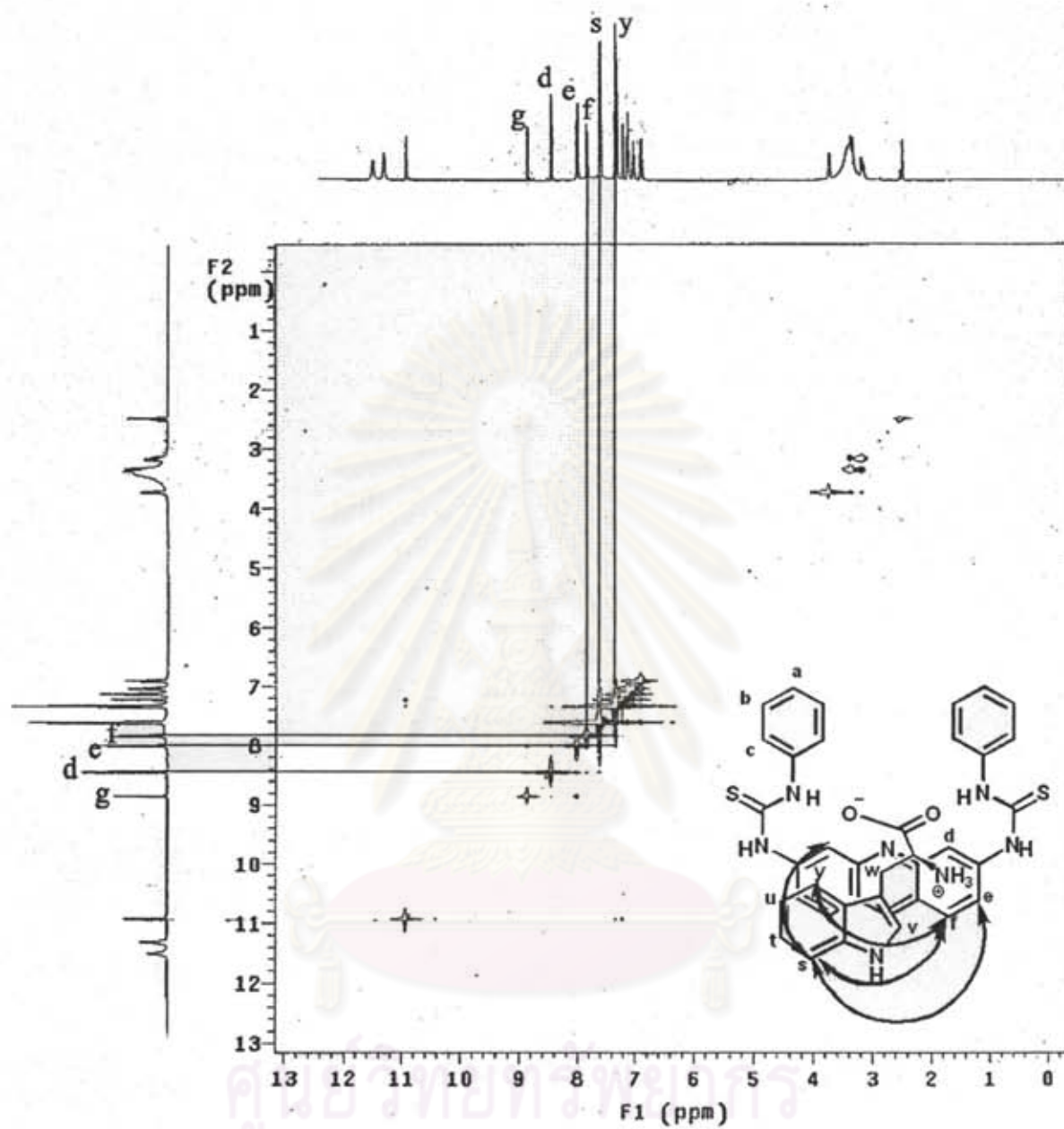


Figure 2.8 ^1H - ^1H ROESY of L1.Trp complex.

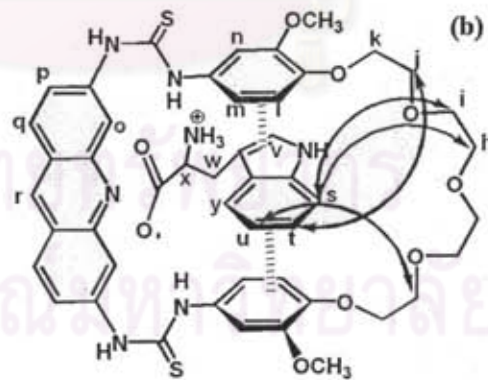
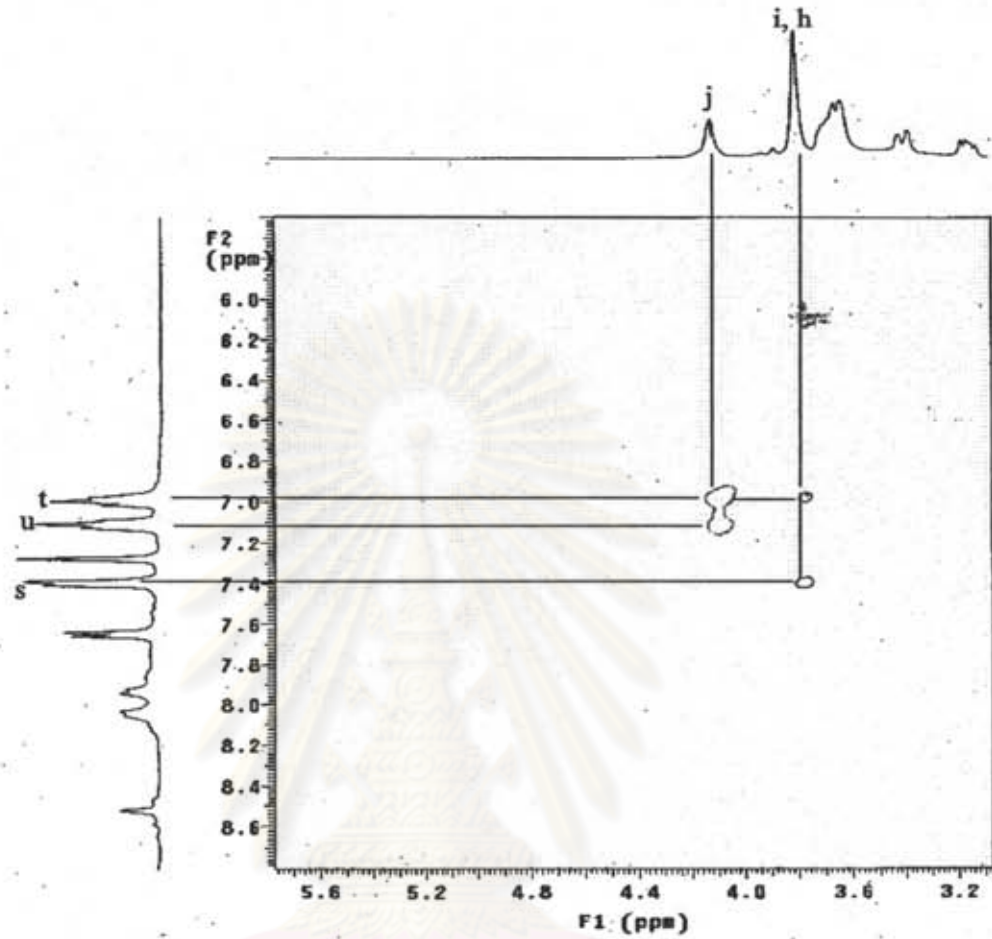


Figure 2.9 ^1H - ^1H NOESY of L2.Trp complex.

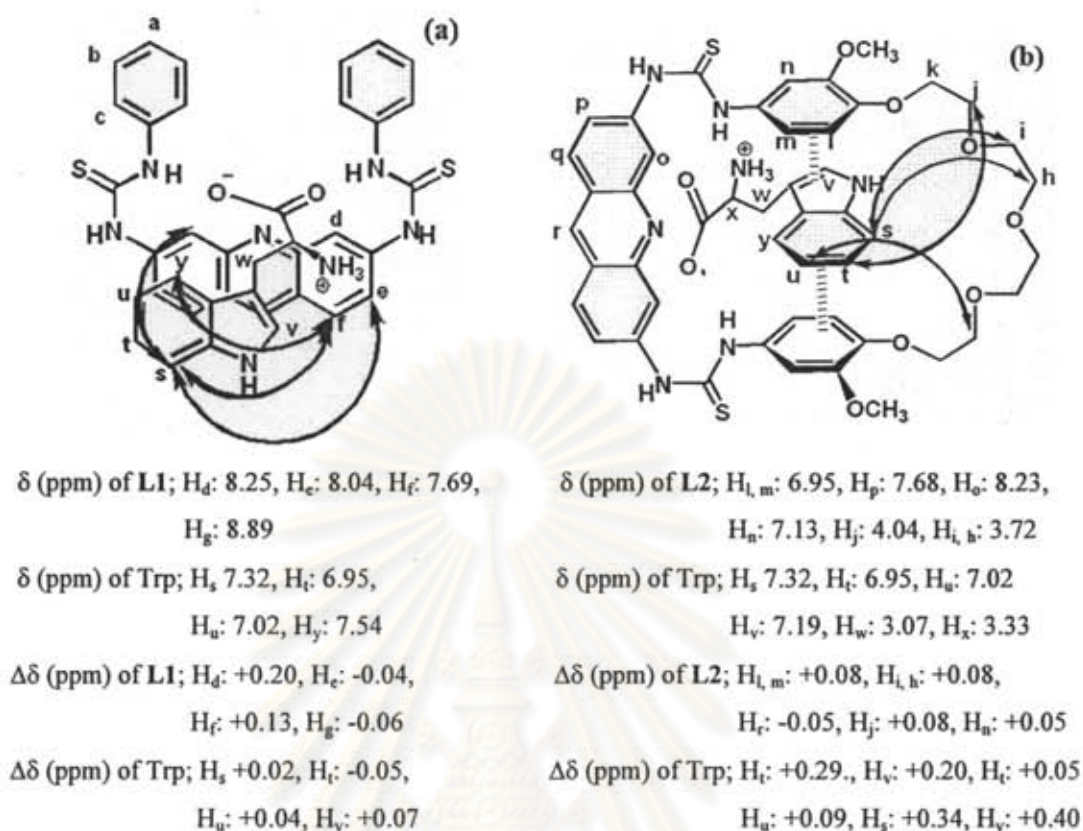


Figure 2.10 The proposed structure of (a) L1.Trp and (b) L2.Trp complexes, consistent with the cross relationship form ROESY and NOESY and the signal of both receptors and Trp.

The downfield shifts of the NH thiourea protons were also monitored in the course of L2 complexation with amino acids. Moreover, an observation of the downfield shifts of phenyl protons (H_l and H_m), acridine protons (H_p and H_o) and crown-like ether protons (H_j) was also found in L2 upon the addition of Trp and Phe. The complex binding of [L2.Trp] was clarified by a NOESY spectrum as shown in Figure 2.9. The cross relation peaks of H_j and H_u as well as H_j and H_t , whereas H_u and H_t are the protons of Trp on the aromatic side chain, were signified for this complex. The cross relation peaks of acridine protons and Trp side chain protons were not observed. It can be rationalized that it is possibly the complementary π - π stacking interaction between

aromatic amino acids and phenyl ring of host. The proposed structures of the complexes of both ligands with Trp are shown in Figures 2.10a and 2.10b. The Job's plots of **L1.Trp**, **L1.Phe**, **L2.Trp** and **L2.Phe** are symmetric and show a maximum mole fraction of guest at 0.5, which indicated a 1:1 guest-host stoichiometry as shown in Figure 2.11.

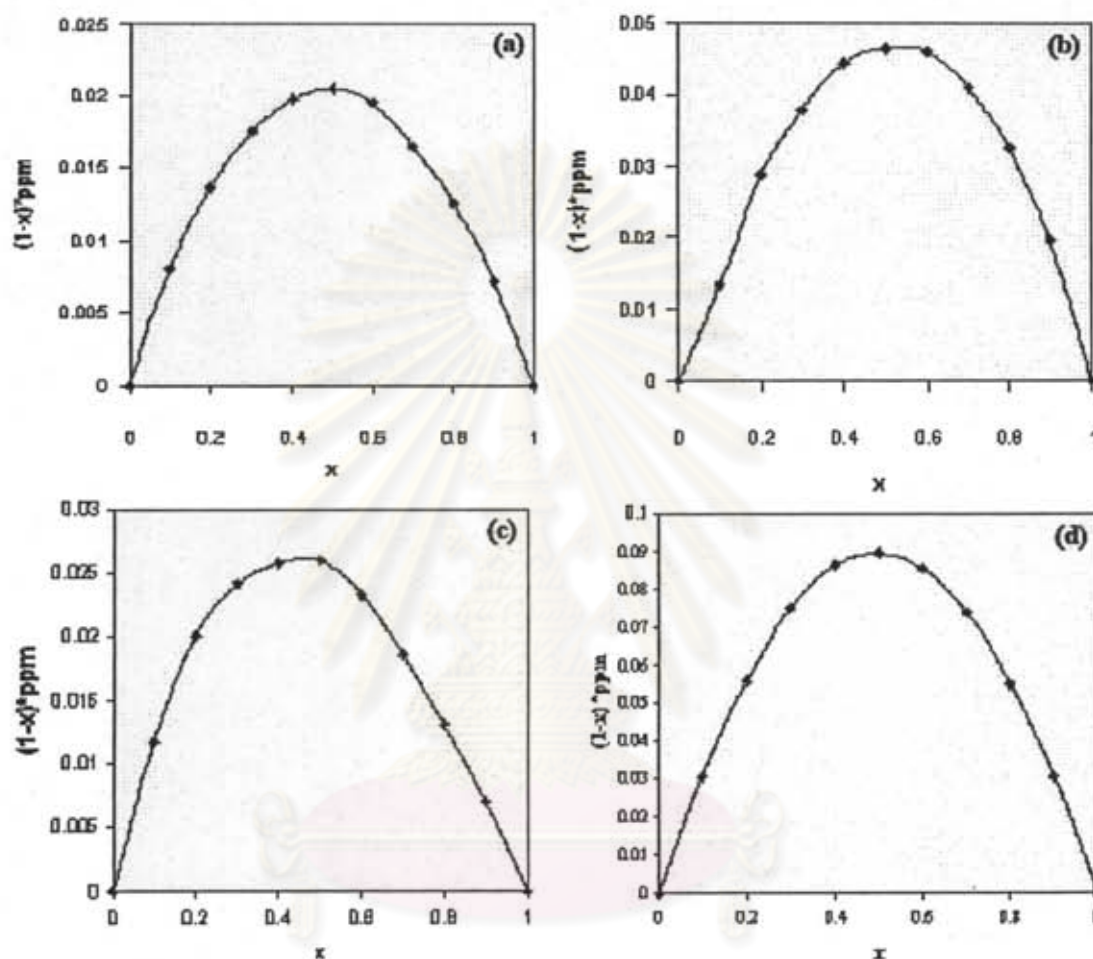


Figure 2.11 Job's plots of the complexation of (a) **L2.Phe**, (b) **L2.Trp**, (c) **L1.Phe** and (d) **L1.Trp** on the chemical shift of NH thiourea.

Beside the confirmation of 1:1 complex stoichiometry using Job's plot NMR technique, a result from mass spectrum of **L2.Trp** complex at $m/z = 938.987$ [$M + 4H^+$] (shown in Figure 2.12) is one evidence to support the complex formation at 1:1 ratio. Unfortunately, it was unsuccessful for obtaining the mass spectra of **L1.Trp**, **L1.Phe** and **L2.Phe** complexes.

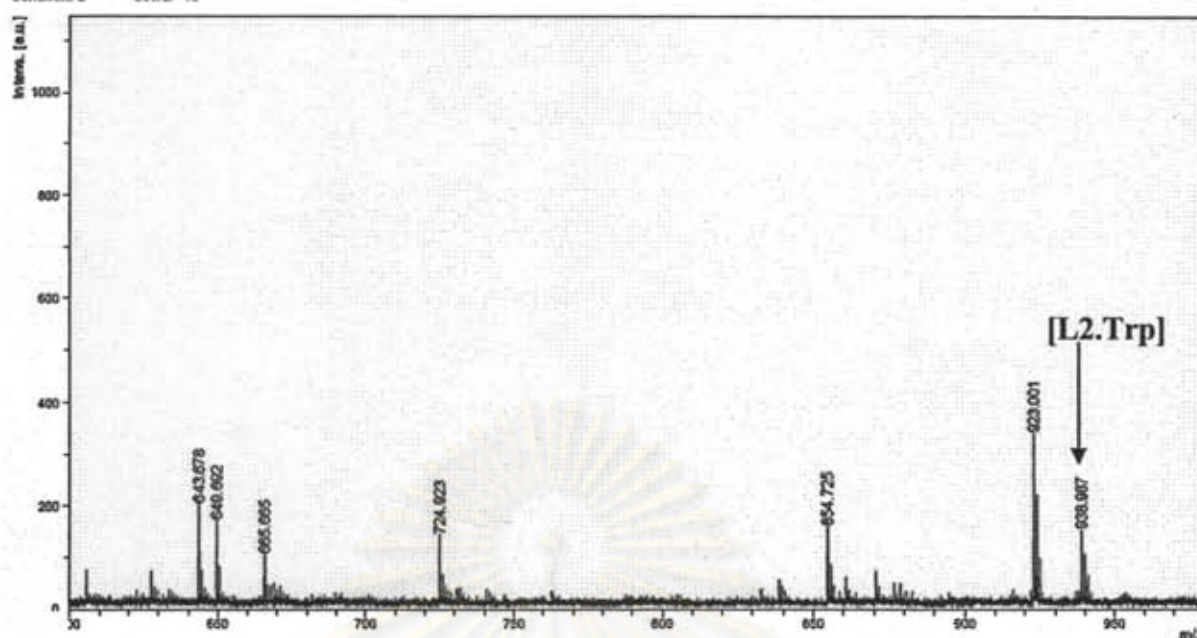


Figure 2.12 The mass spectrum of L2.Trp complex.

2.3.3 The complexation studies by UV-vis technique

2.3.3.1 The complexation studies of ligands L1 and L2 with amino acids by UV-vis technique

Interaction between ligands L1 and L2 with amino acids have been generally studied by $^1\text{H-NMR}$ technique. However, this method suffers from low sensitivity resulting from the relatively high concentrations in both hosts and guests required in order to obtain NMR signals ($10^{-2} - 10^{-3}$ M or more). This makes a limitation in the solubility of amino acids, especially aliphatic amino acids. Moreover, $^1\text{H-NMR}$ signals of the active hydrogen (generally NH) measured becomes very broad upon the complexation with amino acids and overlapping with the aromatic peaks, thereby, making it somewhat more difficult to determine the stability constant of the complex by this method. Thus, it is possible to study the complexation by other techniques such as UV-vis and fluorescence because both ligands (L1 and L2) consist of acridine as a

fluorophore. Herein, we report binding properties of ligand **L1** and **L2** by UV-vis technique.

Absorption or emission intensity of acridine was derived from an inversion of two singlet excited states; $n-\pi^*$ and $\pi-\pi^*$ transition.[67] In aprotic solvent (DMSO in this experiment), the $n-\pi^*$ state is presumably lowest.[67] The characteristic spectra of 3×10^{-5} M of ligand **L1** and 2.5×10^{-5} M of ligand **L2** according to a light yellow solution in DMSO display the same wavelength of a broad band at 400 nm (shown in Figure 2.13).

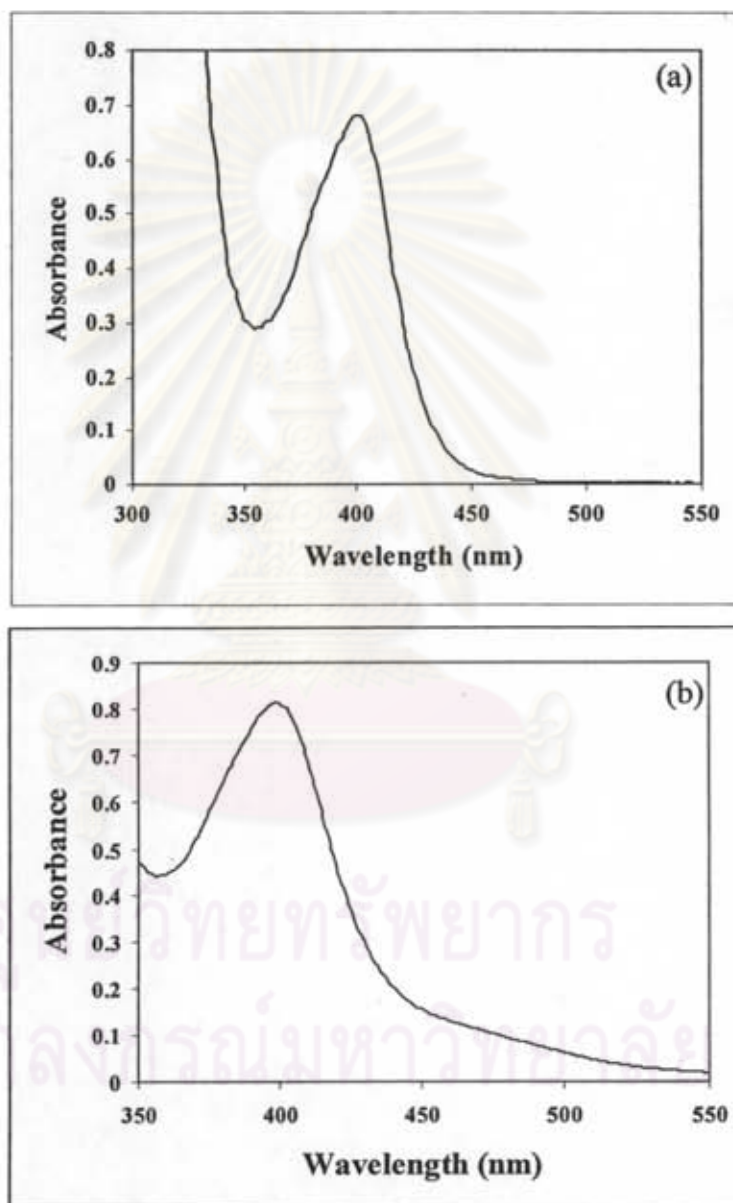


Figure 2.13 The UV-vis absorption spectra of (a) ligand **L1** (3×10^{-5} M) and (b) ligand **L2** (2.5×10^{-5} M).

Absorption spectra of L1 and L2 were measured in DMSO in absence and presence of amino acids (tetrabutylammonium hexafluorophosphate as supporting electrolyte) at 25°C.

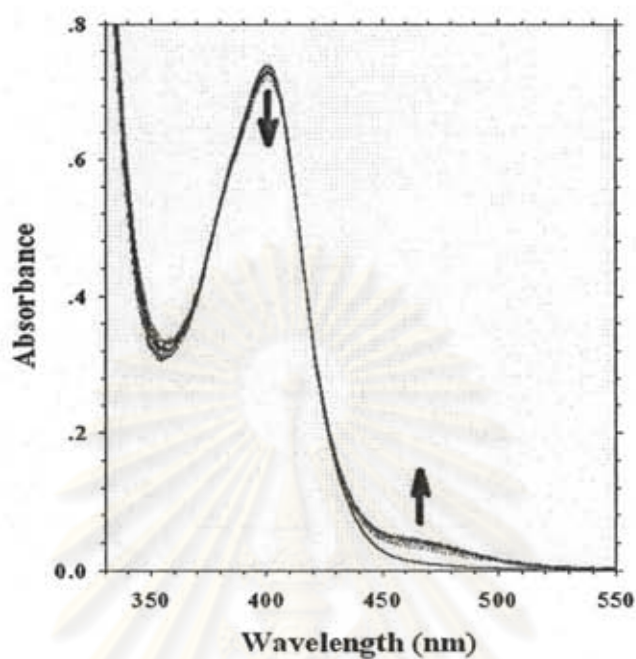


Figure 2.14 Absorption spectra of ligand L1 upon addition of Phe 50 equiv.

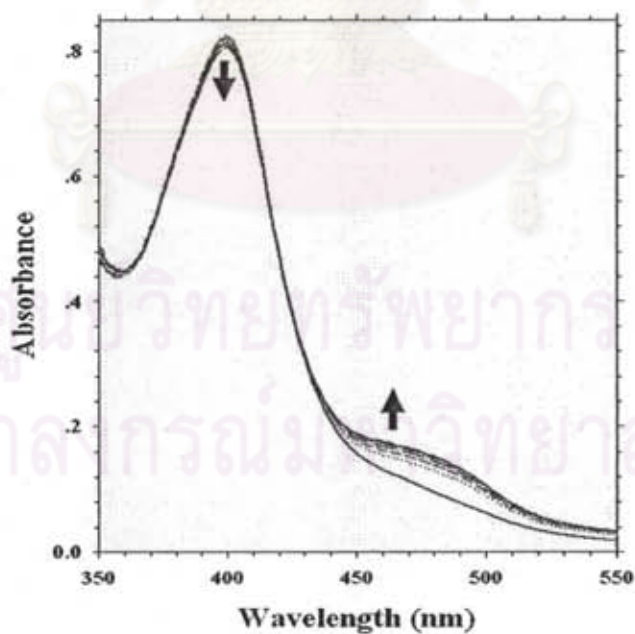


Figure 2.15 Absorption spectra of ligand L2 upon addition of Phe 40 equiv.

Upon the addition of amino acids, the band at 400 nm of **L1** decreased slightly with a concomitant of the appearance of a new band at 460 nm, in particular of Phe added but none in case of other guests whose maximum bands decreased slightly without the appearance of a new band. This result was similarly found in **L2** after adding of aliphatic amino acids (Leu, Ala and Gly). Presumably, the new absorption band at 460 nm corresponds to the acridinium ion produced by the protonation at N-acridine from amino acids. Topp and Diverdi reported that in protic solvent, the “n” electrons on the nitrogen atom in acridine are more tightly bound hydrogen bond in a solvate complex. This hydrogen bond stabilized π - π^* excited state, caused the inversion of level of the lowest excited state and subsequent to the red shift of its absorption band.[67] From titrations, the changes in spectra of **L1** and **L2** were not notable even by adding excess amount of amino acids (as shown in Figures 2.14 and 2.15). This implies that both ligands have not enough efficiency to bind with amino acids. It is presumably due to a repulsion between electron density at N-acridine and a negative charge at carboxylate group of amino acids.

2.3.3.2 The complexation studies of ligands **L1H** and **L2H** with amino acids by UV-vis technique

To solve this problem about the weak complexation of **L1** and **L2** with amino acids, ligands **L1H** and **L2H** were designed and prepared. Electron density at N-acridine was reduced by protonation to obtain NH^+ -acridinium ion. We expected that **L1H** and **L2H** will improve the binding ability with amino acids.

As mentioned before, the absorption or emission intensity of acridine was derived from an inversion of two excited states; n - π^* and π - π^* transition. After the protonation at N-acridine, the π - π^* excited state is presumably lowest because the “n” electrons on the nitrogen atom are more tightly bound with protons. This resulted in a shift of absorption band to a longer wavelength.[67] The characteristic spectra of 2.5×10^{-5} M of ligand **L1H** and 2.0×10^{-5} M of **L2H** according to an orange solution in DMSO showed a broad band at 460 nm as shown in Figure 2.16.

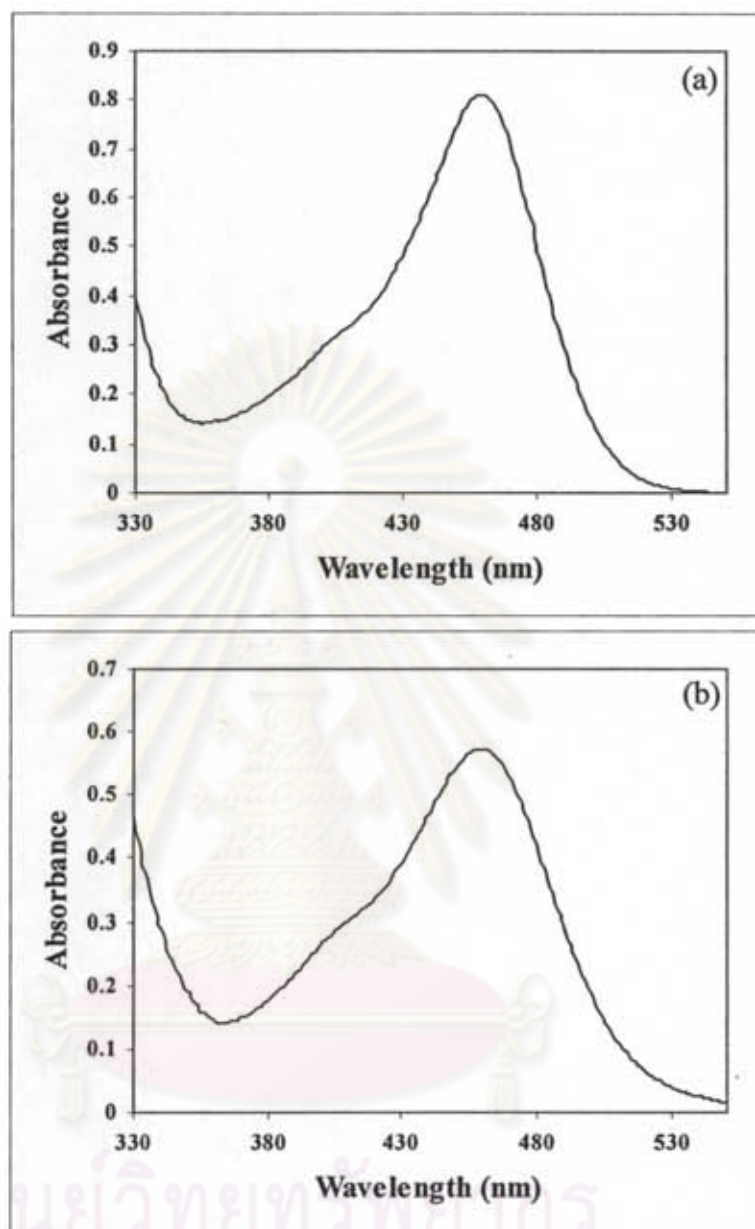


Figure 2.16 The UV-vis absorption spectra of (a) ligand L1H (2.5×10^{-5} M) and (b) ligand L2H (2.0×10^{-5} M).

Absorption spectra of L1H and L2H were carried out in DMSO in absence and presence of amino acids (tetrabutylammonium hexafluorophosphate as supporting electrolyte) at 25°C.

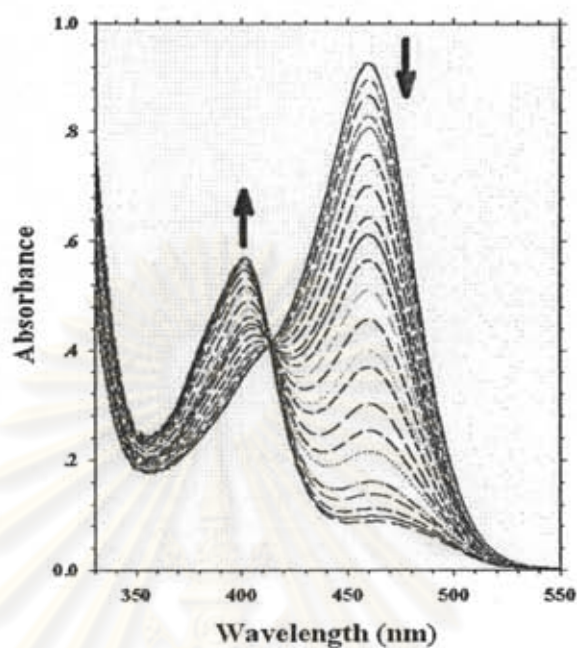


Figure 2.17 Absorption spectra of ligand L1H upon addition of Phe 30 equiv.

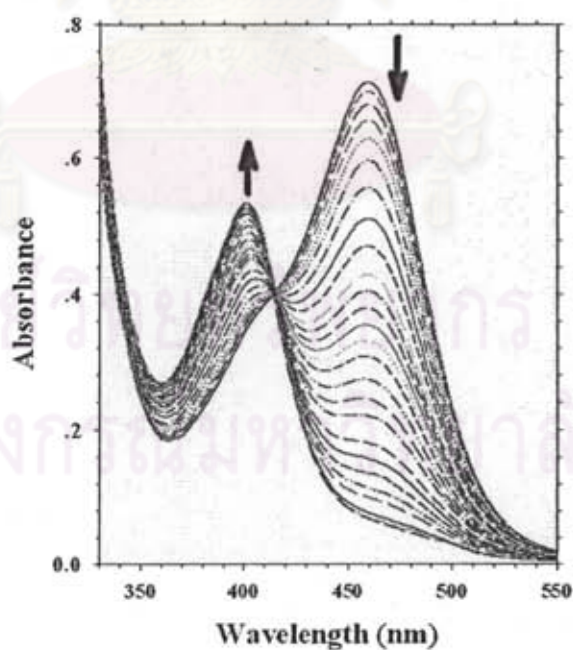


Figure 2.18 Absorption spectra of ligand L2H upon addition of Phe 30 equiv.

More interestingly, a study of UV-visible spectra of **L1H** and **L2H** upon addition of Phe displays dramatic changes (shown in Figure 2.17 and 2.18, respectively). The absorption band of **L1H** and **L2H** at 460 nm is progressively decreased while a new band at 400 nm forms and develops upon adding amino acids. An isobestic point at 415 nm revealed that only two species coexisted at the equilibrium. Similar UV-vis spectra were found with other amino acids addition. This change in absorption spectra reflects the transformation from NH^+ -acridinium to neutral N-acridine, observing from the disappearance of the band at 460 nm and the appearance of the band at 400 nm. This means that the carboxylate group of the added zwitterionic amino acid can bind strongly with NH^+ -acridine moiety and consequently induce the proton transfer of NH^+ -acridinium ion.

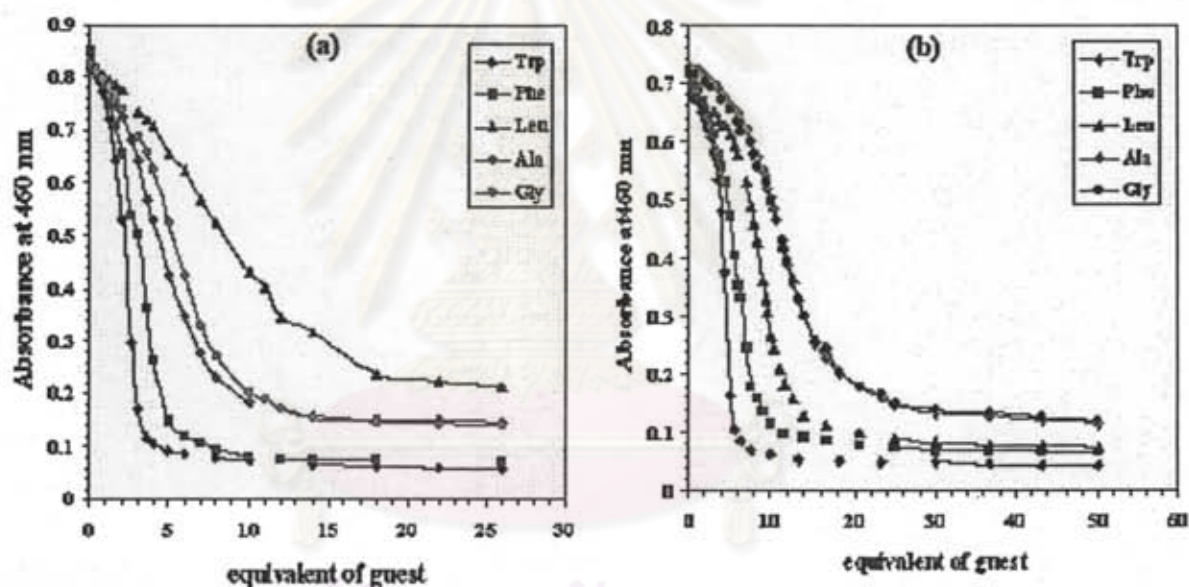


Figure 2.19 Plot of absorbance of (a) **L1H** (2.5×10^{-5} M) and (b) **L2H** (2.0×10^{-5} M) at 460 nm in DMSO as a function of equivalent of amino acids addition.

In addition, Figure 2.19 depicts the titration curve of **L1H** and **L2H** with different amino acids by monitoring the decrease of the absorption band at 460 nm. It was found that ligands **L1H** and **L2H** have a factor to bind Trp over other guests observing from the significant change of spectral in both receptors. From Figure 2.19a, the addition of 5

equiv of Trp induced the complete disappearance of the absorption band at 460 nm of **L1H** while the other amino acids need more than 10 equiv to suppress this band completely. The same results observed in Figure 2.19b for **L2H** exhibited the complete disappearance of the absorption band at 460 nm with 10 equiv Trp and more than 20 equiv of other amino acids. Presumably, the basicity of Trp at carboxylate group is over other amino acids (Table 2.10) resulting in the fast proton transfer with acridinium ligand which was held by hydrogen bonding interaction between carboxylate and NH^+ in form of $\text{R-COO}^- \cdots \text{H} \cdots \text{N}^+$ -acridinium and the complementary electrostatic force. The results showed that the protonation at N-acridine can improve the binding ability with amino acids.

Table 2.10 The basicity of various amino acids.[9]

Amino Acid	pK_1	pK_2	pI
Glycine	2.34	9.60	5.97
Alanine	2.34	9.69	6.00
Leucine	2.36	9.60	5.98
Valine	2.32	9.60	5.98
Proline	1.99	10.60	6.30
Phenylalanine	1.83	9.13	5.48
Tryptophan	2.83	9.39	5.89
Tyrosine	2.20	9.11	5.66

2.3.4 The complexation studies of ligands **L1H** and **L2H** with amino acids by $^1\text{H-NMR}$ titration technique

The binding properties of **L1H** and **L2H** toward various amino acids were examined by $^1\text{H-NMR}$ titration in $\text{DMSO-}d_6$ to deduce the intermolecular proton transfer at NH^+ -acridinium by amino acids.

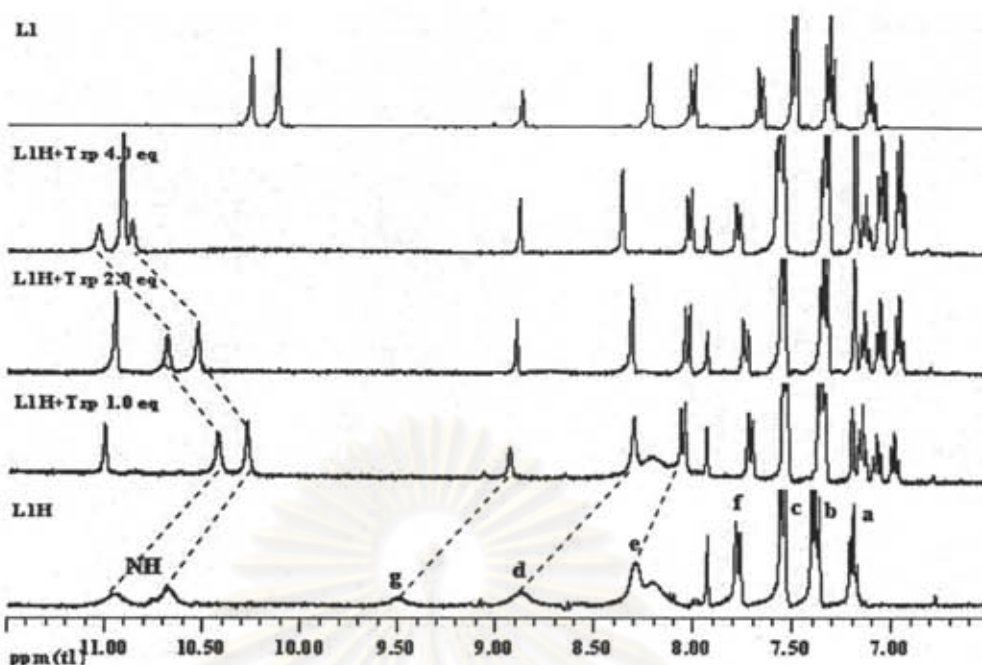


Figure 2.20 ¹H-NMR titration spectra of L1H (3.0×10^{-3} M) in DMSO- d_6 upon addition of Trp 1.0, 2.0 and 4.0 equivalent, in comparison with ¹H-NMR spectra of L1 (3.0×10^{-3} M).

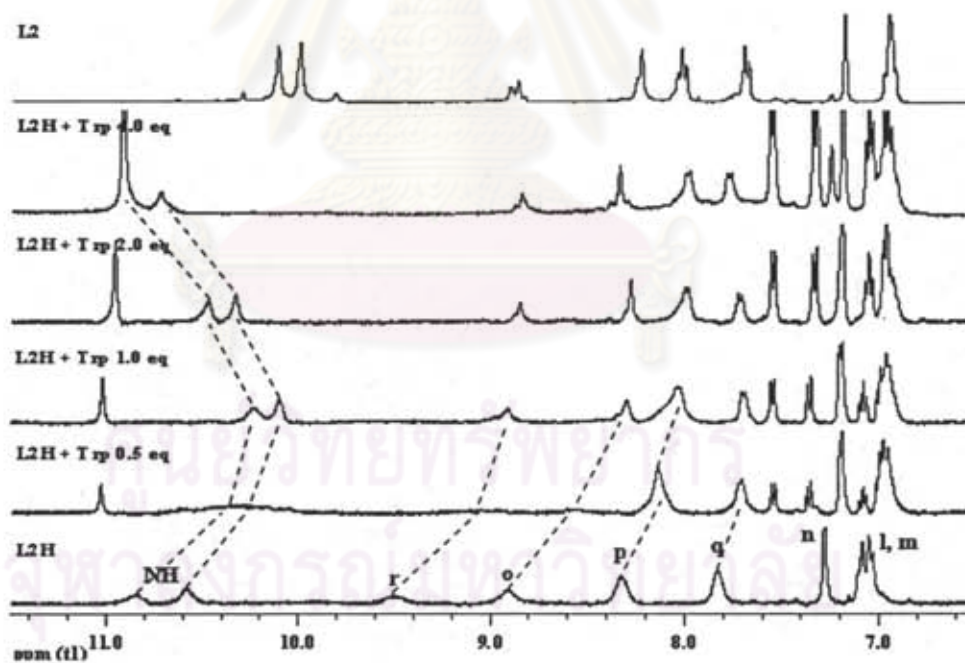


Figure 2.21 ¹H-NMR titration spectra of L2H (3.0×10^{-3} M) in DMSO- d_6 upon addition of Trp 0.5, 1.0, 2.0 and 4.0 equivalent, in comparison with ¹H-NMR spectra of L2 (3.0×10^{-3} M).

Considering $^1\text{H-NMR}$ titration techniques, the results gave the strong evidence to support the deprotonation process of **L1H** and **L2H** in the presence of amino acids. As seen from the spectra shown in Figures 2.20 and 2.21, the NH thiourea and acridine protons (H_g , H_d , H_e , H_f , H_r , H_o , H_p and H_q) exhibited the gradual upfield-shift at the beginning of Trp added and all protons did not further shift to highfield after adding Trp reached 1 equiv. At this point, the proton signals of **L1H** are not at the same position as **L1** signals. This revealed that the transformation of NH^+ -acridinium to N-acridine took through the intermolecular proton transfer not the deprotonation process. The addition of Trp beyond 1 equiv induced the downfield shift of the NH thiourea protons. This shift was a consequence of the binding of amino acids to the thiourea binding site under hydrogen bonding interaction. In case of Phe shown in Figure 2.22 and aliphatic amino acids, the proton transfer processes of **L1H** by Phe were not completed and the downfield shift of the thiourea protons is not observed even adding the excess amount of amino acids but the NMR titration spectra of **L2H** in Figure 2.23 showed the shift to downfield of the thiourea protons after adding Phe more than 2.5 equivalents. It is probably due to the highest pK_1 of carboxylate group in Trp which causes a good intermolecular proton transfer at NH^+ -acridinium ion to carboxylate group of amino acids.



ศูนย์วิทยทรัพยากร
จุฬาลงกรณ์มหาวิทยาลัย

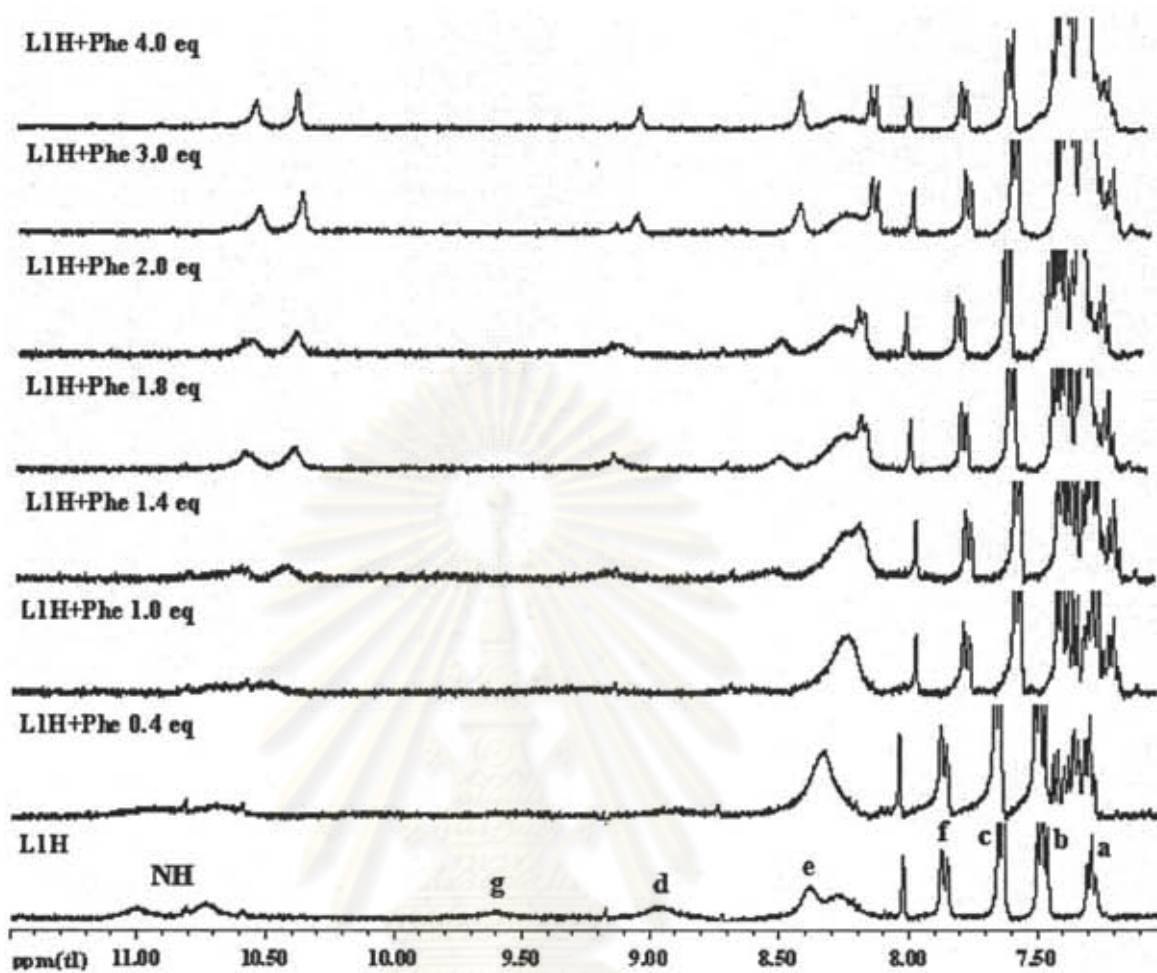


Figure 2.22 ^1H -NMR titration spectra of L1H (3.0×10^{-3} M) in $\text{DMSO-}d_6$ upon addition of Phe 0.4, 1.0, 1.4, 1.8, 2.0, 3.0 and 4.0 equivalent.

ศูนย์วิทยทรัพยากร
จุฬาลงกรณ์มหาวิทยาลัย

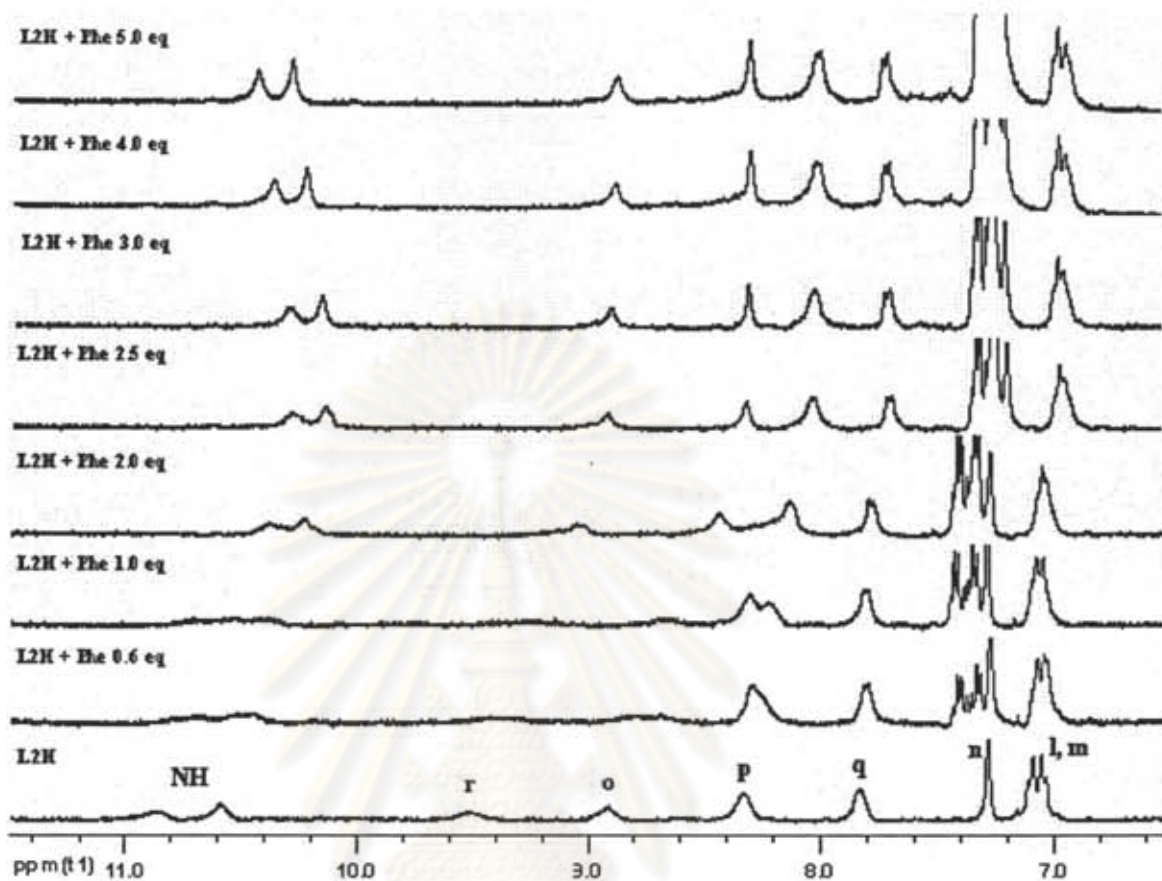


Figure 2.23 $^1\text{H-NMR}$ titration spectra of L2H (3.0×10^{-3} M) in $\text{DMSO-}d_6$ upon addition of Phe 0.6, 1.0, 2.0, 2.5, 3.0, 4.0 and 5.0 equivalent.

ศูนย์วิทยทรัพยากร
จุฬาลงกรณ์มหาวิทยาลัย

2.3.5 The complexation studies of ligands L1, L2, L1H and L2H with amino acids by fluorescence technique

The fluorescence intensity of acridine is strongly dependent on solvent and varies from being extremely weak in hydrocarbon solvents to moderately strong in aqueous solution. For example, the acridine fluorescence quantum yields were found to be about 1.2% and < 0.1% in formamide (hydrogen bonding) and dimethylformamide (non-hydrogen bonding but similarly polarity), respectively. This dependence of fluorescence quantum yield on solvent has been postulated to derive from an inversion of two close-lying singlet states, $^1n-\pi^*$ and $^1\pi-\pi^*$. [67, 68] In this experiment, DMSO which is non-hydrogen bonding solvent was used. Thus, the fluorescence intensities of acridine and acridinium group in L1, L2, L1H and L2H are very low.

Ligands L1 and L2 showed emission band at 520 and 528 nm, respectively. These emission bands were derived from a transition to $^1n-\pi^*$ excited state. [67] From fluorescence titration studies of both ligands with amino acids, a similar fluorescence emission change of L1 (shown in Figures 2.24 and 2.25) and L2 (shown in Figures 2.26 and 2.27) showed a slightly enhancement of emission band at 520 nm and 528 nm for L1 and L2, respectively. A large enhancement was observed for aromatic amino acid (Trp and Phe), especially in the case of L2. This means that L2 bound with aromatic amino acids more effectively. It can be rationalized from a more rigid structure of L2 (cyclic structure) and a forming of multiple $\pi-\pi$ stacking interaction between aromatic amino acid side chain and the phenyl ring of the host as seen in Figure 2.10. The lacking of $\pi-\pi$ stacking interaction in case of aliphatic amino acids reduced the binding efficiency. The nonemissive via PET mechanism of the unbound L1 and L2 might be ascribed that the electron-donating ability of heteroatom in acridine behaves under the electron transfer quenching pathway. For bound L1 or L2 with amino acids, this quenching pathway was eliminated possibly due to the protonation on N-atom of acridine by amino acids.

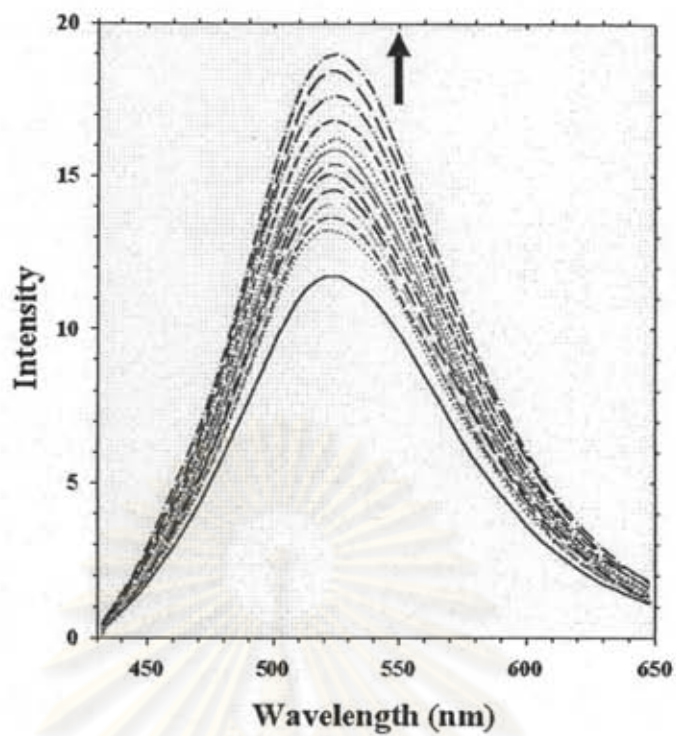


Figure 2.24 The emission spectra of L1 (2.0×10^{-4} M) upon adding Trp 30 equivalent.

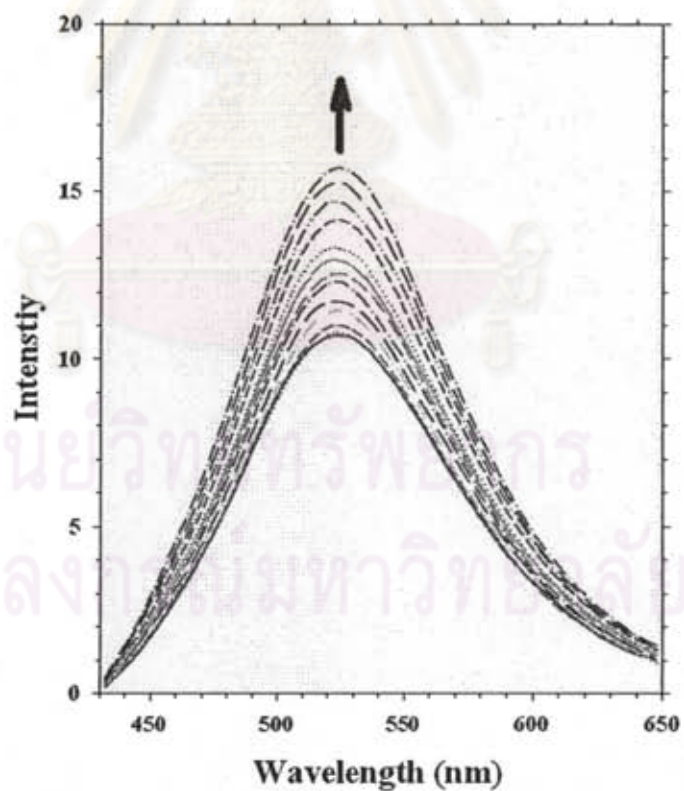


Figure 2.25 The emission spectra of L1 (2.0×10^{-4} M) upon adding Phe 30 equivalent.

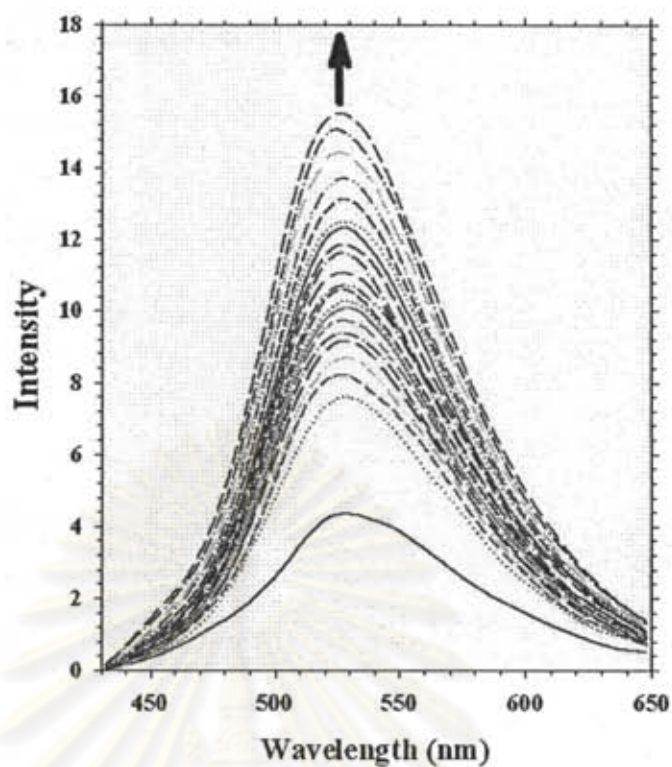


Figure 2.26 The emission spectra of L2 (2.0×10^{-4} M) upon adding Trp 30 equivalent.

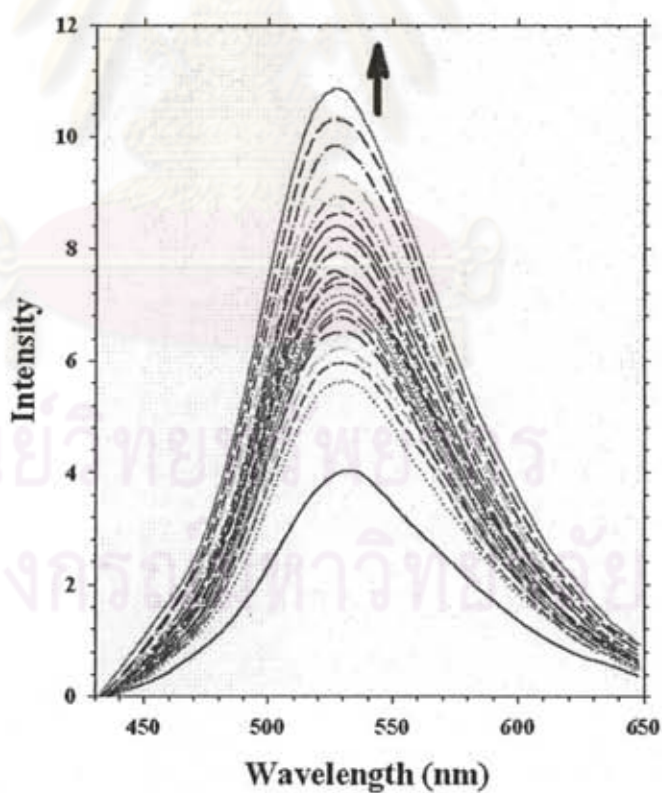


Figure 2.27 The emission spectra of L2 (2.0×10^{-4} M) upon adding Phe 30 equivalent.

The emission bands of **L1H** and **L2H** were observed at 535 and 545 nm, respectively. These bands undergo a small hypsochromic shift (15 nm and 17 nm in comparison with emission band of **L1** and **L2**, respectively). These red shifts are presumably due to the inversion from $n-\pi^*$ to $\pi-\pi^*$ excited state. More interestingly, a study of fluorescence titration spectra of **L1H** and **L2H** upon addition of amino acids displayed dramatically changes. From Figures 2.28 and 2.29, the fluorescence intensity of **L1H** at 535 nm was gradually enhanced upon gradual increase of the concentration of Trp and Phe, respectively. It was found not only the enhancement but also the shift of emission band from 535 to 520 nm. This blue shift reflects the transformation from acridinium to acridine via the intermolecular proton transfer by amino acids. The titration with other amino acids also showed dramatically enhancement in particular of Trp inducing the largest enhancement. Upon addition of Trp to **L2H** as shown in Figures 2.30 and 2.31, the enhancement of emission band at 545 nm was also observed and the blue shift was found from 545 to 528 nm instead. The titration results of **L2H** with all amino acids gave the same results as those of **L1H**.

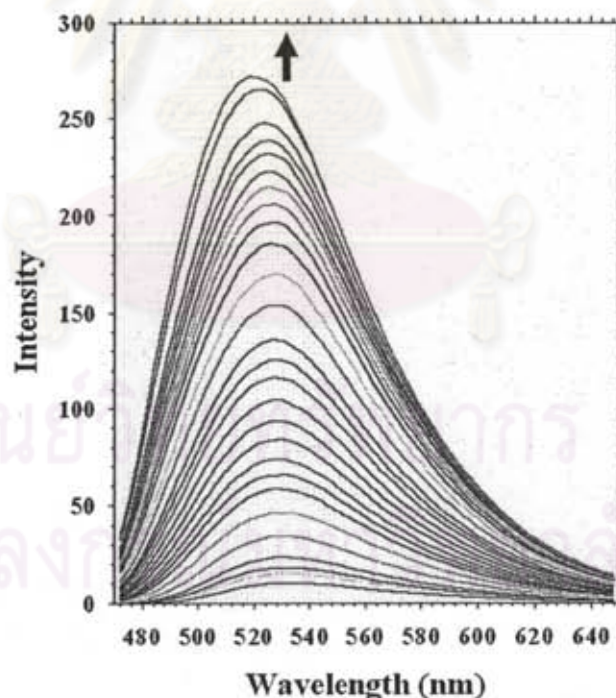


Figure 2.28 The emission spectra of **L1H** (2.0×10^{-4} M) upon adding Trp 25 equivalent.

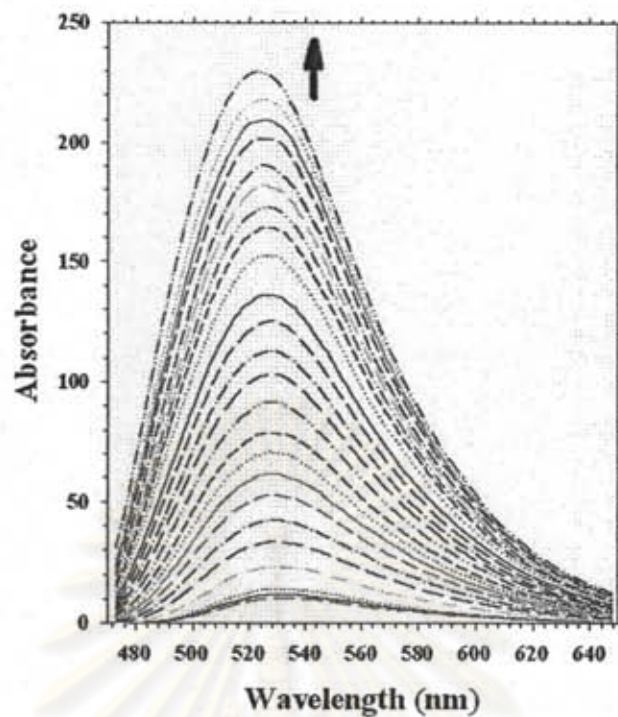


Figure 2.29 The emission spectra of L1H (2.0×10^{-4} M) upon adding Phe 25 equivalent.

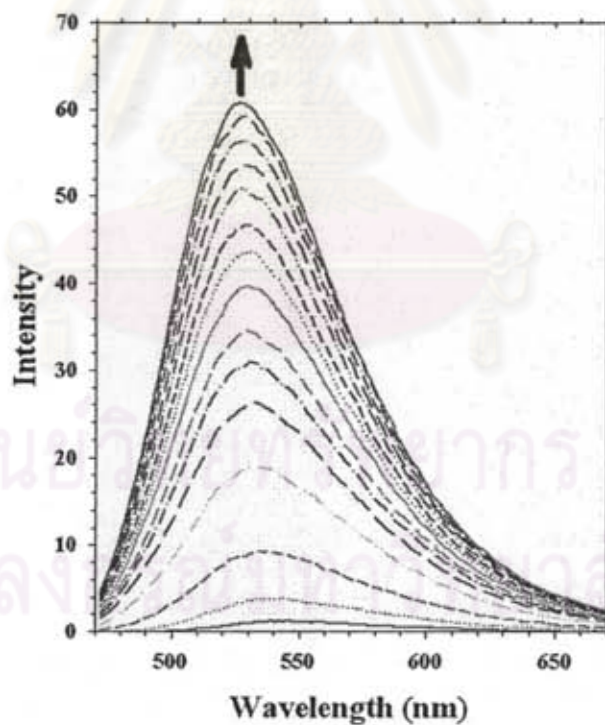


Figure 2.30 The emission spectra of L2H (2.0×10^{-4} M) upon adding Trp 30 equivalent.

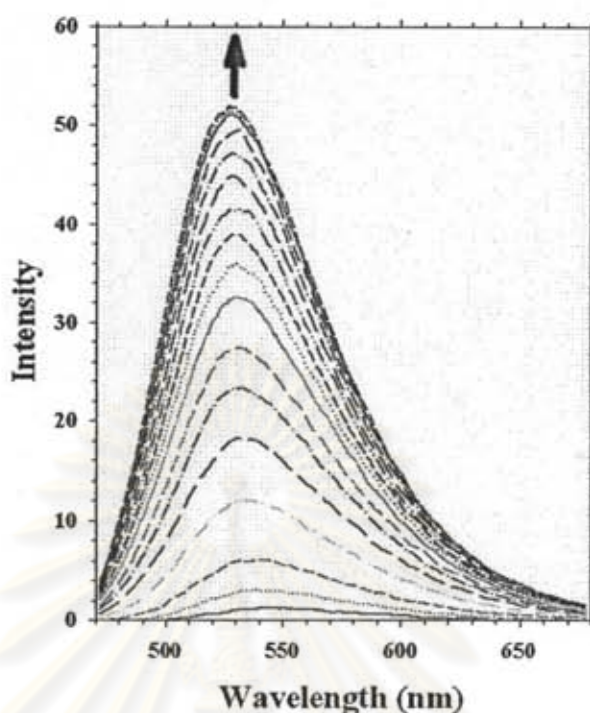


Figure 2.31 The emission spectra of L2H (2.0×10^{-4} M) upon adding Phe 30 equivalent.

Fluorescence titration experiments were carried out repeatedly in the presence of amino acids for investigating the binding constants and the fluorescence enhancement factor (FE) of the complex formation of all ligands with amino acids. The binding constants were calculated using Benesi-Hildebrand equation[51] for 1:1 association between host and guest. The FE values were determined as the ratio of fluorescence intensity in the presence and in the absence of amino acids. Tables 2.11 and 2.12 summarized the binding constants (K) and the fluorescence enhancement factor (FE), respectively, for all receptors in the presence of various amino acids.

จุฬาลงกรณ์มหาวิทยาลัย

Table 2.11 The binding constants of interaction between **L1**, **L1H**, **L2** and **L2H** with amino acids calculated from fluorescence titration using Benesi-Hildebrand equation.

	K				
	Trp	Phe	Leu	Ala	Gly
L1	266	<i>a</i>	<i>a</i>	<i>a</i>	<i>a</i>
L1H	2873	2365	1418	1483	1367
L2	307	578	<i>a</i>	219	<i>a</i>
L2H	3157	2748	855	900	957

a = cannot be calculated

Table 2.12 Fluorescence enhancement factors^b (FE) of receptors **L1**, **L1H**, **L2** and **L2H** with various guests.

	FE				
	Trp	Phe	Leu	Ala	Gly
L1	1.53	1.42	1.29	1.35	1.28
L1H	24.17	20.98	18.86	17.55	17.99
L2	3.12	2.42	1.22	1.77	1.73
L2H	34.42	31.43	27.42	26.13	22.52

^b FE values were calculated as the ratio of fluorescence intensity in the presence and in the absence of each guest.

Corresponding of the data in both tables demonstrated that the FEs of **L2** (cyclic structure) with aromatic amino acids exhibit the higher value than those of **L2** with aliphatic amino acids. It is shown that the rigidified **L2** containing the crown-like ether selectively bound with aromatic amino acids which were fitted the cavity inside. On the contrary, there is no significant difference in FE values of **L1** (acyclic structure) with all amino acids possibly caused by the preferential binding of open form (**L1**) toward all guests. From Tables 2.11 and 2.12, **L1H** and **L2H** showed much higher binding constants and FE values than **L1** and **L2**, respectively. This suggested that the acridinium receptor

improved the binding ability to amino acids. Rebek and Nemeth have been reported that lacking ionic character at N-acridine and a well-placed aromatic ring showed no evidence of binding to aromatic amino acids.[62] In the case of **L1** and **L2**, the binding properties with amino acids are poor because there is a repulsion from electron density at N-acridine and a negative charge at carboxylate group of zwitterion amino acids. After acridine is turned to be acridinium form, both **L1H** and **L2H** have abilities to bind with amino acids effectively due to the losing of electron density at N-acridine by the protonation. Interaction between acridinium ligands and amino acids is proposed by a combination of proton transfer from NH^+ -acridinium to carboxylate group of entering zwitterionic amino acids with hydrogen bonds, hydrogen bonding interaction of carboxylate with thiourea and also the complementary electrostatic force. Considering the K and FE values for **L1H** and **L2H**, the binding with Trp showed the highest value because of the strongest basicity of Trp (pK_1 for Trp, Phe, Leu, Ala and Gly are 2.83, 1.83, 2.36, 2.34 and 2.34, respectively).[9] It is indicative of the strong complex formation over other amino acids.



ศูนย์วิจัยทรัพยากร
จุฬาลงกรณ์มหาวิทยาลัย

CHAPTER III

STEROIDAL RECEPTOR FOR AMINO ACIDS

3.1 Introduction

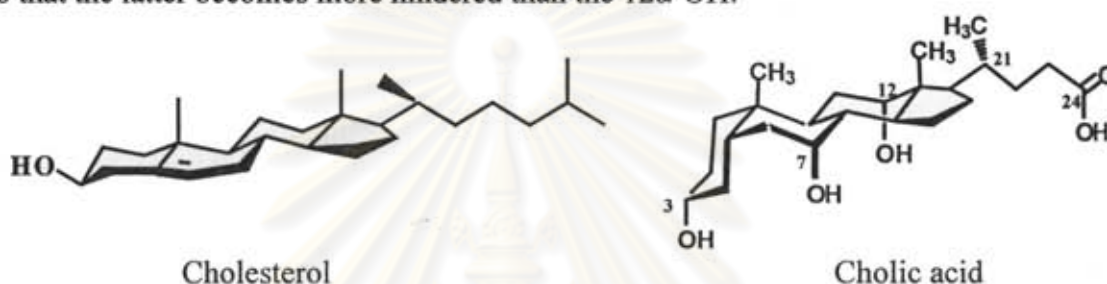
3.1.1 Steroids in Supramolecular Chemistry [69]

Receptor design is governed largely by the concept of preorganization, the creation of a binding site of well-defined shape which complements the structure of the target species. Nature achieves this goal with flexible, linear molecules which fold into particular conformations. This approach is not yet realistic for the supramolecular chemist. Modelling software cannot be relied upon to predict the conformation of complex linear structures and the creative exploitation of folding is still more difficult. In practice, the design of synthetic receptors is strongly reliant on rigid subunits which can be used to define clefts and cavities and can serve as scaffolds for organized arrays of functional groups.

When supramolecular chemists require a rigid unit, the most obvious choice is usually an aromatic ring. However, fused alicyclic systems may be equally rigid and can play a complementary role. They have certain intrinsic advantages; for example, they are usually chiral and possess two valencies (and thus two orientations) at each non-bridging center. One fragment which has been under-utilized is the steroid nucleus. It is one of the largest rigid units which are readily available. Moreover, because of the importance of steroids in biochemistry and medicine, their chemistry is understood in great detail.

The steroid nucleus which is one of the largest rigid units consists of four fused rings covering an area of ca. $10 \times 6 \text{ \AA}$. It presents two options for substitution (axial or equatorial) at most positions and occurs in homochiral form. There are many steroids which are commercially available and might be chosen as starting materials for more elaborate frameworks. There are two examples; cholesterol and cholic acid. Cholesterol is functionalized at one end and can easily be appended to a structure. Moreover, oxidative degradation of the side chain gives a second point of attachment, allowing the

nucleus to be used as a rigid spacer. However, the lack of functional groups in the central portion of the framework limits cholesterol's potential. In contrast, Cholic acid is more promising. The nucleus is substituted with three secondary hydroxyl groups, while the side-chain is terminated by a carboxyl. The hydroxyl groups are fairly evenly spaced around the periphery and usefully, from the point of view of receptor design, are co-directed. The *cis*-AB ring junction imparts a curved profile (again useful for receptor design), and assists in differentiating between the hydroxyl groups. The 3 α group is rendered equatorial while the others are axial. This group is less hindered than the axial 7/12 α hydroxyls. Also, a CH₂ unit is placed in a 1,3-diaxial relationship with the 7 α -OH, so that the latter becomes more hindered than the 12 α -OH.



Recently, many research groups have been exploring the potential of steroids as scaffolds in supramolecular chemistry, with special emphasis on the exploitation of cholic acid. A substantial part of many works has been in the area of anion recognition, where the steroid can contribute by providing a scaffold on which to mount polar functional groups and lipophilic surfaces to promote solubility in non-polar media.[70, 71]

3.1.2 Steroid-based anion and amino acid receptors[69]

Cholic acid can be converted into a series of neutral anionophores targeted at inorganic anions or amino acids. Interestingly, it is extended and able to support well-separated functional groups and rigid, such that these groups cannot easily interact with each other. The curved profile of cholic acid and co-directed hydroxyl groups naturally lend themselves to the creation of macrocyclic or cleft-type architectures with polar interiors and apolar exteriors. The hydroxyl groups at C3, C7 and C12 may be

differentiated and converted to a range of other functional groups, while side chain carboxyl affords further possibilities.

As H-bond donors in supramolecular chemistry, NH units are far more versatile than OH groups. The third valence on the nitrogen can be exploited structurally and can also be used to tune the hydrogen bond donor strength. These advantages were exploited in a series of steroid-based receptors, represented schematically by a structure in Figure 3.1. Instead of constructing elaborate frameworks derived from more than one steroid unit, synthetic effort was focused on modifying the functional groups on a single molecule of cholic acid. In the resulting cholapod with multiple NH units converge on a binding site beneath the α -face of the steroid. The NH groups may belong to amides, sulfonamides, carbamates, ureas or thioureas. NH acidity and hydrogen bond donor strength can be controlled by variation of electron withdrawing groups Z.

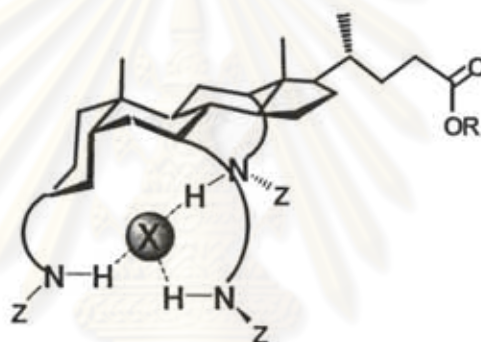
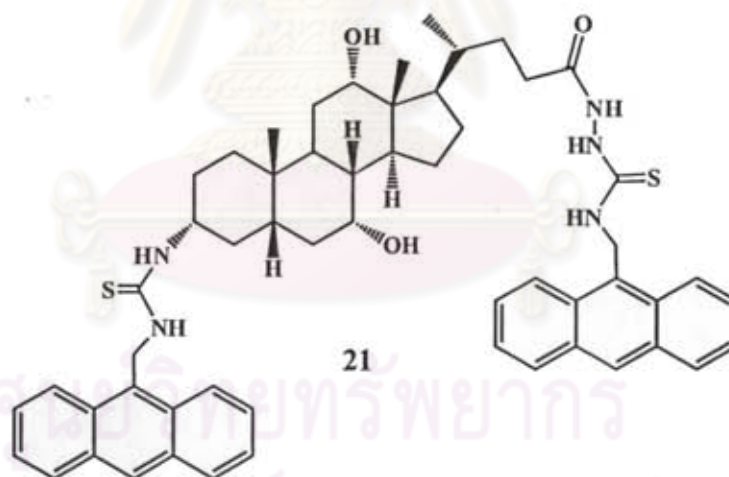


Figure 3.1 Structure of cholapod with multiple NH units.

In case of the binding with amino acids, amino and carboxyl groups in amino acids are expected to act as binding sites for hydrogen bonding and electrostatic interactions. Beside urea and thiourea units, guanidinium cation is well-established as a center for carboxylate recognition through formation of hydrogen bonded complexes. Placed these units on a steroidal scaffold at the secondary hydroxyl groups, they can position a carboxylate within a well-defined environment created by other substituents at C3, C7 or C12 position providing a varieties of enantioselective receptors for chiral carboxylate or amino acids. The steroidal framework provides a chiral scaffold which is created as binding sites for a small to medium size molecule. Chiral discrimination would presumably be enhanced by differential substitution at positions 7 and 12.

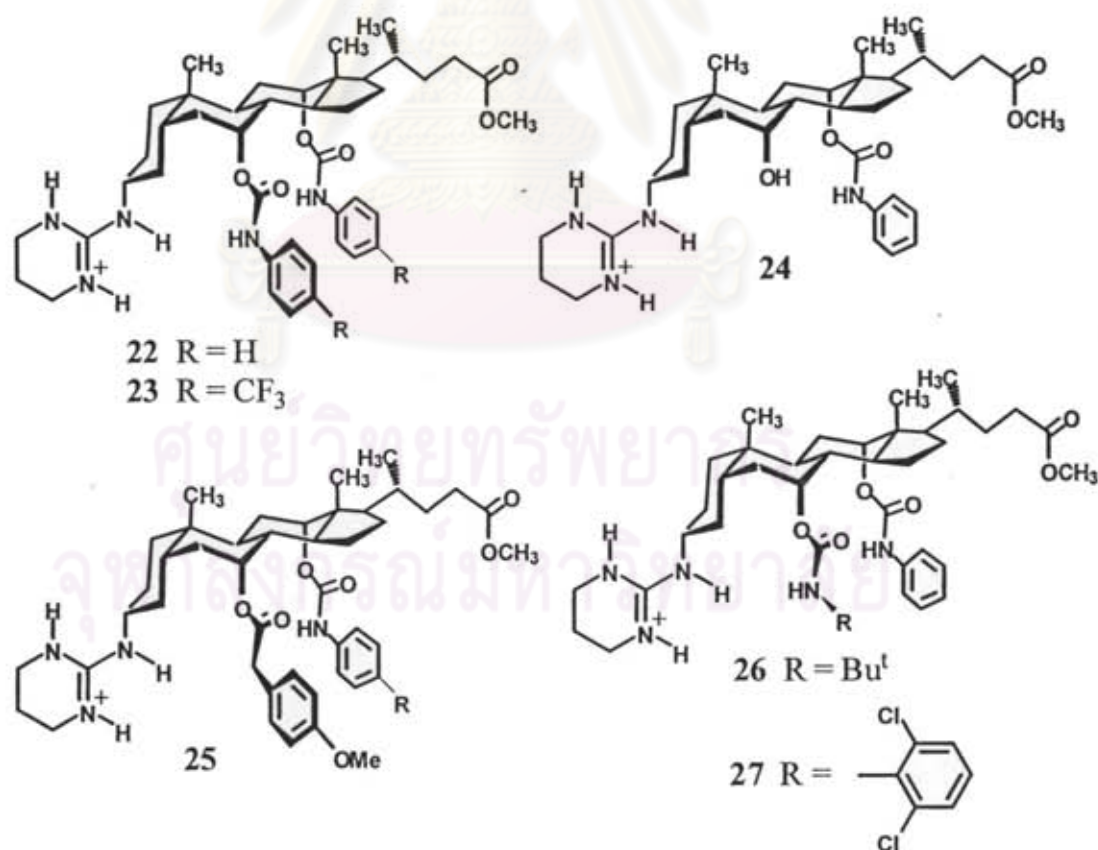
3.1.3 Literature Review for Steroidal Receptors for Amino Acids

A fluorescent ditopic receptor **21** for binding dicarboxylates and acidic amino acids was synthesized by incorporation of aminothiourea and amidothiourea groups to the C3 and C24 of cholic acid, respectively. Methylene anthracene groups were appended onto the receptor for a construction of fluorescent sensors. This receptor was designed as a water-soluble artificial receptor. For fluorimetric study, in methanol/water (1:1), fluorescent emission of **21** was quenched by about 10% and 20% when treated with dicarboxylate anions (malonate, succinate, glutarate, adipate, suberate and sebate) and amino acids (L-aspartate, glutamate, N-acetyl-L-aspartate and N-acetyl-L-glutamate), respectively. The small quenching is caused by the competition of methanol and water via hydrogen bonding with thiourea binding sites. A 1:1 complex of **21** with dicarboxylates and the highest affinity with adipate was found. The binding of the host with dicarboxylate is rather distinct in size and electronic environment. In case of amino acids, **21** showed a much stronger affinity to L-glutamate and its N-protected derivatives than dicarboxylates.[72]

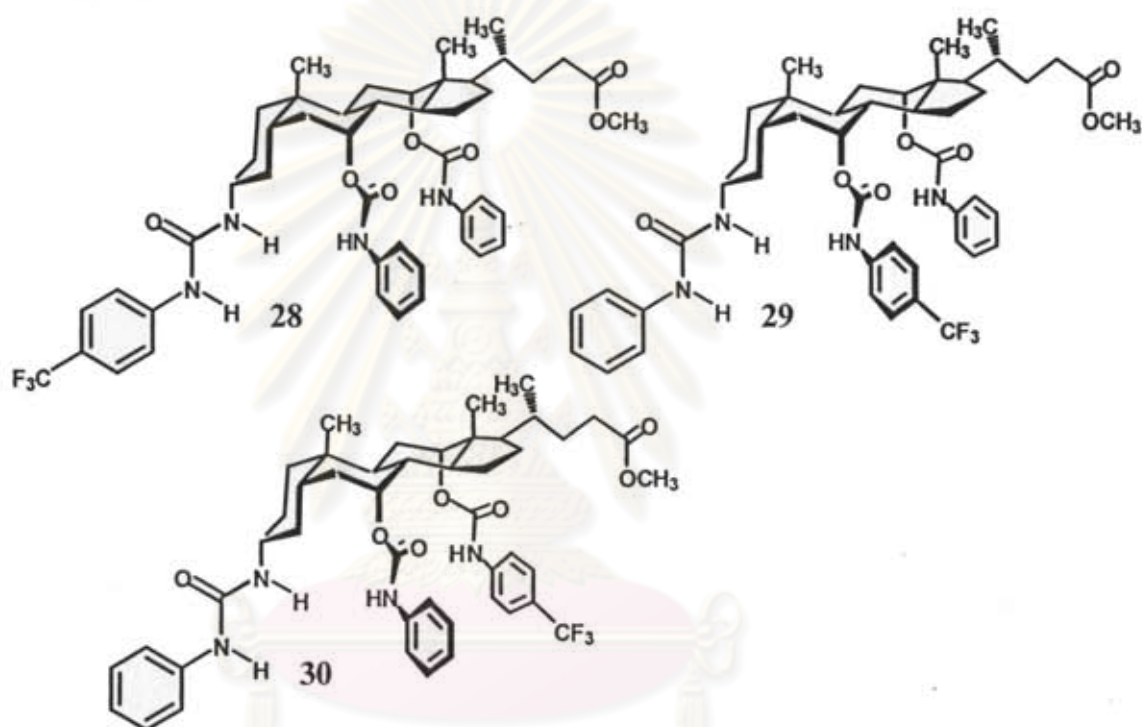


Steroidal guanidinium receptors **22-27** were employed for enantioselective recognition of *N*-acetyl α -amino acids; *N*-Ac-alanine, *N*-Ac-phenylalanine, *N*-Ac-tryptophan, *N*-Ac-valine, *N*-Ac-*tert*-leucine, *N*-Ac-methionine, *N*-Ac-proline *N*-Boc-valine, *N*-Boc-histidine and *N*-Ac-asparagine using extraction method. Extraction

efficiency and enantioselectivity could be followed by NMR. Good enantioselectivities were obtained for the symmetrically derivatized receptors **22** and **23**. The results were insensitive to the bulk of the amino acid side-chain; the receptors performed as well with alanine as with valine or phenylalanine derivatives. However, the hydrophilic asparagines derivative resisted extraction. *N*-Boc amino acids were extracted with greater efficiencies but lower selectivities. Replacement of the acetyl group by a Boc-group in the substrate increased the extraction efficiency but lowered the enantioselectivity. Receptor **22** showed ability to differentiate between enantiomers (enantioselectivity L:D = 7:1). The less symmetric receptors **23-26** gave lower selectivities, while **27** showed higher extraction abilities, possibly due to the greater acidity of the dichlorophenylcarbamoyl NH, and more sensitive to side-chain structure. *N*-Ac-*tert*-leucine gave the lowest selectivity. More selectivity for L-form of amino acids was investigated from the modeling studies of the complex between **27** and *N*-Ac-L-valinate. It was found that the carboxylate accepted H-bonds from the 7-carbamoyl and two guanidinium NH groups, while the acetyl oxygen is bound to the 12-carbamoyl NH.[73, 74]

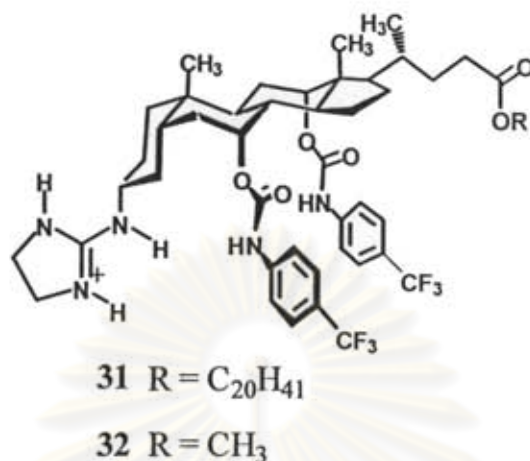


The steroidal ureas **28**, **29** and **30** can extract an N-acetyl amino acid salt from aqueous into organic phase with significant enantioselectivities measured by mass spectroscopy on isotopically labeled “pseudoracemates” technique. The studies focused on the extraction of the L- and D-deuterated phenylalanine. The results showed that all three receptors extracted around 17 mol% of L-/D-form and each showed a significant preference for the L-derivative. The selectivity ranged from 5:1 for **28** to 3:1 for **30**. In comparison, receptor **28** has a potential for enantioselectivity over receptors **29** and **30** which were designed for the better preorganized prior to bind to guest with a higher selectivity.[75]



Amino acids transport studies were undertaken using receptors **31** and **32**, based on **42** with two minor modifications. Firstly, a lipophilic C20 side-chain was introduced to avoid loss of receptor from organic into aqueous phase. Secondly, the six-membered ring guanidinium moiety was replaced by a five-membered ring. Extraction with methyl ester **32** confirmed that the enantioselectivity was not degraded. In experiments with a ‘U-tube’ apparatus, guanidinium **31** proved capable of transporting *N*-acetyl-DL-phenylalanine through dichloromethane with nearly 70% enantiomeric excess. About 20 equivalents of the substrate were transferred during the experiment. Receptor **31** was also

used in a 'hollow-fiber membrane' separator, an apparatus for large-scale aqueous-organic-aqueous transport. Lower %e.e. was obtained in this case, probably because the apparatus enforced a change in non-polar solvents (from DCM to 2.5% octanol in hexane).[76]



3.1.4 Objectives and Scope of this research

The main goal of this research is to synthesize steroidal receptor **L3** for study enantioselective recognition of amino acids. The chiral receptor **L3** employed NH-based urea as binding sites and azobenzene as a sensory unit. Amino acids in both L- and D-forms were studied in this work including L-Trp, D-Trp, L-Phe, D-Phe, L-Leu, D-Leu, L-Ala, D-Ala and Gly. The complexation studies are also investigated using ¹H-NMR spectroscopy, UV-vis spectrophotometry and mass spectroscopy.

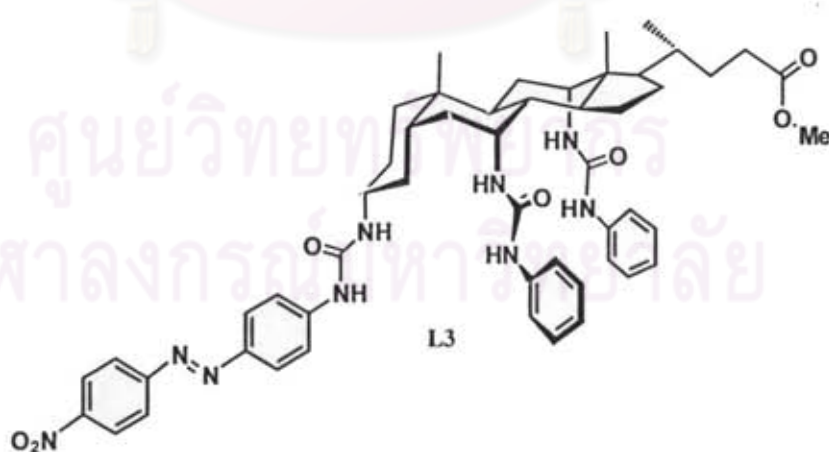
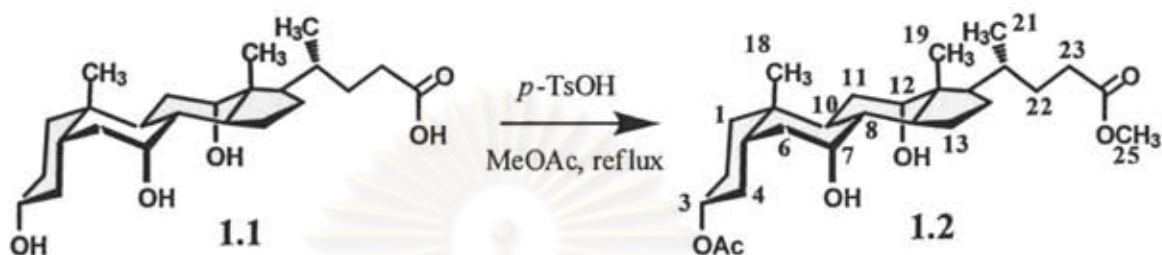


Figure 3.2 Structure of the steroidal receptor **L3**.

3.2 Experimental Section

3.2.1 Synthesis of steroidal receptor

3.2.1.1 Preparation of methyl 3 α -acetoxy-7 α , 12 α -dihydroxy-5 β -cholan-24-oate (1.2)



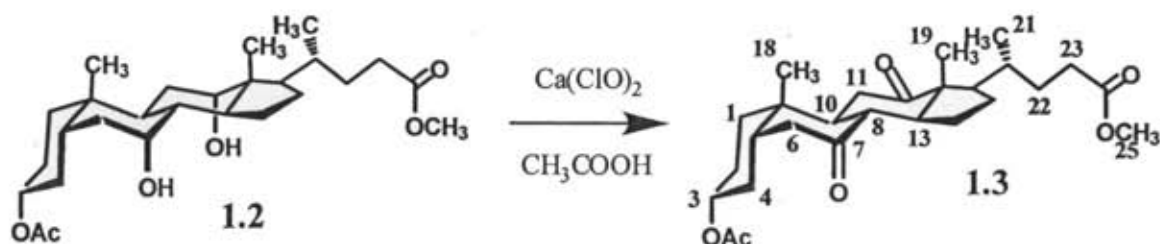
A suspension of cholic acid **1.1** (30.00g, 73.43 mmol) and *p*-toluenesulfonic acid monohydrate (1.45g, 7.63 mmol) in methyl acetate (370 mL) was stirred and refluxed for 48h under air atmosphere. After this suspension was cooled down, NaHCO₃ powder (0.64g, 7.62 mmol) was added and kept stirring for 30 mins. Then the mixture was filtered through a plug of silica (20g) and washed thoroughly with EtOAc and the solvent was removed under reduced pressure. The residue was dissolved in dichloromethane and washed with sat. aq. NaHCO₃. The organic layer was dried over magnesium sulfate and evaporated under reduced pressure. The diol **1.2** (26.20g, 78% yield) was obtained as a white solid after crystallization in dichloromethane/methanol.

Characterization data for **1.2**:

TLC: R_f = 0.57 (diethyl ether)

¹H-NMR spectrum (CDCl₃, 400 MHz): δ = 0.68 (3H, s, 18-H₃), 0.89 (3H, s, 19-H₃), 0.96 (3H, d, *J* = 6.30 Hz, 21-H₃), 1.99 (3H, s, CH₃COO), 2.16-2.42 (4H, m), 3.66 (3H, s, COOCH₃), 3.84 (1H, br s, 7 β -H), 3.97 (1H, br s, 12 β -H), 4.56 (1H, m, 3 β -H).

3.2.1.2 Preparation of Methyl 3 α -acetoxy-7 α , 12 α -dioxo-5 β -cholan-24-oate (1.3)



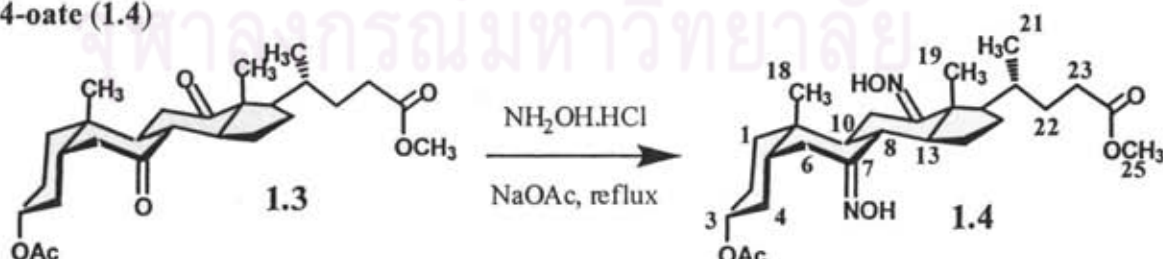
A solution of diol **1.2** (26.70g, 57.47 mmol) in glacial acetic acid (350 mL) was cooled in an ice bath and then added dropwise of a solution of $\text{Ca}(\text{ClO})_2$ in water. The reaction was left stirring overnight at room temperature. Isopropanol (8.00 mL) was then added into the mixture and the stirring was continued for 1.5 hours at room temperature. The mixture was poured into ice-water bath under vigorous stirring. The precipitate was filtered and washed thoroughly with water. The crude product was purified by column chromatography (eluent CH_2Cl_2 : EtOAc 3:1) to give diketone product **1.3** (26.00g, 99%) as a white solid.

Characterization data for 1.3:

TLC: $R_f = 0.68$ (CH_2Cl_2 : EtOAc 3:1)

$^1\text{H-NMR}$ spectrum (CDCl_3 , 400 MHz): $\delta = 0.82$ (3H, d, $J = 9.44$ Hz, 21- H_3), 1.01 (3H, s, 18- H_3), 1.28 (3H, s, 19- H_3), 1.97 (3H, s, CH_3COO), 2.22-2.43 (4H, m), 2.71 (2H, q, $J = 18.08$ Hz), 2.81 (1H, m), 3.64 (3H, s, COOCH_3), 4.66 (1H, m, 3 β -H).

3.2.1.3 Preparation of Methyl 3 α -acetoxy-7 α , 12 α -dioximino-5 β -cholan-24-oate (1.4)



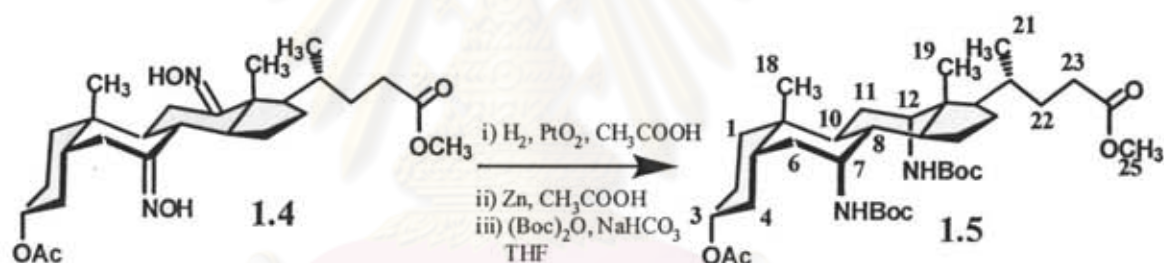
A mixture of diketone **1.3** (26.00g, 56.64 mmol), sodium acetate (22.56g, 275.07 mmol) and hydroxylamine hydrochloride (11.74g, 168.90 mmol) was dissolved in methanol (540 mL) and refluxed overnight under air atmosphere. Then, the reaction mixture was cooled in an ice bath and the precipitate was filtered to obtain dioximino product **1.4** (22.00g, 79.23%) as a white solid.

Characterization data for 1.4:

TLC: $R_f = 0.67$ (diethyl ether)

¹H-NMR spectrum (CDCl₃, 400 MHz): $\delta = 0.91$ (6H, d, $J = 7.84$ Hz, 21-H₃ + 18-H₃), 1.14 (3H, s, 19-H₃), 1.99 (3H, s, CH₃COO), 2.35-2.43 (2H, m), 3.07-3.12 (1H, dd), 3.23-3.26 (1H, dd), 3.65 (3H, s, COOCH₃), 4.70 (1H, m, 3 β -H).

3.2.1.4 Preparation of Methyl 3 α -acetoxy-7 α , 12 α -di[N-(t-butylloxycarbonyl) amino]-5 β -cholan-24-oate (1.5)



A mixture of dioximino compound **1.4** (10.00g, 20.40 mmol) and platinum(IV)oxide monohydrate (Adams' catalyst) (1.01 g, approx. 10% by weight) in glacial acetic acid (52 mL) was stirred under hydrogen atmosphere for a week. The reaction mixture was filtered and washed with glacial acetic acid. The filtrate was added with zinc powder (20g) and stirred overnight under air atmosphere. The resultant mixture was filtered and the solvent was evaporated under reduced pressure. The residue was dissolved in THF (160 mL) and then sat. aq. NaHCO₃ and di-t-butylidicarbonate (11.30g, 60.80 mmol) were added and the solution was stirred under air atmosphere for 2 days. The organic layer was dried over magnesium sulfate and the solvent was evaporated under reduced pressure to give yellow crude product. The crude was purified by column

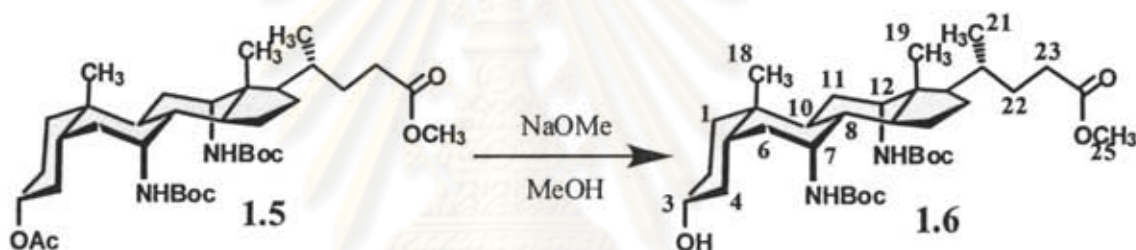
chromatography (eluent EtOAc:CH₂Cl₂ 1:4) affording bis-Boc product **1.5** (9.64g, 73%) as a white solid.

Characterization data for 1.5:

TLC: R_f = 0.55 (hexane:EtOAc 1:1)

¹H-NMR spectrum (CDCl₃, 400 MHz): δ = 0.78 (3H, s, 18-H₃), 0.82-0.92 (6H, m, 21-H₃ + 19-H₃), 1.42 (18H, s, (CH₃)₃C), 2.01 (3H, s, CH₃COO), 2.14-2.25 (1H, m), 2.45 (1H, m), 3.65 (1H, br s, 7β-H), 3.69 (3H, s, COOCH₃), 3.96 (1H, br s, 12β-H), 4.56 (1H, br s, 3β-H), 5.05 (1H, br s, 7-CH-NHR), 5.24 (1H, br s, 12-CH-NHR).

3.2.1.5 Preparation of Methyl 3α-hydroxy-7α, 12α-di[N-(t-butyloxycarbonyl) amino]-5β-cholan-24-oate (1.6)



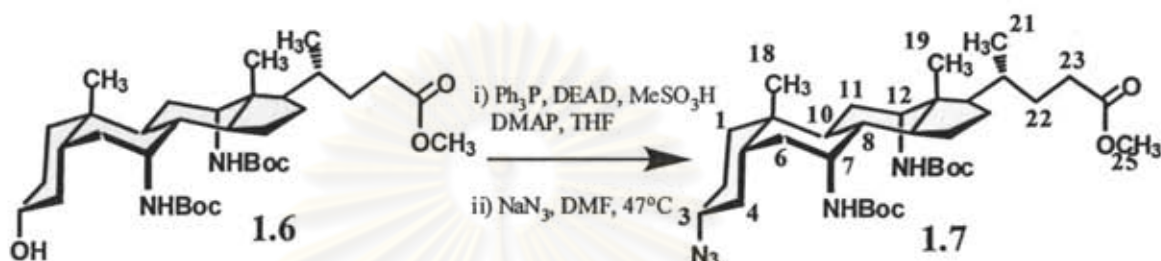
Bis-Boc product **1.5** (10.05 g, 15.50 mmol) was dissolved in dry methanol (70 mL) and added into a solution of sodium methoxide (1.22 g, 22.60 mmol) in dry methanol. The reaction mixture was stirred at 0°C for 4h and then the stirring was continued at room temperature overnight. The solvent was evaporated under reduced pressure and the crude product was dissolved in diethylether. The solution was washed thoroughly with water and dried over magnesium sulfate and the solvent was evaporated under reduced pressure. The hydroxyl compound **1.6** (9.30 g, 97%) as a white solid was obtained after recrystallization.

Characterization data for 1.6:

TLC: R_f = 0.47 (CH₂Cl₂:EtOAc 2:1)

¹H-NMR spectrum (CDCl₃, 400 MHz): δ = 0.79 (3H, s, 18-H₃), 0.92 (6H, s, 21-H₃ + 19-H₃), 1.44 (18H, s, (CH₃)₃C), 2.16-2.30 (1H, m), 2.38-2.50 (1H, m), 3.51 (1H, br s, 3β-H), 3.69 (4H, s, COOCH₃ + 7β-H), 3.98 (1H, br s, 12β-H), 4.95 (1H, br s, 7-CH-NHR), 5.09 (1H, br s, 12-CH-NHR).

3.1.2.6 Preparation of Methyl 3α-azido-7α, 12α-di[N-(*t*-butyloxycarbonyl) amino]-5β-cholan-24-oate (1.7)



A mixture of hydroxy compound **1.6** (3.50 g, 5.63 mmol), DMAP (1.81 g, 14.83 mmol) and triphenylphosphine (4.44 g, 16.88 mmol) was dissolved in dry THF under nitrogen atmosphere and the mixture was cooled in an ice bath. Methanesulfonic acid (0.98 mL, 15.02 mmol) was added to give a white precipitate and then DEAD (2.82 mL, 16.8 mmol) was added dropwise over a period of 20 min. The reaction mixture was turned to a pale yellow slurry. The slurry was warmed to room temperature and stirred for 2 days. The reaction was filtered and the filtrate was evaporated under reduced pressure. The residue was purified by flash column chromatography using eluent hexane:EtOAc 3:1 to 1:1 as eluent to give the 3β-methanesulfonate intermediate: R_f = 0.3 (EtOAc:hexane 1:1).

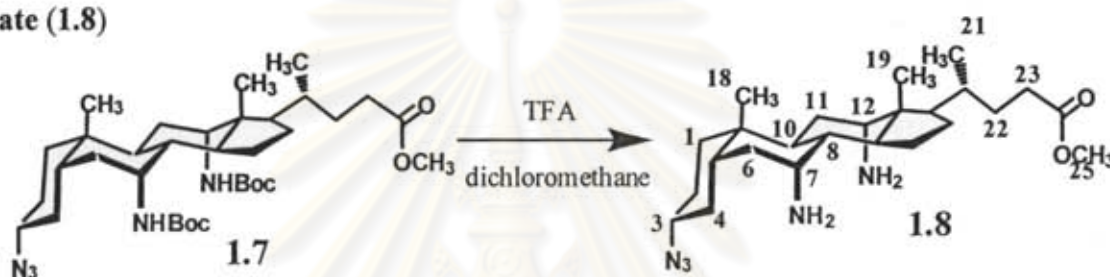
The 3β-methanesulfonate and sodium azide (4.83 g, 7.42 mmol) were dissolved in dry DMF and the reaction was stirred at 47 °C for 3 days. The dry residue was dissolved in ethyl acetate and washed with water. The solution was dried over magnesium sulfate and the solvent was evaporated under reduced pressure. The crude product was purified by flash column chromatography (eluent hexane:EtOAc 4:1) to give the desired azide **1.7** (2.27 g, 63%) as a white solid.

Characterization data for 1.7:

TLC: $R_f = 0.2$ (hexane:EtOAc 4:1)

$^1\text{H-NMR}$ spectrum (CDCl_3 , 400 MHz): $\delta = 0.78$ (3H, s, 18- H_3), 0.90 (3H, d, $J = 6.12$ Hz, 21- H_3), 0.93 (3H, s, 19- H_3), 1.41 (9H, s, $(\text{CH}_3)_3\text{C}$), 1.42 (9H, s, $(\text{CH}_3)_3\text{C}$), 2.16-2.22 (1H, m), 2.42-2.54 (1H, m), 3.26 (1H, br s, 3 β -H), 3.64 (1H, br s, 7 β -H), 3.71 (3H, s, COOCH_3), 3.97 (1H, br s, 12 β -H), 5.17 (1H, br s, 7-CH-NHR), 5.36 (1H, br s, 12-CH-NHR).

3.2.1.7 Preparation of Methyl 3 α -azido-7 α , 12 α -bis-amino-5 β -cholan-24-oate (1.8)



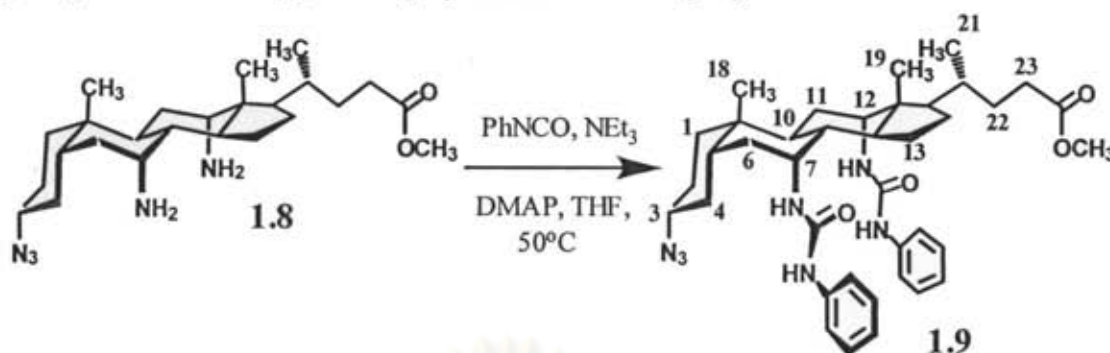
The azide with bis-Boc protected **1.7** (2.27g, 3.52 mmol) was dissolved in dry dichloromethane (55 mL) and placed in an ice bath. Trifluoroacetic acid (34 mL) was added dropwise and the mixture was stirred at 0°C for 1 hour. Then, the reaction mixture was further stirred at room temperature for 4 hours. The solvent was evaporated under reduced pressure and washed with sat. aq. NaHCO_3 and then dried over magnesium sulfate and the solvent was evaporated under reduced pressure. The yellow crude product was precipitated by CH_2Cl_2 /hexane to obtain the diamine product **1.8** (1.24g, 79%) as a white solid.

Characterization data for 1.8:

TLC: $R_f = 1.80$ (EtOAc:MeOH 9:1)

$^1\text{H-NMR}$ spectrum (CDCl_3 , 400 MHz): $\delta = 0.71$ (3H, s, 18- H_3), 0.91 (3H, s, 19- H_3), 0.96 (3H, d, $J = 6.32$ Hz, 21- H_3), 2.02-2.15 (2H, m), 2.18-2.27 (1H, m), 2.32-2.52 (2H, m), 3.07-3.21 (3H, m, 3 β -H + 7 β -H + 12 β -H), 3.66 (3, s, COOCH_3).

3.2.1.8 Preparation of Methyl 3 α -azido-7 α , 12 α -bis-[(phenylaminocarbonyl) amino]-5 β -cholan-24-oate (1.9)



To a solution of diamine **1.8** (1.27 g, 2.84 mmol) in dry THF (30 mL), DMAP (0.33 g, 2.70 mmol), triethylamine (0.74 mL, 5.30 mmol) and phenylisocyanate (620 μ L, 5.68 mmol) were added, respectively. The reaction mixture was stirred at 50°C for 24 h and the solvent was evaporated under reduced pressure. The crude product was purified by flash column chromatography (eluent DCM/methanolic ammonia 99:1) to provide the product bis-urea **1.9** (1.86 g, 96%) as a white solid.

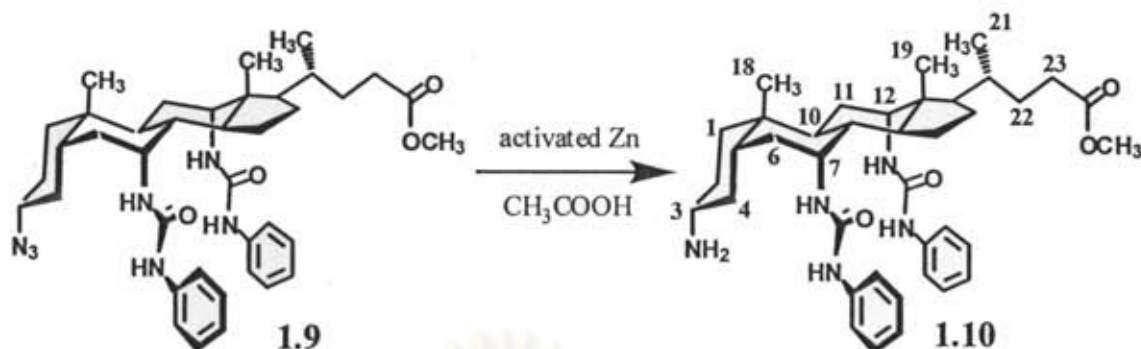
Characterization data for **1.9**:

TLC: R_f = 0.20 (DCM/methanolic ammonia 98:2)

¹H-NMR spectrum (CDCl₃, 400 MHz): δ = 0.75 (3H, s, 18-H₃), 0.85 (3H, d, J = 6.36 Hz, 21-H₃), 0.91 (3H, s, 19-H₃), 1.96-2.06 (1H, m), 2.25-2.32 (1H, m), 3.15 (1H, br s, 3 β -H), 3.93 (1H, br s, 7 β -H), 4.05 (1H, br s, 12 β -H), 5.33 (1H, br s, NH), 5.63 (1H, br s, NH), 6.85 (1H, br s, NH), 6.98-7.06 (2H, m, Ar-CH), 7.25-7.39 (8H, m, Ar-CH).

ศูนย์วิทยทรัพยากร
จุฬาลงกรณ์มหาวิทยาลัย

3.2.1.9 Preparation of Methyl3 α -amino-7 α , 12 α -bis-[(phenylaminocarbonyl) amino]-5 β -cholan-24-oate (1.10)



Activated zinc powder (3.77 g, 58.74 mmol) was added to a solution of azido compound **1.9** (2.00 g, 2.93 mmol) in glacial acetic acid (120 mL) and the mixture was stirred vigorously for 24h. Acetic acid was completely removed under reduced pressure by adding toluene several times. The residue was dissolved by saturated aqueous solution of NaCl (60 mL) and basified by excessive triethylamine and then extracted with EtOAc. The organic phase was dried over magnesium sulfate and the solvent was evaporated under reduced pressure. The desired amine product **1.10** (1.76 g, 91%) was obtained from flash column chromatography purification (eluent DCM/ methanolic ammonia 97:3 to 9:1) as a white solid.

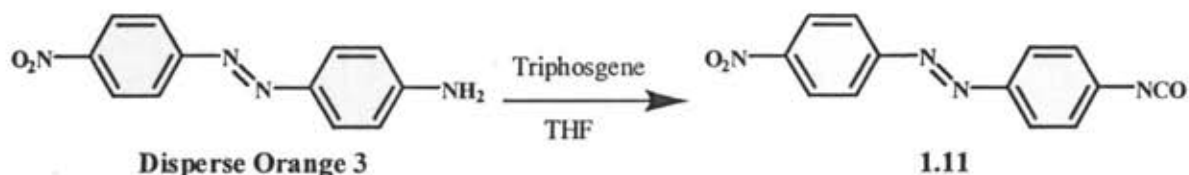
General procedure to activate zinc powder: Zinc dust (5 g) in 1M aqueous HCl (50 mL) was stirred at room temperature for 30 min, then filtered and washed with water (2 x 50 mL) and Et₂O (50 mL). Finally, the material was dried under high vacuum with a heatgun.

Characterization data for **1.10**:

TLC: R_f = 0.3 (DCM/ methanolic ammonia 92:8)

¹H-NMR spectrum ((CD₃)₂CO): δ = 0.88 (3H, s, 18-H₃), 0.90 (3H, d, J = 9.76 Hz, 21-H₃), 1.04 (3H, s, 19-H₃), 3.16 (1H, br s, 3 β -H), 3.54 (3H, s, COOCH₃), 4.04 (1H, br s, 7 β -H), 4.15-4.21 (1H, br s, 12 β -H), 5.86 (1H, br s, CH-NH-CO), 5.94 (1H, br s, CH-NH-CO), 6.86-6.94 (2H, m, Ar-CH), 7.18-7.26 (4H, m, Ar-CH), 7.51 (4H, d, J = 5.88 Hz, Ar-CH), 8.10 (2H, d, J = 8.30 Hz, Ar-NH-CO).

3.2.1.10 Preparation of 4-Isocyanato-4'-nitroazobenzene (1.11)

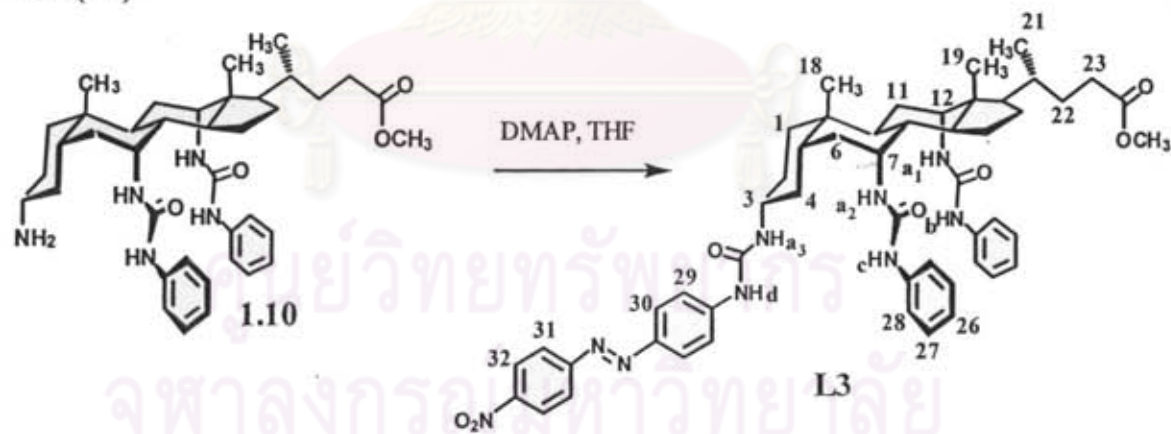


Disperse orange 3 (0.20g, 0.83 mmol) was dissolved in dry THF (15 mL) and a solution of triphosgene (2 equivalents) in THF (15 mL) was added and the reaction mixture was stirred at room temperature for 2 hours. The resultant reaction as a red brown solution was checked using FT-IR (The product showing IR bands of -NCO at 2257 and -NHCOCI at 1734 cm^{-1}). Compound **1.11** was used in the next step immediately without any purification. The yield was considered quantitative.

Characterization data for 1.11:

FT-IR spectrum (cm^{-1}) 2252, 1731, 1597, 1518, 1337, 1247, 1032.

3.2.1.11 Preparation of Methyl 3 α -[(4-nitroazobenzene-4'-aminocarbonyl) amino]-7 α ,12 α -bis-[(phenylamino carbonyl)amino]-5 β -cholan-24-oate (L3)



To a solution of compound **1.11** in dry THF, a mixture of amino compound **1.10** (0.55g, 0.83 mmol) and DMAP (0.13g, 1.08 mmol) in THF was added and the reaction mixture was heated for 2 hours. Then, the solvent was evaporated under reduced pressure. The crude product was purified by column chromatography using

dichloromethane /methanolic ammonia 94:6 as eluent to provide the desired product L3 (0.30g, 38.77%) as a red solid.

Characterization data for L3:

TLC: Rf = 0.2 (DCM/methanolic ammonia 94:6)

¹H-NMR spectrum ((CD₃)₂CO): δ = 0.81 (6H, s, 18-H₃ + 21-H₃), 0.99 (3H, s, 19-H₃), 3.26 (1H, m, 3β-H), 3.48 (3H, s, COOCH₃), 3.99 (1H, br s, 7β-H), 4.09 (1H, br s, 12β-H), 5.56 (1H, d, *J* = 5.85 Hz, CH-NH_a-CO), 5.79 (1H, m, CH-NH_a-CO), 6.82-6.86 (2H, m, Ar_{phenyl}-CH₂₆), 7.21-7.15 (4H, m, Ar_{phenyl}-CH₂₇), 7.40-7.44 (4H, s, Ar_{phenyl}-CH₂₈), 7.56-7.58 (2H, d, *J* = 9.0 Hz, Ar_{org3}-C₂₉), 7.79-7.83 (3H, d, *J* = 4.8 Hz, Ar_{org3}-CH₃₀ + Ar_{phenyl}-NH_c-CO), 7.96-7.98 (2H, d, *J* = 9.0 Hz, Ar_{org3}-CH₃₁), 8.03 (1H, br s, Ar_{phenyl}-NH_b-CO), 8.16 (1H, br s, Ar_{org3}-NH_d-CO), 8.33-8.35 (2H, d, *J* = 9.0 Hz, Ar_{org3}-CH₃₂).

¹³C{¹H}-NMR spectrum ((CD₃)₂CO): δ = 12.27, 15.71, 21.82, 22.31, 25.74, 26.17, 26.86, 29.45, 29.80, 31.92, 33.78, 34.15, 34.73, 35.56, 36.45, 41.14, 43.65, 43.78, 45.22, 47.28, 49.67, 50.44, 51.84, 116.73, 116.86, 120.29, 120.36, 122.14, 123.82, 127.75, 139.98, 144.26, 146.11, 147.42, 153.18, 153.41, 153.59, 155.13, 172.62.

IR spectrum (KBr, cm⁻¹) 3385, 2941, 2867, 1676, 1544, 1439, 1341, 1228, 1139

Elemental analysis:

Anal. Calcd for C₅₂H₆₃N₉O₇+1.5 H₂O C, 65.54; H, 6.93; N, 13.24.

Found C, 65.48; H, 6.87; N, 13.03.

MS (ESI): m/z for C₅₂H₆₃N₉O₇ = 948 [M+Na]⁺, 926 [M+H]⁺.

3.2.2 Experimental procedures in complexation studies

3.2.2.1 $^1\text{H-NMR}$ titration studies for complexes of ligand L3 with amino acids

Typically, a 0.004 M solution of a ligand L3 (1.4×10^{-6} mol) in DMSO- d_6 (0.35 mL) was prepared in a 5-mm NMR tube. An initial $^1\text{H-NMR}$ spectrum of the solution of the ligand was recorded. A 0.018 M stock solution of guest molecules (7.48×10^{-6} mol) in DMSO- d_6 (0.4 mL) was prepared in a vial (shown in Tables 3.1). The solution of a guest molecule (0.3 mL) was portion added *via* microsyringe (10 and 50 μL portions) to the NMR tube to have guest:host ratios shown in Table 3.2. $^1\text{H-NMR}$ spectra were recorded after each addition.

Table 3.1 Amounts of amino acids that used in complexation studies with ligand L3 for NMR titration studies.

Ligand	Amino acids	Weight (gram)
L3	Glycine	0.00056
	Alanine	0.00067
	Leucine	0.00098
	Phenylalanine	0.00124
	Tryptophan	0.00152

ศูนย์วิทยทรัพยากร
จุฬาลงกรณ์มหาวิทยาลัย

Table 3.2 Amounts of solutions of amino acids used to prepare various amino acids:L3 ratios for NMR titration studies.

ratio of guest:host	volume guest added (μL)	ratio of guest:host	volume guest added (μL)
0.0:1.0	0	1.0:1.0	7.5
0.1:1.0	7.5	1.2:1.0	15
0.2:1.0	7.5	1.4:1.0	15
0.3:1.0	7.5	1.6:1.0	15
0.4:1.0	7.5	1.8:1.0	15
0.5:1.0	7.5	2.0:1.0	15
0.6:1.0	7.5	2.5:1.0	37.5
0.7:1.0	7.5	3.0:1.0	37.5
0.8:1.0	7.5	3.5:1.0	37.5
0.9:1.0	7.5	4.0:1.0	37.5

3.2.2.2 UV-vis titration studies for complexes of ligand L3 with amino acids

Typically, 0.01 M solution of $[\text{Bu}_4\text{N}][\text{PF}_6]$ (0.3874 g) in 100 mL of DMSO (spectroscopic grade) was prepared and used as a solvent in all UV-vis experiments. Solution of 0.00002 M of the ligand L3 (2.00×10^{-7} mol) in 10 mL of DMSO were prepared in a volumetric flask. The ligand solution (2 mL) was pipetted into a 1 cm pathlength quartz cuvette and absorption spectrum of each ligand was recorded from 300 to 550 nm at room temperature. A solution of a guest in DMSO was prepared in a 10 mL volumetric flask (shown in Table 3.3). The solution of a guest (total volume 1.5 mL) was added directly to the cuvette by microburette and stirred for 30 sec prior to measurement. The absorption spectra of solution were recorded after each addition.

Table 3.3 Amounts of amino acids that used in complexation studies with ligand **L3** for UV-vis titration studies.

Ligands	Amino acids	Weight (gram)	Ligand:Guest (equiv)
L3	Glycine	0.00600	1:300
	Alanine	0.00713	1:300
	Leucine	0.01050	1:300
	Phenylalanine	0.01322	1:300
	Tryptophan	0.00218	1:40

3.3 Results and Discussion

3.3.1 Design Concept

It is known that the steroidal framework, derived from cholic acid, provides a chiral scaffold that positions the codirected legs so as to create a binding site for a small-to-medium size molecule. The side chain may be used to control solubility, or to link the scaffold to a polymer backbone for solid-phase synthesis. Cholapod libraries prepared by “split and mix” solid phase synthesis have already been used for sequence-selective peptide recognition[77] and for studies in enzyme modeling[78]. Moreover, many researchers have demonstrated that many steroid derivatives have an efficiency to bind and transport N-acetyl α -amino carboxylates with significant enantioselectivities.[74, 79] These results suggest that the cholapod architecture is intrinsically suitable for enantioselective recognition.

On the basic of this strategy, ligand **L3** were synthesized as a steroidal derivative by attaching urea binding site at C3, C7 and C12 positions of cholic acid framework. **L3** has three-dimension binding sites and the intrinsic chiral structure. Thus, the binding properties with significant enantioselectivity are expected in complex formation of this compound with amino acids.

3.3.2 Synthesis and characterization of steroidal receptor L3

The synthetic pathways for receptor L3 is shown Figure 3.3. Methods for the synthesis of compounds 1.2-1.10 were followed from the literature.[80]

3.3.2.1 Synthesis and characterization of methyl 3 α -acetoxy-7 α , 12 α -dihydroxy -5 β -cholan-24-oate (1.2)

Hydroxyl group at 3-position and carboxylic group of cholic acid (1.1) were converted to acetyl and ester group by one pot esterification and acetylation of 1.1 using methyl acetate as the source of methoxy and acetyl and p-toluenesulfonic acid monohydrate as a catalyst. This reaction was done to obtain methyl acetoxycholinoate (1.2) as a white powder in 78% yield. The equatorial C3 hydroxyl group was acetylated selectively although the C7 and C12 axial hydroxyl group are the active groups in the molecule.

The ¹H-NMR spectrum of 1.2 showed two singlet signals and one doublet signal of methyl protons (18-H₃, 19-H₃ and 21-H₃) at 0.68, 0.89 and 0.96 ppm, respectively. Acetoxy protons (CH₃COO) and methyl ester protons (COOCH₃) appeared as two singlet signals at 1.99 and 3.66 ppm, respectively. In addition, proton signals at 3 β -H, 7 β -H and 12 β -H were observed as multiplet signals at 3.84, 3.97 and 4.56 ppm, respectively.

3.3.2.2 Synthesis and characterization of methyl 3 α -acetoxy-7 α , 12 α -dioxo-5 β -cholan-24-oate (1.3)

The oxidation of the hydroxyl groups at the C7 and C12 with glacial acetic acid and Ca(ClO)₂ provided diketone product (1.3) as a white solid in 98% yield after purification by silica gel column using dichloromethane:ethyl acetate = 3:1 as eluent. The ¹H-NMR spectrum of 1.3 showed the shift of protons signal which are adjacent to diketone such as an upfield shift of 21-H₃ protons at 0.82 ppm as a doublet signal and downfield shifts of 18-H₃ and 19-H₃ protons at 1.10 and 1.28 ppm, respectively. A disappearance of 7 β -H and 12 β -H protons signal was observed. Acetoxy protons

(CH₃COO) and methyl ester protons (COOCH₃) still appeared as two singlet signals at the same region (1.97 and 3.64 ppm, respectively). These results were in good agreement with the proposed structure which the hydroxyl groups were changed to be ketone.

3.3.2.3 Synthesis and characterization of methyl 3 α -acetoxy-7 α , 12 α -dioximino-5 β -cholan-24-oate (1.4)

The diketone at the C7 and C12 position was changed to dioxime compound (1.4) by the dioximation reaction of 1.3 with sodium acetate and hydroxylamine hydrochloride. Acetoxydioxime 1.4 was obtained as a white solid in 79%. The ¹H-NMR spectrum of 1.4 showed a combination of 18-H₃ and 21-H₃ protons at the same position (0.91 ppm) as a doublet signal. Acetoxy protons (CH₃COO) and methyl ester protons (COOCH₃) still appeared as two singlet signals at the same region (1.99 and 3.65 ppm, respectively). The characteristic signal of the dioxime compound is an appearance of two doublet of doublet signals (NH dioxime protons) at the range of 3.07-3.36 ppm.

3.3.2.4 Synthesis and characterization of methyl 3 α -acetoxy-7 α , 12 α -di[N-(*t*-butyl oxycarbonyl) amino]-5 β -cholan-24-oate (1.5)

Diamine compound was obtained from a catalytic hydrogenation of dioxime compound (1.4) with Adam's catalyst (H₂, PtO₂ and CH₃COOH) followed by a treatment with zinc in acetic acid. After the reaction of 1.4 with Adam's catalyst, dioxime group of 1.4 was reduced to obtain a mixture of imine and amine products. This mixture was reacted with zinc to afford only diamine product. This is an enantioselective hydrogenation to provide only amine groups at C7 and C12 at axial orientation. The diamine was protected using saturated NaHCO₃ and di-*t*-butyldicarbonate to give bis-Boc compound 1.5 as a white solid in 73% yield after purification by silica gel column using ethyl acetate:dichloromethane = 1:4 as eluent.

The ¹H-NMR spectrum of compound 1.5 showed signals of 18-H₃, 19-H₃ and 21-H₃ protons in the range 0.78-0.92 ppm. ¹H-NMR signals show a reappearance of 7 β -H and 12 β -H protons as two broad singlet peaks at 3.65 and 3.96 ppm, respectively and new

signals of Boc protons ($(\text{CH}_3)_3\text{C}$) as a singlet peak at 1.42 ppm and *NHBoc* protons as two broad singlet peaks at 5.05 and 5.24 ppm. Acetoxy protons (CH_3COO) and methyl ester protons (COOCH_3) were found as two singlet signals at 2.01 and 3.69 ppm, respectively.

3.3.2.5 Synthesis and characterization of methyl 3 α -hydroxy-7 α , 12 α -di[N-(*t*-butyl oxycarbonyl) amino]-5 β -cholan-24-oate (1.6)

The acetoxy group at the C3 position of compound **1.5** was removed using a reaction with sodium methoxide in dry methanol to give an alcohol product **1.6** in 97% yield as a white solid after recrystallization.

The $^1\text{H-NMR}$ spectrum of compound **1.6** showed signals of 18- H_3 and a combination of 19- H_3 and 21- H_3 protons at 0.79 and 0.92 ppm, respectively, as two singlet peaks. $^1\text{H-NMR}$ spectrum showed a disappearance of acetoxy protons (CH_3COO) and upfield shift of 3 β -H proton as a broad singlet peak to 3.51 ppm. A singlet signal of Boc protons ($(\text{CH}_3)_3\text{C}$) was found at 1.44 ppm and *NHBoc* protons appeared as two broad singlet peaks at 4.95 and 5.09 ppm. Methyl ester protons (COOCH_3) and 7 β -H proton appeared at the same position as one singlet signal at 3.69 ppm.

3.3.2.6 Synthesis and characterization of methyl 3 α -azido-7 α , 12 α -di[N-(*t*-butyl oxycarbonyl) amino]-5 β -cholan-24-oate (1.7)

The hydroxyl group at C3 position was used as substrate for the Mitsunobu reaction to convert this α -hydroxyl group to C3- α azide group. A reaction of compound **1.6** with Ph_3P , DEAD, MeSO_3H and DMAP in THF gave C3- β methanesulfonate as an intermediate after purification by flash column chromatography using hexane:ethyl acetate 3:1 to 1:1 as eluent. This transformation is quite difficult to accomplish because the intermediate methanesulfonate can give an olefinic product after elimination of the mesylate moiety. Purification to remove the olefinic product using flash column chromatography was necessary. It was found that the amount of the olefinic compound increased when the intermediate was left in the column for a long time. The intermediate (methanesulfonate) was reacted with sodium azide to provide the C3- α azide product as a

white solid in 63% yield after purification by flash column chromatography using hexane:ethyl acetate as 4:1.

The $^1\text{H-NMR}$ spectrum of compound **1.7** showed signals of 18- H_3 , 19- H_3 and 21- H_3 protons at 0.78, 0.90 and 0.93 ppm, respectively. A broad singlet peak of 3 β -H proton showed the highfield at 3.26 ppm. 7 β -H and 12 β -H protons as two broad singlet peaks were observed at 3.6 and 3.97 ppm, respectively. Boc protons (CH_3)₃C splitted to two singlet peaks at 1.41 and 1.42 ppm and *NHBoc* protons as two broad singlet peaks appeared at 5.17 and 5.36 ppm. Methyl ester protons (COOCH_3) were observed at 3.71 ppm as a singlet peak.

3.3.2.7 Synthesis and characterization of methyl 3 α -azido-7 α , 12 α -bis-amino-5 β -cholan-24-oate (**1.8**)

Diamine compound **1.8** was obtained in 79% yield as a white solid by Boc-deprotection reaction of the azide **1.7** with trifluoroacetic acid in dichloromethane. The $^1\text{H-NMR}$ spectrum of compound **1.8** showed signals of 18- H_3 , 19- H_3 and 21- H_3 protons at 0.71, 0.91 and 0.96 ppm, respectively. The $^1\text{H-NMR}$ spectrum showed a disappearance of Boc protons (CH_3)₃C and *NHBoc* protons. 3 β -H, 7 β -H and 12 β -H protons were found as a multiplet signal in the range 3.07-3.21 ppm. Methyl ester protons (COOCH_3) were observed at 3.66 ppm as a singlet peak.

3.3.2.8 Synthesis and characterization of methyl 3 α -azido-7 α , 12 α -bis-[(phenyl aminocarbonyl) amino]-5 β -cholan-24-oate (**1.9**)

Bis-urea compound **1.9** was synthesized using a coupling reaction of the diamine **1.8** with 2 equiv. of phenylisocyanate in THF in the presence of triethylamine as based and DMAP as a catalyst. This product was obtained in 96.0% yield as a white solid after purification by flash column chromatography using 99:1 ratios of DCM:methanolic ammonia as eluent.

The $^1\text{H-NMR}$ spectrum of compound **1.9** showed signals of 18- H_3 , 19- H_3 and 21- H_3 protons at 0.75, 0.91 and 0.85 ppm, respectively. 3 β -H, 7 β -H and 12 β -H protons were

found as three broad singlet signals at 3.15, 3.93 and 4.05 ppm, respectively. Methyl ester protons (COOCH_3) showed a singlet peak at 3.65 ppm. The characteristic signals of this compound are showed new signals of three NH-urea protons as broad singlet peaks at 5.33, 5.63 and 6.85 ppm. Phenyl protons were found as two multiplet signals at the range of 6.98-7.06 ppm and 7.25-7.39 ppm. The fourth NH-urea proton was overlapped with phenyl protons at the range of 7.25-7.39 ppm.

3.3.2.9 Synthesis and characterization of methyl 3α -amino- 7α , 12α -bis-[(phenyl aminocarbonyl) amino]- 5β -cholan-24-oate (1.10)

The azide group at C3 position of the bis-urea **1.9** was successfully reduced using activated zinc in acetic acid to give C3-amino compound **1.10** as a white solid in 91% yield after purification by flash column chromatography using dichloromethane :methanolic ammonia = 98:2 as eluent.

The $^1\text{H-NMR}$ spectrum of compound **1.10** showed signals of 18-H_3 , 19-H_3 and 21-H_3 protons at 0.88, 1.04 and 0.90 ppm, respectively. $3\beta\text{-H}$, $7\beta\text{-H}$ and $12\beta\text{-H}$ protons were found as three broad singlet signals at 3.16, 4.04 and 4.19 ppm, respectively. A singlet peak of methyl ester protons (COOCH_3) was observed at 3.54 ppm. Two NH-urea protons adjacent to steroid backbone appeared at 5.86 and 5.94 ppm as broad singlet peaks while other NH-urea protons adjacent to the phenyl ring was found at 8.10 ppm as a broad doublet signal. Phenyl protons were observed as three multiplet signals at 6.90, 7.22 and 7.51 ppm.

3.3.2.10 Synthesis and characterization of 4-isocyanato-4'-nitro azobenzene (1.11)

Isocyanate compound **1.11** was prepared from a reaction of disperse orange 3 with triphosgene without any base. The same reaction of disperse orange 3 with triphosgene in the presence of DIPEA as based was unsuccessful. In fact, DIPEA should activate the reaction by attacking the triphosgene. The isocyanate product was found to be very sensitive to air and easy to decompose. This reaction was monitored by FT-IR

spectrophotometry. The FT-IR spectra of the product **1.11** showed the characteristic –NCO band at 2250 cm^{-1} and –NHCOCl band at 1730 cm^{-1} . Therefore, two products were obtained as a mixture of –NCO and –NHCOCl. Attempts of purification of the product using column chromatography was not successful due to a decomposition of the product in the column (the product turned back to the amino compound or/and formation of the urea compound between two azobenzene moieties). All isocyanate **1.11** products were thus used immediately without any further purification.

3.3.2.11 Synthesis and characterization of methyl 3α -[(4-nitroazobenzene-4'-amino carbonyl) amino]- 7α , 12α -bis-[(phenylamino carbonyl)amino]- 5β -cholan-24-oate (**L3**)

The 3α -amino compound **1.10** was reacted with the isocyanate nitroazobenzene **1.11** in the presence of DMAP as a catalyst in dry THF to obtain the desired product **L3** as a red solid in 38% yield after purification by silica gel column chromatography using 94:6 ratio of DCM:methanolic ammonia as eluent.

The $^1\text{H-NMR}$ spectrum of compound **L3** in $\text{DMSO-}d_6$ showed singlet signals of 18-H_3 and 21-H_3 at the same position at 0.75 ppm and a singlet signal of 19-H_3 at 0.96 ppm. $3\beta\text{-H}$, $7\beta\text{-H}$ and $12\beta\text{-H}$ protons were found as three broad singlet signals at 3.23, 3.81 and 3.89 ppm, respectively. Methyl ester protons (COOCH_3) were observed at 3.51 ppm as one singlet peak. Three NH-urea protons which attached to steroid backbone appeared at 5.95 ppm as a broad multiplet peak. The NH-urea protons which attached to the phenyl ring were found at 8.45 and 8.61 ppm as two broad singlet signals. Phenyl protons were observed into three multiplet signals at 6.85, 7.19 and 7.38 ppm. New signals of azobenzene protons at C3 position was found as four doublet peaks at 7.56, 7.84, 7.97 and 8.38 ppm. In addition, a new singlet peak at 8.92 ppm was assigned to be NH-urea proton adjacent to azobenzene ring.

ESI mass spectra of **L3** also supported the structure of the desired compound showing an intense line at m/z 948 $[\text{M}+\text{Na}]^+$ and 926 $[\text{M}+\text{H}]^+$ and elemental analysis was in good agreement with the proposed structure.

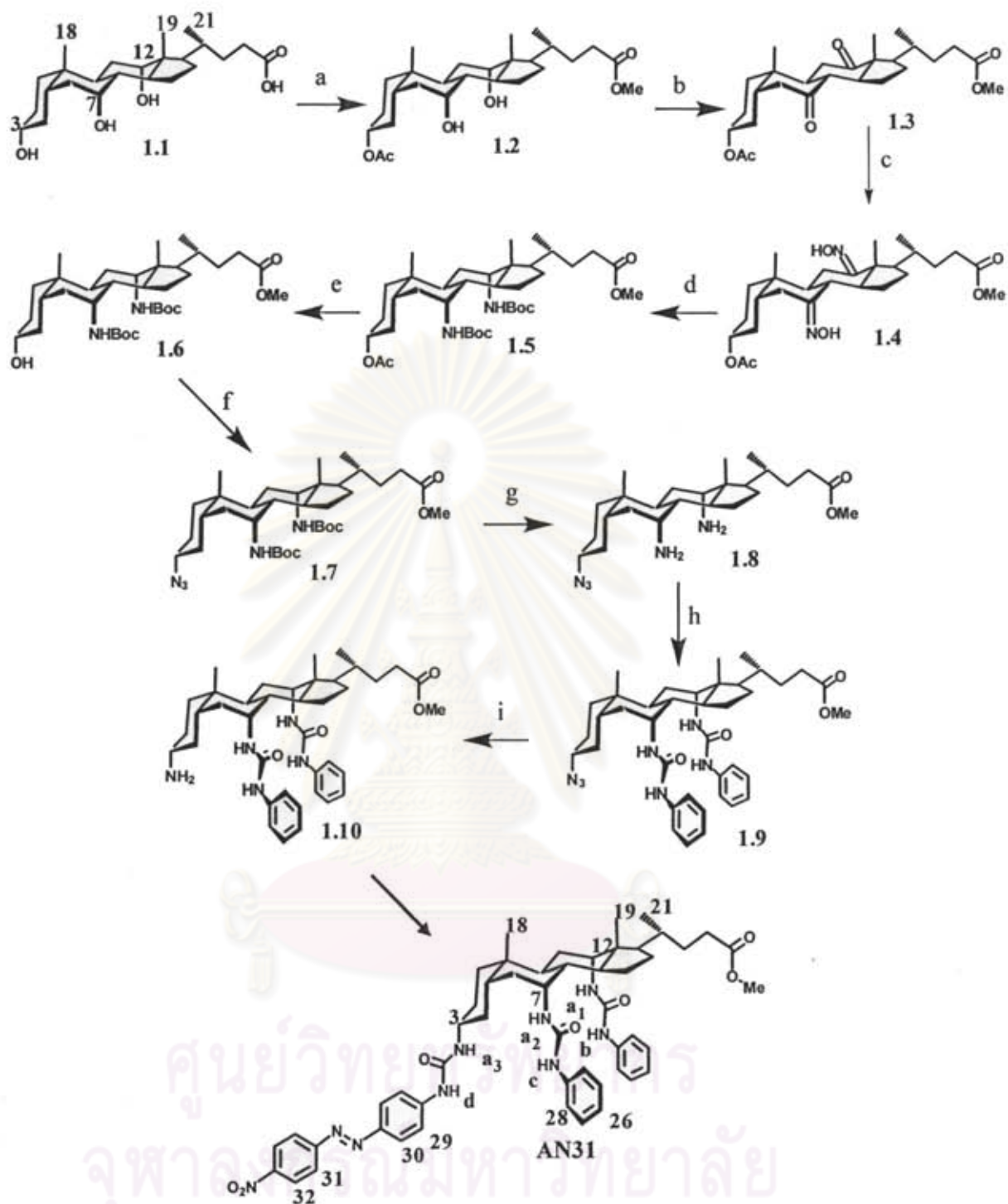


Figure 3.3 Schematic procedures for L3, Reagents and conditions: (a) p-TsOH, MeOAc, reflux; (b) Ca(ClO)₂, HOAc; (c) NH₂OH .HCl, NaOAc, reflux; (d) H₂ (1 atm), PtO₂, HOAc; Zn, HOAc; (Boc)₂O, NaHCO₃ aq., THF; (e) NaOMe, MeOH; (f) Ph₃P, DEAD, MeSO₃H, DMAP, THF; NaN₃, DMF, 47°C; (g) TFA, DCM; (h) PhNCO, Et₃N, DMAP, THF, 50°C; (i) activated zinc, HOAc; (j) 4-Isocyanato-4'-nitroazobenzene 1.11, DMAP, THF.

3.3.3 The complexation studies with amino acids

3.3.3.1 The complexation studies of ligand L3 with amino acids by using $^1\text{H-NMR}$ spectroscopy

$^1\text{H-NMR}$ spectroscopy has been widely employed to investigate receptor-substrate interactions. This technique allows access to the detail of the interaction between a host and a guest molecule. Therefore the binding ability of the multidentate urea receptor based on steroidal building block was investigated by the $^1\text{H-NMR}$ titration technique to determine the interactions and stoichiometry of the complexes.

Compound **L3** contains three urea groups at C3, C7 and C12 positions which are the binding sites for carboxylate group of amino acids. The urea groups at C7 and C12 are constrained by the axial orientation of the C-N bond, such that the NH groups point towards each other. The urea moiety at C3 can also point inwards resulting in the cooperation of hydrogen-bond donation to anionic guests.[81] **L3** is expected to show its ability in a discrimination L- and D-form of amino acid based on the difference of complex formation in space. Thus, complexation studies with 5 amino acids such as Trp, Phe, Leu, Ala and Gly were investigated for searching an enantioselectivity of this ligand for binding with amino acids.

$^1\text{H-NMR}$ titration studies were carried out in the absence and presence of amino acids. From Figure 3.4, $^1\text{H-NMR}$ spectra changes of **L3** upon adding excess amino acids provided preliminary information of the complex formation. The chemical shifts of ligand **L3** and their induced chemical shifts on the formation of complexes with amino acids are listed in Table 3.3.

From Figure 3.4 and Table 3.3, the downfield shift of NH urea ($\text{H}_{\text{a1-a3}}$, H_b , H_c and H_d) after adding amino acids can be explained by a complex formation via hydrogen bonding interactions between carboxylate group of zwitterionic amino acid and urea moieties. Not only the shifts of the urea protons but also the upfield shifts of aromatic protons (H_{27} , H_{28} , H_{29} and H_{30}) were observed. This upfield shift was indicative of an existing of π - π stacking interactions between amino acids side chain and aromatic moieties in **L3**.

Table 3.3 Chemical shifts (ppm) of ligand **L3** and their changes at complexation with various amino acids.*

	H ₂₆	H ₂₇	H ₂₈	H ₂₉	H ₃₀	NH _{a1}	NH _b	NH _c	NH _d
L3	6.86	7.20	7.38	7.84	7.56	6.00	8.46	8.23	8.93
L3.L-Trp	-0.02	-0.03	+0.08	-0.02	-	+0.48	+0.51	+0.34	+0.21
L3.D-Trp	-0.01	-0.03	+0.04	-0.03	-	+0.31	+0.36	+0.20	+0.22
L3.L-Phe	-0.03	-0.04	+0.08	-	-	-	+0.35	+0.19	+0.17
L3.D-Phe	-0.03	-0.04	+0.08	-0.02	+0.02	-	-	-	+0.22
L3.L-Leu	-0.03	-0.04	+0.08	-0.02	+0.03	+0.30	+0.04	-	+0.08
L3.D-Leu	-	-	+0.09	-	+0.05	+0.31	+0.06	+0.02	+0.09
L3.L-Ala	-0.02	-0.03	+0.09	-0.01	+0.03	-	-	-	+0.15
L3.D-Ala	-0.03	-0.04	+0.09	-0.02	+0.05	-	-	-	+0.25
L3.Gly	-0.03	-0.05	+0.12	-0.02	+0.07	-	-	-	+0.25

* Positive value showed downfield shifts and negative value showed upfield shifts.

The binding of **L3** with aromatic amino acids; Trp and Phe showed the largest shifts of the NH urea protons, typically H_b, H_c and H_a. This reflected the strong complex formation of these amino acids with **L3**. It is presumably due to a holding of hydrogen bonding and π - π stacking interactions. In case of aliphatic amino acids, the shifts of aromatic protons of **L3** were subjected to CH- π interactions. Considering the shifts of the aromatic protons, there is no difference in $\Delta\delta$ between complexes with aromatic and aliphatic amino acid. Thus, the selectivity of **L3** with L- and D-form amino acids was investigated by monitoring on the shifts of the NH urea protons.

From Figure 3.4, the difference in ¹H-NMR signals of NH urea protons in **L3.L-Trp** and **L3.D-Trp** complexes was found. L-Trp induced a larger downfield-shift of the urea protons (H_{a1-a3}, H_b and H_c). This indicated that the host **L3** showed more favorable in binding with L-Trp than with D-Trp. The DMSO-*d*₆ solution of the **L3.L-Trp** complex displayed magnificent downfield shifts with $\Delta\delta$ of +0.48, +0.51 and +0.34 ppm owing to H_{a1}, H_b and H_c respectively. In comparison, the shifts of NMR signals of the urea proton (H_d) and aromatic protons (H₂₆-H₃₀) displayed the same shifts in both complexes.

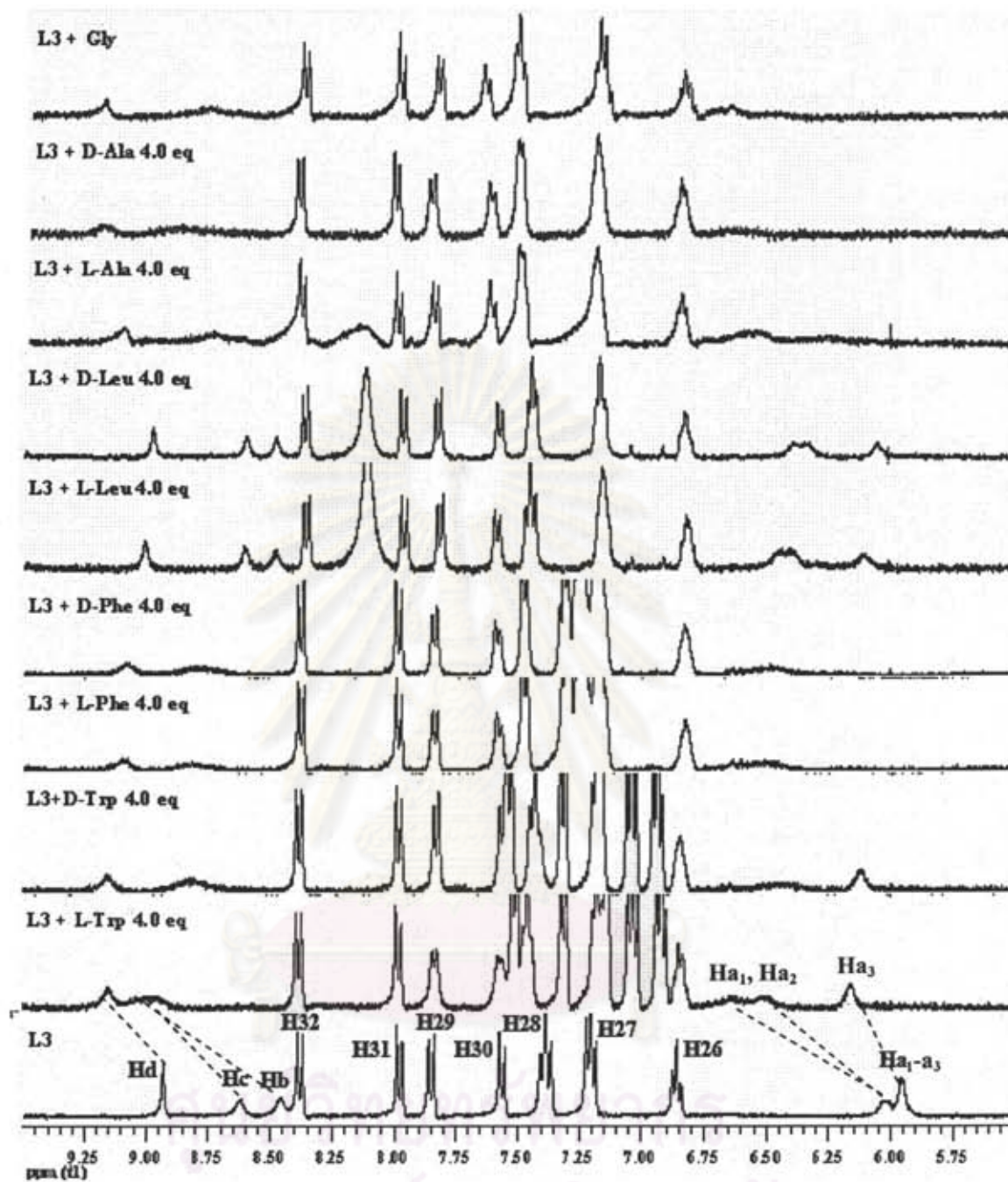


Figure 3.4 Partial ^1H -NMR spectra of L3 and the complexes of L3 with various amino acids.

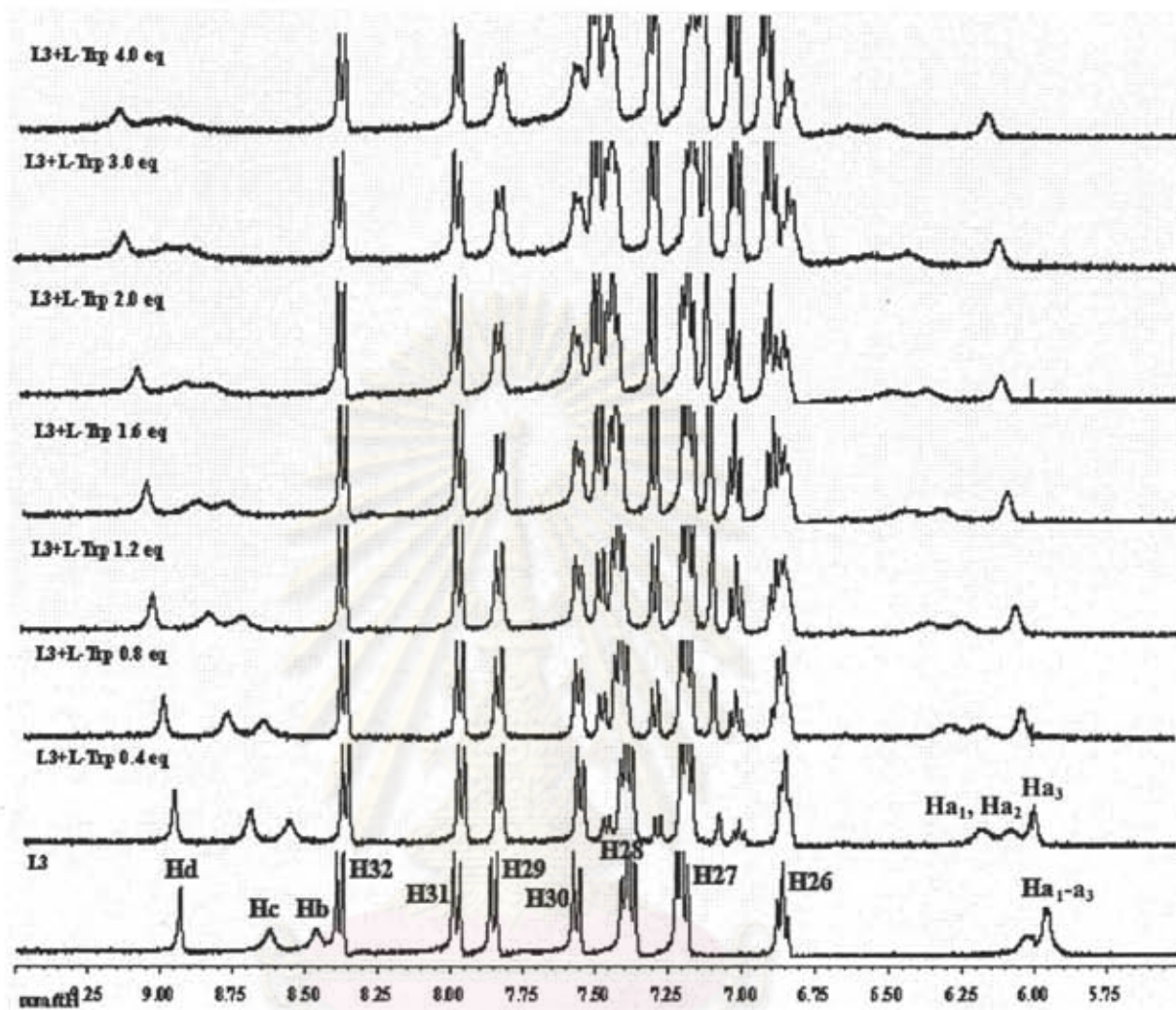


Figure 3.5 Partial $^1\text{H-NMR}$ titration spectra of L3 (4.0×10^{-3} M) upon adding L-Trp 4.0 equivalent in $\text{DMSO-}d_6$.

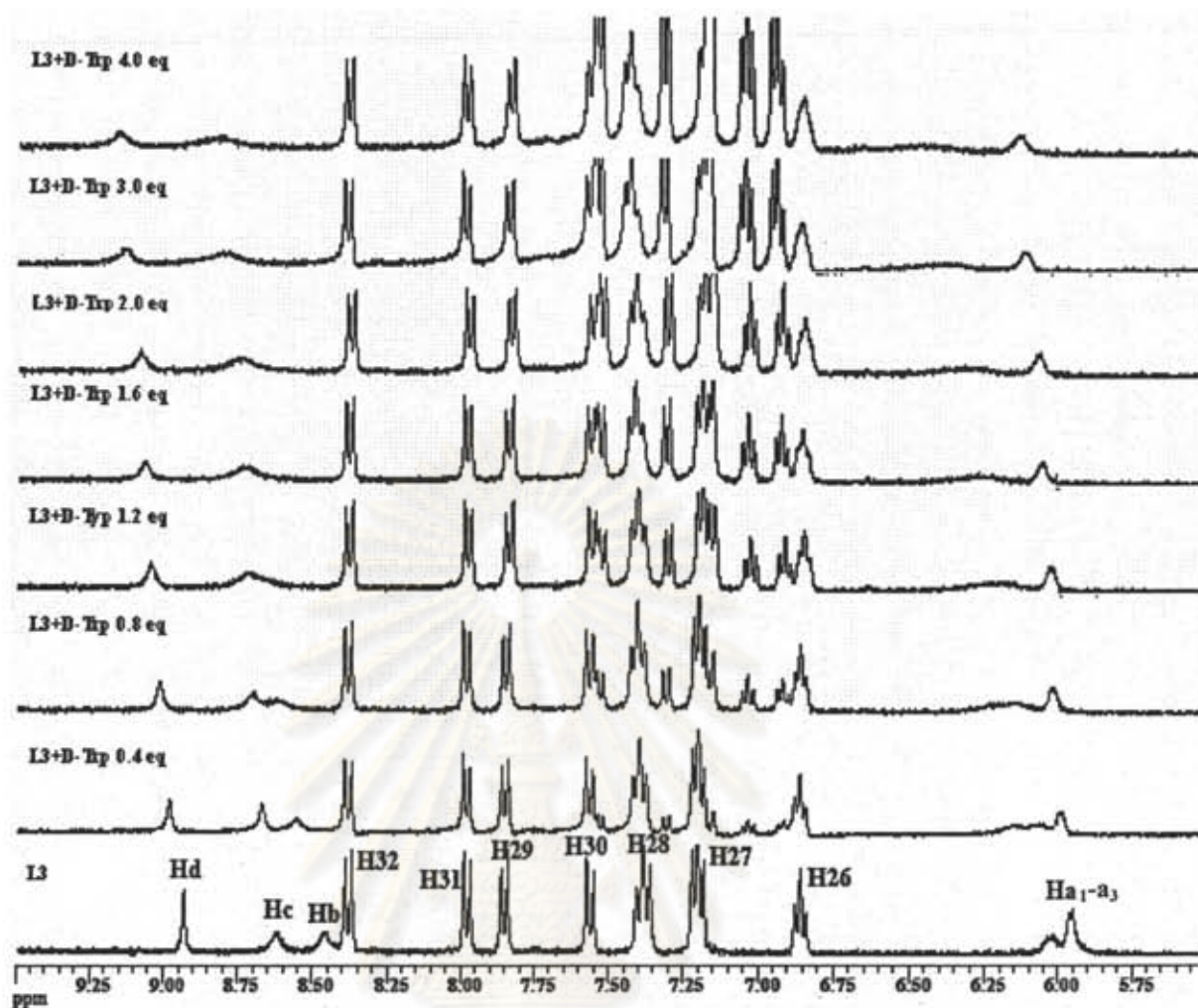


Figure 3.6 Partial ^1H -NMR titration spectra of L3 (4.0×10^{-3} M) upon adding D-Trp 4.0 equivalent in $\text{DMSO-}d_6$.

Titration of a $\text{DMSO-}d_6$ solution of L3 with aliquots of L-Trp and D-Trp guests resulted in several shifts as displayed in Figures 3.5 and 3.6, respectively. In case of the titration with L-Trp, a downfield shift of urea proton; H_d was found with $\Delta\delta$ of +0.21 and other urea protons displayed downfield shifts with $\Delta\delta$ of +0.48, +0.51 and +0.34 ppm corresponding to H_{a1} , H_b and H_c protons, respectively. Beside the downfield shift of NH_a protons, a splitting of the overlapping NH_{a1-a3} protons from two broad signals to three broad signals was observed. Generally, there are three urea binding sites in L3 molecule. Thus, NH_a urea protons displayed two signals owing to one proton at C3 position (H_{a3}) and two protons at C7 (H_{a2}) and C12 (H_{a1}) positions. The association of host L3 and L-

Trp via hydrogen bonding interaction at urea moieties caused the separation of the two protons adjacent to C7 and C12 positions. The more downfield shifts of NH_b and NH_c protons and the splitting of the NH_{a1-a3} protons revealed that the binding between L-Trp and L3 occurred at NH urea protons adjacent to C7 and C12 position.

The binding between L3 and D-Trp resulted in less downfield-shifts of NH_{a1-a3} , NH_b and NH_c with $\Delta\delta$ of +0.31, +0.36 and +0.22 ppm, respectively. In addition, the splitting of NH_{a1-a3} protons was found in the presence of D-Trp 0.4 equivalents but these signals were progressively broaden and then disappeared after adding D-Trp over 0.8 equivalents. From these changes in $^1\text{H-NMR}$ spectra, it was proposed that the binding of D-Trp with NH urea adjacent to C7 and C12 is not strong enough. The results from NMR technique revealed that the steroidal ligand L3 is prefer to bind with L-Trp over D-Trp. It is rationalized that the urea groups adjacent to C7 and C12 are in the axial position. A rigid bond and the NH group pointed inward caused a good preorganization of these urea protons prior to binding with carboxylate group of amino acids. L-form of amino acids which showed better binding affinity to C7 and C12 urea groups displayed the strong hydrogen bonding in complexes. The enantioselectivity of steroidal receptors for L-form amino acids has been reported by Davis groups.[56-57]

In case of a binding of L3 with other amino acids (Phe, Leu, Ala and Gly) in both L- and D-forms, the downfield-shifts of all NH thiourea protons were discovered, except Leu. These results revealed that L3 still has efficiency in the binding with carboxylate group of Phe, Leu, Ala and Gly guests but $^1\text{H-NMR}$ signals of L3 in complexation with L- and D-form of these amino acids showed insignificant changes in $^1\text{H-NMR}$ spectra. It was proposed that a less bulky group of amino acid side chain exhibit a less steric hindrance between amino acid side chain and phenyl ring of host L3. This factor should affect the different binding in the host-guest complexes.

The complexation stoichiometry in $\text{DMSO-}d_6$ solution was judged by Job's plot and was consistent with the titration curve of the $^1\text{H-NMR}$ data. The formation of simple 1:1 complexes in cases of all L3.amino acids complexes (Figure 3.7) was evidenced by the symmetric bell-shaped (the maximum of curve at $X = 0.5$) in Job's analysis.

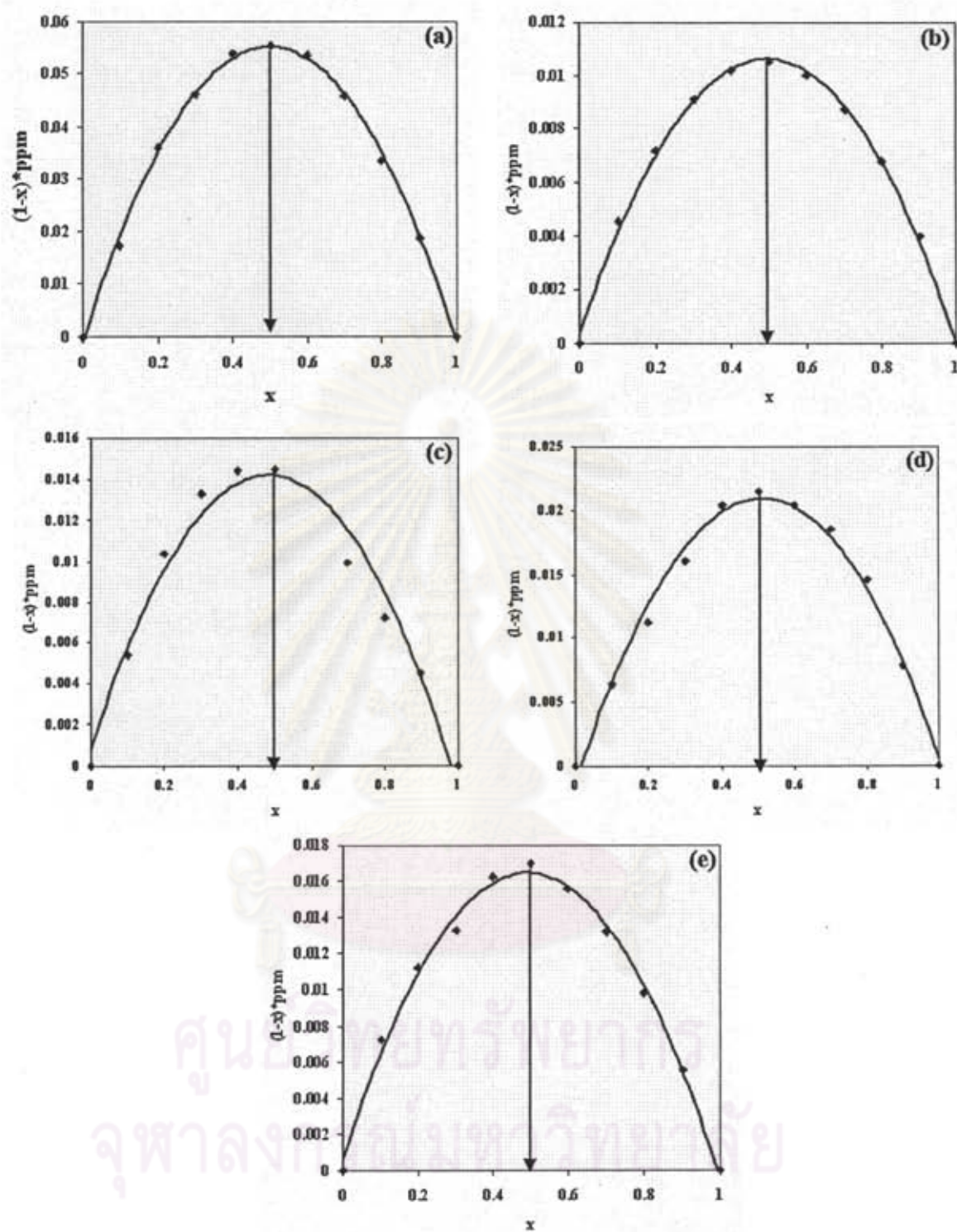


Figure 3.7 Job's plots of NH_3 in (a) L3'L-Trp, (b) L3'L-Phe, (c) L3'L-Leu, (d) L3'L-Ala and (e) L3'Gly complexes.

NOESY spectra of a [L3.D-Trp] clarified the complexation structure observed by the correlation at the aryl protons (T_5 and T_2) of D-Trp and phenyl protons assignments (H_{27} , H_{28} and H_{29}) of L3 and the correlation at NH indole proton of D-Trp and phenyl proton (H_{27}) (shown in Figures 3.8 and 3.9). In Figure 3.10, NOESY spectrum of L3.L-Trp complex showed many correlations of L3 phenyl protons and tryptophan side chain protons consisting of the Trp protons assignments (T_1 , T_2 , T_3 , T_4 and T_5). The correlation between the phenyl protons (H_{28} , H_{29} and H_{30}) and the Trp proton (T_5) were found in spectrum. Moreover, the correlation at urea protons (NH_a) of L3 and Trp protons (T_1 , T_2 and T_4) was seen from the spectrum. This strong evidence showed in agreement with the complex formation between L3 and Trp in both L- and D-forms at urea and phenyl urea underwent the hydrogen bonding interactions and π - π stacking interactions.

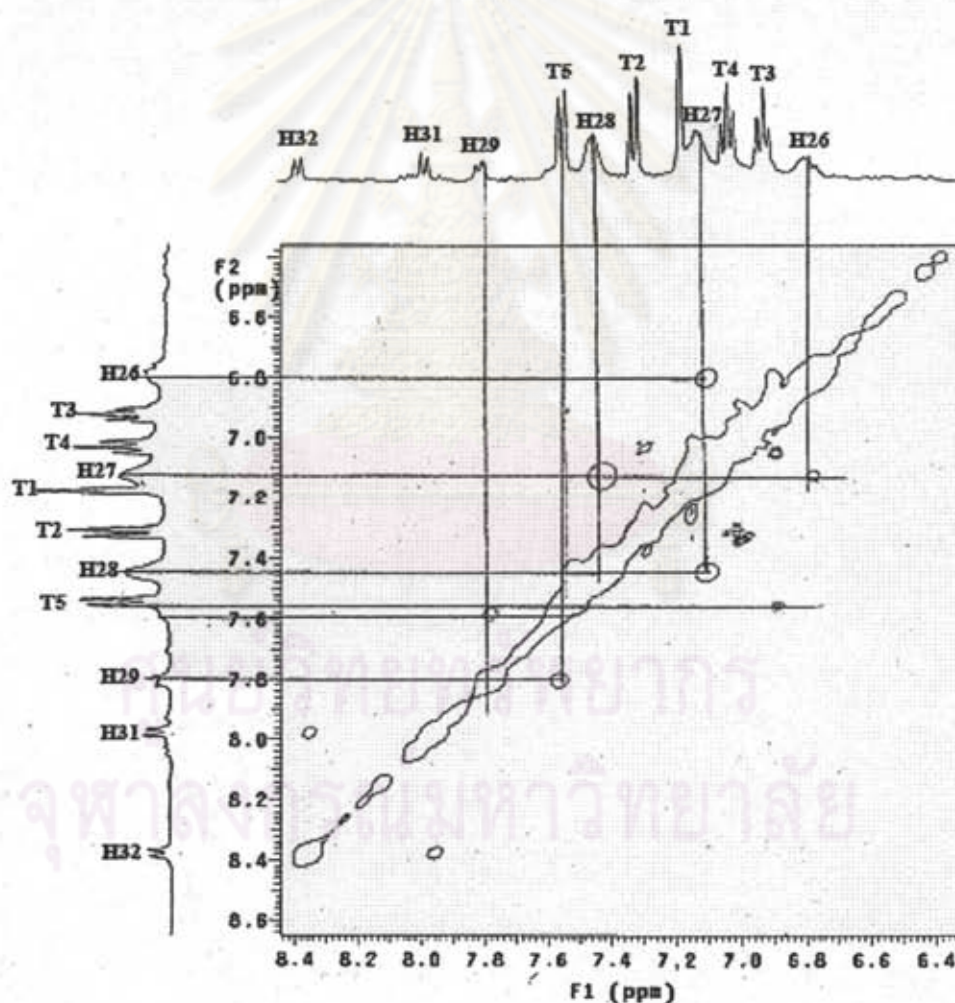


Figure 3.8 ¹H-H NOESY NMR of L3:D-Trp complex.

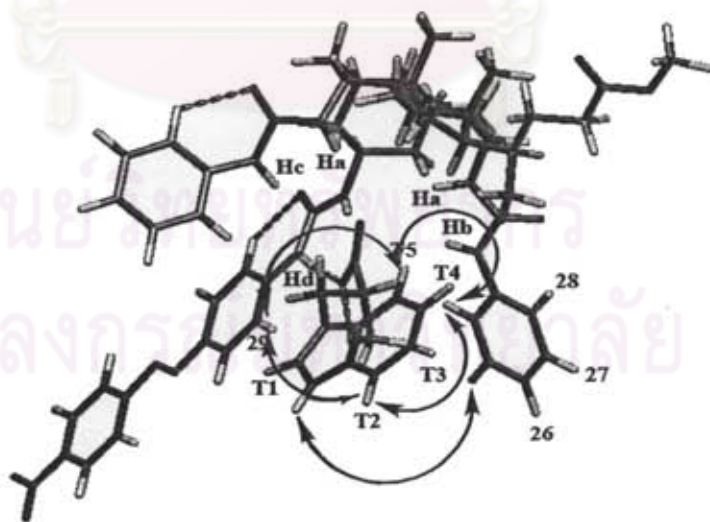
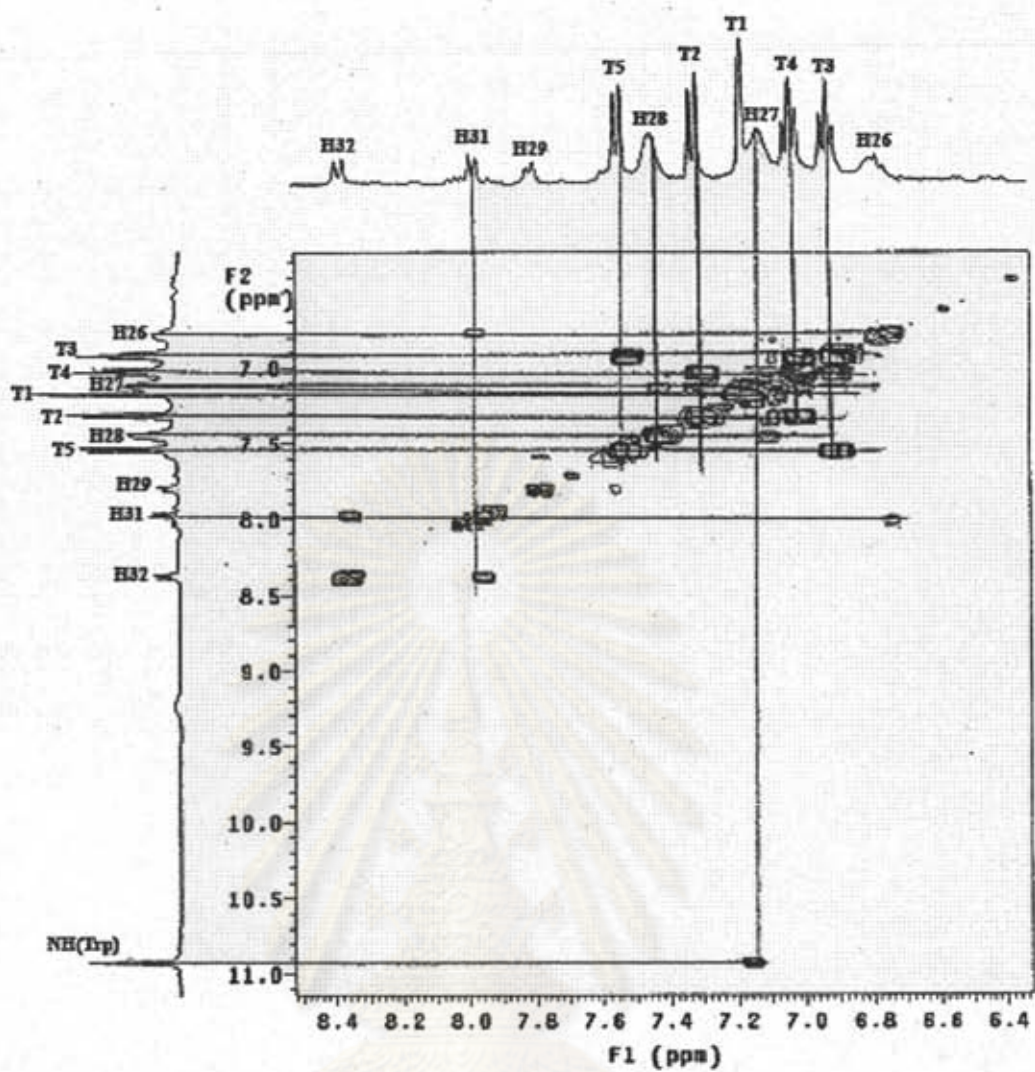
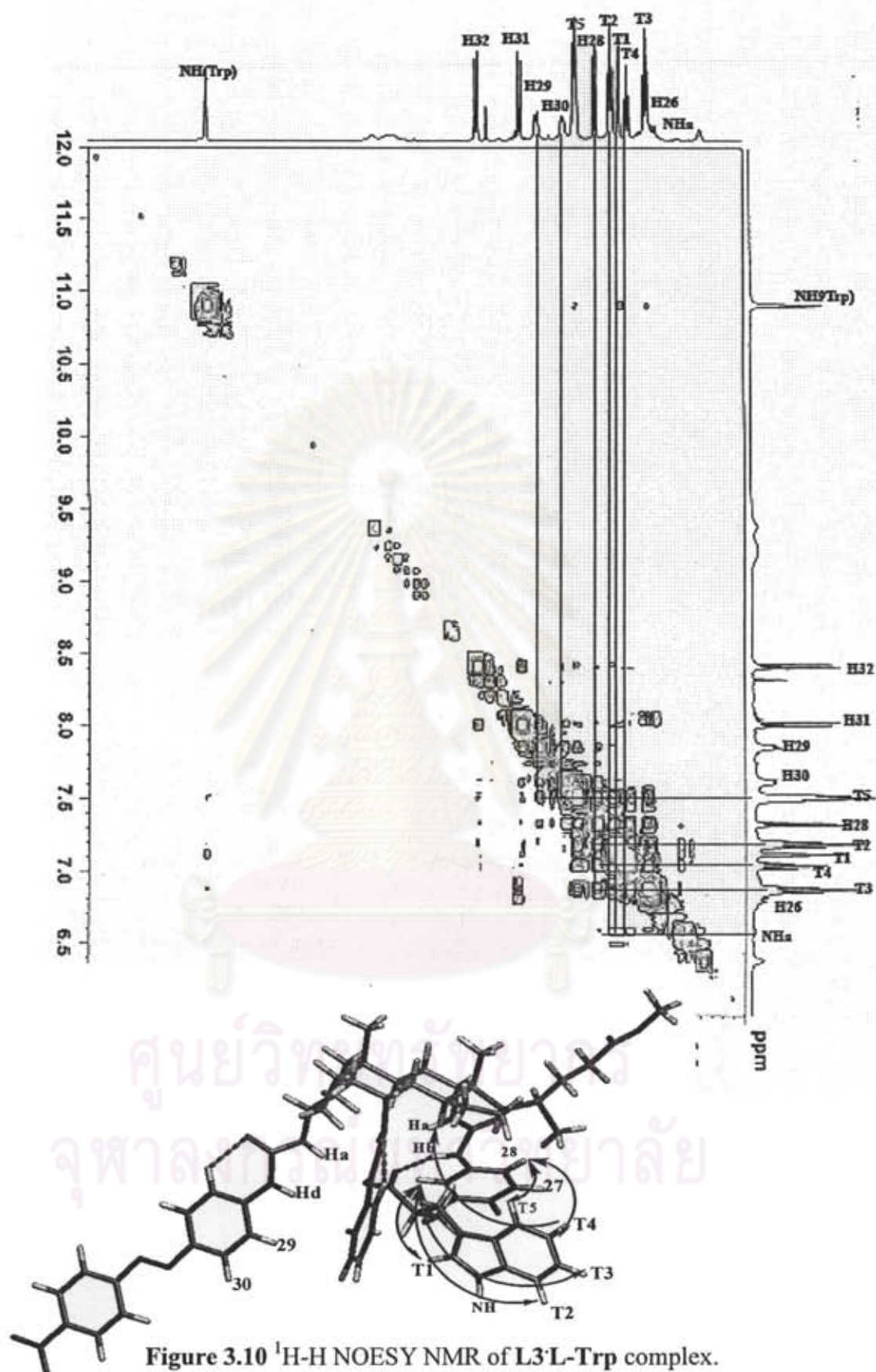


Figure 3.9 ^1H -H NOESY NMR of L3'D-Trp complex.



To gain more insight into the origin of the observed preference of **L3** with L-Trp and D-Trp, modeling studies using Density Functional Theory: DFT (B3LYP/6-31G(d)) in Gaussian03 Program on **L3.L-Trp** and **L3.D-Trp** complexes were carried out since attempts to grow the single crystal of both complexes were unsuccessful. Two energy minima obtained for the diastereomeric complexes are shown in Figure 3.11. Interestingly, differences between the two complexes showed that the carboxylate group of L-Trp located close to the urea NH groups adjacent to C7 and C12 positions, stabilizing by two hydrogen bonds (donor-acceptor distances $d[\text{NH}\cdots\text{O}] = 2.02\text{-}2.09 \text{ \AA}$). In contrast, D-Trp located at NH urea adjacent to C3 processing one hydrogen bonding interaction (donor-acceptor distances $d[\text{NH}\cdots\text{O}] = 2.19 \text{ \AA}$). These results are in agreement with the proposed structure of the **L3.Trp** complex in which the C7 and C12 urea moieties are the suitable binding sites corresponding to the larger downfield-shift of the urea protons (H_a , H_b and H_c) and the splitting of NH_a urea protons. In addition, it was found that an orientation of aromatic side chain of L-Trp positioned perpendicularly to the C7 and C12 phenyl urea moieties of the host. This contributes a forming of CH- π interaction between the phenyl urea and the L-Trp side chain. When the less bulky side chain amino acids is replaced, the changes in $^1\text{H-NMR}$ spectra of the complexes are not different between L- and D-form of amino acids. This means that the steric hindrance of amino acid side chain plays an important role in promoting the different binding of **L3** with L- and D-form of amino acids via the hydrogen bonding interactions with urea groups at C3, C7 or C12 positions.

ศูนย์วิจัยทรัพยากร
จุฬาลงกรณ์มหาวิทยาลัย

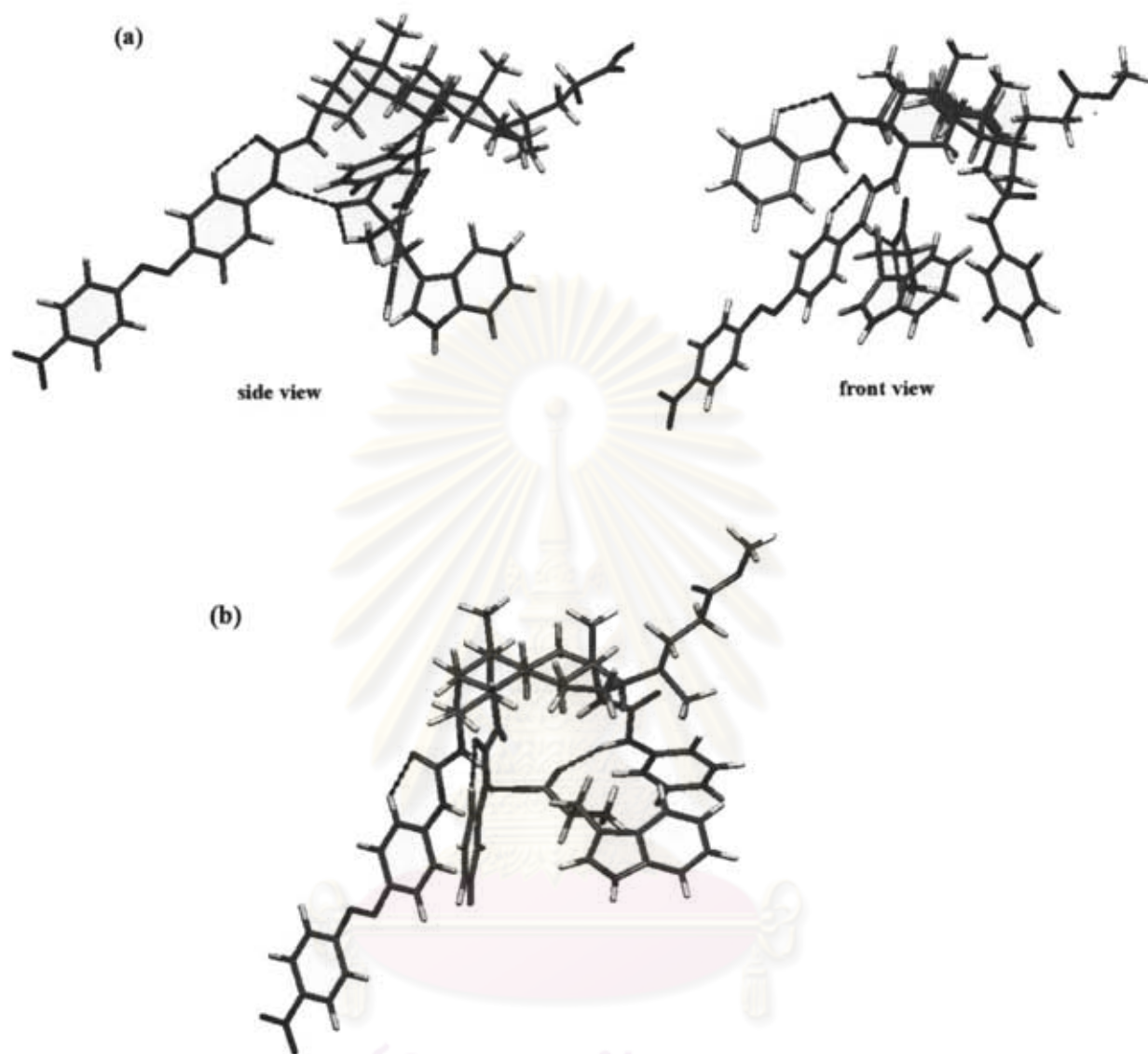


Figure 3.9 Structure of (a) L3.D-Trp and (b) L3.L-Trp complexes derived from computer-based molecular modeling. Intramolecular and intermolecular hydrogens are shown as broken lines.

Table 3.4 Binding constants (K) of ligand **L3** complexes with various amino acids using the EQNMR program.

Amino acids	K
L-Trp	386
D-Trp	9
L-Phe	36
D-Phe	10
L-Leu	<i>b</i>
D-Leu	<i>b</i>
L-Ala	<i>b</i>
D-Ala	15
Gly	49

b = cannot be calculated

According to the results in Table 3.4, ligand **L3** showed a significant preference to L-Trp observing from the highest binding constant. This was attributed to the orientation and the steric hindrance of Trp side chain in the host cavity. In other amino acids, the difference in the complexes of **L3** with L- and D-form was not observed for example Phe case. The binding constants of complexes of **L3** with L-Leu, D-Leu and L-Ala cannot be calculated because of a fluctuation of the shift of **L3** proton signals during the complexation. The complex formations of **L3** with L- and D-form of amino acids are not selective in case of less steric amino acids.

3.3.3.2 The complexation studies of **L3** with amino acids by UV-vis technique

The characteristic spectra of 2×10^{-5} M of ligand **L3** according to a light yellow solution in DMSO shows a broad band around 415 nm (as shown in Figure 3.12). This band attributes to the π - π^* excitation of more stable *trans* form of azobenzene.[82]

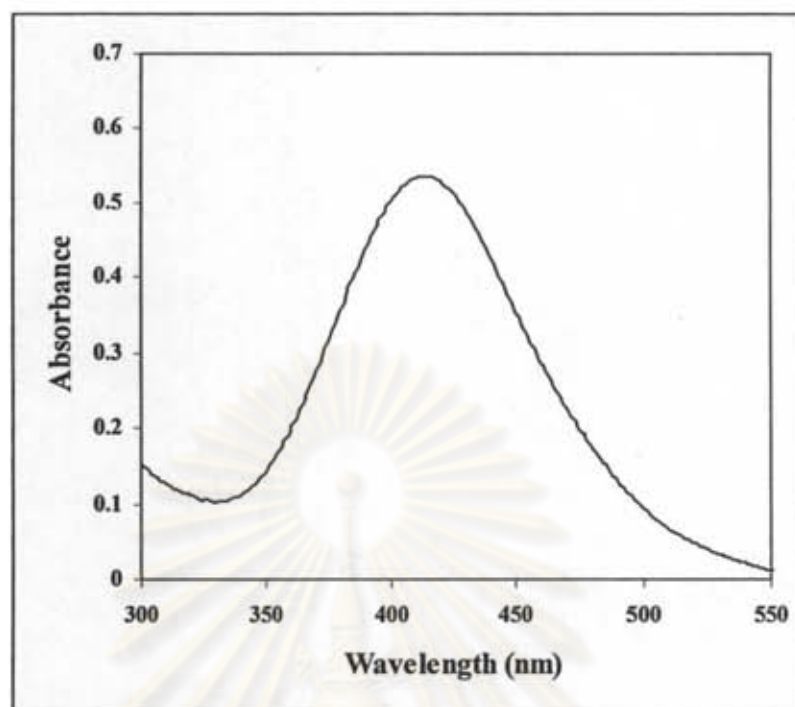


Figure 3.12 The UV-vis absorption spectra of ligand **L3** (2.0×10^{-5} M).

UV-vis titration experiments were carried out repeatedly in the presence of various amino acids to investigate the binding abilities of **L3** with various amino acids toward the association constant (shown in Figures 3.13 and 3.14 for **L3.L-Trp** and **L3.D-Trp** complexes, respectively). The absorption band of **L3** at 415 nm is slightly increased upon adding L- or D-Trp and a small shift of the absorption band to longer wavelength was observed for the addition of D-Trp. No significant change in absorption spectra and color was observed when both L- or D-Trp were exposed in the solution of **L3** in DMSO. In cases of other amino acids, the difference in spectra of **L3** upon adding L- and D-form was not notable as expected. These results were probably due to a position of azobenzene which was attached to urea group at C3 position. As mention previously from the modeling structures, amino acids in both L- and D-form are positioned in the center between the C7 and C12 urea moieties although there is the difference in the forming of the hydrogen bonding interactions between the host and the guest. Thus, the azobenzene

chromophore linking with the C3 urea group which positioned far away from the C7 and C12 urea groups received a little effect on the guest binding. However, the binding constants of complexes could be determined by monitoring the changes in the maximum absorption band of ligand **L3** at 415 nm using the SPECFIT32 program. The binding constants were collected in Table 3.4.

Table 3.5 Summary of the binding constants (log K) of ligand **L3** for various amino acids using the SPECFIT32 program.

Amino acids	Log K
L-Trp	4.54
D-Trp	2.08
L-Phe	2.61
D-Phe	2.62
L-Leu	2.02
D-Leu	2.51
L-Ala	2.72
D-Ala	2.95
Gly	2.33

Corresponding to the results from the $^1\text{H-NMR}$ technique, the binding constants in Table 3.5 showed that ligand **L3** gave the highest log K value (4.54) to L-Trp. The preferential binding of **L3** was significantly observed for L-Trp over D-Trp and other amino acids. In case of Phe, Leu and Ala, the binding affinities of **L3** could not discriminate between L- and D-forms of amino acids in the attribution of the similar log K values. The results from NMR and UV-vis experiments suggested that **L3** has a powerful potential to discriminate between L-Trp and D-Trp. We assumed that this result stemmed from the difference in the orientation and the steric bulkiness of amino acids.

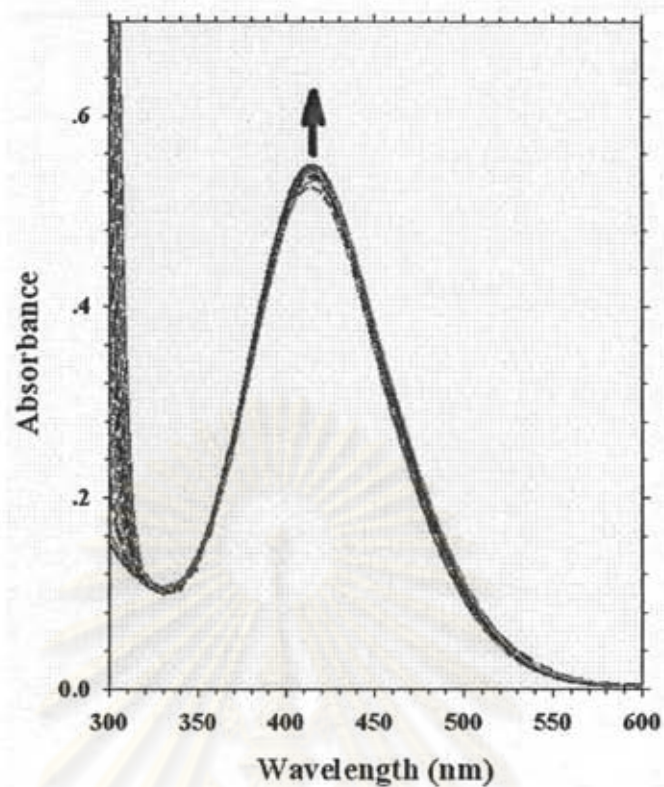


Figure 3.13 UV-vis titration spectra of L3 (2×10^{-5} M) upon adding L-Trp 40 eq.

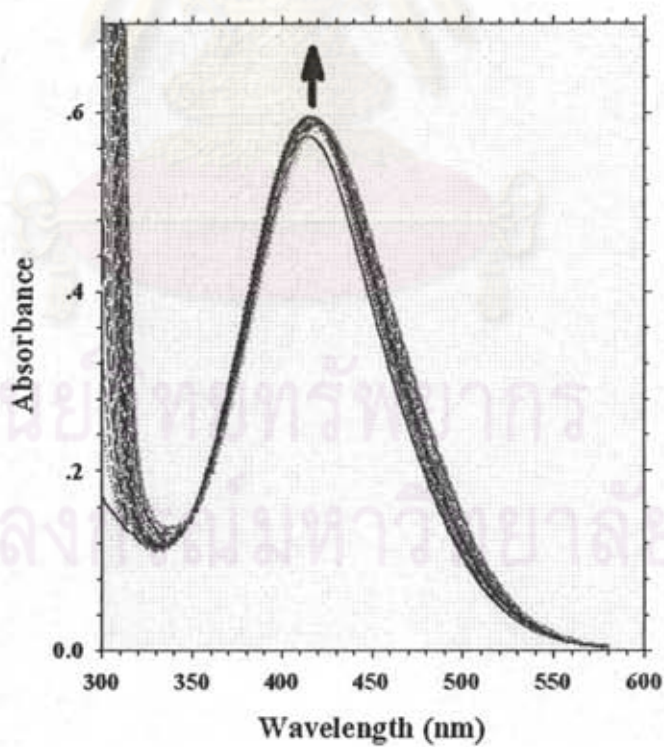


Figure 3.14 UV-vis titration spectra of L3 (2×10^{-5} M) upon adding D-Trp 300 eq.

CHAPTER IV

CONCLUSION

4.1 Conclusion

The synthesis of fluorescent receptor based on acridine derivative **L1** was carried out by a coupling reaction of proflavinedithiocyanate with aniline in 52%. Receptor **L2** was obtained by a nucleophilic substitution reaction of pyrocatechol with iodomethane in the presence of potassium carbonate as base in acetonitrile yielded **1** (54%), then followed by a nitration reaction with acetic acid and nitric acid in acetonitrile to afford compound **2** (10%). After that a coupling reaction of **2** with tetraethyleneglycol ditosylate in the presence of potassium carbonate as base in acetonitrile gave compound **3** (40%). The nitro groups of **3** were reduced using Raney nickel to obtain diamino compound **4** (77%). Upon coupling reaction of **4** with proflavinedithiocyanate produced the desired product **L2** (17%). The receptor **L1H** and **L2H** were accomplished from a reaction of **L1** and **L2** with trifluoroacetic acid, respectively.

Binding recognitions of receptors **L1** and **L2** in DMSO- d_6 were investigated toward amino acids using $^1\text{H-NMR}$ technique. The complexes of both receptors and guests took through the hydrogen bonding interaction between thiourea based on receptors and carboxylate of zwitterionic amino acids. The stoichiometry of the complexes of **L1** and **L2** with Trp and Phe by Job's plot analysis is indicative of 1:1 ratio. The binding with aromatic amino acids was observed a possibility of the complementary π - π stacking interaction of amino acid side chain with acridine ring and phenyl ring for **L1** and **L2**, respectively.

Absorption band of receptors **L1** and **L2** were appeared at 400 nm. This band was attributed to n - π^* transition. Upon adding amino acids, a slightly red-shift of the band at 400 nm to 460 nm was observed in both receptors. This indicated weak complexes formation of **L1** and **L2** with amino acids due to a repulsion between electron density at N-acridine and a negative charge at carboxylate group in amino acids. In the case of receptors **L1H** and **L2H**, the maximum absorption band at 460 nm which concerned to π -

π^* transition dramatically changes in their UV-vis spectra upon addition of amino acids. An observation of a progressive decrease of the band at 460 nm during a developing of a new band at 400 nm was proposed as a transformation from NH^+ -acridinium to neutral N-acridine via the intermolecular proton transfer by amino acids. In addition, the enhancement in fluorescence intensity was found in all receptors upon adding amino acids but **L1H** and **L2H** showed the stronger enhancement meaning more efficiency in amino acid recognition. It was found not only the enhancement but also a blue shift of emission band upon the binding between **L1H** and **L2H** with amino acids. Binding constants ($\log K$) and fluorescent enhancement factor (FE) were determined by fluorescence titration. Corresponding of $\log K$, FE values and the results from the changes in UV-vis spectra demonstrated that **L2** preferred to bind aromatic amino acids over aliphatic amino acids. **L1** showed no selectivity in amino acids binding. **L1H** and **L2H** showed the binding abilities with amino acids over **L1** and **L2** due to the losing of electron density at N-acridine. Among amino acids, Trp established the strongest complex with **L1H** and **L2H**.

The steroidal receptor **L3** was carried out from cholic acid (**1.1**). One pot esterification and acetylation of **1.1** using methyl acetate and p-toluenesulfonic acid monohydrate yielded **1.2** (78%), then followed by oxidation of the C7 and C12 hydroxyl groups with glacial acetic acid and $\text{Ca}(\text{ClO})_2$ afforded diketone **1.3** (98%). After that the diketone was changed to dioxime by the dioximation reaction with sodium acetate and hydroxylamine hydrochloride providing the dioxime **1.4** (79%). Diamine compound was obtained from a catalytic hydrogenation of the dioxime (**1.4**) with Adam's catalyst (H_2 , PtO_2 and CH_3COOH) followed by a treatment with zinc in acetic acid. Then, the diamine was done Boc protection using saturated NaHCO_3 and di-*t*-butyldicarbonate to give bis-Boc protected compound **1.5** (72.9%). The acetoxy group at the C3 position of **1.5** was removed by sodium methoxide in dry methanol to give an alcohol product **1.6** (96.6%). After that the hydroxyl group at C3 position was converted to C3- α azide group by the Mitsunobu reaction using a reaction of **1.6** with Ph_3P , DEAD, MeSO_3H and DMAP in THF. This reaction gave C3- β methanesulfonate as an intermediate which was reacted with sodium azide to provide the C3- α azide product **1.7** (62.9%). Boc-deprotection

reaction of the azide **1.7** with trifluoroacetic acid yielded diamine compound **1.8** (78.6%). Bis-urea compound **1.9** (96%) was synthesized using a coupling reaction of **1.8** with phenylisocyanate in the presence of triethylamine as base and DMAP as a catalyst. The azide group at C3 position of the bis-urea **1.9** was successfully reduced using activated zinc in acetic acid to give C3-amino compound **1.10** (91%). Finally, **1.10** was reacted with the isocyanate nitroazobenzene **1.11** in the presence of DMAP as a catalyst to obtain the desired product **L3** (38%).

Binding properties of **L3** with L- and D-form amino acids were studied with an intrinsic chiral ligand **L3**. Results from $^1\text{H-NMR}$ revealed that the strong complexation of **L3** with amino acids occurred from a holding of hydrogen bonds and π - π stacking interactions. Corresponding between the results from NMR and UV-vis, **L3** is preferable to bind with L-Trp over D-Trp. Although **L3** has an efficiency in binding with Phe, Leu, Ala and Gly, the difference in complexation between L- and D- form of these amino acids did not perform. These results were clarified from the modeling studies which revealed the differences in the complex structures between **L3.L-Trp** and **L3.D-Trp** complexes. The hydrogen bonding interactions between the carboxylate group of Trp took place with the C7 and C12 urea groups in the case of **L3.L-Trp** complex but with the C3 urea group for the **L3.D-Trp** complex. These came from the orientation of Trp side chain in the complexes. **L3** could not be used to differentiate L- and D- form of amino acids which bear a less steric hindrance of side chain.

4.2 Suggestion for future works

The host-guest association of these complexes could be studied with di- or tri-peptide or other amino acids such as *N*-acetyl amino acid derivatives due to the problem in solubility of normal amino acids in DMSO, particularly aliphatic amino acids. Furthermore, attempts to grow the single crystal of complexes are to reveal the solid structure of the complexes.

Crown-ether like part which is a cation binding site in ligand **L2** does not participate in the binding with amino acids. An introduction of using aza-crown ether instead would afford a higher efficiency of this ligand in binding with amino acids. In addition, a new design receptor molecule which has the cation binding site close to the anion binding site will provide a high affinity of binding with amino acids.



ศูนย์วิจัยทรัพยากร
จุฬาลงกรณ์มหาวิทยาลัย

REFERENCES

- [1] Beer, P. D.; Gale, P. A. and Smith, D. K. *Supramolecular Chemistry*. New York: Oxford University Press, 1999.
- [2] Beer, P. D. and Gale, P. A. Anion recognition and sensing: the state of the art and future perspectives, *Angew. Chem. Int. Ed.* 40 (2001) :486-516.
- [3] Bianchi, A.; Bowman-James, K. and Garcia-Espana, E. *Supramolecular Chemistry of Anion*. New York: Wiley-VCH, 1997.
- [4] Martinez-Manez, R. and Sancenon, F. Fluorogenic and chromogenic chemosensors and reagents for anions, *Chem. Rev.* 103 (2003) :4419-4476.
- [5] Hou, X. and Kobir, K. 4-(*N,N*-Dimethylamino)benzoic acid as a new class of simple chromogenic and fluorogenic anion host exhibiting high selectivity to HPO_4^{2-} and SO_4^{2-} , *Chem. Lett.* 35 (2006) :116-117.
- [6] Kovalchuk, A.; Bricks, J. L.; Reck, G.; Rurack, K.; Schulz, B.; Szumna, A. and WeiBhoff, H. A charge transfer-type fluorescent molecular sensor that "Light Up" in the visible upon hydrogen bond-assisted complexation of anions, *Chem. Commun.* (2004) :1946-1947.
- [7] Hsiao, Y. J.; Fang, T. H.; Chang, Y. S.; Chang, Y. H.; Liu, C. H.; Ji, L. W. and Jywe, W. Y. Specific optical signalling of anions via intramolecular charge transfer pathway based on acridinedione fluorophore, *J. of Luminescence.* 126 (2007) :866-870.
- [8] de Silva, A. P.; Gunaratne, H. Q. N.; Gunnlaugsson, T.; Huxley, A. J. M.; McCoy, C. D.; Rademacher, J. T. and Rice, T. E. Signaling recognition events with fluorescent sensors and switches, *Chem. Rev.* 97 (1997) :1515-1566.
- [9] Werner, R. *Essentials of Modern Biochemistry*. Boston: Jones and Bartlett publisher, 1983.
- [10] Lehn, J.-M. and Sirlin, C. Molecular catalysis: enhanced rates of thiolysis with high structural and chiral recognition in complexes of a reactive macrocyclic receptor molecule, *J. Chem. Soc., Chem. Commun.* (1978) : 949-950.

- [11] Peacock, S. C.; Domeier, L. A.; Gaeta, F. C. A.; Helgeson, R. C.; Timko, J. M. and Cram, D. J. Host-guest complexation. 13. High chiral recognition of amino esters by dilocular hosts containing extended steric barriers, *J. Am. Chem. Soc.* 100 (1978) :8190-8202.
- [12] Sogah, G. D. Y. and Cram, D. J. Host-guest complexation. 14. Host covalently bound to polystyrene resin for chromatographic resolution of enantiomers of amino acid and ester salts, *J. Am. Chem. Soc.* 101 (1979) :3035-3042.
- [13] Newcomb, M.; Toner, J. L.; Helgeson, R. C. and Cram, D. J. Host-guest complexation. 20. Chiral recognition in transport as a molecular basis for a catalytic resolving machine, *J. Am. Chem. Soc.* 101 (1979) :4941-4947.
- [14] Peacock, S. S.; Walba, D. M.; Gaeta, F. C. A.; Helgeson, R. C. and Cram, D. J. Host-guest complexation. 22. Reciprocal chiral recognition between amino acids and dilocular systems, *J. Am. Chem. Soc.* 102 (1980) :2043-2052.
- [15] Davidson, R. B.; Bradshaw, J. S.; Jones, B. A.; Dalley, N. K.; Chirstensen, J. J.; Izatt, R. M.; Morin, F. G. and Grant, D. M. Enantimeric recognition of organic ammonium salts by chiral crown ethers based on the pyridino-18-crown-6 structure, *J. Org. Chem.* 49 (1984) :353-357.
- [16] Liu, R.; Sanderson, P. E. J. and Still, W. C. Enantioselective complexation of the alanine dipeptide by a C2 host molecule, *J. Org. Chem.* 55 (1990) :5184-5186.
- [17] Yoon, S. S. and Still, W. C. An exceptional synthetic receptor for peptide, *J. Am. Chem. Soc.* 115 (1993) :823-824.
- [18] Borchardt, A. and Still, W. C. Synthetic receptor for internal residues of a peptide chain. Highly selective binding of (L)X-(L)Pro-(L)X tripeptides, *J. Am. Chem. Soc.* 116 (1994) :7467-7468.
- [19] Pirkle, W. H. and Pochapsky, T. C. Chiral molecular recognition in small bimolecular systems: a spectroscopic investigation into the nature of diastereomeric complexes, *J. Am. Chem. Soc.* 109 (1987) :5975-5982.
- [20] Kuroda, Y.; Kato, Y.; Higashioji, T.; Hasegawa, J.-Y.; Kawanami, S.; Takahashi, M.; Shiraishi, N.; Tanabe, K. and Ogoshi, H. Chiral amino acid

- recognition by a porphyrin-based artificial receptor, *J. Am. Chem. Soc.* 117 (1995) :10950-10958.
- [21] Chen, H.; Ogo, S. and Fish, R. H. Bioorganometallic chemistry. 8. The molecular recognition of aromatic and aliphatic amino acids and substituted aromatic and aliphatic carboxylic acid guests with supramolecular (η^5 -pentamethylcyclopenta dienyl)rhodium-nucleobase, nucleoside, and nucleotide cyclic trimer hosts via non-covalent π - π and hydrophobic interactions in water: steric, electronic, and conformational parameters, *J. Am. Chem. Soc.* 118 (1996) :4993-5001.
- [22] Konishi, K.; Yahara K.; Toshishige, H.; Aida, T. and Inoue, S. A Novel anion-binding chiral receptor based on a metalloporphyrin with molecular asymmetry. highly enantioselective recognition of amino acid derivatives, *J. Am. Chem. Soc.* 116 (1994) :1337-1344.
- [23] Lipkowitz, K. B.; Raghobama, S. and Yang, J. A. Enantioselective binding of tryptophan by alpha-cyclodextrin, *J. Am. Chem. Soc.* 114 (1992) :1554-1562.
- [24] Wallance, K. J.; Fagmemi, R. I.; Folmer-Anderson, F. J.; Morey, J.; Lynth, V. M. and Anslyn, E. V. Detection of chemical warfare simulants by phosphorylation of a coumarin oximate, *Chem. Commun.* (2006) :3886-3888.
- [25] Baskin, S. I. and Brewer, T. G. Medical Aspects of Chemical and Biological Warfare. Washington DC: TMM Publications, 1997.
- [26] Beer, P. D. and Gale, P. A. Anion recognition and sensing: the state of the art and future perspectives, *Angew. Chem., Int. Ed. Engl.* 40 (2001) :486-516.
- [27] Steiner, T. The hydrogen bond in the solid state, *Angew. Chem. Int. Ed.* 41 (2002) :48-76.
- [28] Dale, T. J. and Rebek, Jr. J. Fluorescent sensors for organophosphorus nerve agent mimics, *J. Am. Chem. Soc.* 128 (2006) :4500-4501.
- [29] Deslongchamps, G.; Galan, A.; de Mendoza, J. and Rebek, Jr. J. A synthetic receptor for cyclic adenosine monophosphate, *Angew. Chem., Int. Ed. Engl.* 31 (1992) :61-63.

- [30] Metzger, A.; Lynch, V. M. and Anslyn, E. V. A synthetic receptor selective for citrate, *Angew. Chem. Int. Ed. Engl.* 36 (1997) :862-865.
- [31] Berger, M. and Schmidtchen, F. P. Zwitterionic guanidinium compounds serve as electroneutral anion hosts, *J. Am. Chem. Soc.* 121 (1999) :9986-9993.
- [32] Shinoda, S.; Tadokoro, M.; Tsukube, H. and Arakawa, R. One-step synthesis of a quaternary tetrapyrindinium macrocycle as a new specific receptor of tricarboxylate anions, *Chem. Commun.* (1998) :181-182.
- [33] Abouderbala, L. O.; Belcher, W. J.; Boutelle, M. G.; Cragg, P. J.; Dhaliwal, J.; Fabre, M.; Steed, J. W.; Turner, D. R. and Wallace, K. J. Anion sensing 'Venus Flytrap' hosts: a modular approach, *Chem. Commun.* (2002) :358-359.
- [34] Lehn, J. M.; Meric, R.; Vigneron, J. P.; Bkouche-Waksman, J. and Pascard, C. Molecular recognition of anionic substrates. Binding of carboxylates by a macrobicyclic coreceptor and crystal structure of its supramolecular cryptate with the terephthalate dianion, *J. Chem. Soc., Chem. Commun.* (1991) :62-64.
- [35] Kimura, E. and Koike, T. Dynamic anion recognition by macrocyclic polyamines in neutral pH aqueous solution; development from static anion complexes to an enolate complex, *Chem. Commun.* (1998) :1495-1599.
- [36] Bazzicalupi, C.; Bencini, A.; Bianchi, A.; Cecchi, M.; Escuder, B.; Fusi, V.; Garcia-Espana, E.; Giorgi, C.; Luis, S. V.; Maccagni, G.; Marcelino, V.; Paoletti, P. and Valtanocoli, B. Thermodynamics of phosphate and pyrophosphate anions binding by polyammonium receptors, *J. Am. Chem. Soc.* 121 (1999) :6807-6815.
- [37] Boerrigter, H.; Grave, L.; Nissink, J. W. M.; Chrisstoffels, L. A. J.; van der Maas, J. H.; Verboom, W.; de Jong, F. and Reinhoudt, D. N. (Thio)urea resorcinarene cavitands. Complexation and membrane transport of halide anions, *J. Org. Chem.* 63 (1998) :4174-4180.
- [38] Buhlmann, P.; Nishizawa, S.; Xiao, K. P. and Umezawa, Y. Strong hydrogen bond-mediated complexation of H_2PO_4^- by neutral bis-thiourea hosts, *Tetrahedron* 53 (1997) :1647-1654.

- [39] Sasaki, S. I.; Mizuno, M.; Naemura, K. and Tobe, Y. Synthesis and anion selective complexation of cyclophane-based cyclic thioureas, *J. Org. Chem.* 65 (2000) :275-283.
- [40] Gale, P. A.; Sessler, J. L. and Kral, V. Calixpyrroles, *Chem. Commun.* (1998) :1-8.
- [41] Bucher, C.; Zimmerman, R. S.; Lynch, V. and Sessler, J. L. First cyptand-like calixpyrrole: synthesis, X-ray structure, and anion binding properties of a bicyclic [3,3,3] nonapyrrole, *J. Am. Chem. Soc.* 123 (2001) :9716-9717.
- [42] Woods, C. J.; Camiolo, S.; Light, M. E.; Coles, S. J.; Hursthouse, M. B.; King, M. A.; Gale, P. A. and Essex, J. W. Fluoride-selective binding in a new deep cavity calix[4]pyrrole: experiment and theory, *J. Am. Chem. Soc.* 124 (2002) :8644-8652.
- [43] Sessler, J. L.; Mody, T. D.; Ford, D. A. and Lynch, V. A Nonaromatic expanded porphyrin derived from anthracene – a macrocycle which unexpectedly binds anions, *Angew. Chem., Int. Ed. Engl.* 31 (1992) :452-455.
- [44] Takeuchi, M.; Shioya, T. and Swager, T. M. Allosteric fluoride anion recognition by a doubly strapped porphyrin, *Angew. Chem. Int. Ed.* 40 (2001) :3372-3376.
- [45] Gale, P. A.; Camiolo, S.; Chapman, C. P.; Light, M. E. and Hursthouse, M. B. Hydrogen-bonding pyrrolic amide cleft anion receptors, *Tetrahedron. Lett.* 42 (2001) :5095-5097.
- [46] Dudic, M.; Lhotak, P.; Stibor, I.; Lang, K. and Proskova, P. Calix[4]arene-porphyrin conjugates as versatile molecular receptors for anions, *Org. Lett.* 5 (2003) :149-152.
- [47] Amendola, V.; Fabbrizzi, L.; Mangano, C.; Pallavicini, P.; Poggi, A. and Taglietti, A. Anion recognition by dimetallic cryptates, *Coord. Chem. Rev.* 219-221 (2001) :821-837.
- [48] Fabbrizzi, L.; Licchelli, M.; Rabaieli, G. and Taglietti, A. The design of luminescent sensors for anions and ionizable analytes, *Coord. Chem. Rev.* 205 (2000) :85-108.

- [49] Fielding, L. Determination of association constants (K_a) from solution NMR data, *Tetrahedron* 56 (2000) :6151-6170.
- [50] Macomber, R. S. An introduction to NMR titration for studying rapid reversible complexation, *J. Chem. Ed.* 69 (1992) :375-378.
- [51] Bourson, J. and Valeur, B. Ion-responsive fluorescent compounds. 2. Cation-steered intramolecular charge transfer in a crowned merocyanine, *J. Phys. Chem.* 93 (1989) :3871-3876.
- [52] Fery-Forgues, S.; Le Bris, M. T.; Guette, J. P. and Valeur, B. First crown ether derivative of benzoxazinone ; a new fluoroionophore for alkaline earth metals recognition, *J. Chem. Soc., Chem. Commun.* (1988) :384-385.
- [53] Hortala, M. A.; Fabbrizzi, L.; Marcotte, N.; Stomeo, F. and Taglietti, A. Designing the selectivity of the fluorescent detection of amino acids: a chemosensing ensemble for histidine, *J. Am. Chem. Soc.* 125 (2003) :20-21.
- [54] Ipe, B. I.; Mahima, S. and Thomas, G. Light-induced modulating of self-assembly on spiropyran-capped gold nanoparticles: a potential system for the controlled release of amino acid derivatives, *J. Am. Chem. Soc.* 125 (2003) :7174-7175.
- [55] Schmuck, C. and Bickert, V. N'-Alkylated guanidiniocarbonyl pyrroles: new receptors for amino acid recognition in water, *Org. Lett.* 5 (2003) :4579-4581.
- [56] Grawe, T.; Schrader, T. and Finocchiaro, P. A new receptor molecule for lysine and histidine in water: strong binding of basic amino acid esters by a macrocyclic host, *Org. Lett.* 3 (2001) :1597-1600.
- [57] Ballistreri, F. P.; Notti, A.; Pappalardo, S.; Parisi, M. F. and Risagatti, I. Multipoint molecular recognition of amino acids and biogenic amines by ureidocalix[5]arene receptors, *Org. Lett.* 5 (2003) :1071-1074.
- [58] Wehner, M.; Schrader, T.; Finocchiaro, P.; Failla, S. and Consiglio, G. A chiral sensor for arginine and lysine, *Org. Lett.* 2 (2000) :605-608.

- [59] Mandl, C. P. and Konig, B. Luminescent crown ether amino acids: selective binding to *N*-terminal lysine in peptides, *J. Org. Chem.* 70 (2005) :670-674.
- [60] Escuder, B.; Rowan, A. E.; Feiters, M. C. and Nolte, R. J. M. Enantioselective binding of amino acids and amino alcohols by self-assembled chiral basket-shaped receptors, *Tetrahedron* 60 (2004) :291-300.
- [61] Feuster, E. K. and Glass, T. E. Detection of amines and unprotected amino acids in aqueous conditions by formation of highly fluorescent iminium ions, *J. Am. Chem. Soc.* 125 (2003) :16174-16175.
- [62] Rebek, J. and Nemeth, D. Molecular recognition: three-point binding leads to a selective receptor for aromatic amino acids, *J. Am. Chem. Soc.* 107 (1985) :6738-6739.
- [63] Galan, A.; Andreu, D.; Echavarren, A. M.; Prados, P. and Mendoza, J. D. A receptor for the enantioselective recognition of phenylalanine and tryptophan under neutral conditions, *J. Am. Chem. Soc.* 114 (1992) :1511-1512.
- [64] Carey, F. A. and Sundberg, R. J. *Advanced Organic Chemistry; part B*, 3rd Edition. New York: Plenum press, 1990.
- [65] Benito, J. M.; Garcia, M. G.; Blanco, J. L. J.; Mellet, C. O. and Fernandez, J. M. G. Carbohydrate-based receptors with multiple thiourea binding sites. Multipoint hydrogen bond recognition of dicarboxylates and monosaccharides, *J. Org. Chem.* 66 (2001) :1366-1372.
- [66] Bordwell, F. G.; Algrim, D. J. and Harrelson, J. A. The relative ease of removing a proton, a hydrogen atom or an electron from carboxamides versus thiocarboxamides, *J. Am. Chem. Soc.* 110 (1988) :5903-5904.
- [67] Diverdi, L. A. and Topp, M. R. Subnanosecond time-resolved fluorescence of acridine in solution, *J. Phys. Chem.* 88 (1984) :3447-3451.
- [68] Kanamaru, N. and Lim, E. C. $T_1(\pi\pi^*) \rightarrow S_0$ radiationless transitions in aromatic molecules with nonbonding electrons, *J. Chem. Phys.* 65 (1976) :4055-4029.

- [69] Davis, A. P. and Joos, J. B. Steroids as organising elements in anion receptors, *Coord. Chem. Rev.* 240 (2003) :143-146.
- [70] Davis, A. P. and Wareham, R. S. Carbohydrate recognition through noncovalent interactions: a challenge for biomimetic and supramolecular chemistry, *Angew. Chem. Int. Ed.* 38 (1999) :2978-2996.
- [71] Davis, A. P. Cholaphanes et al.; steroids as structural components in molecular engineering, *Chem. Soc. Rev.* (1993) :243-255.
- [72] Liu, S. Y.; Fang, L.; He, Y. B.; Chan, W. H.; Yeung, K. T.; Cheng, Y. K. and Yang, R. H. Cholic-acid-based fluorescent sensor for dicarboxylates and acidic amino acids in aqueous solutions, *Org. Lett.* 7 (2005) :5825-5828.
- [73] Davis, A. P. and Lawless, L. J. Steroidal guanidinium receptors for the enantioselective recognition of *N*-acyl α -amino acids, *Chem. Commun.* (1999) :9-10.
- [74] Lawless, L. J.; Blackburn, A. G.; Ayling, A. J.; Perez-Payan, M. N. and Davis, A. P. Steroidal guanidines as enantioselective receptors for *N*-acyl α -amino acids. Part 1. 3α -guanylated carbamates derived from cholic acid, *J. Chem. Soc., Perkin Trans. 1.* (2001) :1329-1335.
- [75] Siracusa, L.; Hurley, F. M.; Dresen, S.; Lawless, L. J.; Perez-Payan M. N. and Davis, A. P. Steroidal ureas as enantioselective receptors for an *N*-acetyl α -amino carboxylate, *Org. Lett.* 4 (2002) :4639-4642.
- [76] Baragana, B.; Blackburn, A.G.; Breceia, P.; Davis, A. P.; de Mendoza, J.; Carrillo, J. M. P.; Prados, P.; Riedner, J. and de Vries, J.G. Enantioselective transport by a steroidal guanidinium receptor, *Chem. Eur. J.* 8 (2002) :2931-2936.
- [77] Cheng, Y.; Suenga, T. and Still, W. C. Sequence-selective peptide binding with a peptido-A,B-*trans*-steroidal receptor selected from an encoded combinatorial receptor library, *J. Am. Chem. Soc.* 118 (1996) :1813-1814.
- [78] Muynck, H. D.; Madder, A.; Farcy, N.; Clercq, P. J. D.; Perez-Payan, M. N.; Ohberg, L. M. and Davis, A. P. Application of combinatorial procedures in the search for serin-protease-like activity with focus on the acyl transfer step, *Angew. Chem., Int. Ed. Engl.* 39 (2000) :145-148.

- [79] Baragana, B.; Blackburn, A.G.; Breccia, P.; Davis, A. P.; de Mendoza, J. PadronlCarrillo, J. M.; Prados, P.; Tiedner, J. and de Vries, J.G. Enantioselective transport by a steroidal guanidinium receptor, *Chem. Eur. J.* 8 (2002) :2931-2935.
- [80] Sisson, A. L., Sanchez, V. D. A.; Margo, G.; Griffin, A. M. E.; Shah, S.; Charmant, J. P. H. and Davis, A. P. Spiraling steroids: organic crystals with asymmetric nanometer-scale channels, *Angew. Chem. Int. Ed.* 44 (2005) :6878-6881.
- [81] Ayling, A. J.; Perez-Payan, M. N. and Davis, A. P. New "Cholapod" anionophores; high-affinity halide receptors derived from cholic acid, *J. Am. Chem. Soc.* 123 (2001) :12716-12717.
- [82] Kumar, G. S. and Neckers, D. C. Photochemistry of azobenzene-containing polymers, *Chem. Rev.* 89 (1989) :1915-1925.



ศูนย์วิทยทรัพยากร
จุฬาลงกรณ์มหาวิทยาลัย



APPENDICES

ศูนย์วิทยทรัพยากร
จุฬาลงกรณ์มหาวิทยาลัย

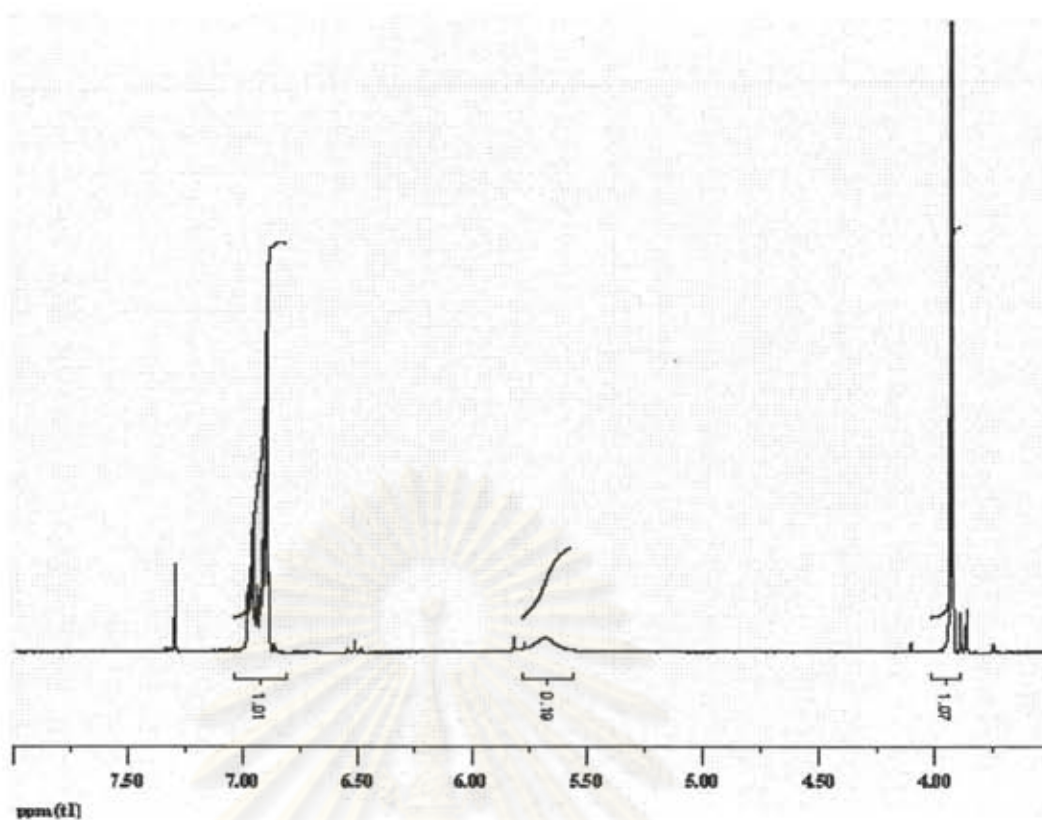


Figure A1. The ¹H-NMR spectrum of *o*-methoxy phenol (1) in CDCl₃ with 400 MHz.

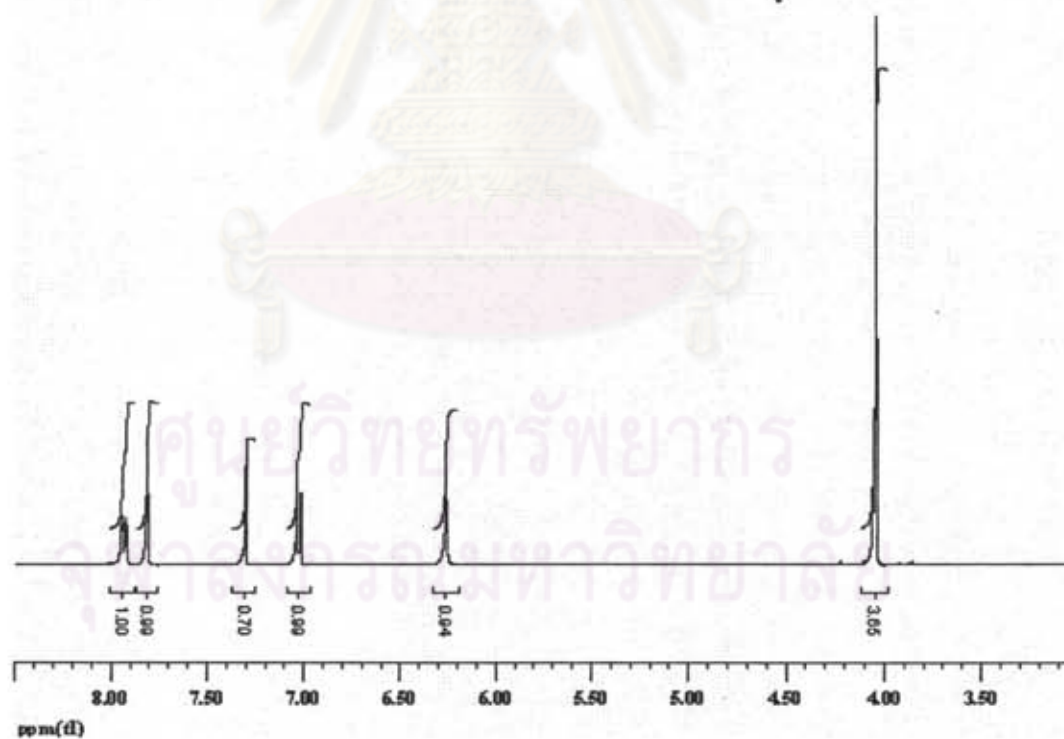


Figure A2. The ¹H-NMR spectrum of 2-methoxy-6-nitrophenol (2) in CDCl₃ with 400 MHz.

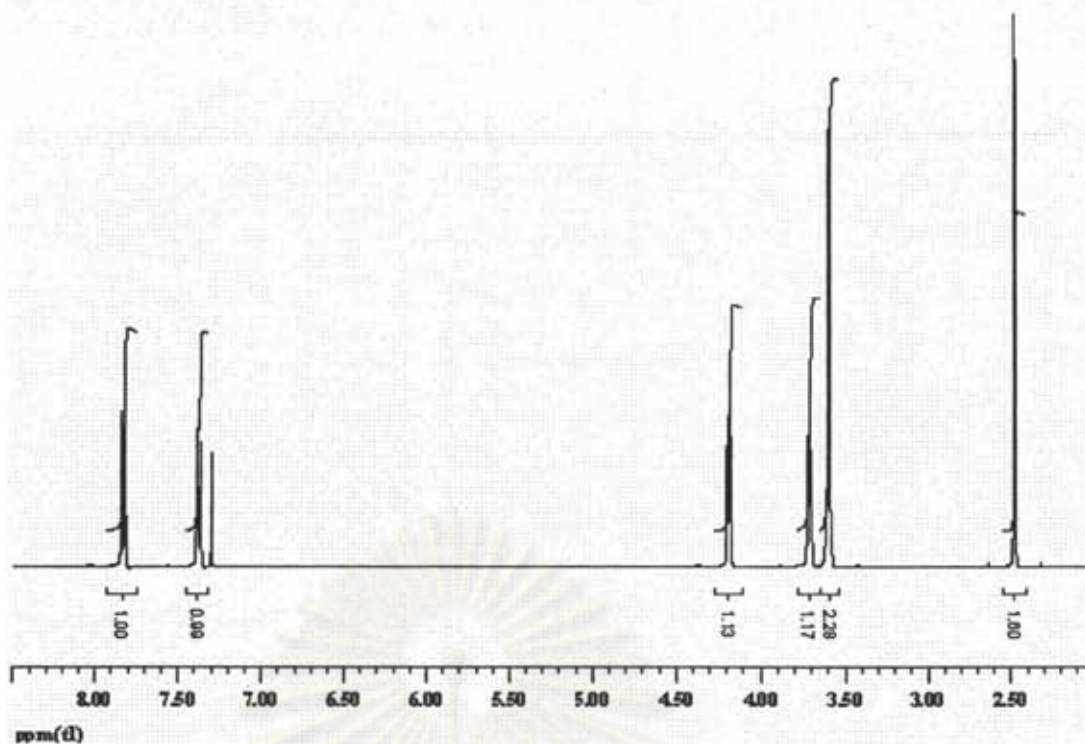


Figure A3. The $^1\text{H-NMR}$ spectrum of tetraethyleneglycol ditosylate in CDCl_3 with 400 MHz.

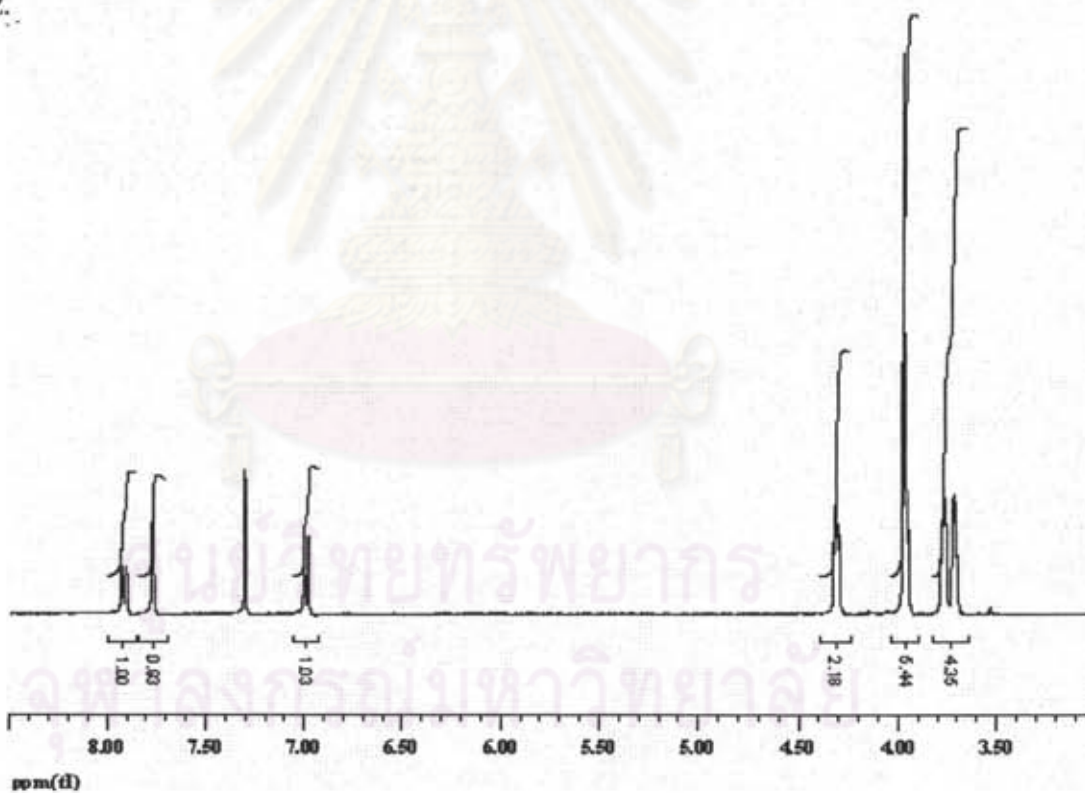


Figure A4. The $^1\text{H-NMR}$ spectrum of 2-methoxy-1-(2-(2-(2-(2-(2-methoxy-4-nitrophenoxy) ethoxy)ethoxy)ethoxy) ethoxy)-4-nitrobenzene (3) in CDCl_3 with 400 MHz.

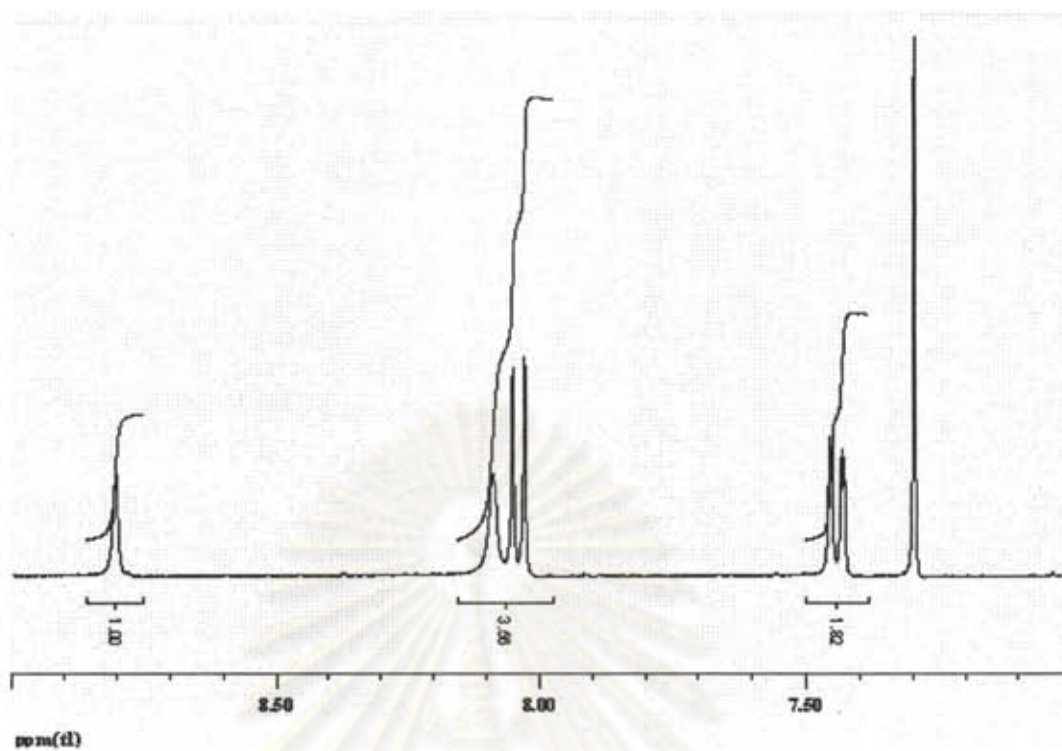


Figure A5. The ^1H -NMR spectrum of proflavine dithiocyanate in CDCl_3 with 400 MHz.

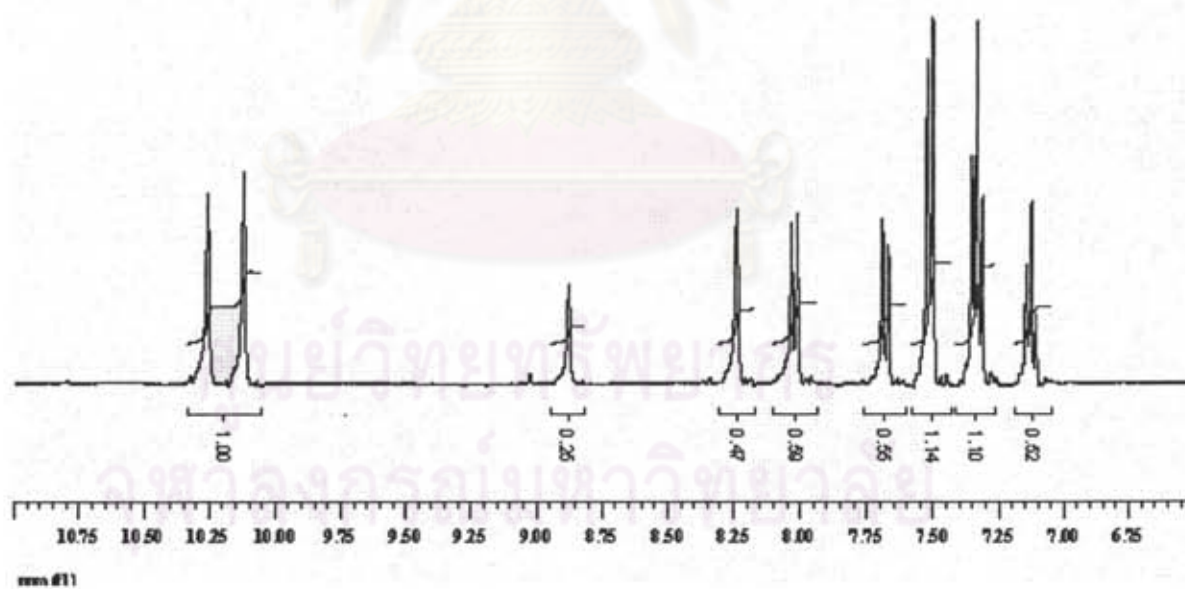


Figure A6. The ^1H -NMR spectrum of 3,6-bis(thioureaphenyl)acridine (L1) in $\text{DMSO}-d_6$ with 400 MHz.

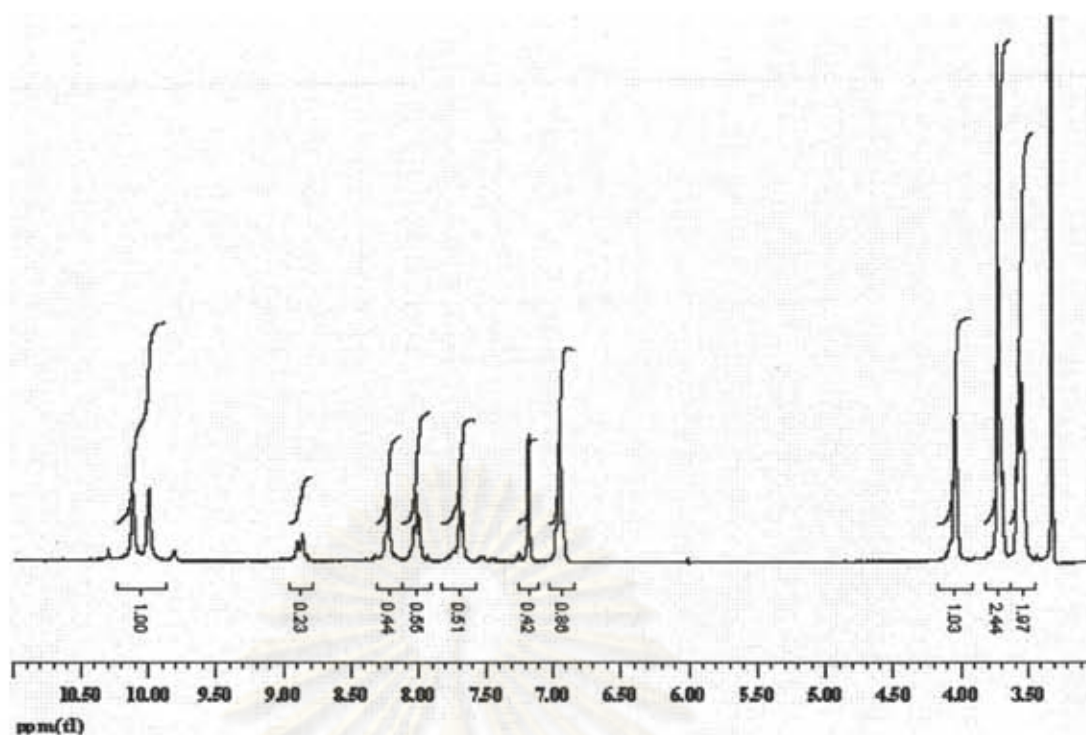


Figure A7. The ^1H -NMR spectrum of 3,6-[3-methoxy-4-(2-(2-(2-(2-(3-methoxy-1-thiourea benzene)ethoxy)ethoxy) ethoxy)ethoxy)-1-thiourea benzene]acridine (L2) in $\text{DMSO-}d_6$ with 400 MHz.

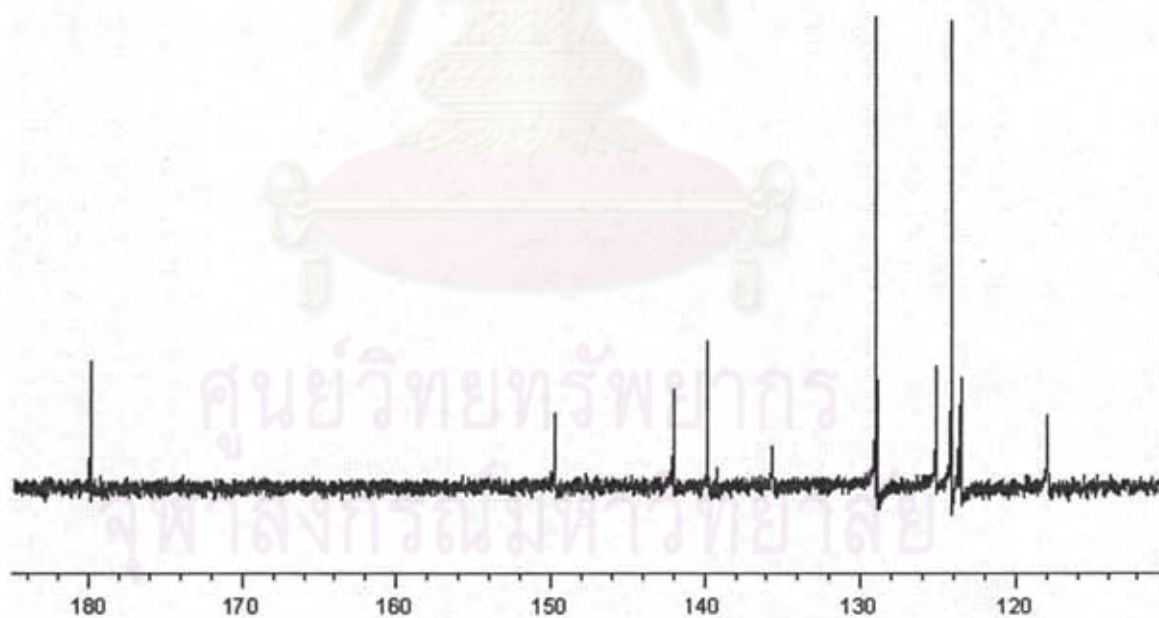


Figure A8. The ^{13}C -NMR spectrum of 3,6-bis(thiourea phenyl)acridine (L1) in $\text{DMSO-}d_6$ with 400 MHz.

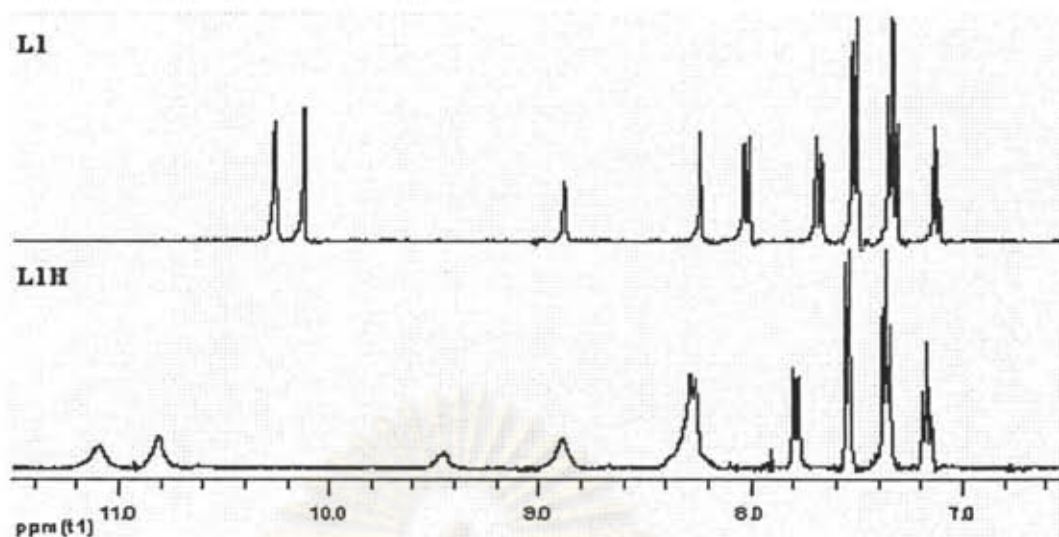


Figure A9. The ^1H -NMR spectrum of L1H in $\text{DMSO-}d_6$ for a comparison with ^1H -NMR spectrum of L1 with 400 MHz.

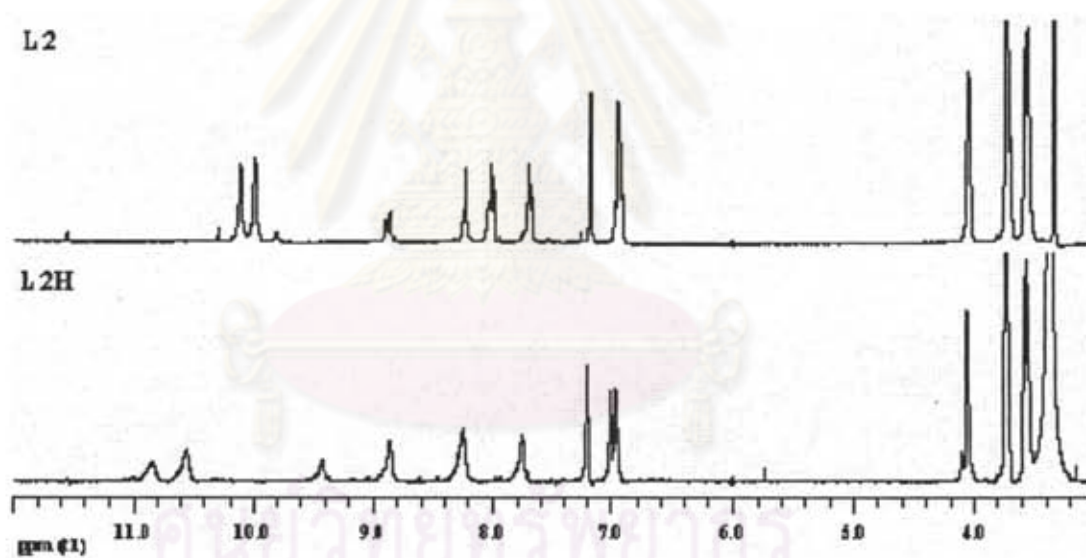


Figure A10. The ^1H -NMR spectrum of L2H in $\text{DMSO-}d_6$ for a comparison with ^1H -NMR spectrum of L2 with 400 MHz.

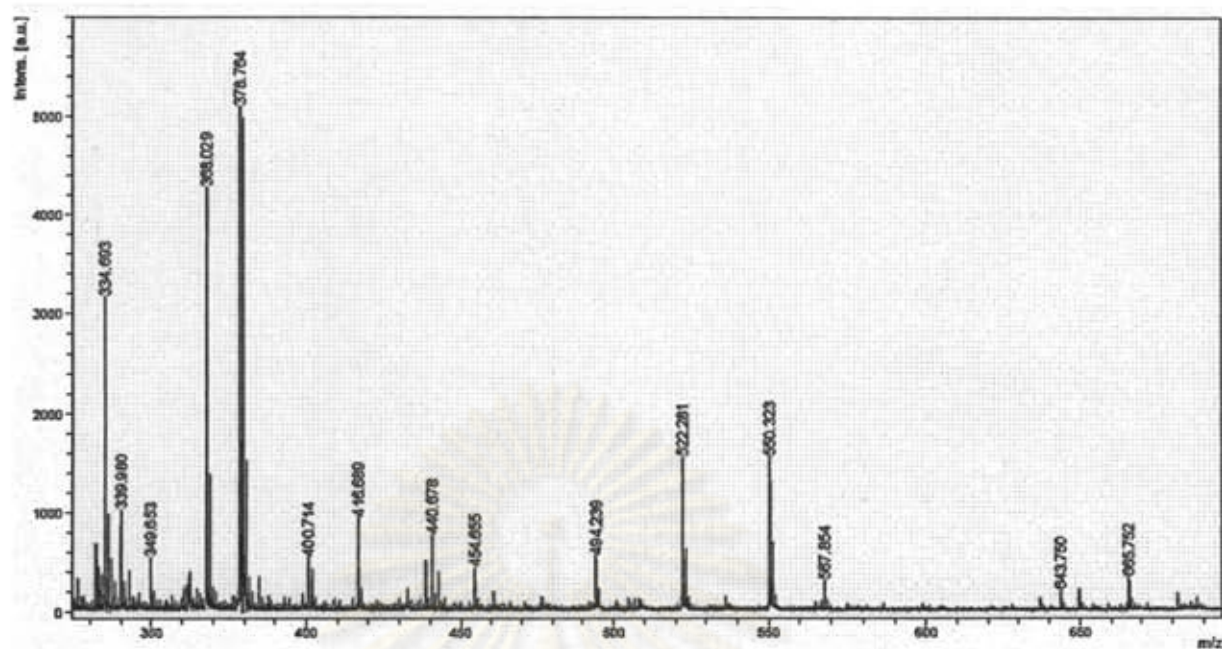


Figure A11. The mass spectrum (ESI) of ligand L1H.

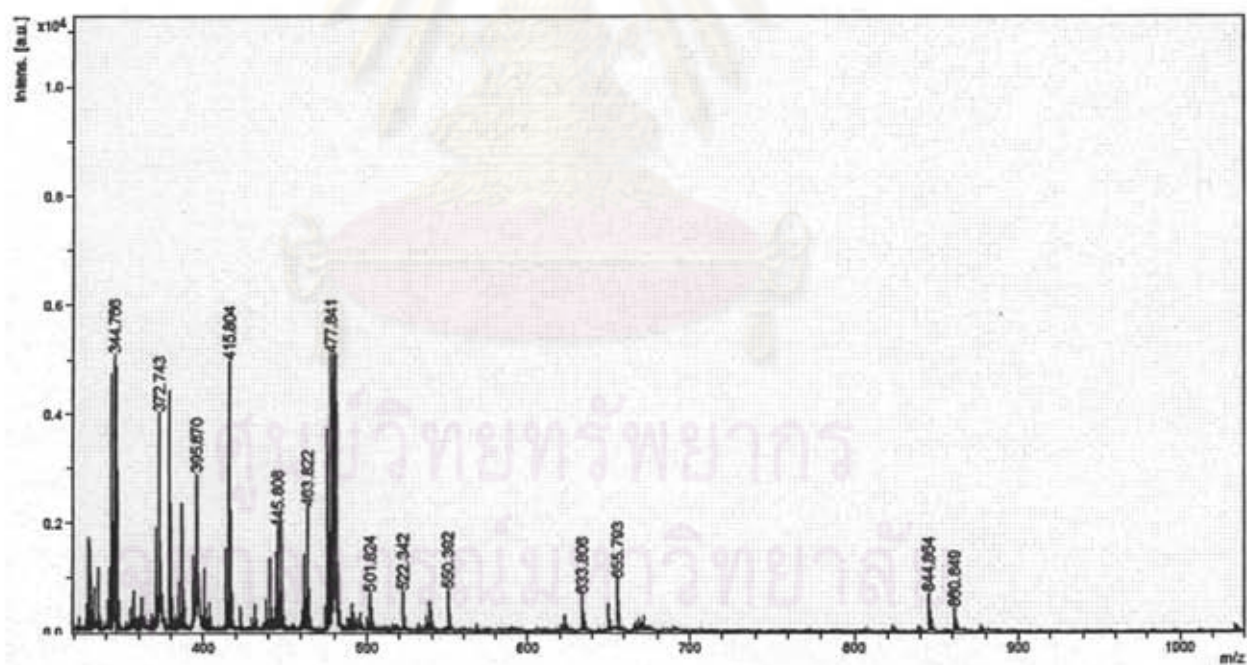


Figure A12. The mass spectrum (ESI) of ligand L2H.

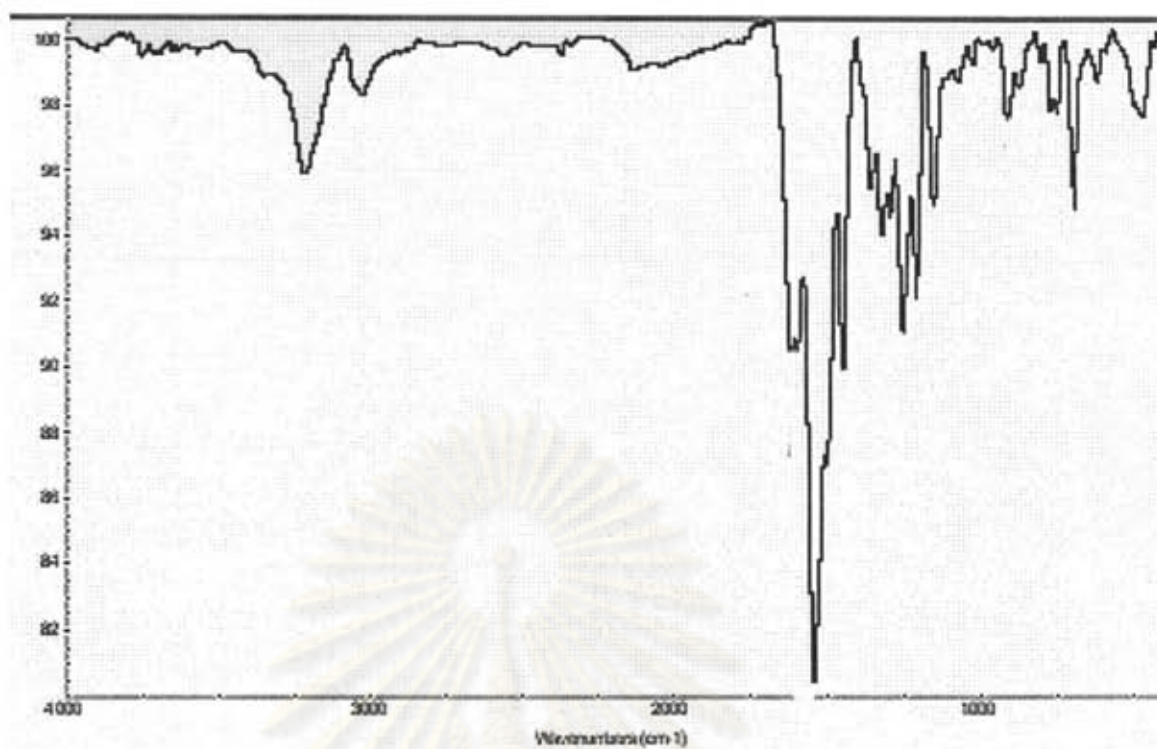


Figure A13. FTIR spectrum (KBr) of ligand L1.

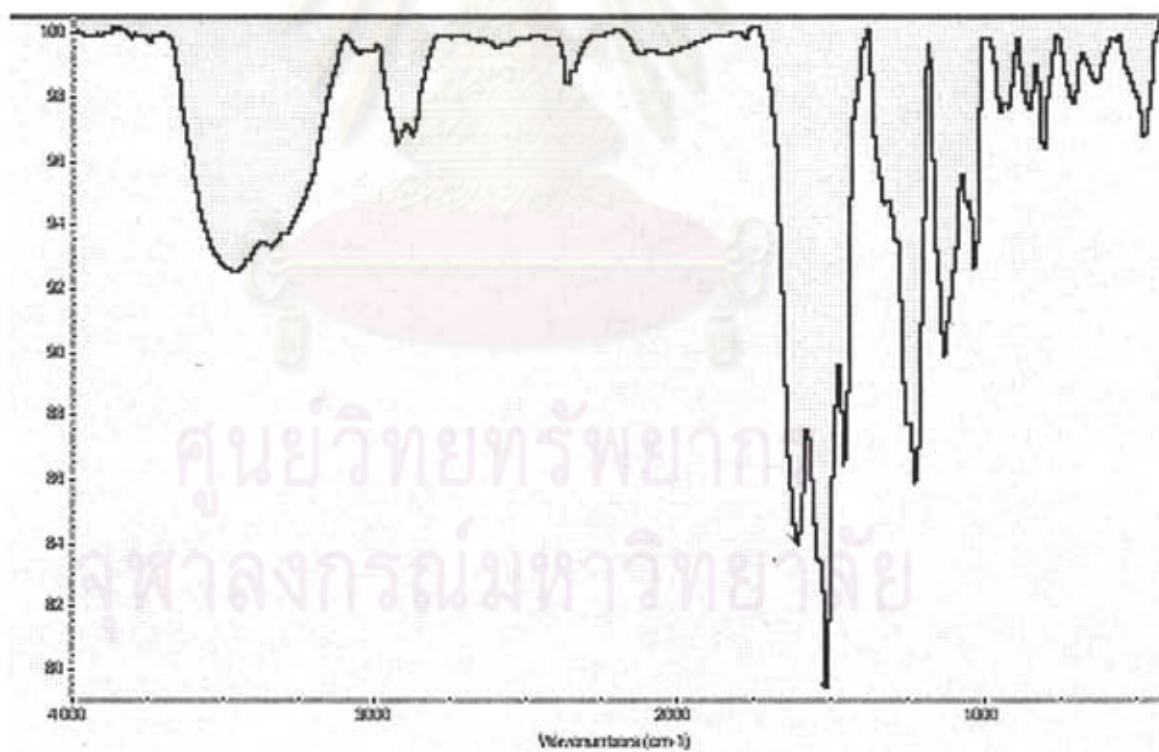


Figure A14. FTIR spectrum (KBr) of ligand L2.

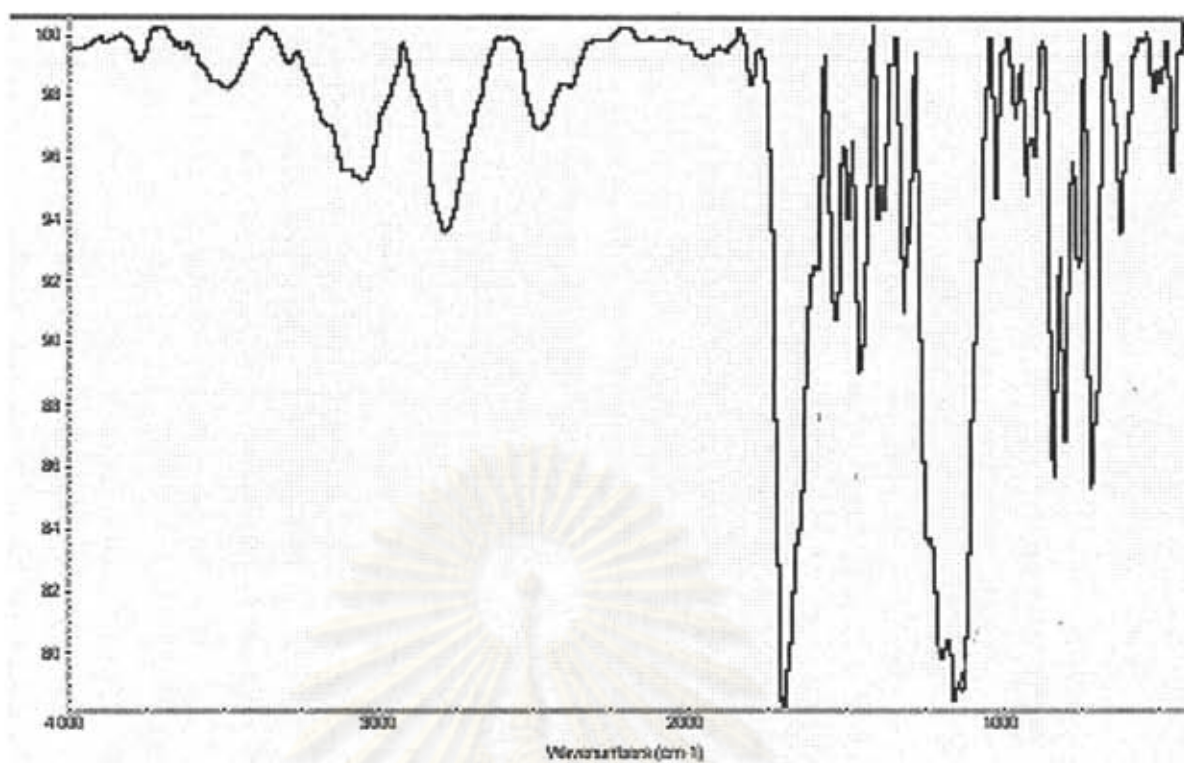


Figure A15. FTIR spectrum (KBr) of ligand L1H.

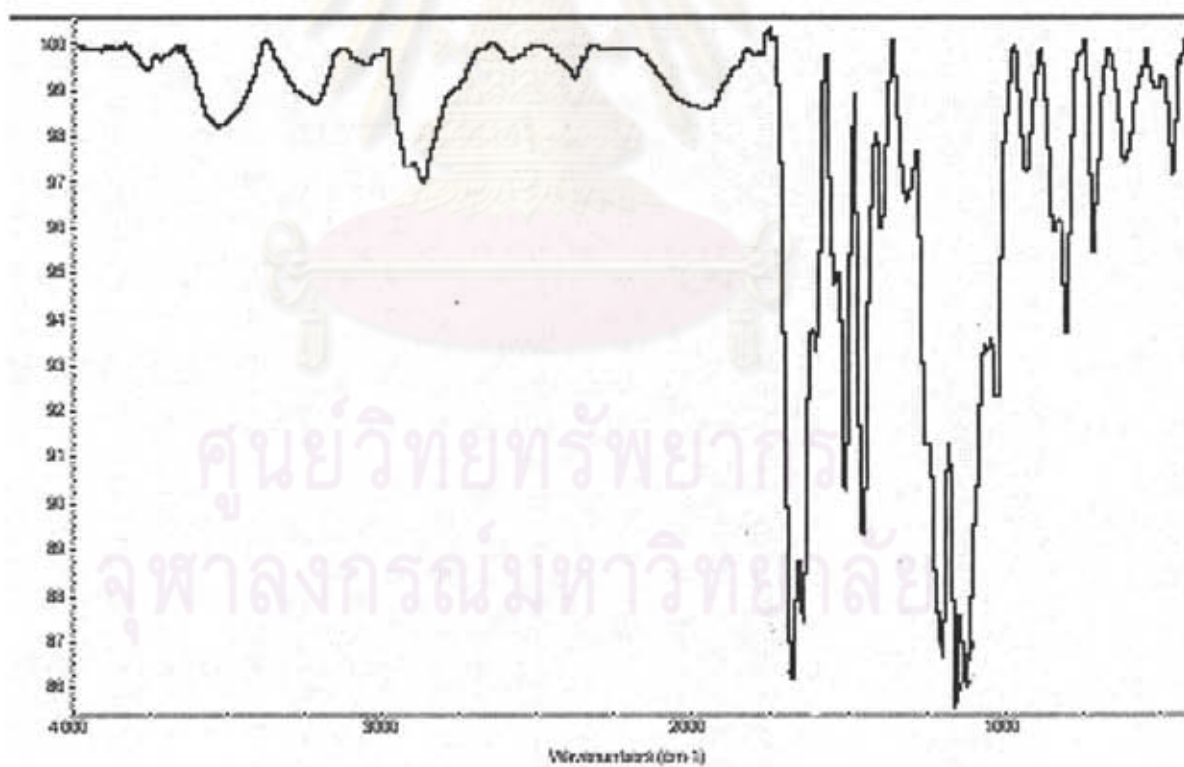


Figure A16. FTIR spectrum (KBr) of ligand L2H.

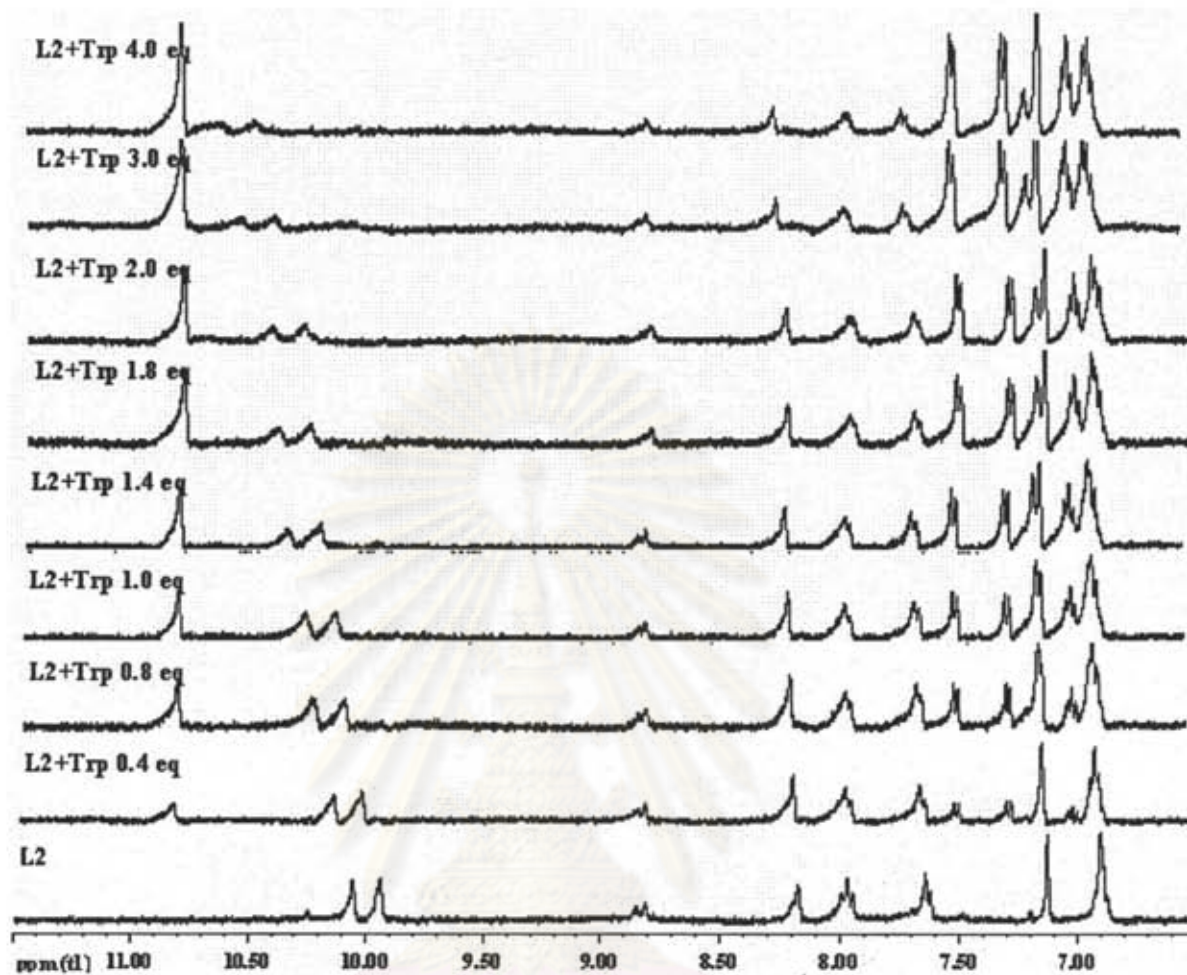


Figure A17. The $^1\text{H-NMR}$ titration spectra of L2 (4×10^{-3} M) in $\text{DMSO-}d_6$ upon adding Trp.

ศูนย์วิทยทรัพยากร
จุฬาลงกรณ์มหาวิทยาลัย

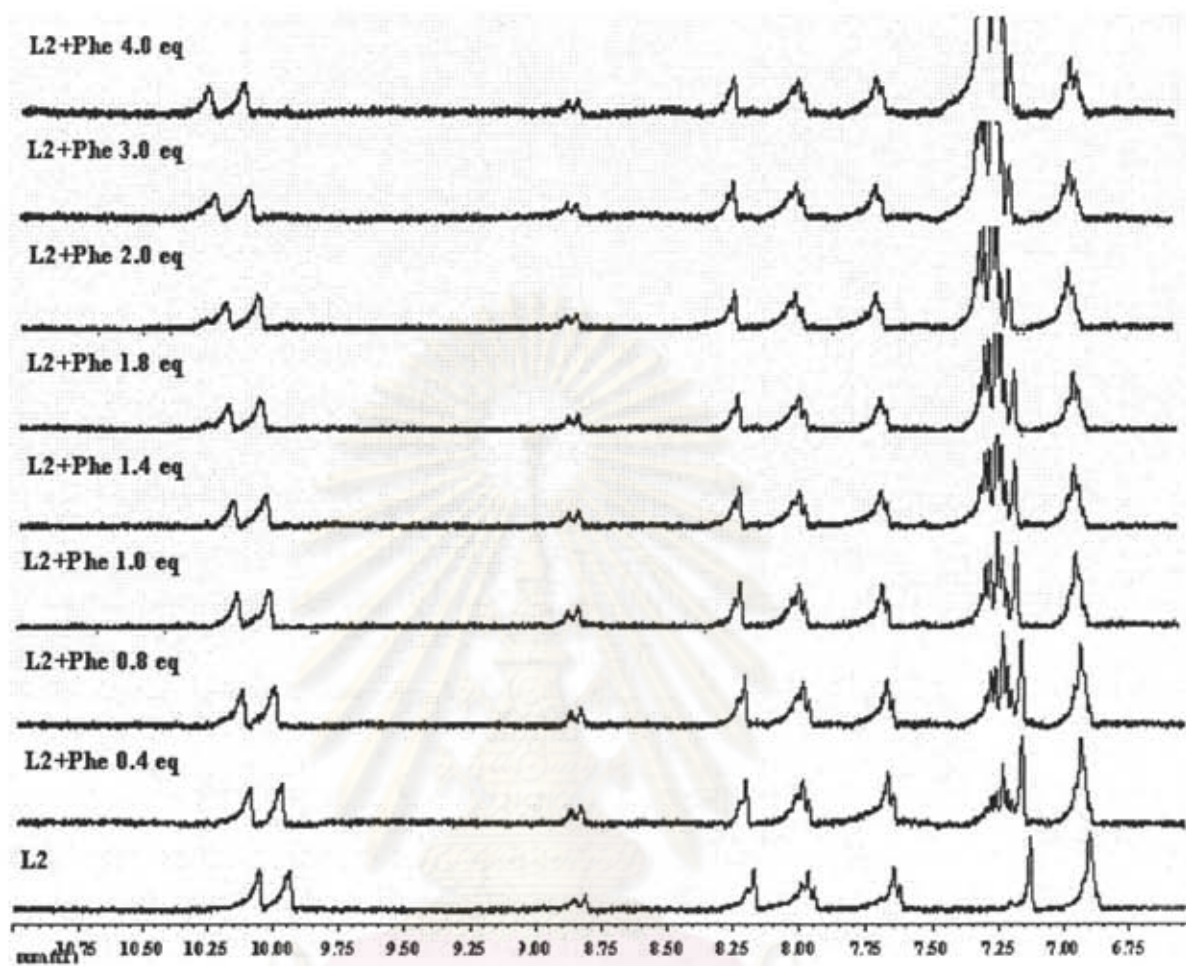


Figure A18. The $^1\text{H-NMR}$ titration spectra of L2 (4×10^{-3} M) in $\text{DMSO-}d_6$ upon adding Phe.

ศูนย์วิทยทรัพยากร
จุฬาลงกรณ์มหาวิทยาลัย

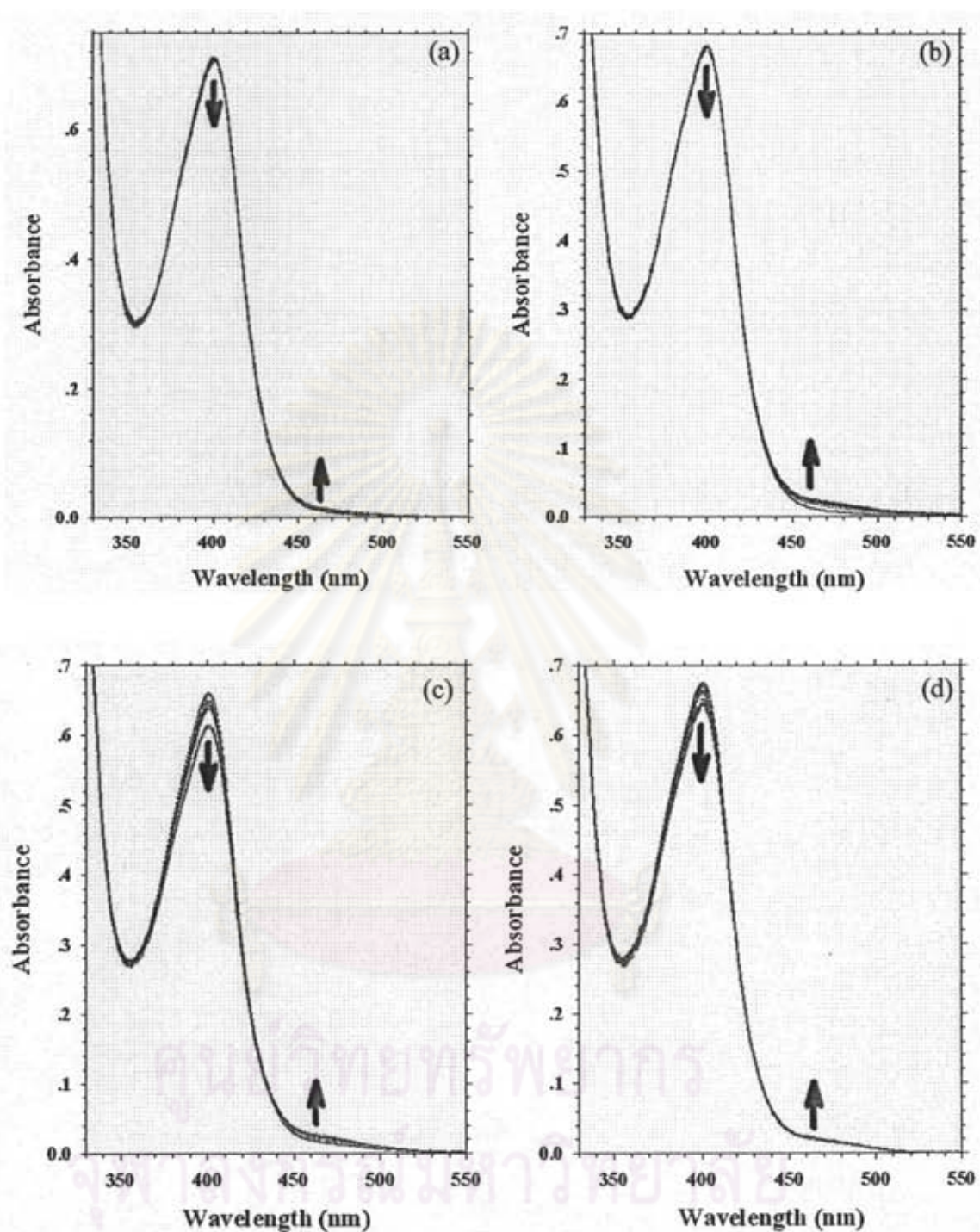


Figure A19. UV-vis titration spectra of ligand L1 upon addition of (a) Trp, (b) Leu, (c) Ala and (d) Gly 50 equiv.

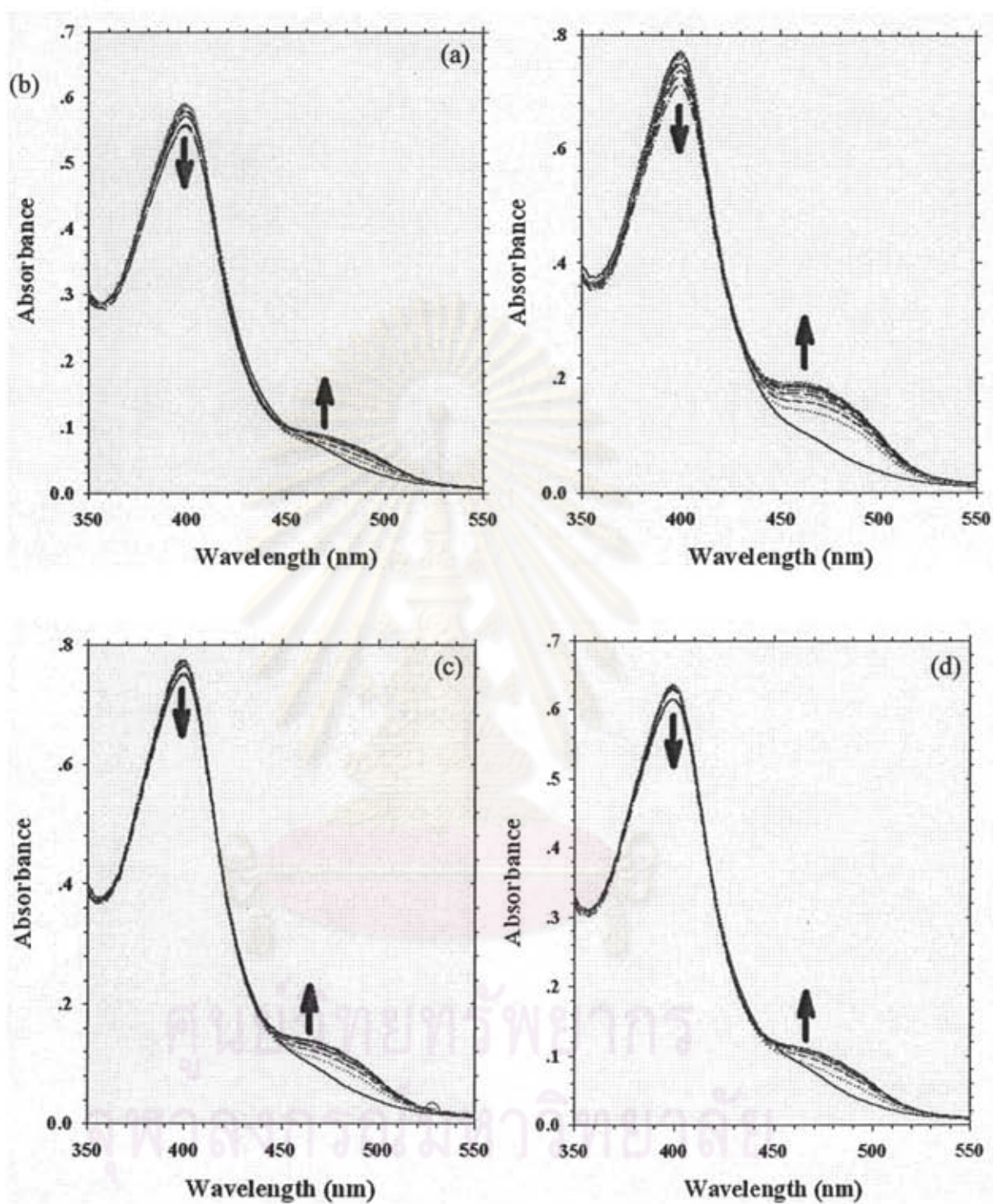


Figure A20. UV-vis titration spectra of ligand L2 upon addition of (a) Trp, (b) Leu, (c) Ala and (d) Gly 40 equiv.

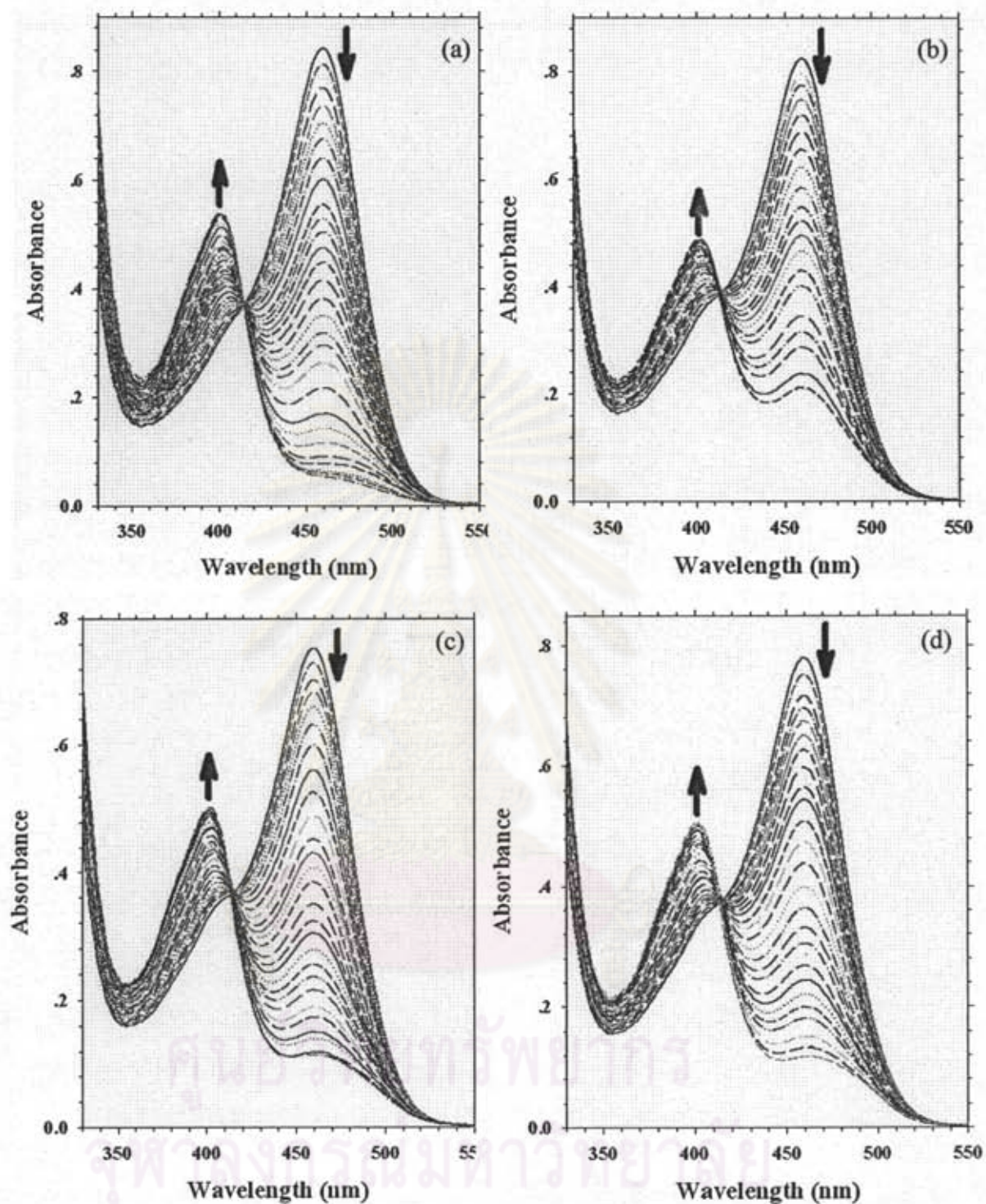


Figure A21. UV-vis titration spectra of ligand L1H upon addition of (a) Trp, (b) Leu, (c) Ala and (d) Gly 30 equiv.

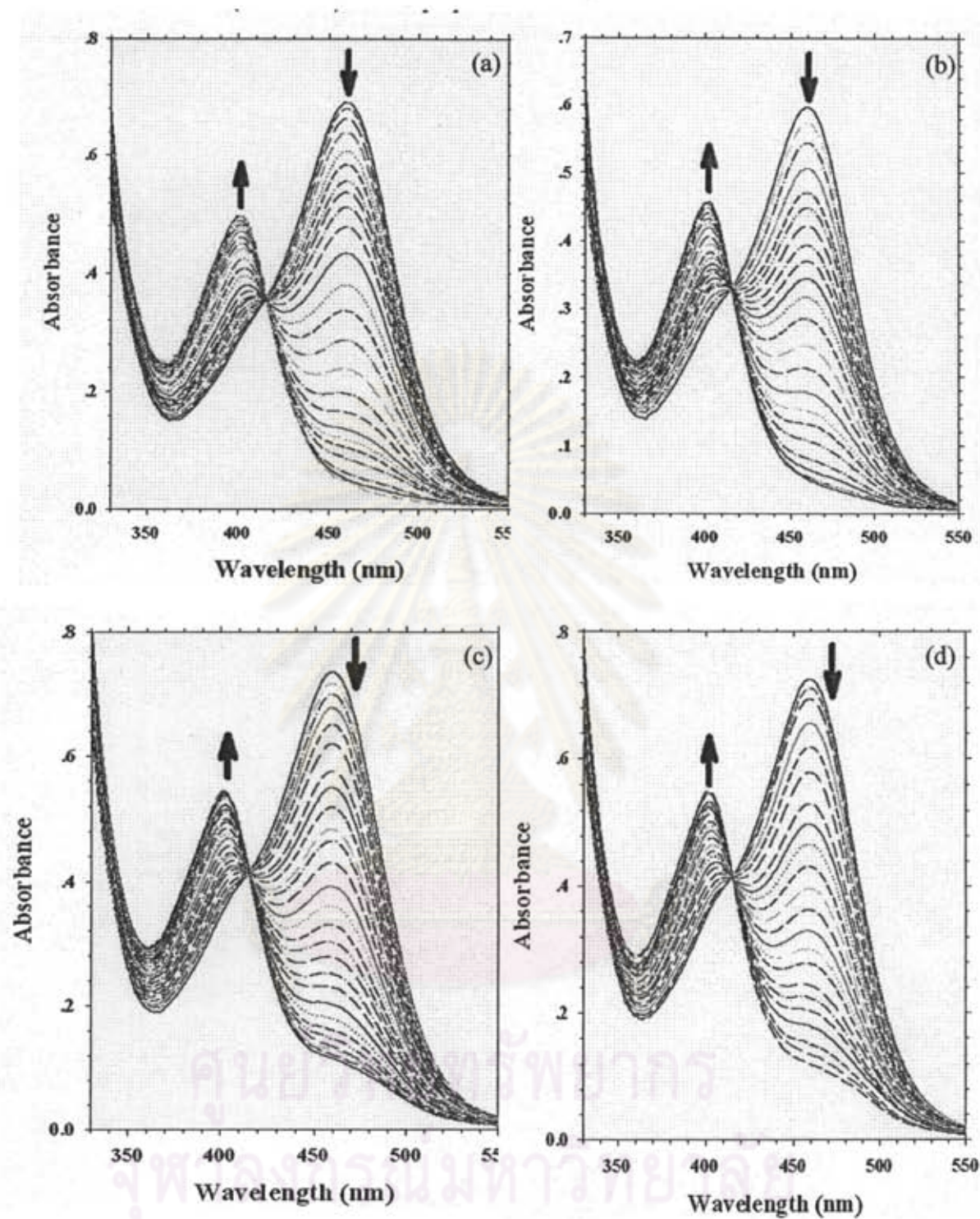


Figure A22. UV-vis titration spectra of ligand L2H upon addition of (a) Trp, (b) Leu, (c) Ala and (d) Gly 30 equiv.

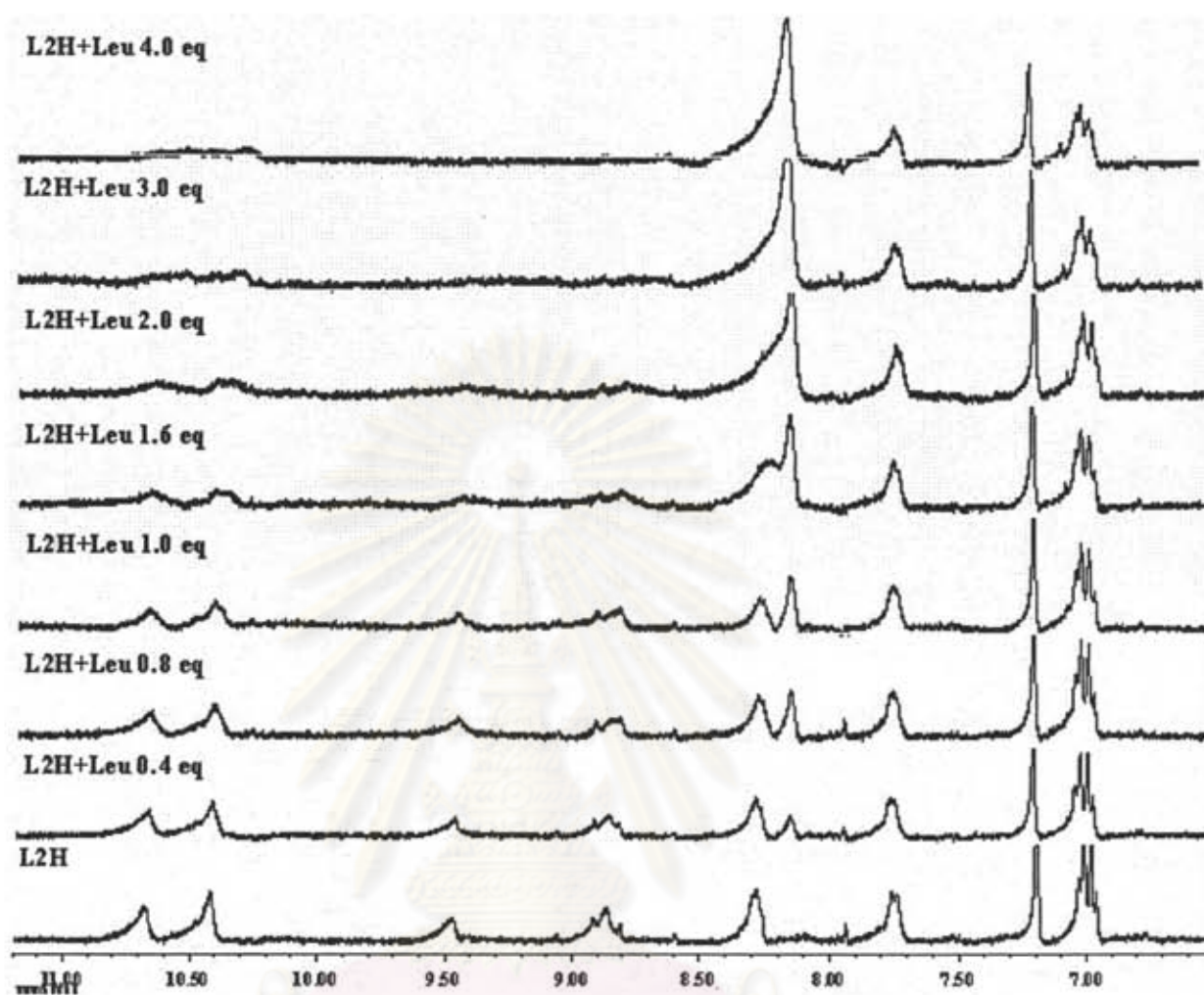


Figure A23. The $^1\text{H-NMR}$ titration spectra of ligand L2H ($2.0 \times 10^{-3} \text{ M}$) in $\text{DMSO-}d_6$ upon adding Leu.

ศูนย์วิทยทรัพยากร
จุฬาลงกรณ์มหาวิทยาลัย

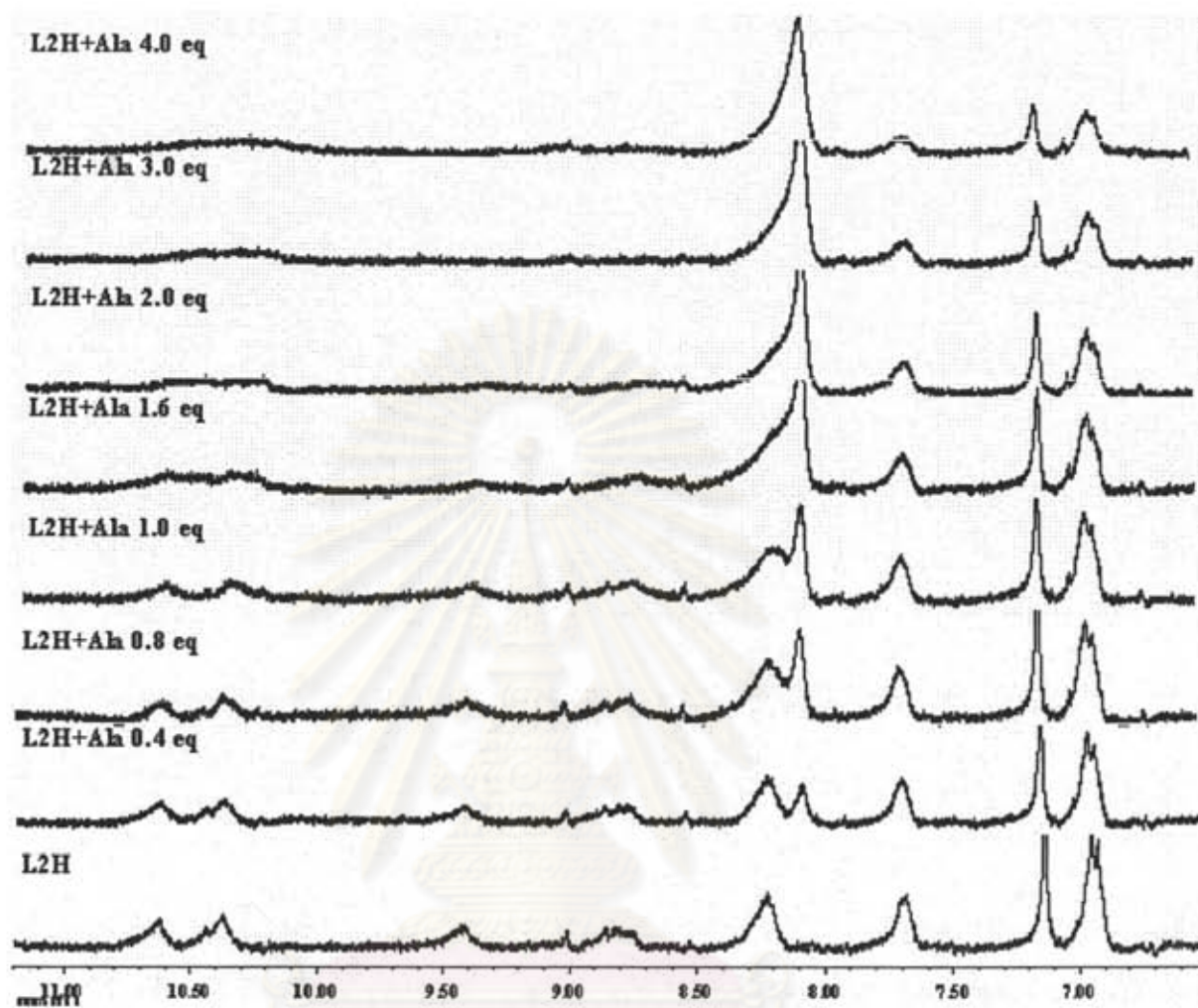


Figure A24. The $^1\text{H-NMR}$ titration spectra of ligand L2H (2.0×10^{-3} M) in $\text{DMSO-}d_6$ upon adding Ala.

ศูนย์วิทยทรัพยากร
จุฬาลงกรณ์มหาวิทยาลัย

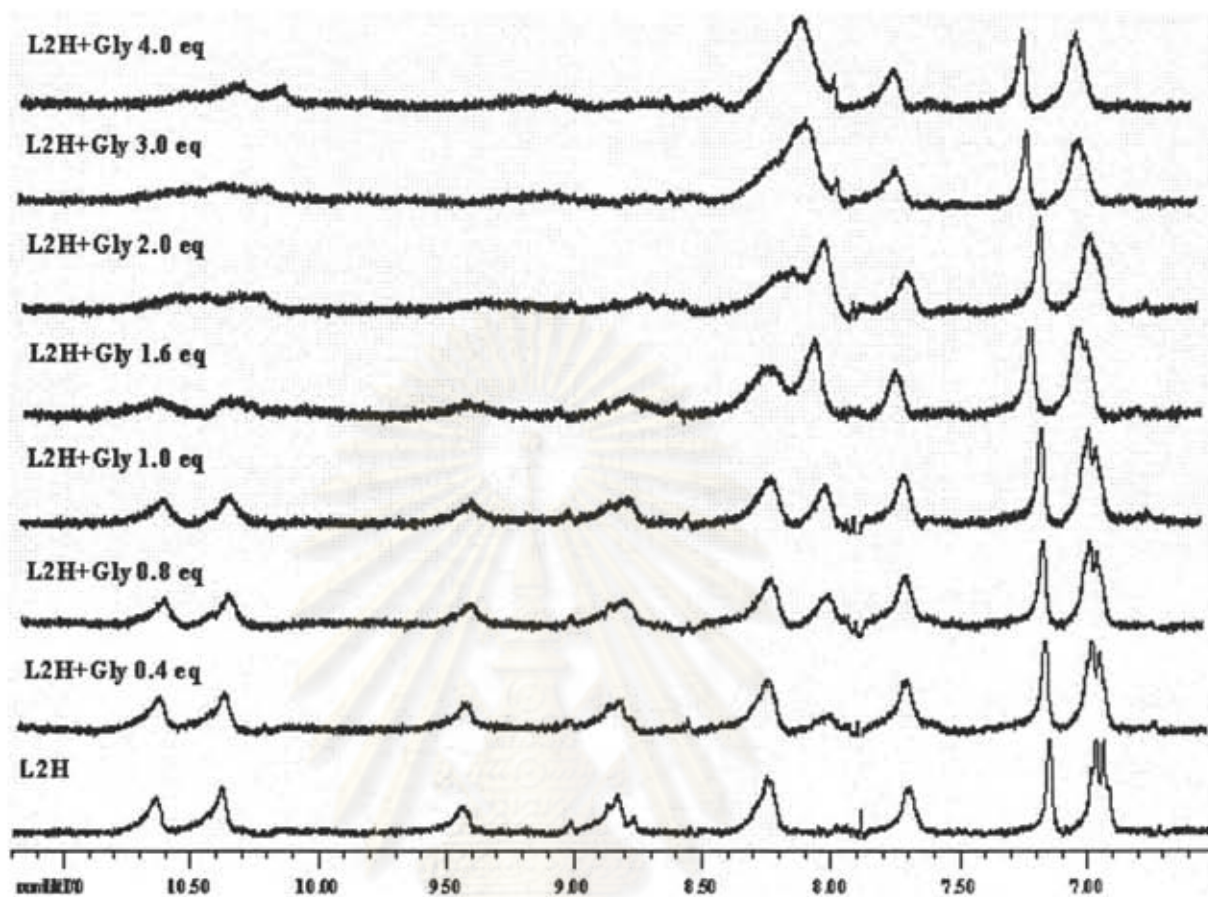


Figure A25. The ¹H-NMR titration spectra of ligand L2H (2.0×10^{-3} M) in DMSO-*d*₆ upon adding Gly.

ศูนย์วิทยทรัพยากร
จุฬาลงกรณ์มหาวิทยาลัย

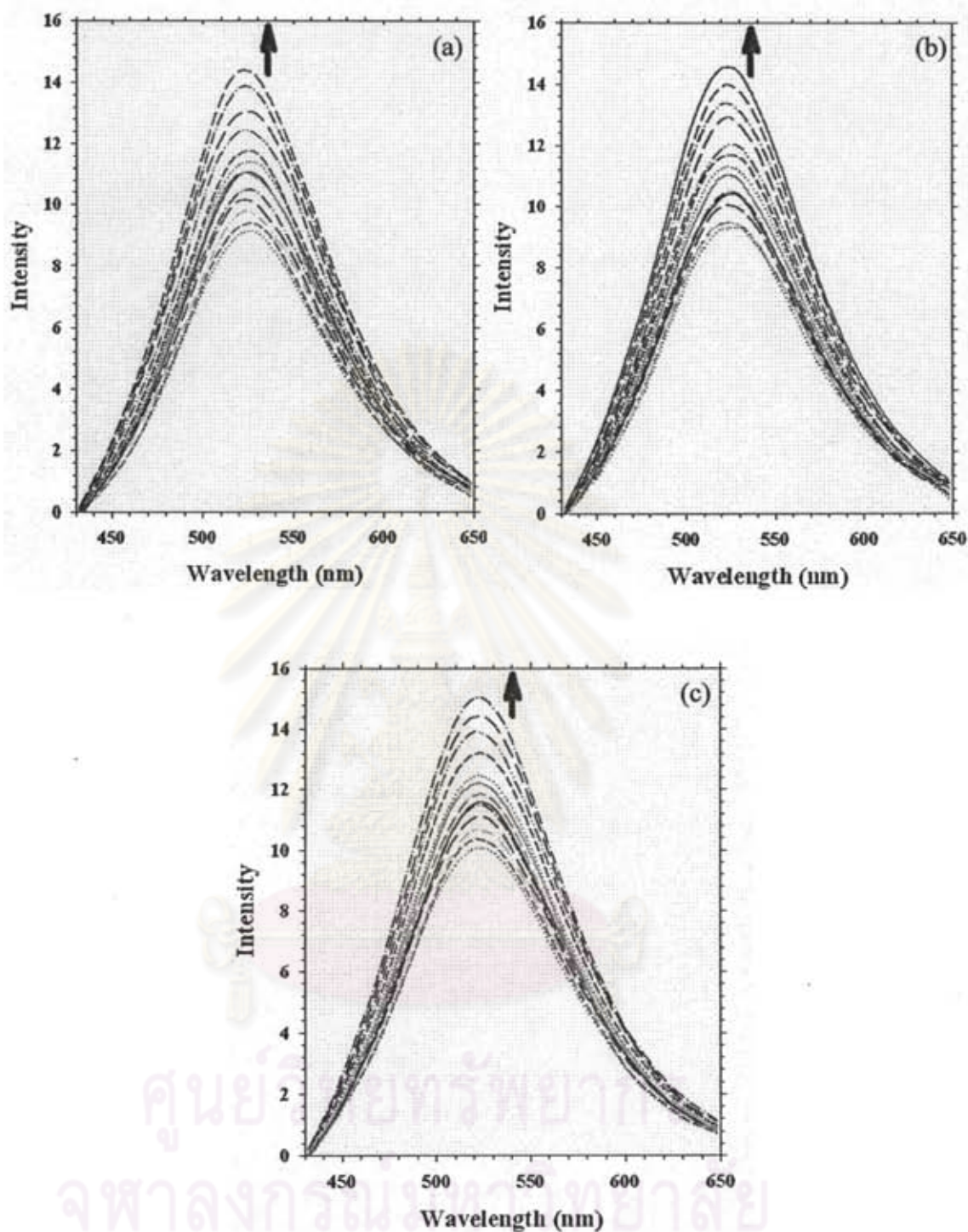


Figure A26. Fluorescence titration spectra of ligand L1 upon addition of (a) Leu, (b) Ala and (c) Gly 30 equiv.

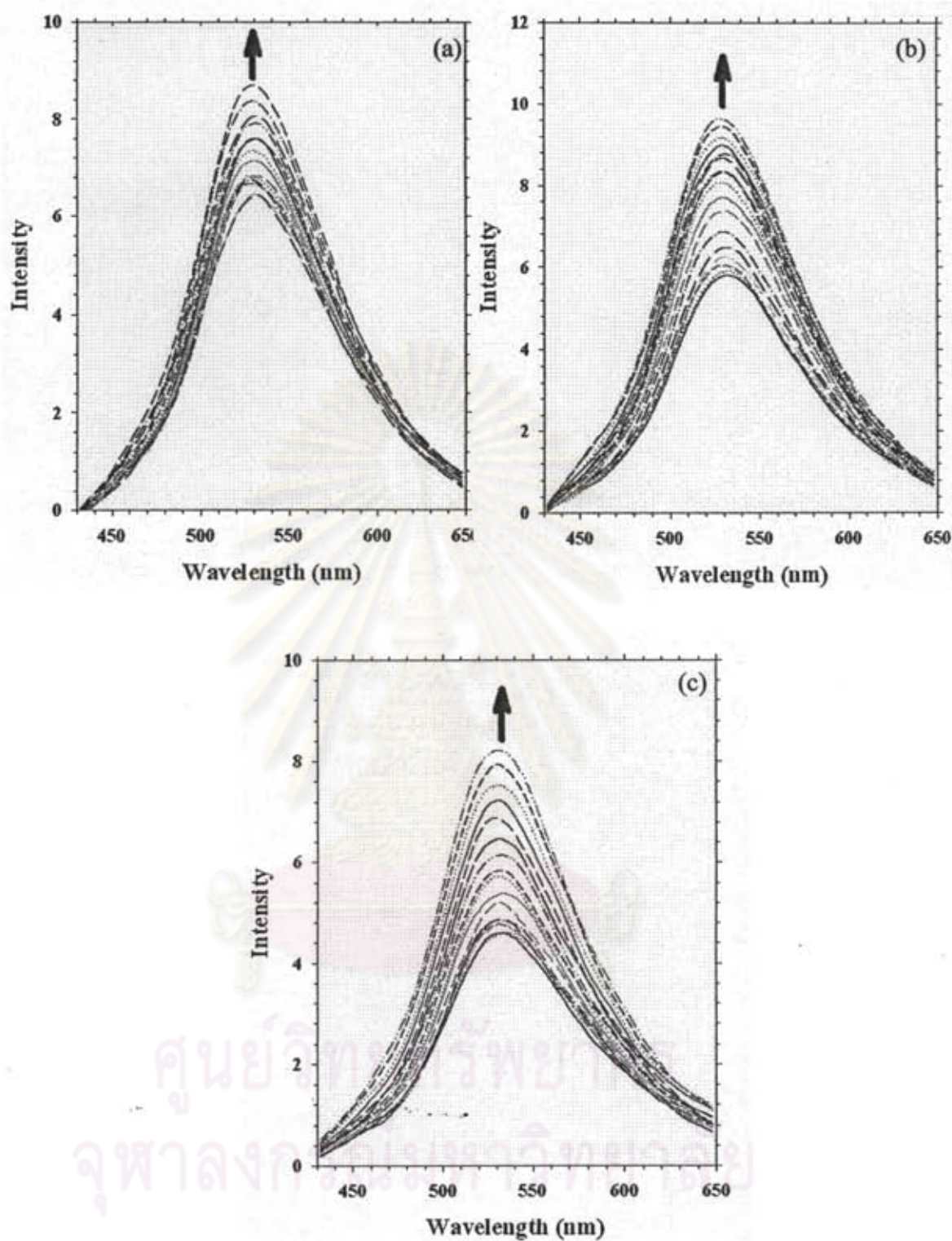


Figure A27. Fluorescence titration spectra of ligand L2 upon addition of (a) Leu, (b) Ala and (c) Gly 30 equiv.

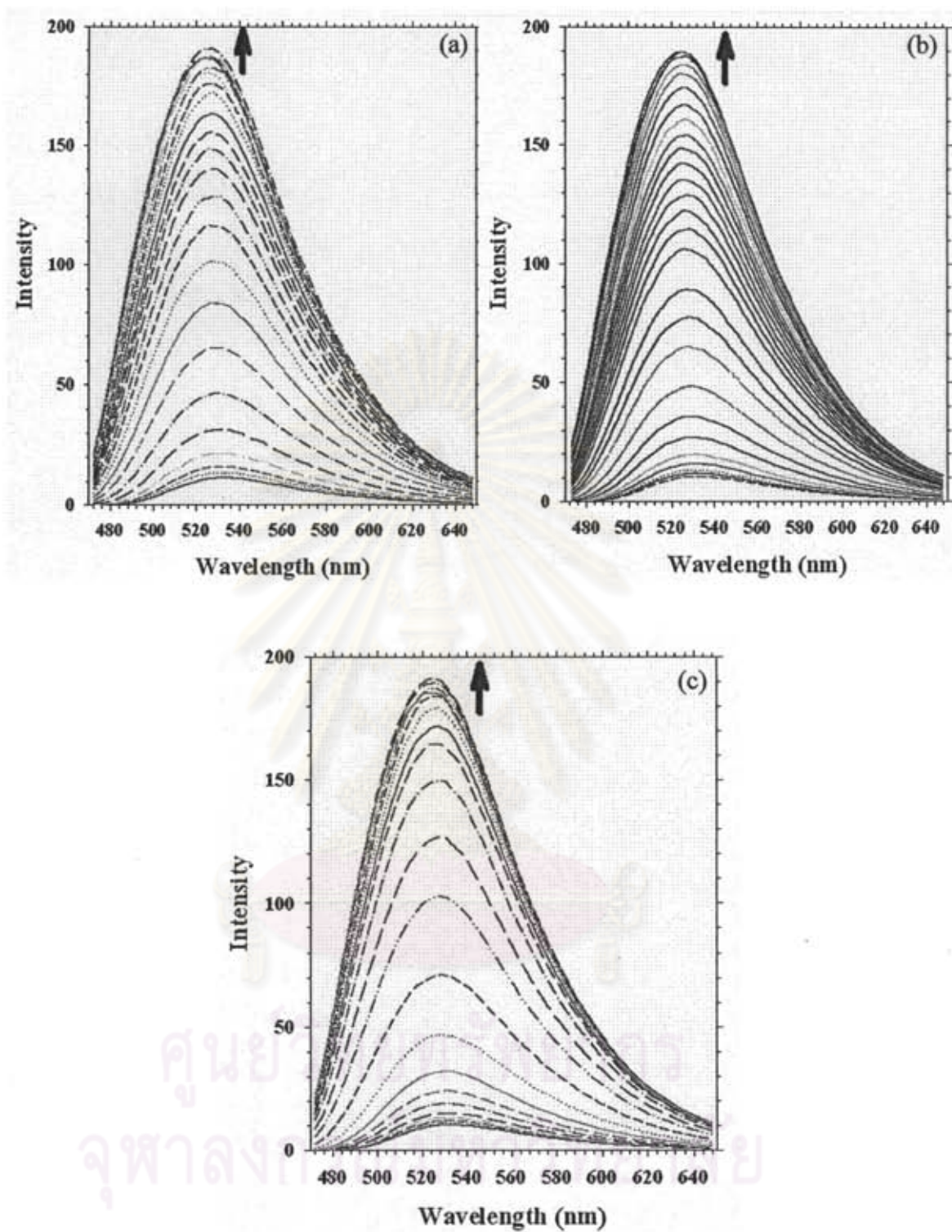


Figure A28. Fluorescence titration spectra of ligand L1H upon addition of (a) Leu, (b) Ala and (c) Gly 30 equiv.

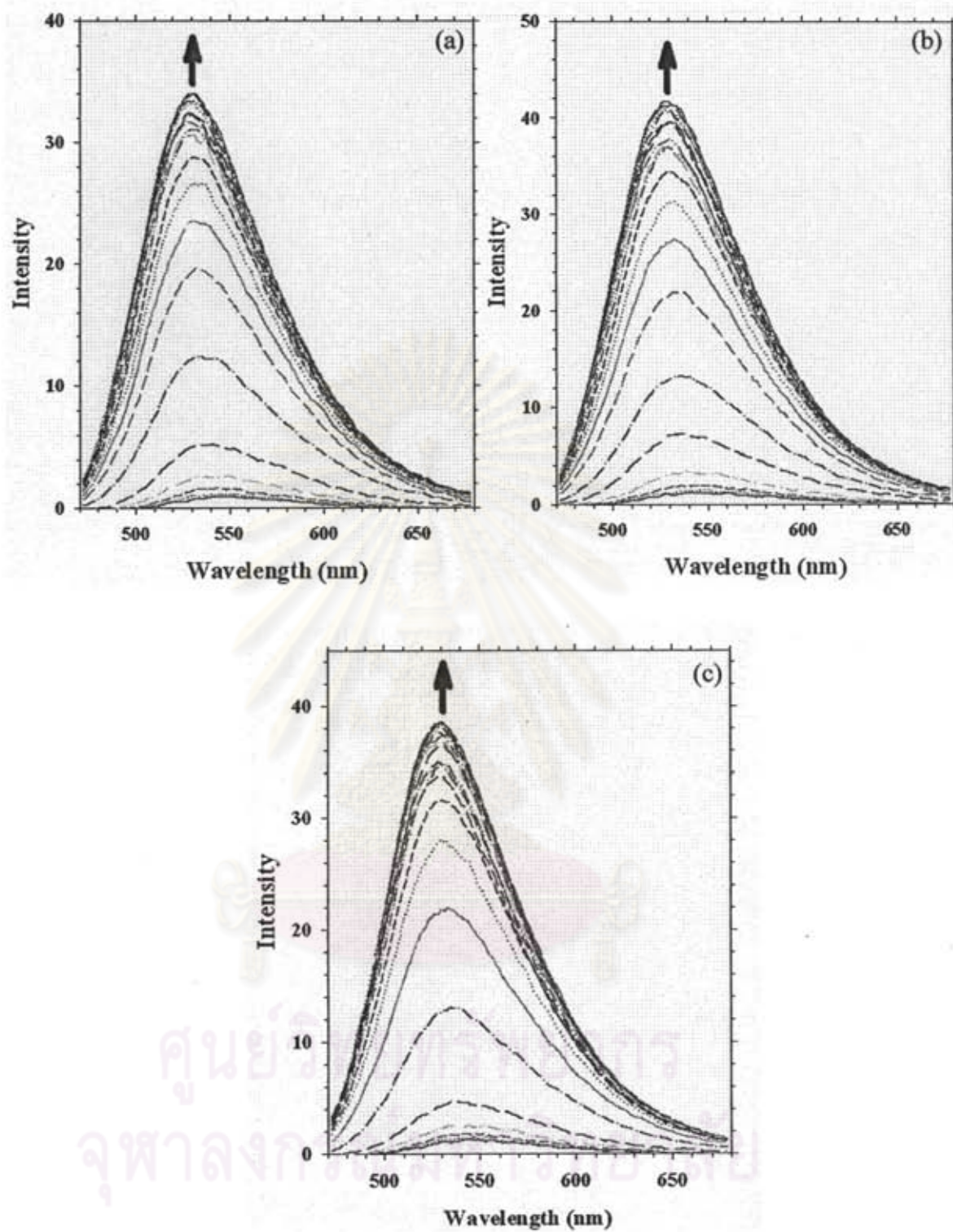


Figure A29. Fluorescence titration spectra of ligand L2H upon addition of (a) Leu, (b) Ala and (c) Gly 30 equiv.

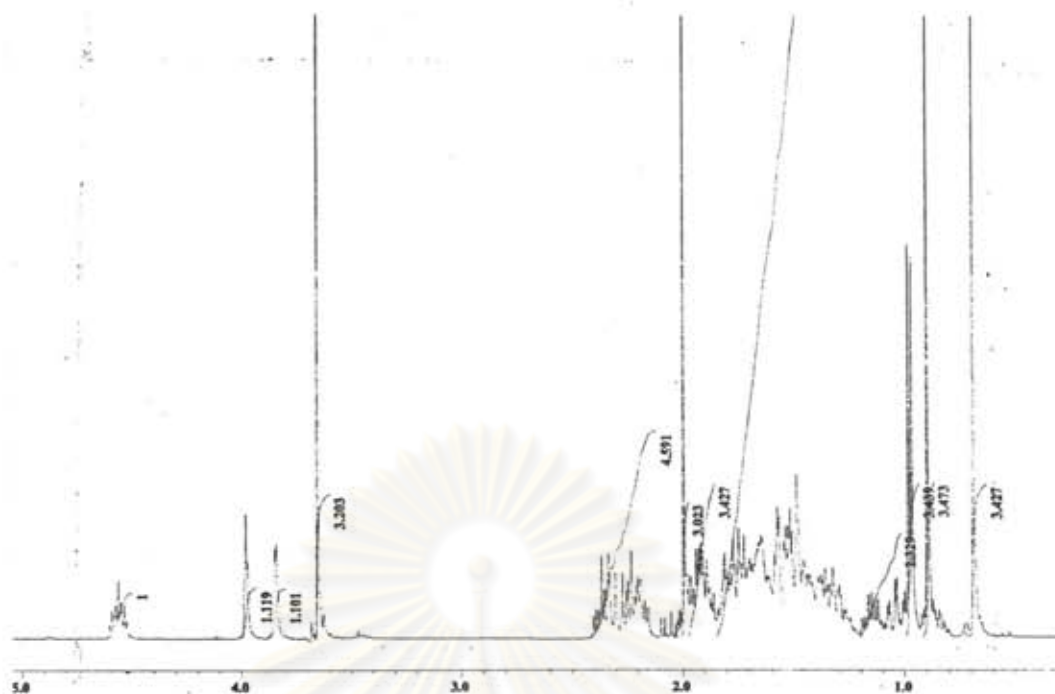


Figure A30. The $^1\text{H-NMR}$ spectra of compound 1.2 in CDCl_3 with 400 MHz.

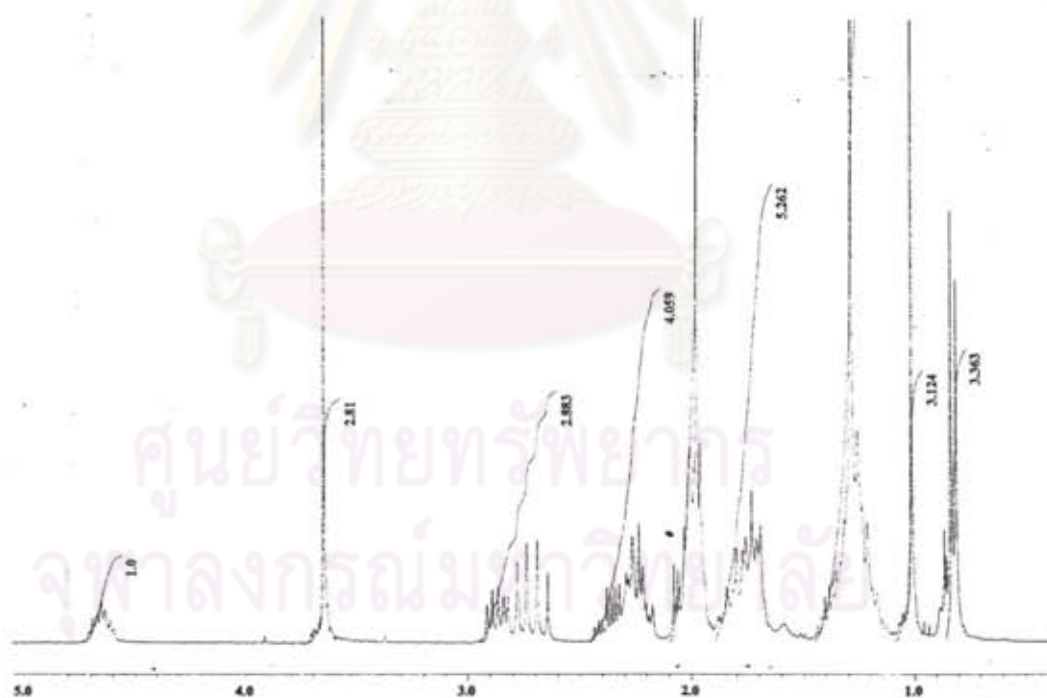


Figure A31. The $^1\text{H-NMR}$ spectra of compound 1.3 in CDCl_3 with 400 MHz.

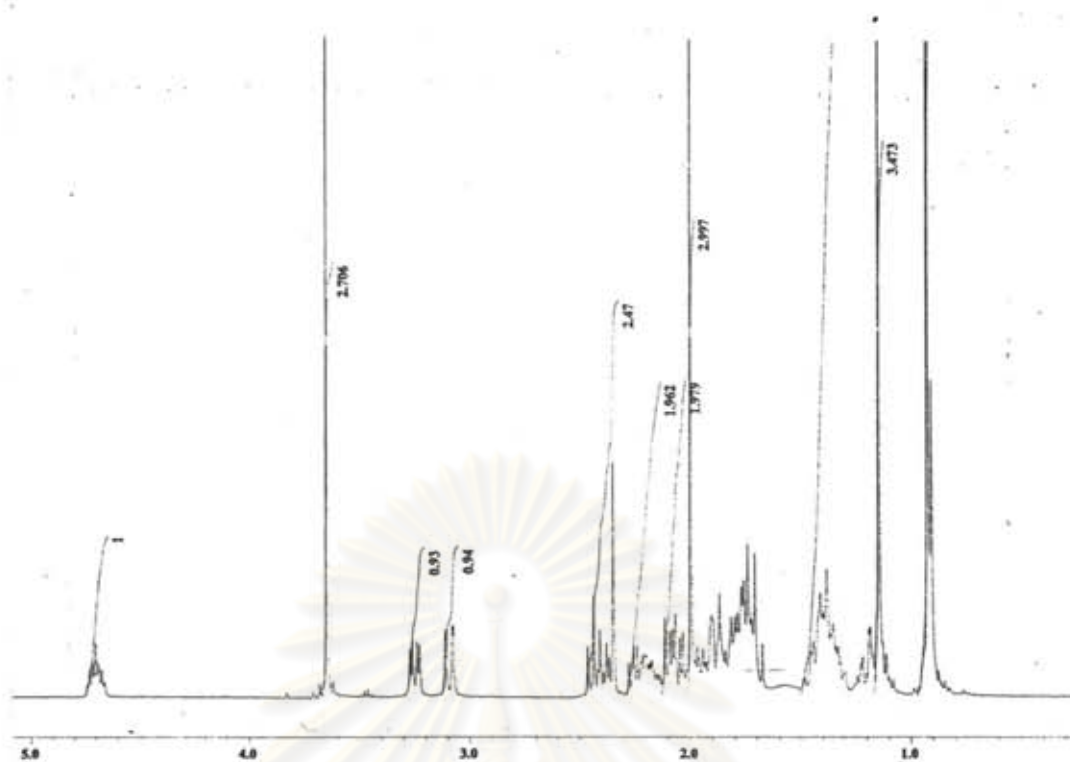


Figure A32. The $^1\text{H-NMR}$ spectra of compound 1.4 in CDCl_3 with 400 MHz.

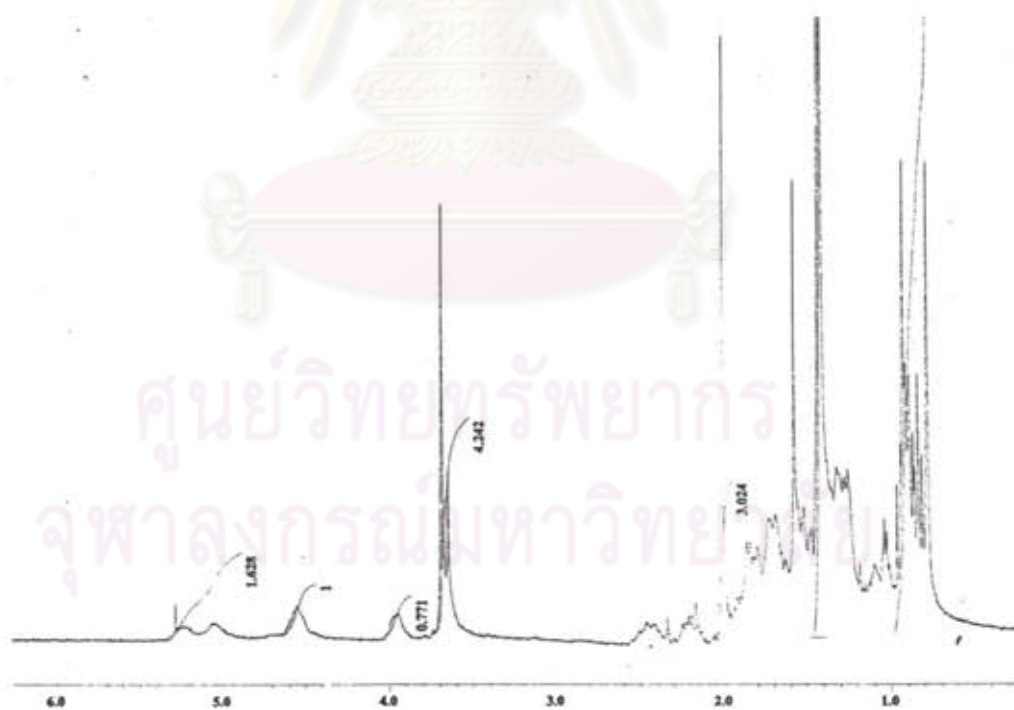


Figure A33. The $^1\text{H-NMR}$ spectra of compound 1.5 in CDCl_3 with 400 MHz.



ต้นฉบับไม่มีหน้า 151

NO PAGE 151 IN ORIGINAL

ศูนย์วิทยทรัพยากร
จุฬาลงกรณ์มหาวิทยาลัย

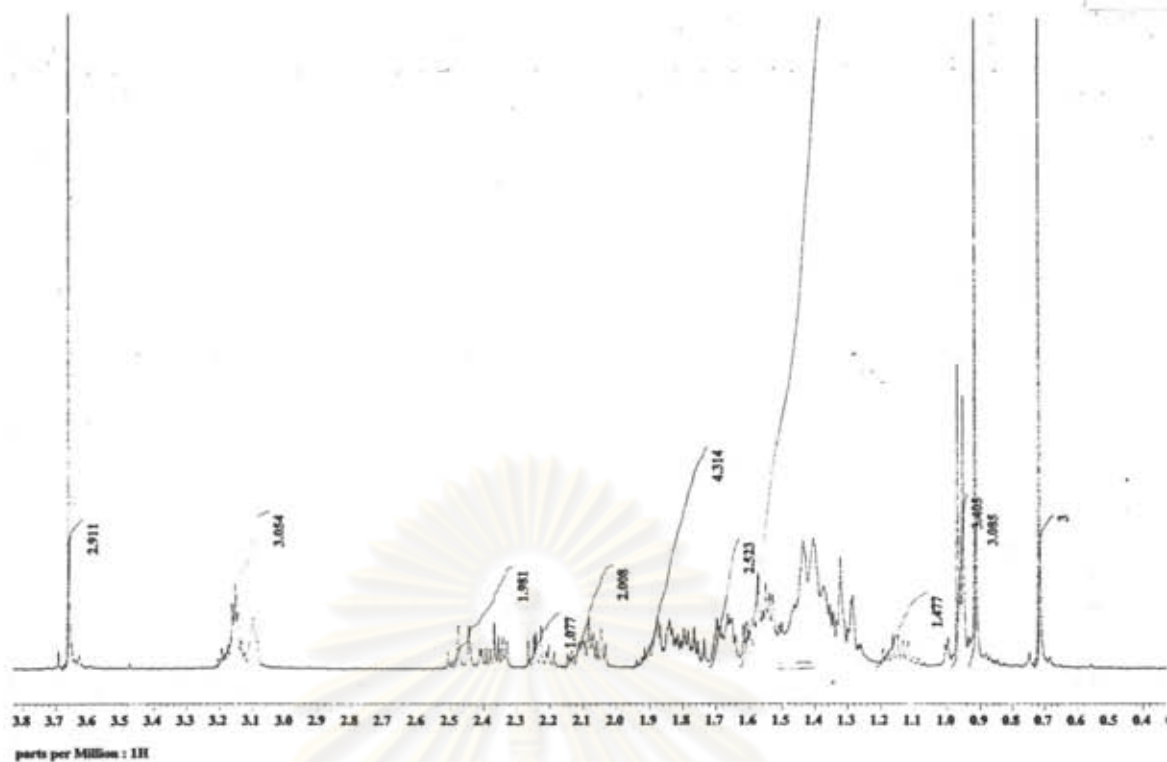


Figure A36. The ^1H -NMR spectra of compound 1.8 in CDCl_3 with 400 MHz.

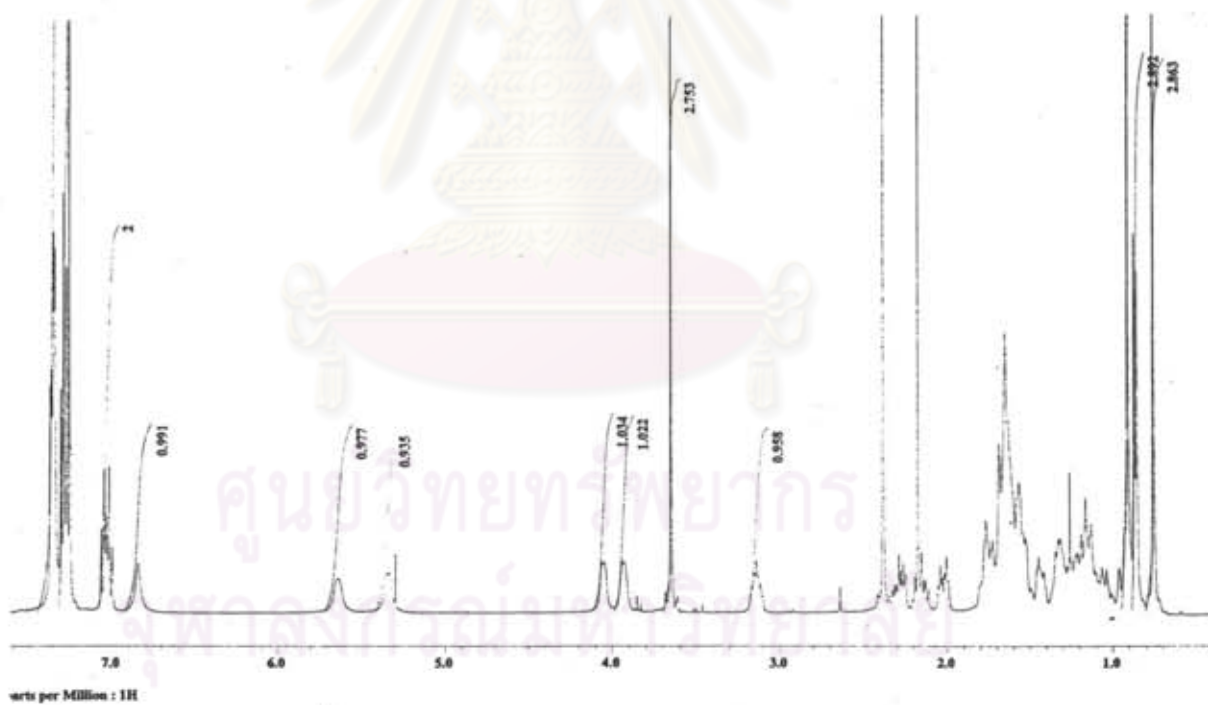


Figure A37. The ^1H -NMR spectra of compound 1.9 in CDCl_3 with 400 MHz.

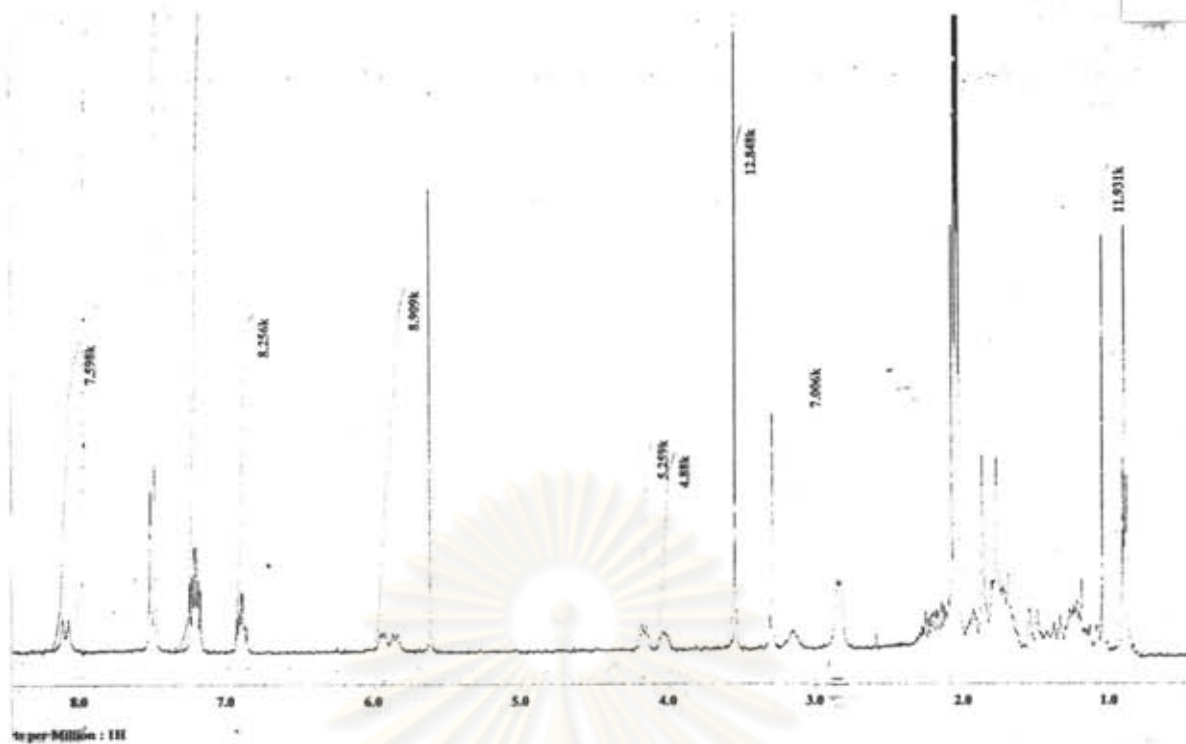


Figure A38. The $^1\text{H-NMR}$ spectra of compound 1.10 in CDCl_3 with 400 MHz.

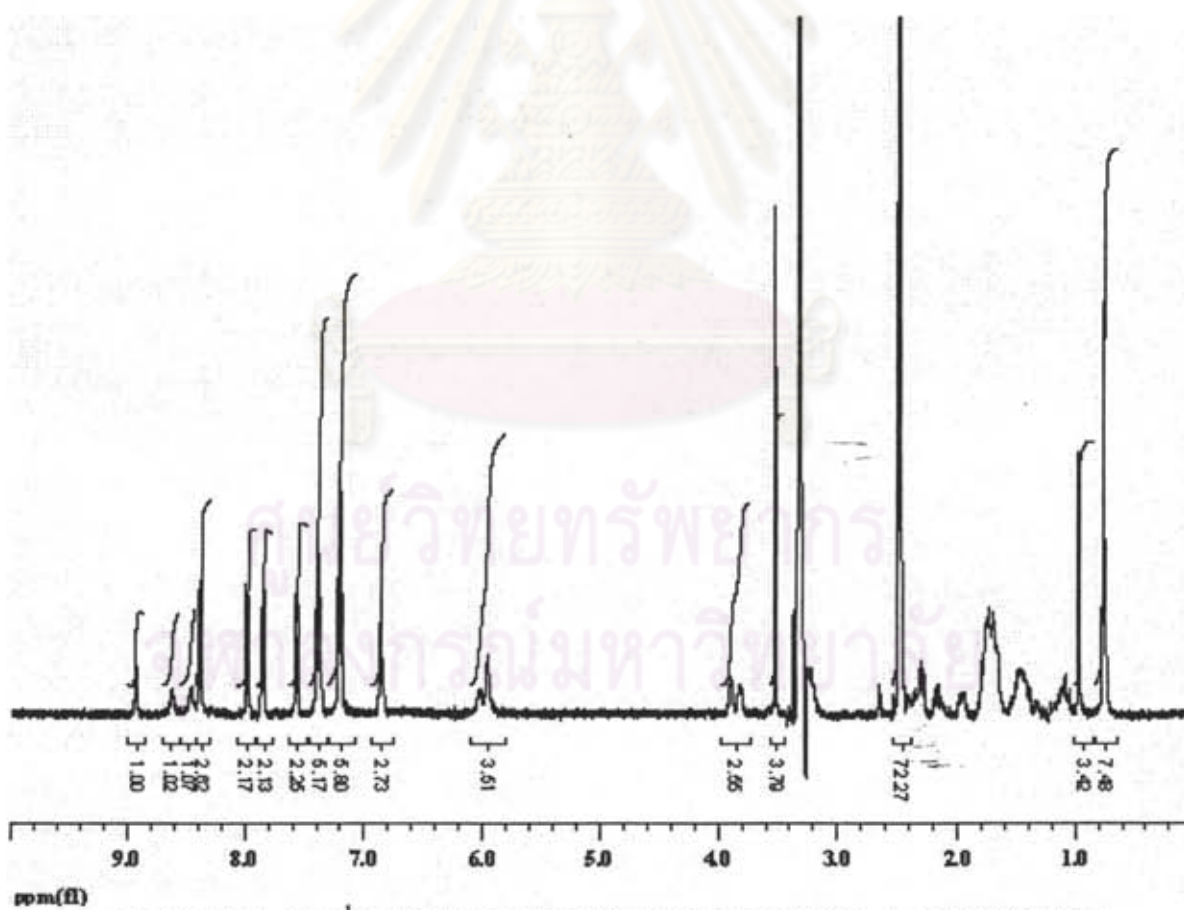


Figure A39. The $^1\text{H-NMR}$ spectra of ligand L3 in $\text{DMSO-}d_6$ with 400 MHz.

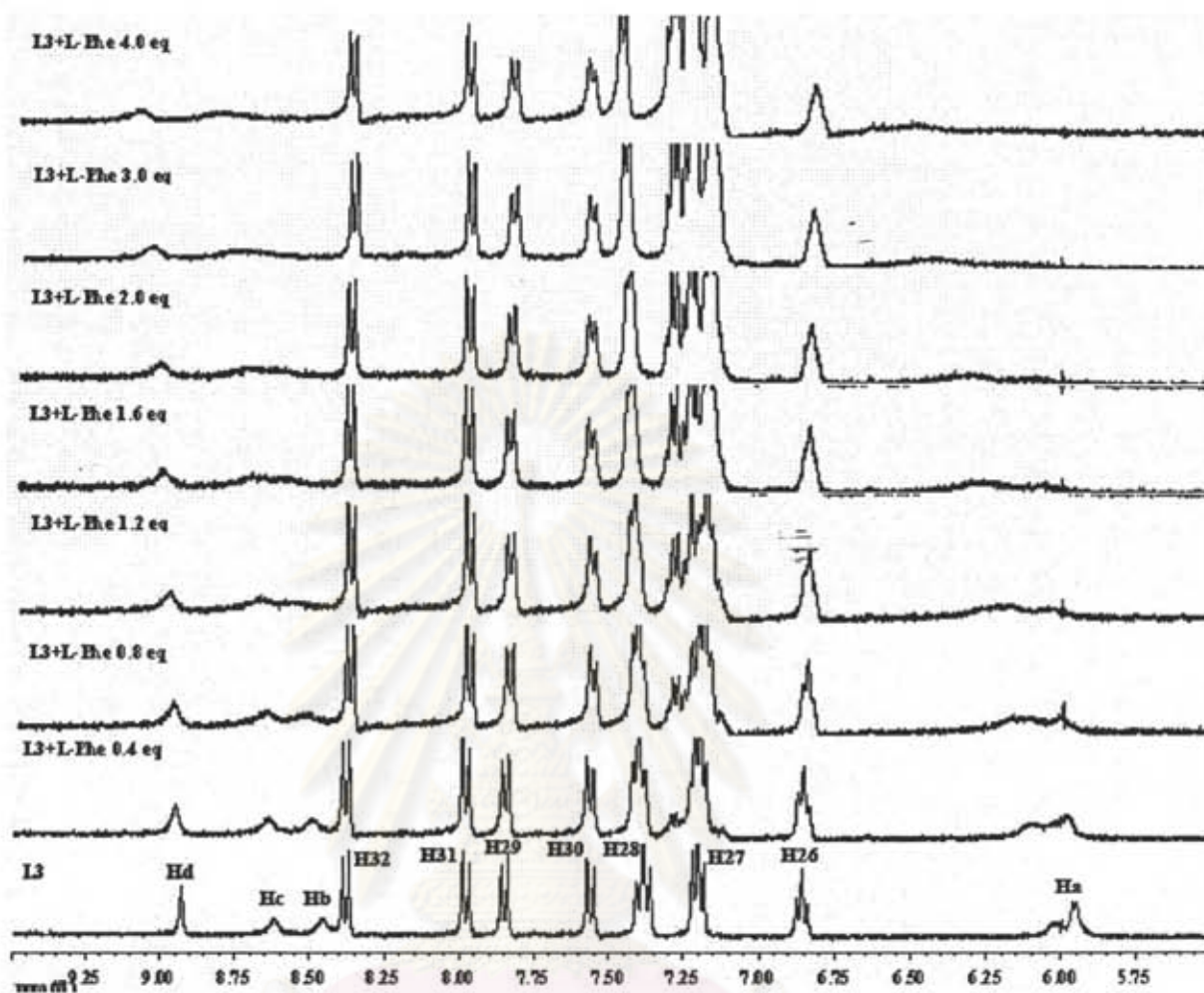


Figure A40. Partial ^1H -NMR titration spectra of L3 (3.0×10^{-3} M) upon adding L-Phe 4.0 equivalent in $\text{DMSO-}d_6$.

ศูนย์วิทยทรัพยากร
จุฬาลงกรณ์มหาวิทยาลัย

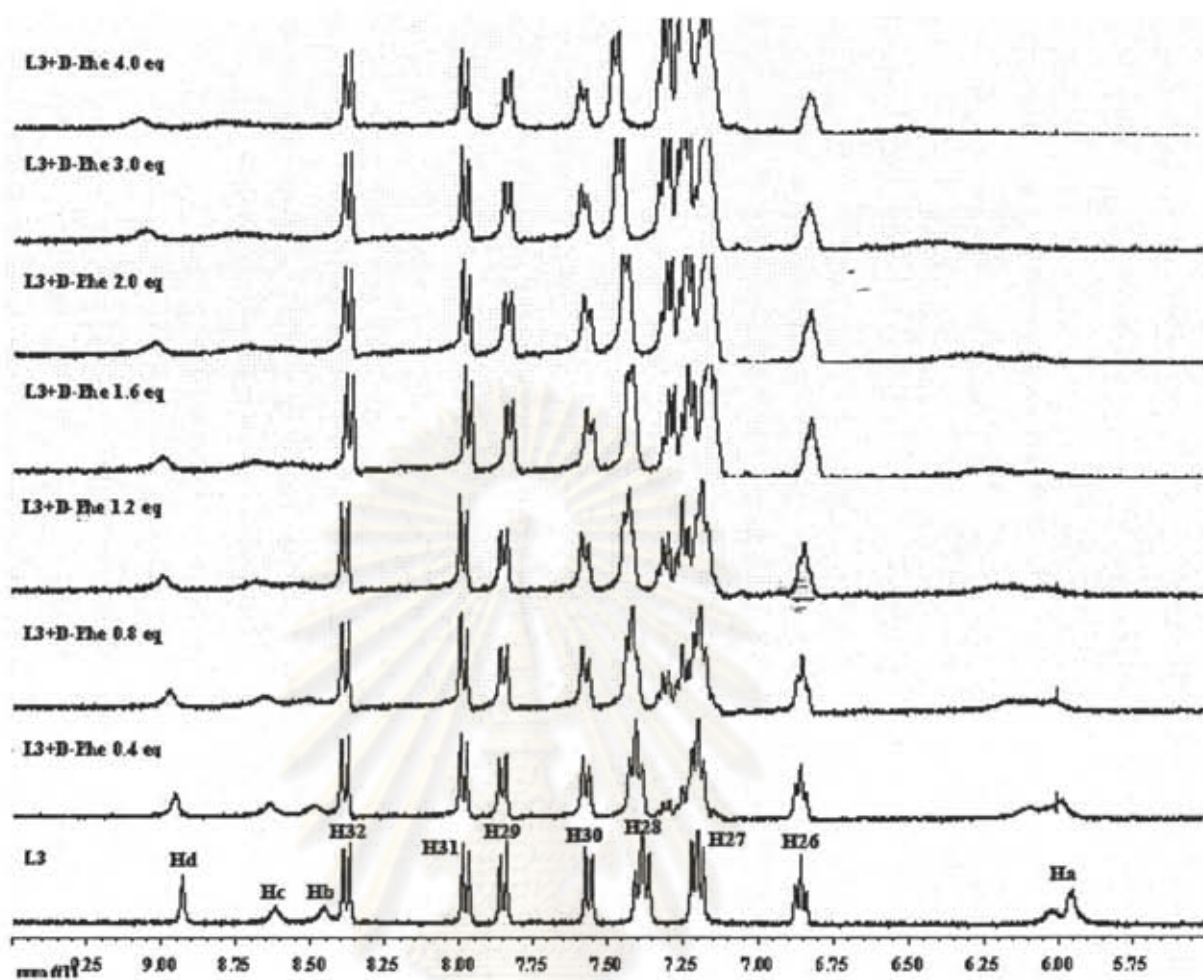


Figure A41. Partial ^1H -NMR titration spectra of L3 (3.0×10^{-3} M) upon adding D-Phe 4.0 equivalent in $\text{DMSO-}d_6$.

ศูนย์วิทยทรัพยากร
จุฬาลงกรณ์มหาวิทยาลัย

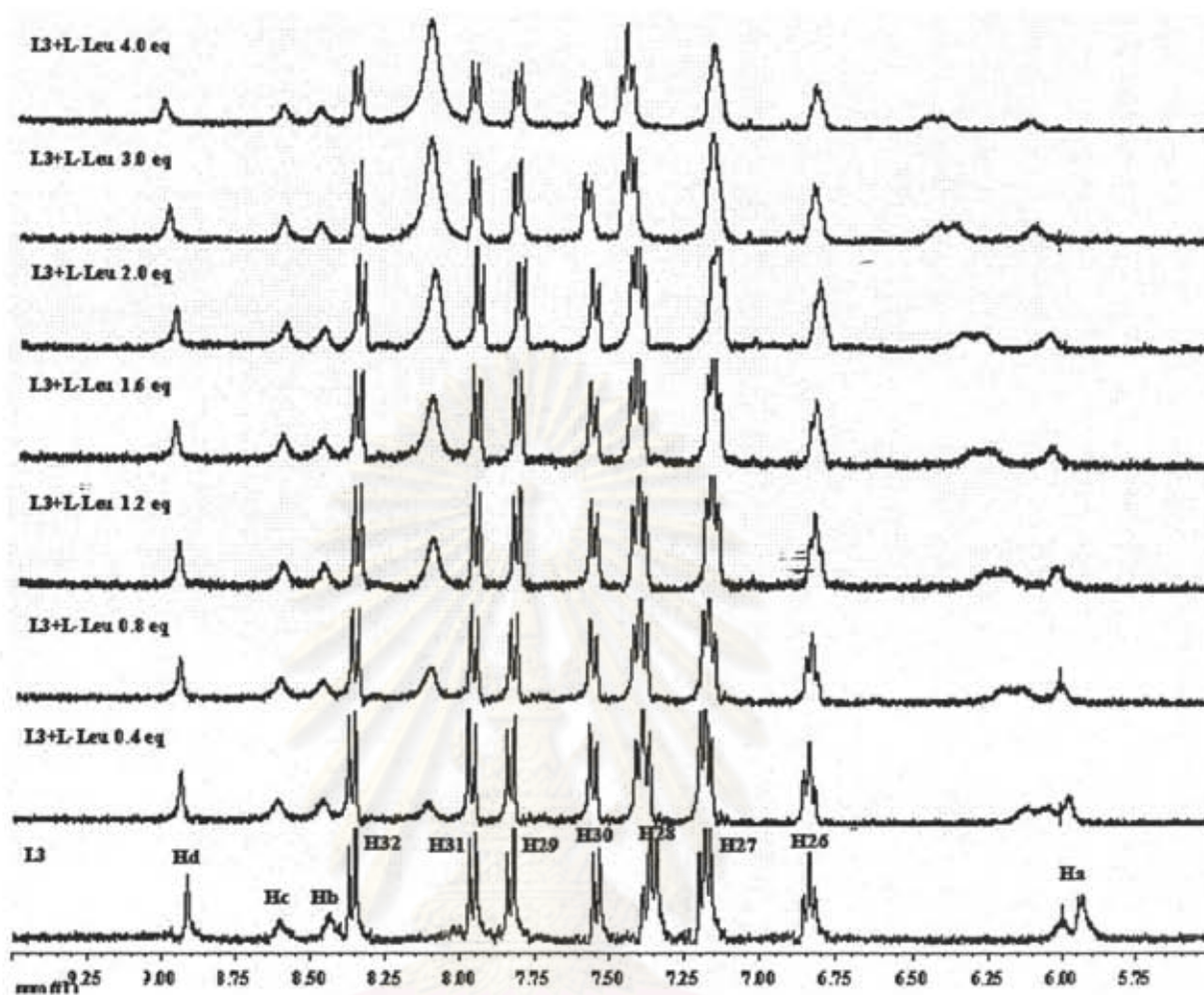


Figure A42. Partial $^1\text{H-NMR}$ titration spectra of L3 ($4.0 \times 10^{-3} \text{ M}$) upon adding L-Leu 4.0 equivalent in $\text{DMSO-}d_6$.

ศูนย์วิทยทรัพยากร
จุฬาลงกรณ์มหาวิทยาลัย

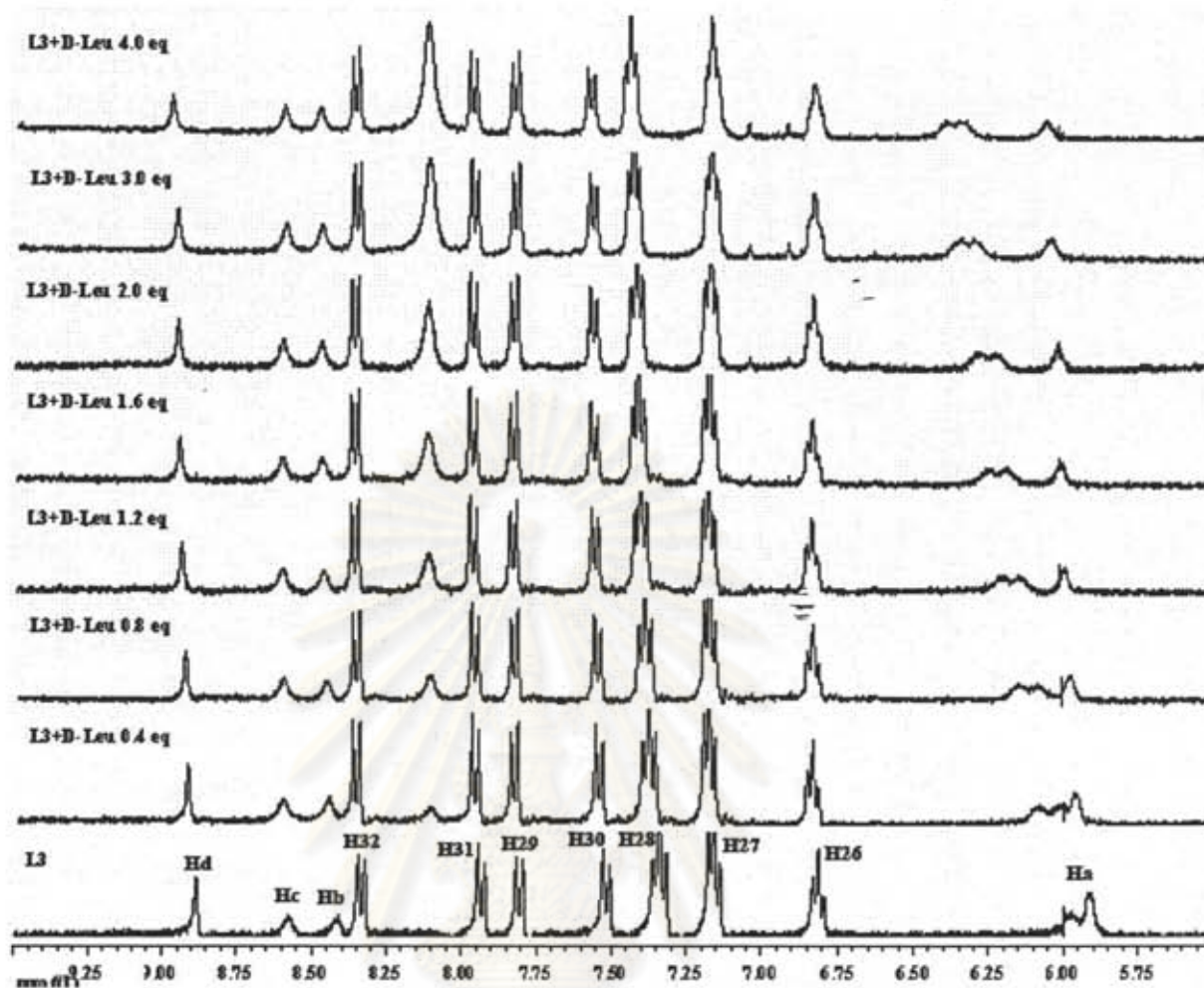


Figure A43. Partial ^1H -NMR titration spectra of L3 (4.0×10^{-3} M) upon adding D-Leu 4.0 equivalent in $\text{DMSO-}d_6$.

ศูนย์วิทยทรัพยากร
จุฬาลงกรณ์มหาวิทยาลัย

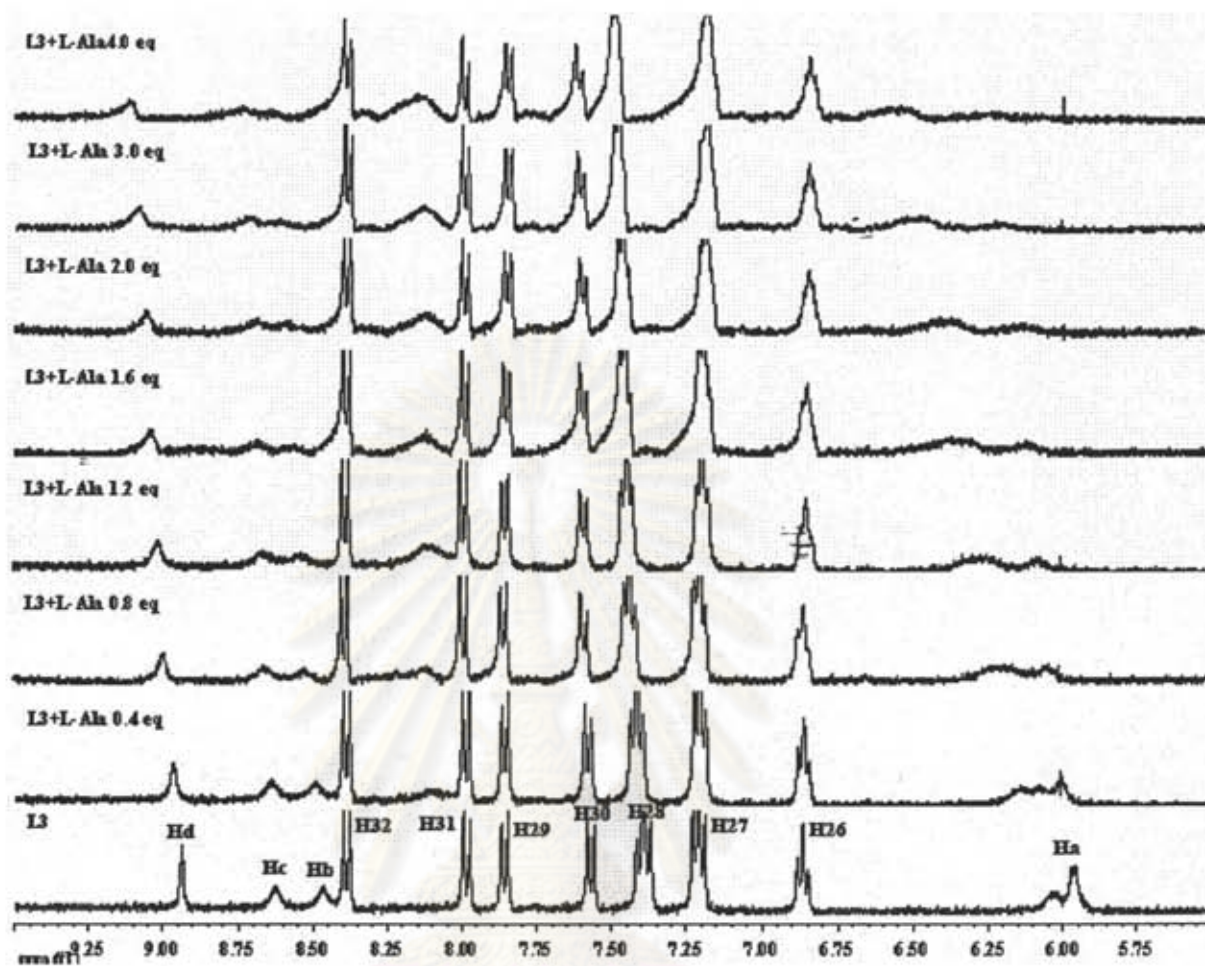


Figure A44. Partial ^1H -NMR titration spectra of L3 (4.0×10^{-3} M) upon adding L-Ala 4.0 equivalent in $\text{DMSO-}d_6$.

ศูนย์วิทยทรัพยากร
จุฬาลงกรณ์มหาวิทยาลัย

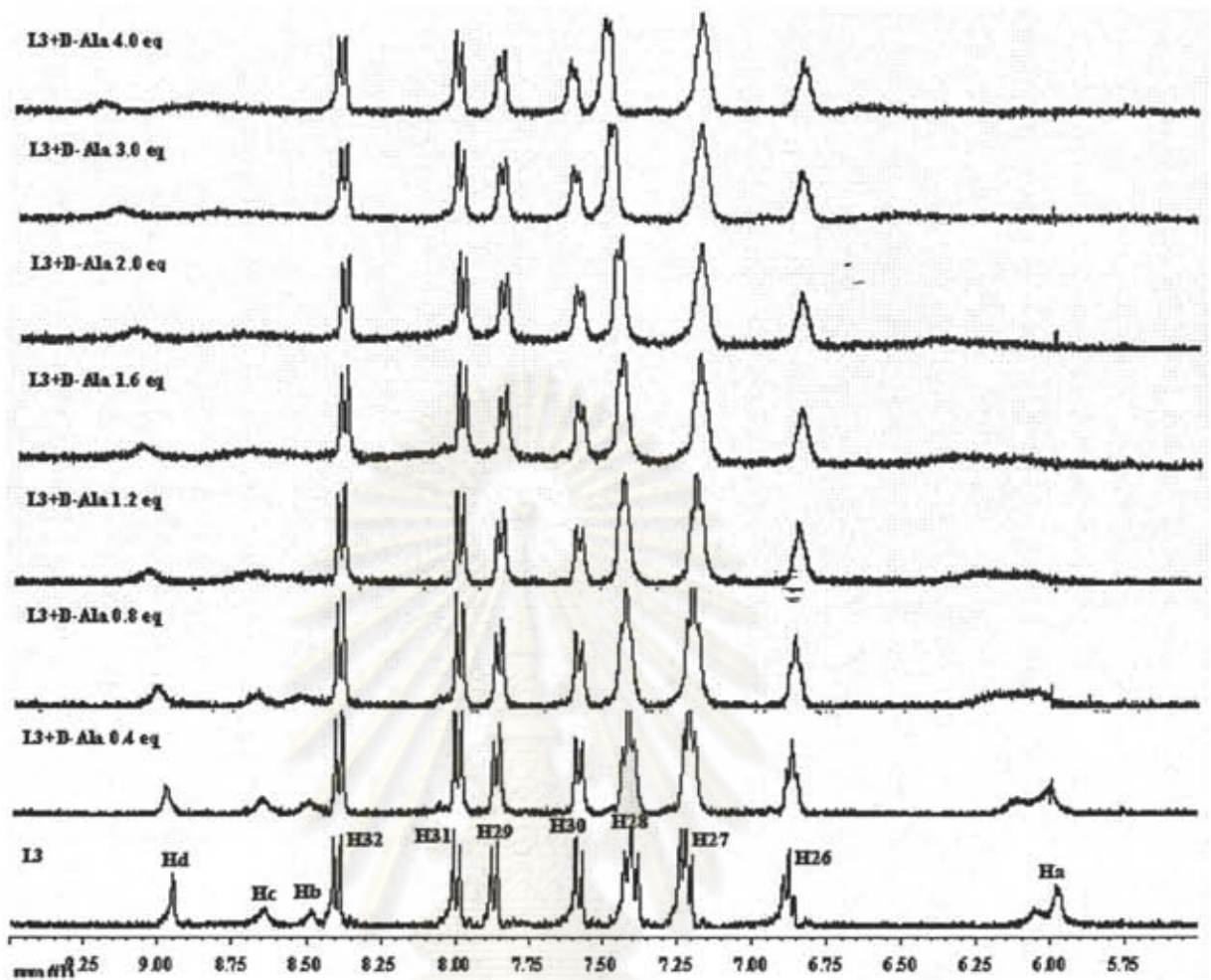


Figure A45. Partial ^1H -NMR titration spectra of L3 (4.0×10^{-3} M) upon adding D-Ala 4.0 equivalent in $\text{DMSO-}d_6$.

ศูนย์วิทยทรัพยากร
จุฬาลงกรณ์มหาวิทยาลัย

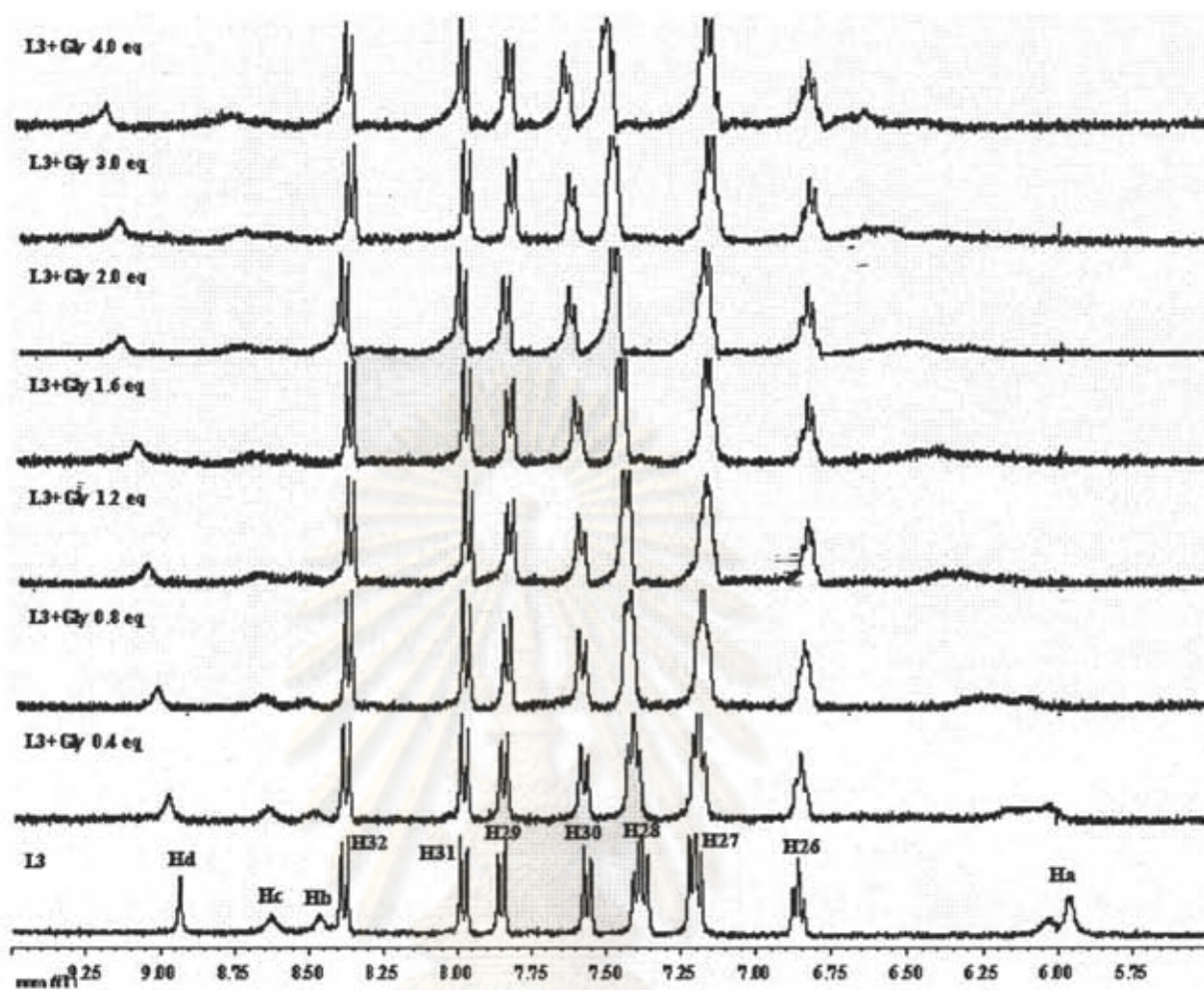


Figure A46. Partial ^1H -NMR titration spectra of L3 (4.0×10^{-3} M) upon adding Gly 4.0 equivalent in $\text{DMSO-}d_6$.

ศูนย์วิทยทรัพยากร
จุฬาลงกรณ์มหาวิทยาลัย

VITA

Miss Anchalee Sirikulajorn was born on December 9, 1978 in Chiang Mai, Thailand. She was a student under “The Development and Promotion of Science and Technology Talent Project (DPST)” from 1997 till 2006. She received her Bachelor’s degree of Science in Chemistry from Chiang Mai University in 1999. Then, she received her Master’s degree of Science in Chemistry from Chulalongkorn University in 2002. Since then, she has been a postgraduate student studying inorganic chemistry and become a member of Supramolecular Chemistry Laboratory under the supervision of Assoc. Prof. Thawatchai Tuntulani. During this period, the DPST gave her an opportunity to do the research under the supervisor of Prof. Anthony P. Davis at University of Bristol, United Kingdom during April 2006-March 2007. She graduated with a doctorate degree in chemistry in the academic year 2007.



ศูนย์วิทยทรัพยากร
จุฬาลงกรณ์มหาวิทยาลัย